Displays for Exploration and Comparison of Nested or Intersecting Surfaces

by
Christopher Charles Weigle

A dissertation submitted to the faculty of the University of North Carolina at Chapel Hill in partial fulfillment of the requirements for the degree of Doctor of Philosophy in the Department of Computer Science.

Chapel Hill
2006

Approved by:

Russell M. Taylor II, Advisor

Elizabeth Bullitt, Reader

Christopher G. Healey, Reader

Stephen M. Pizer, Reader

Mary Whitton, Reader

ABSTRACT

CHRISTOPHER CHARLES WEIGLE: Displays for Exploration and Comparison of Nested or Intersecting Surfaces.

(Under the direction of Russell M. Taylor II.)

The surfaces of real-world objects almost never intersect, so the human visual system is ill prepared to deal with this rare case. However, the comparison of two similar models or approximations of the same surface can require simultaneous estimation of individual global shape, estimation of point or feature correspondences, and local comparisons of shape and distance between the two surfaces. A key supposition of this work is that these relationships between intersecting surfaces, especially the local relationships, are best understood when the surfaces are displayed such that they do intersect. For instance, the relationships between radiation iso-dose levels and healthy and tumorous tissue is best studied in context with all intersections clearly shown.

This dissertation presents new visualization techniques for general layered surfaces, and intersecting surfaces in particular, designed for scientists with problems that require such display. The techniques are enabled by a union/intersection refactoring of intersecting surfaces that converts them into nested surfaces, which are more easily treated for visualization. The techniques are aimed at exploratory visualization, where accurate performance of a variety of tasks is desirable, not just the best technique for one particular task. User studies, utilizing tasks selected based on interviews with scientists, are used to evaluate the effectiveness of the new techniques, and to compare them to some existing, common techniques. The studies show that participants performed the user study tasks more accurately with the new techniques than with the existing techniques.

ACKNOWLEDGMENTS

I thank my advisor, Russell Taylor, and my committee members, Elizabeth Bullitt, Christopher Healey, Steven Pizer, and Mary Whitton, for their advice and guidance in this work.

I thank the scientists, Elizabeth Bullitt, Ed Chaney, Micheal Falvo, and Amitabh Varshney, for discussing their research with me and for helping determine the direction of this work.

I thank the faculty and staff of the computer science department for their many years of support and for providing all the little things that make up an excellent learning environment.

I thank the National Science Foundation and the National Institutes of Health for financial support.

I thank family and friends who supported and encouraged me throughout my at Carolina. Most especially, I thank my wife, Michele.

TABLE OF CONTENTS

LIST OF TABLES

LIST OF FIGURES

Chapter 1

Introduction

The ultimate goal for layered-surface visualization is to simultaneously present nested or intersecting surfaces such that the shape of each is just as understandable as if it were displayed alone while enabling comparisons amongst the surfaces. The surfaces of real-world objects almost never intersect, so the human visual system is ill prepared to deal with this rare case. However, the comparison of two similar models or approximations of the same surface can require simultaneous estimation of individual global shape, estimation of point or feature correspondences, and local comparisons of shape and distance between the two surfaces. A key supposition of this work is that these relationships between intersecting surfaces, especially the local relationships, are best understood when the surfaces are displayed such that they do intersect.

This work presents novel visualization techniques for general layered surfaces, designed for scientists with problems that require such display. The techniques developed for this work are enabled by two algorithms also presented here. The first algorithm refactors intersecting surfaces into non-intersecting, nested surfaces. The second algorithm computes a bijective map between two surfaces, where the map is suitable for use in visualizing integral lines of point correspondence between surfaces (as an aid to perceiving inter-surface distance).

The effectiveness of the two new techniques at conveying the shape of layered surfaces is evaluated by a series of user studies. The tasks included in the user studies are distilled from interviews with scientists whose research includes exploring and understanding layered-surface data. The scientists

interviewed work in a range of fields, including medicine, biology, physics, and chemistry.

The user study tasks derived from these domains and domain-specific questions are the following:

- estimating and comparing inter-surface distances,
- estimating and comparing local shape, and
- recognizing global shape.

Other tasks were also identified through interviews with the scientists, such as identification of the intersection and volume estimation and comparison, but these were not evaluated by user study for reasons explained in Chapter 2.

1.1 Thesis Statement

The thesis of my dissertation is the following:

> Union/intersection refactoring of intersecting surface geometry into non-intersecting components enables the effective application of existing nested-surface visualization techniques to general layered-surface data. Two novel layered-surface display techniques, relying on the refactoring algorithm and utilizing 1) cast shadows or 2) point-correspondence glyphs, enable better shape perception for a pair of general, layered surfaces than a set of previous techniques. The novel techniques also preserve the ability to comprehend the global shape of the individual surfaces.

This work, only a step toward the ultimate goal for layered-surface visualization, takes the following approach:

- collect domain-specific layered-surface questions from scientists,
- synthesize domain-independent layered-surface questions suitable for guiding the design of shape tasks for evaluation studies,

- design layered-surface display techniques that present two surfaces in a manner enabling the simultaneous perception of surface shape and the comparison of shapes and related metrics between surfaces, and
- run evaluation studies to quantify the effectiveness of these techniques at displaying layered surfaces in general, and the synthesized questions specifically.

1.2 Organization

Chapter 2 motivates this work by describing the scientists' research and enumerating their major questions involving the shapes of and relationships between layered surfaces. The scientists work in a variety of fields, and each could benefit from displays of intersecting surfaces. The scientists questions are generalized and categorized to show how the disparate questions relate to a small number of shape metrics. The chapter concludes with the synthesis of performance tasks for evaluating techniques that address the scientist' questions.

Chapter 3 presents the relevant factors of visual perception, shape analysis, and visualization that drive the development of effective visual display. It describes existing techniques for displaying multiple nested surfaces and surfaces with positional uncertainty, which this work draws upon.

Chapter 4 describes five techniques, three existing and two new, included in the user study evaluations. For completeness, two proposed techniques not included in the user study are also described. The new techniques are enabled by a union/intersection refactoring of intersecting surfaces (also described in Chapter 4) that converts intersecting surfaces into nested interior and exterior surfaces. The first of the new, studied techniques uses shadows cast from the exterior surface onto the interior surface to enhance the perception of depth and separation between the surfaces. The second of the new, studied techniques instead uses point-correspondence glyphs to do the same.

Chapter 5 describes user studies designed to evaluate the effectiveness of the two techniques. The performance tasks utilized in the user study are derived from the scientist interviews. The novel layered-surface visualization techniques are also compared to existing visualizations often employed

as layered-surface visualizations.

Chapter 6 summarizes the dissertation work and the reviews the contributions made to intersecting-surface visualization in particular, and layered-surface visualization in general.

Chapter 2

Driving Problems

This work is particularly focused on visualization techniques that enable scientists to perform multiple comparisons between surfaces. A common difficulty in introducing new visualization techniques to a scientist's workflow is proving the value of the new technique to the scientist's research. Therefore, this work undertook identification of the key questions of interest to a group of scientists working in different domains. The questions then inform the design of user studies to indicate how well a given visualization conveys the information in which the scientists are interested.

The following sections will explore the scientists' expectations for layered-surface visualization and how those expectations are transformed into user-study tasks. First, each scientist's area of research will be described and specific investigations described. Then generic questions will be synthesized. Finally, measurable performance tasks suitable for user studies evaluating shape perception of layered-surface visualization techniques will be derived from the set of questions.

The hypothesis that many domain-specific questions map to a small number of generic tasks was shown to be reasonable; the 15 domain-specific questions from 4 domains mapped to 6 generic tasks. The questions posed by a new scientist caused no new generic questions, suggesting that the set tested in this study may be approaching full coverage.

2.1 Scientists: Domains and Investigations

This section contains background information on the scientists, their research areas, and their investigations as they pertain to intersecting surfaces.

2.1.1 Medicine: Evaluating Tumor Image Segmentation Algorithms

Many medical image volumes are collected by computed tomography (CT) or magnetic resonance imaging (MRI). CT image volumes represent the amount of radiation absorbed by the different tissues in the scanned region. Tissues with different absorption properties produce different intensity levels in the CT image volume. MRI image volumes primarily represent the resonant response of hydrogen atoms to radio frequency excitation. Tissues with different hydrogen content produce different responses to the imaging signal, which translates to different intensity levels in the MRI volume. Whatever the imaging method, structures are identified within the image volume by a process called image segmentation.

Computer-aided image segmentation techniques distinguish groups or regions of pixels[1] or voxels[2] that form an object or objects separate from the background of an image [ACKT96]. Some segmentation methods require hand-selecting image elements, some are fully computer-automated, and some lie in between. The result of the image segmentation is a labeled image representing the object or objects of interest found in the image volume. The labeled image may then be used to construct shape representations of the individual labeled regions. It is not important to this work what the representation is, except that it can be readily converted to a boundary representation.

Dr. Elizabeth Bullitt (Department of Neurosurgery at UNC Chapel Hill) is interested in layered-surface display for applications involving brain tumors extracted from MRI volumes. Dr. Bullitt is especially interested in tools for comparing different segmentations of the same data (i.e. human versus computer) and tools for assisting surgical or chemotherapy planning for tumor treatment.

[1]The word *pixel* comes from the phrase *picture element*. A pixel represents a single sample of the data represented by a 2D image. The amount of data summarized by a single pixel depends on the details of the image capture or generation method.

[2]The word *voxel* comes from the phrase *volume element*. It is the extension of the pixel to volume, or 3D, images.

One of Dr. Bullitt's goals is to develop image segmentation algorithms capable of segmenting brain tumors from MRI volumes with at least the same accuracy and reliability as expert radiologists. Such algorithms might then be trusted by clinicians to help with treatment planning. Understanding the differences between automatic segmentations and expert segmentations can help determine how to tune the automatic algorithms. A particular question is whether differences between two segmentations are correlated to shape features (see Figure 2.1). For instance, if the automatically-extracted tumor boundary consistently overestimates the height and width of similar small protrusions, as compared to the expert-extracted tumor boundary, this may indicate that the parameters controlling the contribution of small-scale features in the image data are too sensitive.

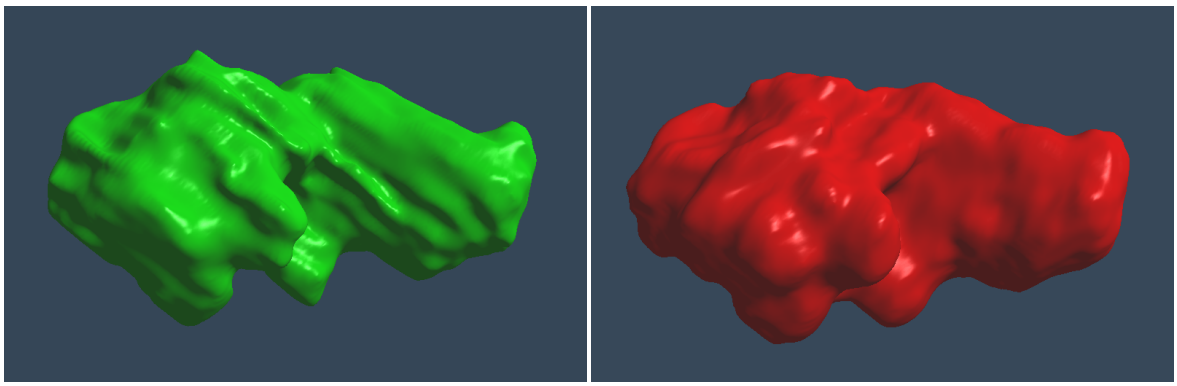

Figure 2.1: On the left, a tumor segmented from MRI data by hand. On the right, the same tumor segmented from the same MRI data by automatic algorithm.

2.1.2 Medicine: Tumor Radiation Treatment Planning

There are three main methods of treating tumors: chemotherapy, surgery, and radiation. Treatment of tumors by radiation involves arranging multiple low-dose radiation beams to deliver a high dose at their intersection. The planning of the positions, shapes, and magnitudes of the low-dose radiation beams is very complex, and fully-automated planning remains an area of active research. Thus, radiation treatment planning is still guided by human experts who must fully understand the relationships between tumors, healthy tissue, and the radiation concentration levels.

The tumor and surrounding tissues are imaged and segmented to produce the *gross tumor volume*

(GTV). The GTV does not contain extensions of the tumor smaller than the resolution of the imaging technology, nor does it contain regions of surrounding tissue experts expect to be damaged by the presence and growth of the tumor. The extent of these extensions and regions can be predicted from tumors with similar pathology. Thus, a radiologist defines a *clinical target volume* that encompasses the GTV and these un-imaged regions. Finally, a *planning target volume* (PTV) is defined to contain the CTV and a small margin allowing for patient motion between and during treatments.

Each low-dosage beam should deliver minimal radiation to healthy tissues while the intersection of the beams should deliver a high level of radiation within the PTV. Typically, radiologists determine the arrangement of beams manually with the aid of 2D planning images of the tumor and surrounding tissues. Software tools for determining the placements and strengths of radiation sources often present radiation iso-dose boundaries that depict treatment regions receiving up to selectable threshold of radiation dose. The most commonly used software tools still present planning images in 2D, both to facilitate the experience of current radiological experts and to satisfy regulations governing records and approval of radiation treatment.

Dr. Edward Chaney (Department of Radiology/Oncology at UNC Chapel Hill) is interested in layered-surface display for applications involving the planning of radiation treatment of tumors. His interests include development of segmentation techniques for the tumor and organs and their combined 3D display along with iso-dose surfaces (see Figure 2.2). Dr. Chaney leads research into the development of 3D displays for radiation planning applications. He is interested in effective displays of tumor, organs, and iso-dose surfaces enabling clinicians to choose appropriate dose levels and allow for the typical day-to-day shifting of anatomy in a patient undergoing radiation therapy. For instance, radiologists may be able to make better treatment plans from 3D displays that enable the surgeon to understand the relationships between radiation iso-dose surfaces, the tumor, and surrounding healthy tissues (relationships such as intersection and penetration depth).

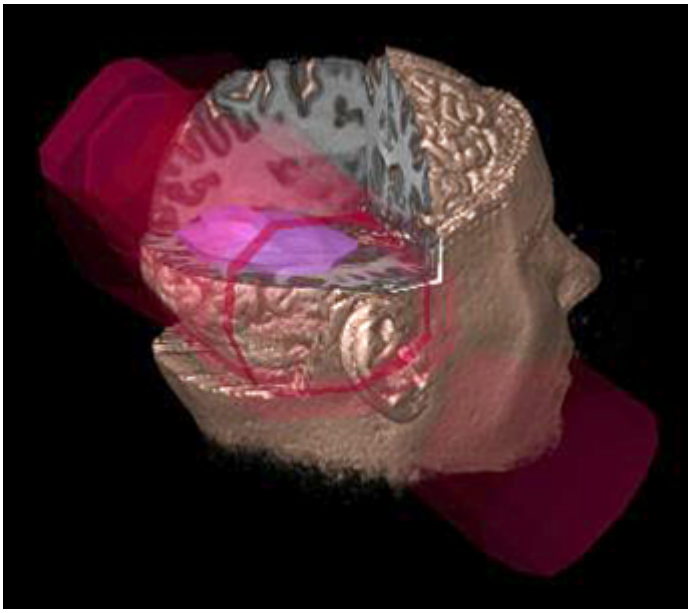

Figure 2.2: An example of an image from a 3D radiation treatment planning system [LFP+90]. Such systems enable a clinician to layout the position, shape, and magnitude of multiple low-dose radiation beams to focus the beams' intersection on the tumorous tissue. The beams' intersection delivers a high dose of radiation to the tumor while individual beams deliver acceptably low doses to nearby healthy tissues.

2.1.3 Materials Science: Atomic-Force Microscopy

An atomic-force microscope (AFM) is capable of imaging many physical properties along the surface of a microscopic specimen, such as height, conductivity, friction, and viscosity [BQG86]. AFMs collect height images of specimens by feedback-controlled scanning of the surface of the specimen with a probe. The tip is scanned to an image coordinate, at which point the height data is recorded. The probe typically has a tip tens of nanometers across, enabling an AFM to image structures as small as an individual virus or strand of DNA. The resulting height data, effectively a dilation of the specimen by the tip, can be used directly to construct a height field for surface display.

Dr. Michael Falvo (Curriculum of Applied Materials Science at UNC Chapel Hill) is interested in layered-surface display for comparing AFM scans of real specimens with simulated scans computed from models of the specimen and the microscope. An AFM simulator performs geometric dilation of a specimen model by a model tip. Understanding the differences between the real and simulated scans can help determine what changes need to be made to the specimen model. For instance, if peak

heights are not significantly different between the two surfaces but the slopes are different, the most likely explanation is that the tip model is the wrong shape.

One of Dr. Falvo's particular interests is the structure of human lung cilia (see Figure 2.3). Height images of cilia taken by AFM show length-wise, striated ridges that may be the result of a fiber-bundle structure within the cilia. Comparison to simulated AFM scans of modeled fiber bundles may help determine the likely size and number of fibers in an individual cilium.

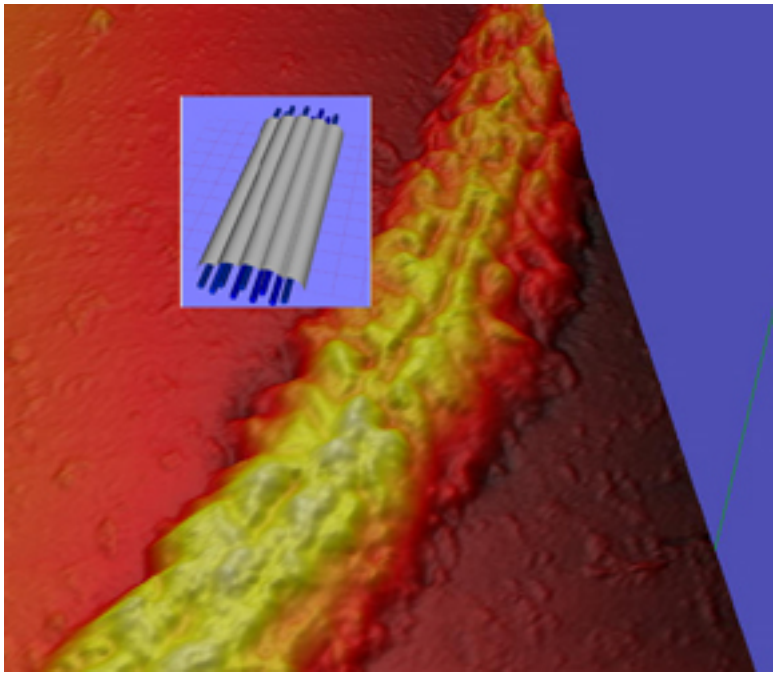

Figure 2.3: An AFM scan of a cilium specimen overlaid with a geometric model of the internal structure of cilia. Note the striations along the length of the AFM scan of the specimen; it is these features the geometric model is intended to capture.

2.1.4 Molecular Docking: Protein Interfaces

Molecular docking applications aid in understanding the minimum-energy configuration and geometric arrangement of molecules as they bond to form more complex compounds. These applications must make use of chemistry, geometry, hydrophilic properties, atomic charge, etc., between two molecules to produce probable docking configurations. Often, these probable docking configurations are visually inspected by displaying solvent-accessibility surfaces [LR71, Con83]. There are multi-

ple algorithms for computing solvent-accessibility surfaces, but the general approach is to determine contact points between a fixed probe and the computed electron density shells of all the atoms in the interacting molecules.

Dr. Amitabh Varshney (Department of Computer Science at the University of Maryland) is interested in layered-surface display of computed protein docking configurations. Dr. Varshney has developed many algorithms to produce probable docking geometries for pairs of molecules. More recently, his research group has developed algorithms that produce only the interaction sites, called interface surfaces, of the solvent-accessible surfaces for a pair of molecules (see Figure 2.4). He wants to visually inspect the interface surfaces as a high-speed filtering step to determine if the docking arrangement is probable. The filtering step should enable easy identification of arrangements where the interface surfaces intersect. The filtering step should also enable easy identification of arrangements where there is insufficient clearance between interface surfaces to allow enzymes to span the two surfaces and form a molecular bond.

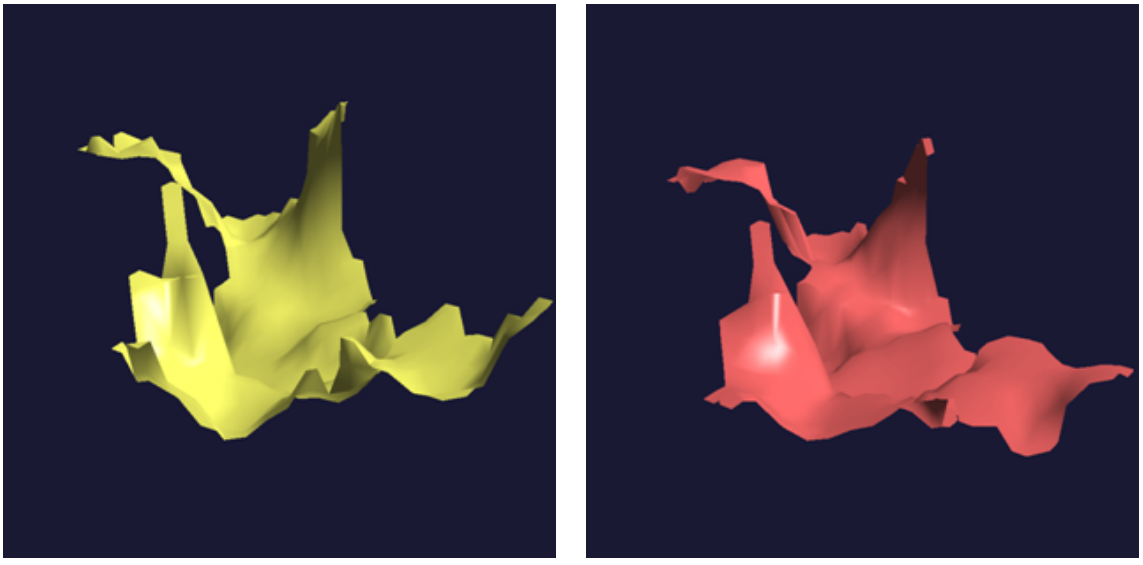

Figure 2.4: These two surfaces make up the interface between two molecules in a potential docking configuration. The interfaces contain only the solvent-accessible surface geometry in the region contributing to the molecular bond.

2.2 Mapping to Generic Questions

This section describes the mapping from domain-specific scientist questions to generic questions. The aim is to show that domain-specific questions from a variety of sources can be mapped to just a few general questions. Later, these generic questions will be used to identify the measurable performance tasks to be tested via user studies.

I anticipate that the set of domain-specific questions from scientists in a broad spectrum of disciplines will map to a small number of generic goals for layered-surface display. In that case, it will be possible to evaluate different techniques with respect to their ability to effectively provide answers to this small number of goals. Then, by selecting the appropriate goal, the best technique for each domain-specific question can be determined.

2.2.1 Mapping: Scientist Questions

Table 2.1 presents the list of scientists, their domains of interest, and their high-level questions. The table also shows a breakdown of the high-level questions into more specific questions, revealing how the scientists expect to explore their data sets to answer their high-level questions.

Table 2.1: Domain-specific questions asked by scientists.

Scientist	Domain	High-level Question	Detail Questions
Bullitt	Brain Tumor Segmentation	Does our tumor segmentation algorithm produce a reliable segmentation of the image data?	– Where do hand-generated and algorithmic segmentations differ? – How significant is each difference (penetration depth)? – What fraction of the surface area of the two segmentations differ? – Are differences between segmentations correlated to shape features (symptom of improper feature contribution to segmentation)?

continued on next page

continued from previous page

Scientist	Domain	High-level Question	Detail Questions
Falvo	Real vs. Simulated AFM Scans	Does the geometric model of the specimen explain the features found in the real AFM scan?	– Does one scan contain significant features not found in the other? – Does the simulated scan appear to be wider or narrower near the specimen substrate than the real scan (symptom of incorrect tip shape)? – Does the simulated scan appear to be higher or lower near the object peaks than the real scan (symptom of incorrect specimen shape)? – Are the shape differences consistent with misalignment of the two scan surfaces?
Chaney	Tumor Radiation Planning	Is the planned dose level a good fit to the organs and tumor?	– Where is the dose not a good fit to the tumor (penetration depth)? – Where is the dose not a good fit to the organs (penetration depth)?
Chaney	Kidney Segmentation	How does the shape of the segmentation vary with the weighting of two heuristics for thresholding the image?	– Where are the segmentations not a good match? – Where the segmentations are not a good match, how much difference is there? – Do the two segmentations have a high percentage of volume overlap?
Varshney	Docked Protein Interface Surfaces	Does the interface between two proteins suggest a probable docking configuration?	– Do the two surface intersect? – Where is there insufficient clearance between the two surfaces?

2.2.2 Mapping: Specific to Generic Questions

Table 2.2 presents domain-specific questions and their mapping to generic questions. The generic questions are numbered to show overlap between domains. The fifteen domain-specific questions from four scientists in three different domains map to eight generic questions (six questions are numbered, but question number 4 comes in three related forms that depend on the transformation being hypothesized between the two surfaces). Two are very local questions (2, 6), two consist of statistics about how the local questions vary across the surfaces (1, 4), and two are summary statistics on these

variations or the volumes of space enclosed by the surfaces (3, 5). As described in the next section, the summary statistics are better found through calculation than visualization. Also described is a method for reducing the set of hypothesis questions to a single shape task.

Table 2.2: Mapping of domain questions to generic questions.

Source Domain	**Detail Question**	**Generic Question**
Brain Tumor Segmentation	Where do the segmentations differ?	(1) Where are the two surfaces separated by more or less than some threshold?
Brain Tumor Segmentation	How significant is each difference?	(2) What distance separates the two surfaces here?
Brain Tumor Segmentation	What fraction of the two segmentations differ?	(3) What percent of the two surfaces are separated by more or less than some threshold?
Brain Tumor Segmentation	Are the differences between segmentations correlated to feature shape?	(4a) Are the apparent differences between the two surfaces consistent with feature shape distortion?
Real vs. Simulated AFM Scans	Does one scan contain significant features not found in the other?	(4b) Are the apparent differences between the two surfaces consistent with missing features?
Real vs. Simulated AFM Scans	Does the simulated scan appear to be higher or lower near the object peaks than the real scan?	(4a)
Real vs. Simulated AFM Scans	Does the simulated scan appear to be wider or narrower near the specimen substrate than the real scan?	(4a)
Real vs. Simulated AFM Scans	Are the shape differences consistent with misalignment of the two scan surfaces?	(4c) Are the apparent differences between the two surfaces consistent with surface misalignment?
Tumor Radiation Planning	Where is the dose not a good fit to the tumor?	(1)
Tumor Radiation Planning	Where is the dose not a good fit to the organs?	(1)
Kidney Segmentation	Where are the segmentations not a good match?	(1)
Kidney Segmentation	Where the segmentations are not a good match, how much difference is there?	(2)

continued on next page

continued from previous page

Source Domain	Detail Question	Generic Question
Kidney Segmentation	Do the two segmentations have a high percentage of volume overlap?	(5) What percent of the total (union) volume is contained in the overlap (intersection) volume?
Docked Protein Interface Surfaces	Are the two surfaces free of intersections?	(6) Where are the surface intersections?
Docked Protein Interface Surfaces	Is there sufficient clearance between the two surfaces?	(1)

2.3 Mapping: Grouping Questions Toward Tasks

This section explores the similarities between many of the generic questions. In particular, it describes the mapping of the generic questions onto tasks appropriate for user-study evaluation of layered-surface visualizations. In some cases it is argued that no evaluation be performed. Such cases involve generic questions that do not map well to shape perception tasks because the human visual system is not well suited to estimating the shape property to be explored.

Questions 1, 2, and 3 are strongly related. All three questions are concerned with estimating the distance between the surfaces. Question 1, *Where are the two surfaces separated by more or less than some threshold?*, asks to compare the distance separating two surfaces at some local region with some reference distance. Question 2, *How far apart are the two surfaces here?*, asks what the actual distance is between the surfaces given a point of reference on one surface. Question 3, *What percent of the two surfaces are separated by more or less than some threshold?*, asks what fraction of the surfaces satisfies question one. If user studies show that participants can compare separating distances accurately with a particular two-surface visualization technique, then it is predicted that questions one and three can be answered accurately. Question 2, however, asks for a direct measurement. This is not a task the human visual system performs well. Our ability to visually measure distance relies on our ability to compare apparent distances to some reference such as a ruler or other known distance. In as much as the human visual system can estimate distance, answering question two accurately follows from answering question one accurately.

Question 6, *Where are the surface intersections?*, is related to the distance questions (1, 2, and 3). The intersections are the regions where the surface separation is zero. Though it could be grouped with the distance questions, the most direct way to enable intersection questions is to explicitly compute and display them (with an unused perceptual cue) as part of the visualization. Assuming a perceptually salient, direct display of the intersection can be added to any display techniques developed in this dissertation, specifically measuring user study performance at identifying the intersection is unnecessary.

Question 4 appears in three related parts, *Are the apparent differences consistent with **some hypothesis**?* The three hypotheses are *misalignment*, *missing features*, and *feature distortion*. All three hypotheses are concerned with comparing the shape of the two surfaces. The misalignment hypothesis tests whether the two surfaces are the same shape but were not brought into a common coordinate system. The missing-feature hypothesis tests whether the surfaces are different shapes. The feature distortion hypothesis tests whether corresponding features are systematically exaggerated on one surface.

These domain-specific shape hypotheses require understanding of their meaning (i.e., what does it mean for a feature to be dilated) that goes beyond low-level shape perception into cognition and are more difficult to isolate from the problem domain. Also, there are many more possible hypotheses than the ones solicited from this group of scientists. In this dissertation, the combination of a local shape perception task and a broad shape perception task (such as global shape recognition) serves to cover the visual-perception aspects of the hypothesis questions. The global shape task also serves to show whether the visualization techniques greatly interfere with the comprehension of the individual objects.

Question 5, *What percent of the union volume is contained in the intersection volume?*, asks a completely global question. This is more than a perception question, as one must estimate volume of two complex, composite shapes resulting from the intersection of the two principal shapes (the union-of-two-shapes boundary and the intersection-of-two-shapes boundary). Unfortunately, the human visual system is not well suited to volume estimation tasks even for single physical objects. It is therefore unnecessary to include a volume estimation task. Scientists who wish to know volume

overlap statistics about their surface would be better served by computing them outright.

2.4 Tasks

This section lists the tasks proposed to cover the synthesized questions. Recall that these questions were about distance, shape, volume, or the intersection itself. Also recall that a volume task was deemed unnecessary due to the human visual system's poor ability to estimate volume and that an intersection task was deemed unnecessary because it is dominated by directly displaying the intersection curves via a salient perceptual cue. The following tasks appear to exercise the remaining synthesized generic questions.

- **Distance Task**: Indicate in which of two regions the two surfaces are closest together. This task addresses generic questions one, two, and three – the distance questions.
- **Local Shape Task**: Indicate in which of two regions the two surfaces are most nearly parallel. This task addresses generic question four – the shape hypothesis question – at a small scale.
- **Global Shape Task**: Identify which, if either, of the two shapes contains a target shape. This task addresses generic question four at a large scale. This task also shows the interference the different visualization techniques cause for recognizing shapes.

The implementation of these tasks in user studies is the subject of Chapter 5.

Chapter 3

Background

As stated in the introduction, the ultimate goal for layered-surface visualization is to simultaneously present nested or intersecting surfaces such that the shape of each is just as understandable as if it were displayed alone while enabling local comparison amongst the surfaces. To approach this, it must be understood what is meant by shape, how it is perceived by the human visual system, and what techniques have proven to best present single and multiple surfaces.

This chapter presents background and related work in geometric shape, visual perception, and surface visualization. The first section describes the geometry of shape as it pertains to display and comprehension of shape. The second section describes perceptual cues commonly used to display a single surface and their relationship to geometric shape. The final section describes existing visualization techniques for displaying multiple surfaces, organized by intended interpretation of the display, with special attention given to those leveraging perceptual cues.

3.1 Geometry of Shape

The following sections, indeed the majority of this chapter, deal with the display and visual perception of object shape. This chapter begins with a discussion of what constitutes object shape. This section will introduce terms and concepts used in describing the geometry of shape[1]

[1]Often, shape and depth are used to denote similar visual concepts. For instance, the manner in which visual depth, the distance from the observer to a point in space, changes along a surface is dependant on surface shape. In this chapter,

3.1.1 Mathematics of Shape

This section introduces many important concepts and terms used in the study of geometric shape. The content of this section is heavily influenced by readings of Jan Koenderink's excellent text on the subject, *Solid Shape* [Koe90].

The *geometric shape* of an object is an operational concept describing, to a linear approximation, how the object's surface changes within a neighborhood. The shape of the object at some point on its surface depends not only on the object, but also on the size of the neighborhood (the scale) considered.

The first-order approximation of an object's surface at a point is the *tangent plane*[2] of the surface at that point. The tangent plane serves as a reference frame for understanding how the surface changes within the neighborhood of the surface point. The tangent plane is the first derivative of object shape.

On the surface, the tangent plane is a 2D reference frame. The direction orthogonal to the tangent plane is called the *surface normal*. The surface normal is a more computationally convenient entity than the tangent plane and is more commonly used in computer graphics as a local approximation of shape. Together the surface normal and tangent plane define a 3D reference frame for the neighborhood about a point on the surface of an object.

As the tangent plane is only a local linear approximation to the surface at a point, the true surface deviates from the tangent plane as you move about the surface away from that point. The *curvature* at that point on the surface is the measure of the rate of this deviation, and is the second derivative of surface shape.

The *shape operator* reveals how the tangent plane changes for a step within the local neighborhood, so it captures the complete local curvature. Specifically, the shape operator is a matrix operator that gives the change in the surface normal for a step along each basis vector of the tangent plane (thus it contains partial derivatives of the surface normal with respect to the basis vector directions). The shape operator describes a linear system, so the change in surface normal direction due to a step in an

however, the term depth will be used exclusively to denote ordering of objects, or part of objects, in the scene with respect to the observer.

[2]Let (x_0, y_0, z_0) be any point on the surface $z = f(x,y)$. If the lines tangent to all smooth curves on the surface passing through (x_0, y_0, z_0) lie in a common plane, then we call that plane the *tangent plane* to $z = f(x,y)$ at (x_0, y_0, z_0).

arbitrary direction can be composed of a linear combination of steps along the basis vectors.

By solving for the eigen terms of the linear system represented by the shape operator, the minimum and maximum change in the surface normal for a step in the tangent plane can be determined. The eigen vectors of the shape operator give basis vectors for the tangent plane that are also the directions of maximum and minimum change in surface normal. The associated eigen values are then the minimum and maximum curvatures. Specifically, the maximum direction and associated curvature are referred to as the *first principal direction* and *first principal curvature*. The minimum direction and curvature are referred to as the *second principal direction and curvature*. These eigen vectors are, of course, orthogonal. An important property of the principal directions is that they are pure nose-dive curvatures; for a step along the direction of principal curvature, the surface normal changes only toward or away from that same direction of principal curvature (according to the sign of the curvature).

The determinant of the shape operator is called the *Gaussian curvature*. The magnitude of Gaussian curvature is a measure of the spread of the surface normals within a neighborhood. The sign of the Gaussian curvature in a local area of the surface can easily be estimated just be viewing the surface. Concave areas have a negative Gaussian curvature. Convex areas have a positive Gaussian curvature. Flat areas have zero Gaussian curvature. The Gaussian curvature is so named because of its relationship to the *Gauss map* of a surface. The Gauss map maps points on a surface, via their surface normal, to points on a unit sphere (in this case called the Gaussian sphere). Gaussian curvature is also a measure of the magnification of a locality when mapped to the Gaussian sphere.

The trace of the shape operator divided by two is the *mean curvature*. The mean curvature is an average of the change of the surface normal over all directions.

3.1.2 Geometric Shape and View Projection

Many features of surface shape have special importance for understanding the shape of a projection of an object as viewed from some vantage point. These features contribute to the depth discontinuities seen in the viewing projection of the object. They also contribute to the boundaries of cast

shadows – shadow boundaries are the projections of these same features from the light source onto the shadow receiver.

The *fold* is the locus of all points on the surface that are tangent to the viewing direction. Though it may be composed of several loops, the fold is always closed. For a given viewing direction, however, parts of the fold may be occluded by the surface itself.

The *occlusion boundary* of the surface is the locus of points that divide the surface into visible and invisible regions. The occlusion boundary is that portion of the fold that is not occluded by the surface. Though concave regions of the surface may contribute to the fold, they can never contribute to the occlusion boundary as they would be simultaneously occluded.

The *contour* is the projection of the occlusion boundary onto an image. The contour may contain T-junctions, cusps, and terminations. As the view direction moves, changes in the apparent shape of the projection of the surface originate along the contour.

The external portions of the contour are called the *silhouette* of the surface. The silhouette is the closed boundary of projection and separates the visible object from the background.

The contour conveys important global shape information about the projected shape. The sign of the curvature of the contour indicates the local Gaussian curvature in that area, an area necessarily orthogonal to the current view direction. Where the contour is convex, the surface is convex. Where the contour is concave, the surface is saddle shaped. Where the contour is flat, the surface is cylindrical or planar. Similar information can be determined from the shadow boundaries.

Geometry of Illumination

The amount of light reflected off a region of surface and reaching an observer is called the *luminance*. Surface shape plays a key role in determining how luminance is distributed, that is how the light from the light source is spread out as it reflects off a surface. In the section, the total luminance from a surface reaching a single observer will be referred to as the *luminance image*.

This section will focus on the geometric properties of two commonly modeled luminance func-

tions; the luminance of a Lambertian surface, which reflects incident light uniformly in all directions, and the luminance of specularities, which are images of the light source reflected onto the observer.

The luminance of a Lambertian surface follows Lambert's cosine law and varies in intensity according to the cosine of the angle between the direction of incident light and the direction of the surface normal. Features of the shape of a Lambertian surface appear as similar features of the intensity of the luminance image of the surface [Koe90]. Generic regions of the surface, local shape features that continue to exist after a random perturbation of the surface (elliptics, hyperbolics, etc.), appear as generic regions of the luminance. Singularities of surface curvature, local shape features that may be annihilated by a random perturbation of the surface (saddle points, cusps, etc.), appear as singularities of the luminance.

Specularities follow the Snell's law reflection of a point light about the surface normal and onto the viewing direction. Given a point on a surface with unit surface normal n and a direction l to a point light source, specularities appear in the reflection direction r when $r = l - 2(n \cdot l)n$. The Gauss map of a surface is formed by taking the direction of all unit surface normals as the coordinates on the unit sphere. So a single point on the surface maps to coordinates on the Gauss map through that point's unit normal. If a path along the surface crosses a parabolic point (a point with zero Gaussian curvature), the corresponding path along the Gauss map will contain a fold. Pairs of specularities are generated and annihilated at parabolic points on the surface [Koe90], so the number of folds on the Gauss map (also called the multiplicity of the Gauss map) determines the maximum number of specularities on the surface. Note that even non-generic shapes that contain no parabolic points (a sphere) or only parabolic points (a plane) still display a single specularity.

3.2 Displaying a Single Surface

Much work in visual perception explores the perception of shape from shading [BB90, CK97, CJ96, DHEN95, Gib50, Ram88]. Specifically, the human visual system interprets shape with a built-in bias toward scenes that are diffusely lit from overhead [Gib50] - though sufficient cues from other perceptual channels can influence this bias. Perception research suggests a variety of other visual cues

that also elicit the perception of shape, such as texture [CJ96], specular highlights [BB90], shadows [EKK93], and object boundaries [Ram88].

3.2.1 Depth Cues

Monocular depth cues are important for understanding the arrangement of objects in a scene and their relative sizes. However, only some of these depth cues appear frequently in scientific or medical visualization. Occlusion and linear perspective are depth cues present in most 3D scientific or medical visualizations. The kinetic depth effect is commonly found in visualization either through user interaction (i.e. interactive applications) or precomputed motion (i.e. animations). Depth of field and atmospheric attenuation are not commonly found in scientific or medical visualization.

Occlusion is an important monocular depth cue where a point near the observer obscures more distant points. The occlusion boundaries are key elements in conveying relative depth between objects. Occlusion is also important to the understanding of the global shape of objects, as an object's internal contours tell the observer both about the relative ordering of regions of the surface and about the shape of the surface at the region forming the contour.

Perspective foreshortening is the name for the most commonly observed artifact of projecting a 3D scene onto a 2D imaging device (a digital camera, a retina, etc.). Distant objects appear smaller than nearby objects. The perspective projection maps 3D space such that parallel lines receding from the imaging device are mapped into lines converging to a single vanishing point in the projected image. Because this projection preserves straight lines, it is often referred to as linear perspective. One side effect of perspective projection is that the apparent depth of familiar objects is related to their apparent size. For instance, if in the same scene a child appears larger than an adult, the natural interpretation is that the adult is much further away than the child.

Depth of field is an "out of focus" effect on unattended objects at depths different from the attended object. Due to the lens of the eye focusing the attended object onto the fovea, other objects in the view appear blurred. Atmospheric attenuation is an effect of diminishing contrast due to atmospheric scattering of light rays. Objects that are further from the viewer appear more attenuated. Depth

of field and atmospheric attenuation are not commonly included in visualization for two reasons. First, graphics hardware has only recently been capable of producing depth-of-field and atmospheric-attenuation effects at interactive rates. More importantly, both effects reduce overall detail in the visualization. They are more often used to focus attention than to enhance depth relationships.

The kinetic depth effect is a strong depth cue derived from motion cues. An object near the observer moving transverse to the line of sight at a fixed velocity traverses a greater visual angle per unit time than does an identical object with a similar absolute motion but at a greater depth from the observer. Figure 3.1 illustrates this phenomenon. This is similar in effect to parallax, the change in relative apparent positions of objects produced by a change in the position of the observer.

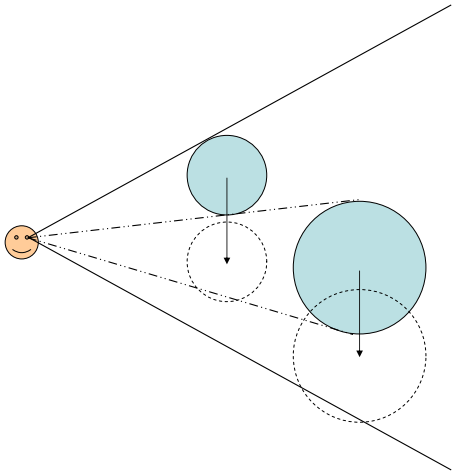

Figure 3.1: This figure illustrates the phenomenon of the *kinetic depth effect*. The two objects move with the same absolute velocity relative to the observer. The difference in apparent velocity reveals their relative depths from the observer.

The kinetic depth effect also applies to the understanding of shape of a single object in motion. The difference in appearant velocities of multiple regions of an object in motion reveal depth and shape information about the full object.

Depth cues also result from stereo vision. Because this work does not use or evaluate stereo as an active perceptual component of layered-surface display, it will not be discussed in detail here. It should be noted, however, that the kinetic depth effect is a stronger shape cue than stereo vision. So for most visualizations, interactive control is a more important feature than stereo display for providing

good shape perception.

3.2.2 Direct Illumination

The most common illumination model used in computer graphics, the empirical Phong lighting model, may convey shape cues in a manner similar to certain real objects under natural illumination. The Phong lighting model approximates diffuse and specular lighting according to Lambert's cosine law and Fresnel's laws of reflection, respectively [Pho75]. Under the appropriate conditions, Phong illumination has been shown to convey shape and depth [JC96]. Phong's diffuse term captures the view-independent Lambert's Law reflection of a point light about the surface normal. Phong's specular term captures the Snell's law reflection of a point light about the surface normal and onto the viewing direction.

Johnston *et al.* investigated whether the illusion of curvature in Phong-illuminated, computer-generated surfaces mimic cues appearing on solid objects under real light [JC96]. Specifically, they looked at three-dimensional curvature contrast and the illuminant-position effect. Three-dimensional curvature contrast is a simultaneous contrast effect for curved surfaces, in that the apparent curvature of a surface defined by shading is influenced by the surrounding surface curvature. The illuminant-position effect predicts that the perceived magnitude of curvature of a surface patch is a function of the position of the light source. The illuminant-position effect can be mitigated by texture cues and specularities. Johnston *et al.* found the perceived curvature magnitudes influenced by both investigated effects to be the same whether the objects were real or computer generated – the Phong lighting model works.

The Phong illumination model is used in all of the techniques presented here.

3.2.3 Shadows

Shadows on surfaces can be categorized into two types – attached shadows and cast shadows. Attached shadows contain points on a surface facing away from the light source. Cast shadows contain points on a surface that are occluded from the light source. In both cases, the boundaries of the shadow

correspond to light rays that just graze the surface producing the shadow. Generically, attached shadow boundaries denote the curve along the surface where surface normal vectors are perpendicular to the incoming light direction. Cast shadow boundaries are the projection of the attached shadow boundary.

Shadow formation shares similarities with specular hightlights. Shadows are created and destroyed at parabolic points on the surface. Shadows also occur in pairs, just as specularities do. A shadow pair consists of one attached and one cast shadow. Other shape-related properties of shadow boundaries and their interaction with surface features are described in Knill *et al.* [KMK97].

Research into the perception of attached shadows finds that they are perceived similarly to occlusion contours [EKK93, Cas01, KMK97, MKK98]. Occlusion contours separate objects from background and also reveal the global structure of surfaces, providing evidence of the presence of bumps, dimples, and other features [Koe84].

Cavanagh and Leclerc report that cast shadows help disambiguate light direction and help place objects in space but do not appear to strongly suggest shape [CL89]. Cavanagh and Leclerc also find that shape perception is diminished for shadows that do not obey appropriate contrast rules – the region in shadows should be darker than the surround. Indeed, "light" shadows, false shadows that geometrically behave like real shadows but are brighter than their surroundings instead of darker, appear to be processed differently from "dark" shadows in visual search tasks.

Sinha reports that viewers are not very sensitive to inconsistencies in the directions of cast shadows for disconnected objects in doctored photographs [Sin00].

Shadows in motion produce a strong sense of 3D object motion but not illuminant motion. Mamassian *et al.* report that even when available visual information suggests otherwise, shadows in motion are interpreted as if the light source were fixed [MK96]. Other assumptions and biases can be overridden by shadow motion as well, such as constant object size, linear object motion, and assumed viewpoint.

Another benefit of shadows is that they can enforce the perception of proximity or contact between objects [TSS$^+$98]. Physically inaccurate, artificial shadows placed near the region of closest proximity between two objects enforces the precept that the objects are in or near contact. This can be critical to

understanding the layout of a scene.

One of the techniques presented here uses dark cast shadows from a fixed light source as a depth cue.

3.2.4 Texture

Texture has long been known to be an excellent shape cue. Gibson showed that the slant of a textured plane extending to the horizon could be perceived, though the slant is typically underestimated [Gib50]. Here Gibson uses slant to refer to the degree of rotation of the surface out of the image plane and toward the horizon. Cumming *et al.* described the three shape cues due to apparent variation in texture on a uniformly textured surface: *compression* – due to surface orientation relative to the image plane, *density* – due to distance and obliqueness of view, and *perspective* – due to distance from the view point [CJP93]. Of these, texture compression has been shown to be the most significant for surface shape perception under stereo viewing.

A number of studies have found that certain directional components of surface texture seem to enable better shape and depth perception than some other directions [IFP96, IFP97, KHSI03, KHSI04, LZ00, SW04]. Li and Zaidi find that (sinusoidal) surface shape is best perceived when noise-like textures project significant energy along the first principal curvature direction [LZ00], which is the direction of highest local curvature. Interrante *et al.* found that brush strokes laid along the first principal curvature direction, through well spaced points on the surface, also convey surface shape [IFP97].

Some cautions against using first principal curvature alone have been put forth [TO02a, SW04] concerning the poor shape cues present in principal-curvature textures under non-generic views where the viewing direction follows the curvature direction. Viewing a ridge transversely is one such non-generic view. However, using both principal curvature directions can convey shape better than either one alone [KHSI03], and additional non-principal directions can further improve the recognition of some shapes [KHSI04]. Because the two principal directions are orthogonal, textures using both directions address concerns about non-generic views. Sweet and Ware describe a highly effective

and inexpensive two-direction texture hash not designed to follow principal curvature [SW04]. The texture produces a grid on the surface that provides texture compression cues and can also be used to judge distances along the surface.

Several of the techniques presented here use principal-direction texture to enhance perception of surface shape.

3.3 Displaying Multiple Surfaces

The key problem in investigating the surfaces of multiple objects is occlusion. A simple, but often ineffective, approach to displaying multiple surfaces is to display all of the surfaces as opaque geometry. Should any of the objects project to the same pixels in the view image, only the outer most regions of their surfaces are visible for investigation. This solution is often insufficient for understanding the relationships among a set of objects under investigation.

Techniques such as side-by-side display, color mapping, texture, glyphs, and translucency have historically been used to mixed effect in an effort to display multiple occluding surfaces.

3.3.1 Side-by-side

Comparing surfaces side by side is a common technique. In the context of computer display, side-by-side is often chosen because it is so natural and familiar – it is a direct analog to what we do with real objects or images of objects. Side-by-side display was not tested because it was not expected to enable accurate performance on the inter-surface distance tasks or the local shape tasks. A key supposition of this work is that these relationships between intersecting surfaces, especially the local relationships, are best understood when the surfaces are displayed such that they do intersect. It is not clear how to establish a common frame in which to compare the two surfaces in a side-by-side display.

3.3.2 Color Mapping

Many visualization tools apply color maps to one visible surface to convey the shape of an hidden surface (see Figure 3.2). The color map conveys some metric about the relationship between the two surfaces, typically a distance metric. A typical distance metric is the Euclidean distance between points of closest approach.

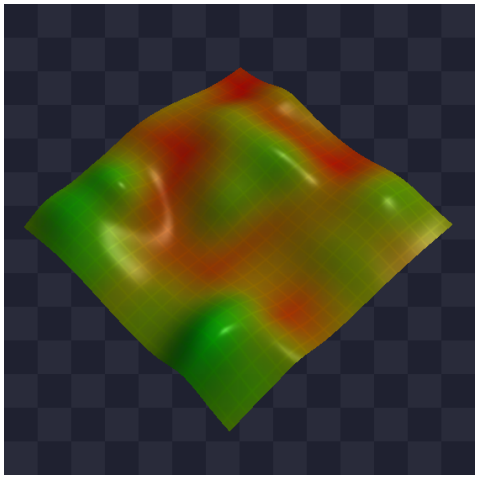

Figure 3.2: This image presents an example of using a color map to encode distance between two surfaces on the geometry of one surface. It is clearly difficult to infer the shape of the hidden surface from the color encoding on the visible one.

There are at least two geometric problems with this distance map. First, the Euclidean shortest distance between points on different surfaces is not symmetric (see Figure 3.3). Point A_0 on surface X has a set of closest points B on surface Y. For a point B_i in the set B, there is no guarantee that point A_0 is in its set of closest points on surface X.

Second, shown in Figure 3.4 the shape of visible surface X and its distance-mapped color texture M does not uniquely identify the shape of the second, hidden surface Y.

There are also perceptual issues in choosing an appropriate color scale. In particular, some color scales are best for conveying metric values, while others are best for conveying shape [War88]. Spectral maps convey metric value best, because they best avoid simultaneous contrast – an effect where the perception of a stimulus is influenced by its contrast with neighboring stimuli. Luminance maps convey shape best. Ware found that a map combining spectrum and luminance best conveys shape

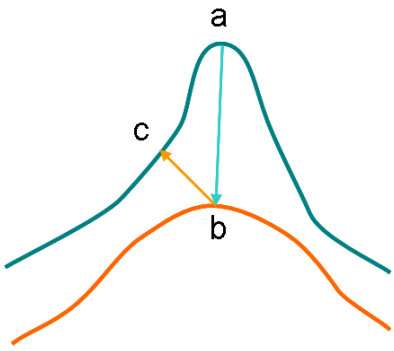

Figure 3.3: These two surfaces illustrate the asymmetry in Euclidean shortest distance between points on surfaces. Point b is the closest to point a, but point a is not the closest to point b. Also note that the distances $||a-b||$ and $||b-c||$ are not equal.

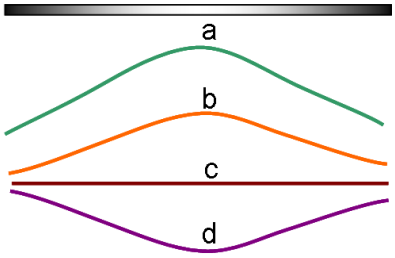

Figure 3.4: Using color to encode the Euclidean shortest distance between surfaces can by ambiguous. As a 2D example, the color bar on top can represent the distance between curve a and any of lines b, c, or d.

and metric value simultaneously [War88]. However, Ware was not investigating color maps on smooth surfaces, but rather smooth univariate maps in 2D images. Luminance is not available for mapping metric values on smooth surfaces, because luminance is required to convey the surface shape (via illumination).

In this study, two color scales are used. Both use hue to label the two ends of the scale. The first scale interpolates saturation, passing through a desaturated grey between in the middle of the scale. The second scale interpolates between the two end hues alone.

3.3.3 Cut-away Geometry

There are a number of very simple and frequently employed techniques which remove some geometry in order to remove some occlusion. Neither occlusion order nor shape perception are criteria

for how geometry is removed, so these techniques are not necessarily appropriate for direct use in general layered-surface visualization.

One method of removing occluding geometry is to render some of the layered objects in wireframe (only the edges of the polygonal facets of the surface geometry are actually rendered). Unfortunately, this approach reveals more of the approximation to the surface than it reveals the represented shape (see Figure 3.5). A common compromise is to use a simple texture with regular regions of translucence, such as a grid (see Figure 3.6). This gives uniformity to the pattern of opacity and translucency and enables the possibility of user control. However, finding non-distorted texture coordinates for a surface of arbitrary topology is an area of active research, and I know of no technique that could guarantee the regularity of the texture on an arbitrary surface.

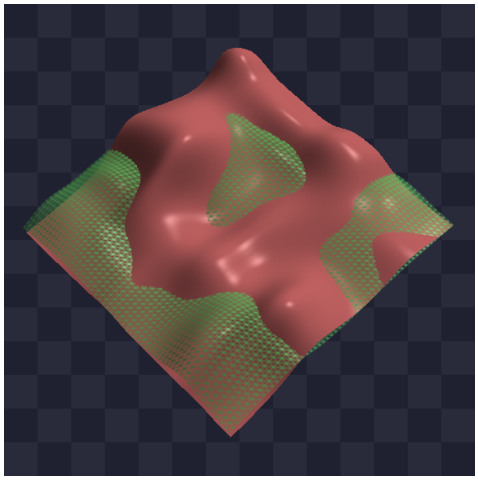

Figure 3.5: Two intersecting surfaces are visualized. One surface is displayed as an opaque triangle mesh, and the second surface is displayed by the edges of the triangle mesh only (a technique commonly referred to as *wireframe*).

Two related methods are planar contours and ribbons. The planar contours technique reveals the intersections of layered surfaces and a stack of evenly-spaced parallel planes. It can be difficult to understand the full surface shape from these contours and more so to understand relationships between surfaces between planes. Ribbon techniques are less aggressive at removing geometry than planar contours. Instead of rendering only the planar intersections, only geometry between alternating pairs of planes are removed. For instance, the geometry between every other pair of planes may be removed. Each ribbon then has sufficient image coverage for good shape perception of the ribbons.

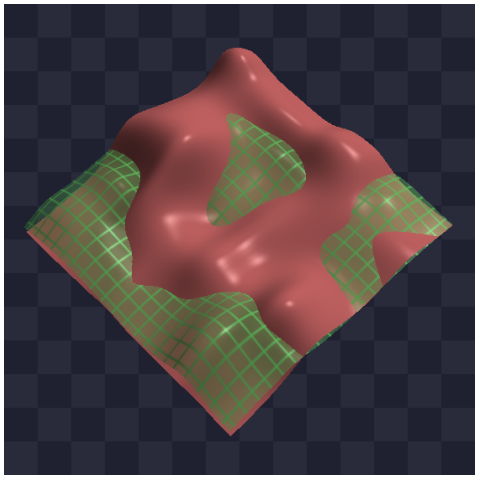

Figure 3.6: Two intersecting surface are visualized. One surface is displayed as an opaque triangle mesh, and the second surface is displayed with a grid texture modulating the surface translucency.

Bauer-Kirpes *et al.* used a ribbon-like technique for displaying nested surfaces in medical applications [BKSBL87] (see Figure 3.7). The technique bears some similarities to a technique proposed, but not implemented, for this work (see Section 4.3).

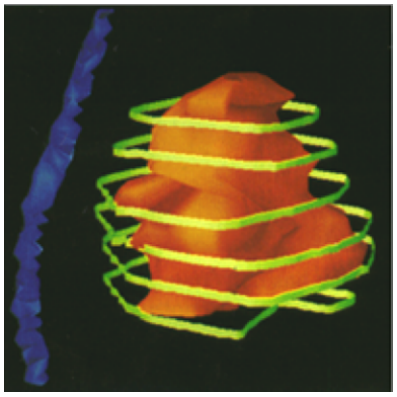

Figure 3.7: The technique of Bauer-Kirpes *et al.* displays only ribbon-like pieces of the exterior surface, called "barrel hoops" [BKSBL87].

Diepstraten *et al.* describe techniques for automatically producing breakaway and cutaway illustrations of nested surfaces [DWE03] (see Figure 3.8). The automatic algorithm can be combined with any non-photorealistic techniques to illustrate the interior of an otherwise solid object. A number of potentially useful cutout styles are proposed. These illustrations remove portions of exterior geometry that occlude important interior surfaces.

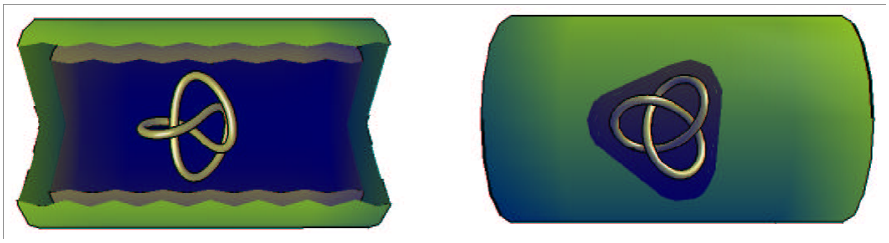

Figure 3.8: This image shows examples of cutaway illustrations from Diepstraten *et al.* [DWE03].

None of these techniques are included for study in this work. They are all interesting techniques for later comparison as part of future work.

3.3.4 Translucence

A common, simple, but perceptually ineffective method to display nested surfaces is to simply render exterior surfaces with uniform translucency. Unfortunately, uniform translucency confounds shape perception away from object silhouettes. Techniques that render occluding surfaces as a mix of translucent and opaque materials generally enable better shape perception than uniform translucency.

Interrante provides an excellent summary of relevant perceptual issues for using translucency in visualizations [IFP97]. The most critical aspect in perceiving that a surface is translucent is apparent contrast reduction. For a surface to be perceived as translucent, the surface must reduce the apparent contrast of the background while preserving relative brightness ordering. Metelli proposed a model requiring an achromatic translucent surface to modulate background reflectance ratios consistently [Met74]. D'Zmura found similar requirements for chromatic translucent layers [DRG00]. However, these models do not explain translucent-layer perception in terms of the transmittance of the layer itself. More recently, Singh found that perception of translucent layers must obey Michelson contrast and that the Metelli and D'Zmura models both converge to Michelson contrast [Sin04].

Diepstraten *et al.* describe a technique for view-dependent translucency, which aims to automatically produce translucent surfaces similar to technical illustrations [DWE02] (see Figure 3.9). The technique is somewhat limited by the use of uniform translucency. Also, as with the Diepstraten technique mentioned previously, the interior object must be relatively small compared to the exterior or

too much of the exterior will be rendered translucent to effectively perceive its shape.

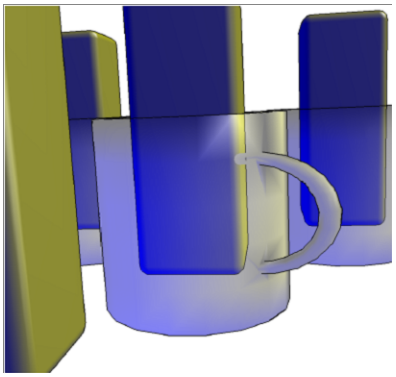

Figure 3.9: This image shows an example of view-dependent transparency for technical illustration from Diepstraten *et al.* [DWE02].

Some successful techniques render an opaque interior surface surrounded by textured, translucent exterior surfaces [IFP96, IFP97, Rhe96]. The texture patterns modulate local translucency, providing better illumination and texture cues to enhance exterior surface shape perception as compared to uniform translucency.

Rheingans re-tiled surfaces so that uniform circle or hexagon textures could be applied around vertices [Rhe96]. Because the surface geometry is uniform, very simple texture patterns produce uniform texture patterns that reveal shape effectively through texture compression (see Figure 3.10). Multiple nested layers may be represented in different colors and even different simple texture patterns. The simple textures tile the surface seamlessly and enable interactive display.

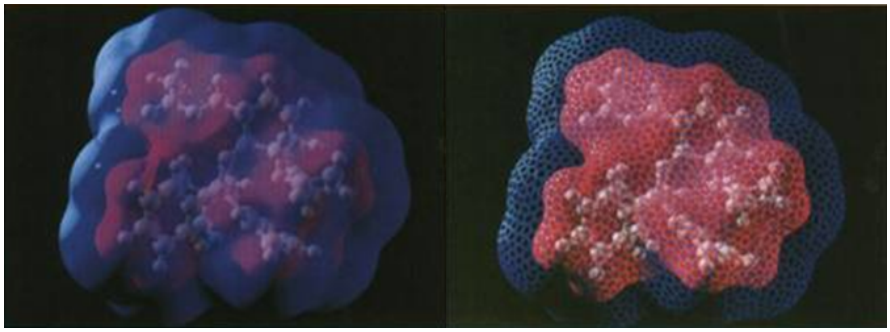

Figure 3.10: Rheingans retiled surfaces and applied simple translucency-modulating textures to convey shape of an exterior surface while enabling the interior surface to be seen as well [Rhe96].

Interrante placed first principal curvature direction strokes along outer surfaces [IFP96, IFP97,

Int97] (see Figure 3.11). Because the texture strokes follow maximum curvature they typically produce a strong texture compression effect, though the effect is susceptible to localized, view-dependent interference. These curvature strokes require non-trivial computation to apply as 2D texture on arbitrary triangle meshes but can be computed at once as a 3D texture for all isosurfaces in an image volume [Int97].

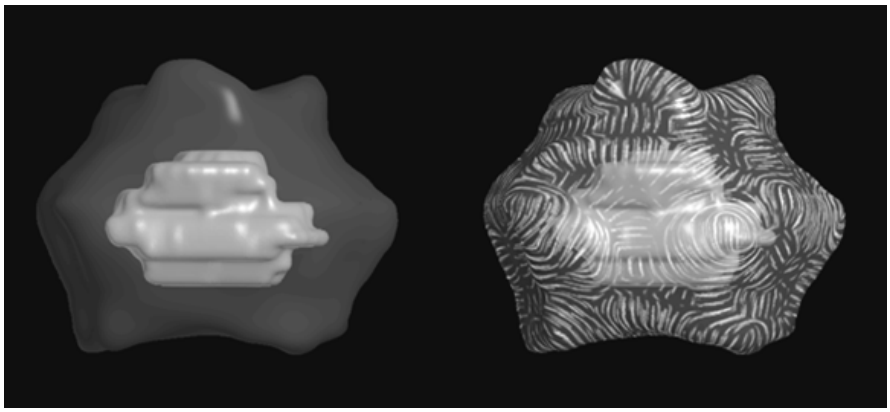

Figure 3.11: Interrante applied translucency-modulating principal curvature strokes to convey shape of an exterior surface while enabling an interior surface to be seen as well [Int97].

Recently, Bair *et al.* published a layered-surface visualization technique using textures selected from a class of visually complex but easily separable repeating patterns [HW02, BHW05] (see Figure 3.12). The class of textures was parameterized by driving a genetic agorithm by user study evaluations. The class of textures use "screen-door" transparency[3] and are very effective at displaying nested surfaces in stereo. Though only stereo displays of nested surfaces were explored in their user study, the technique appears to be very effective for stereo displays of general layered surfaces as well.

Interrante's technique is included in this study, and in fact is extended upon in the two new techniques. These extensions could have been based on other work in this category, but Interrante's technique had other properties (discussed in Chapter 4) that made it a better basis for the new techniques. The other techniques are interesting for later comparison as future work.

[3] Screen-door transparency refers to using numerous small regions alternating between fully opaque and fully transparent to achieve an effect similar to a window or door screen.

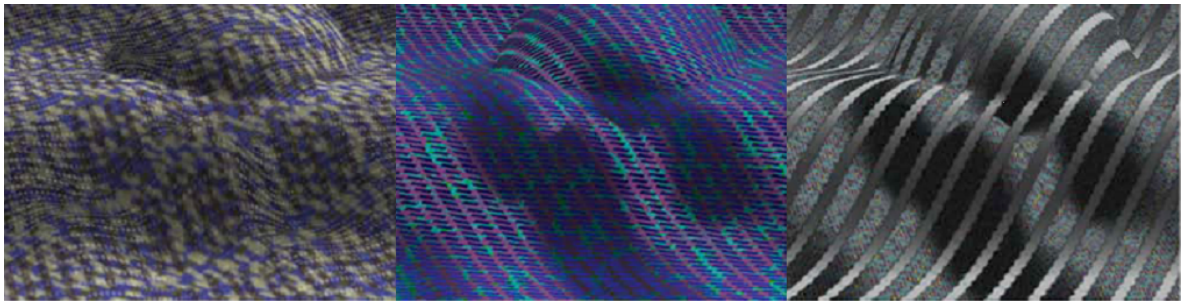

Figure 3.12: Bair *et al.* used complex but visually distinct texture to visualize layered surfaces [BHW05]. The parameters used to define the texture patterns were found by using human subjects to guide a genetic algorithm.

3.3.5 Uncertainty Techniques

Uncertainty visualization is an area of visualization research concerned with representing data along with its associated error or uncertainty. The uncertainty may be due to measurement error, loss of detail during simplification, limited precision computation, or any of a number of processing steps as the data propagates from acquisition to display. This section focuses on that part of uncertainty visualization that is concerned with positional uncertainty in surfaces without concern for the sources. Techniques suitable for layered surfaces may also be suitable for uncertain surfaces, and vice versa. The measured surface and its envelope of uncertainty can be viewed as a layered-surface problem.

Pang *et al.* categorizes many modes of uncertainty visualization with which the authors have experimented [PWL96]. The techniques largely involve modulating some property of a single surface or adorning a single surface with glyphs. The paper indicates areas yet to be explored but does not describe techniques appropriate for layered surfaces.

Wittenbrink *et al.* focus on positional error in surface geometry [WPL95]. The authors discuss sources of uncertainty (measurement, transformation, visual mapping), list several uncertainty techniques, and suggest which technique should be considered appropriate for what type of data (see Figure 3.13). The techniques are fat surfaces, perturbation surfaces, oscillation surfaces, and uncertainty glyphs. A fat surface depicts the range of uncertainty by depicting the envelope as a thick surface and using cutting planes to show cross sections. Perturbation surfaces vary the surface roughness by

applying bump mapping techniques scaled to match the uncertainty. Oscillations describe animation of a single surface through a min/max envelope. Uncertainty glyphs describe using the parameters of geometric probes placed on the surface to represent the local uncertainty.

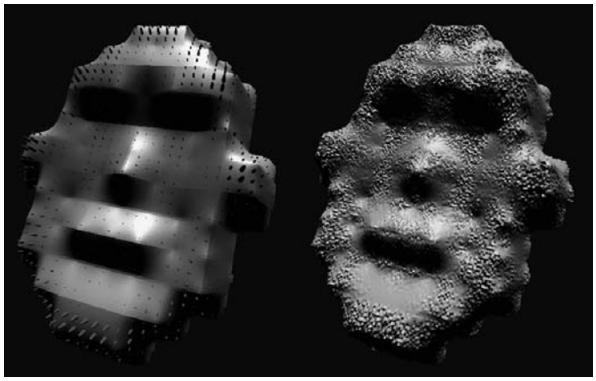

Figure 3.13: This image shows some of the visualizations from Wittenbrink *et al.* [WPL95]. The image on the left uses ellipsoid glyphs to show the uncertainty of vertex position. The image on the right uses vertex perturbation to show the same.

Lodha *et al.* are concerned with interpolation errors for sampling and reconstruction of surfaces and associated data [LSPW96]. Their work describes many techniques the authors found fault with (not from perceptual study or foundation but from anecdotal evidence). Typical techniques (already described in this text) appear: side-by-side, pseudo-color, and uniform transparency. The authors describe overlaying the surfaces as a poor solution, but they do not describe addressing occlusion. The authors also cite previous work using animation [Ger92], which they find inadequate. The authors turn to the use of glyphs. The two most relevant to the task at hand are displacement glyphs and volume-filling glyphs. Displacement glyphs attach some geometric entity (line, box, *etc.*) to one surface (see Figure 3.14). The displacement glyph's geometry encodes some information about the uncertainty (like direction and distance). The volume-filling glyphs are constructed from spheres that are bi-tangent to the two surfaces. As such, they represent some sampling of the medial axis of the space between surfaces.

Grigoryan and Rheingans display position uncertainty by randomly displacing point geometry [GR02, GR04]. The magnitude of the displacement is related to uncertainty along the local surface normal. Less certain points are also rendered less opaque. Color can be used to carry an additional scalar field, which might reinforce the positional uncertainty. Finally, the underlying polygonal model

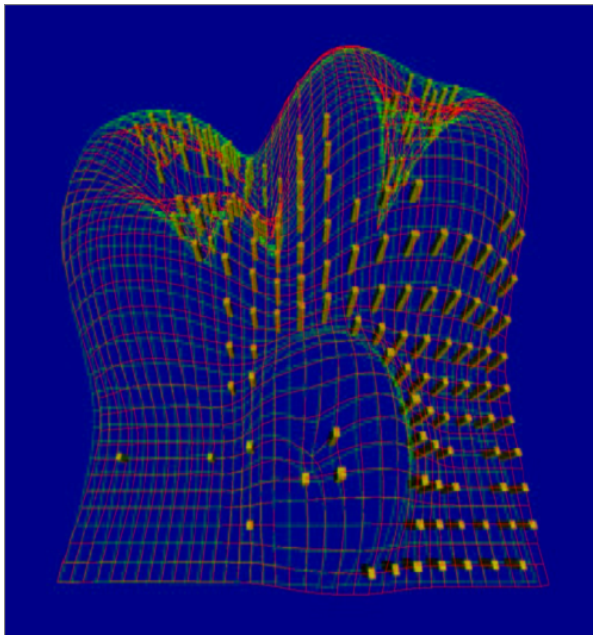

Figure 3.14: This image shows use of displacement glyphs from Lodha *et al.* [LSPW96]. The boxes encode uncertainty information about the surface vertices to which they are attached.

can be combined with the point representation (see Figure 3.15).

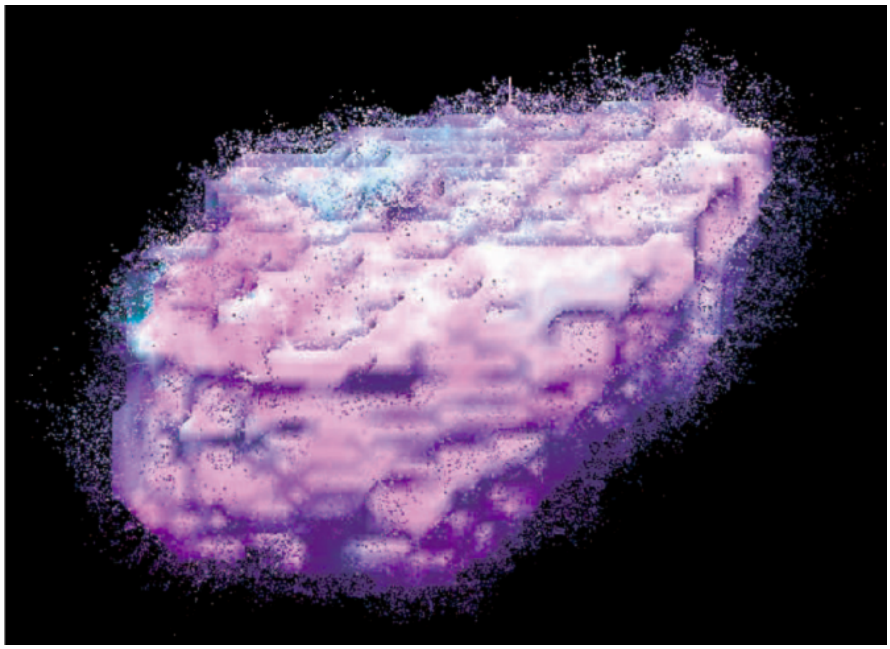

Figure 3.15: This image shows the point-based uncertainty technique of Grigoryan and Rheingans [GR04]. Points are randomly perturbed from the surface according to positional uncertainty. Color is additionally used to encode intensity of the image in the source volume.

This study includes two methods using glyphs denoting correspondence between surfaces that are similar to uncertainty glyphs or displacement glyphs. The other uncertainty techniques are interesting for later comparison as future work.

3.4 Summary

This section summarizes what perceptual cues will be used in the visualization techniques implemented in this dissertation. Also, if a cue is included only to present the best case of a visualization technique for evaluation and is not necessary for a practical implementation, it will be noted here and again where appropriate in Chapter 4. If a cue is inherently part of the technique and can not be omitted for practical implementation, that too will be noted.

All techniques utilize per pixel Phong illumination (via programmable graphics hardware). This is not required for a practical implementation, and can be replaced with standard fixed hardware illumination.

Shadows are used to enhance the perception of distance between intersecting surfaces. In particular, one technique is evaluated explicitly to show the value of shadows as a shape cue. Shadows are not optional but are the very point of that technique.

Shadows are also used to show proximity between objects in another technique. Without the artificial shadows, the objects (which are designed to "touch") do not appear to make contact. In this technique, the proximity shadows are only optional if physically accurate shadows are used instead.

Several techniques evaluated in this dissertation use translucency-modulating texture to enable both interior and exterior surfaces to be seen simultaneously. Specifically, principal curvature texture is used. Although principal curvature texture has been shown to be an effective way to depict nested surfaces, it is only one of many effective texture patterns for such display. This dissertation uses principal curvature texture because it is highly irregular for real surfaces. The irregularity makes it possible to quickly determine the correspondence between a texture element and its shadow, making it easier to judge the distance between them. However, I claim that it is still possible to make the same

distance judgements with regular texture, though I would expect it to take users longer to do so.

Some techniques utilize regular grid texture or noise texture on some surfaces. The use of such texture is not required, but is recommended because large patches of surface appear less like real objects and more like “plastic” or “hard rubber” objects when they are presented without texture using standard hardware graphics.

Chapter 4

Visualization Techniques

This chapter presents seven layered-surface visualization techniques for general layered-surfaces. Five of the techniques were evaluated by user studies (see Chapter 5). The first is a standard technique with standard application. The union/intersection refactoring of intersecting surfaces into nested components presented in section 4.1 enables new applications for the second and third techniques. The fourth and fifth are novel techniques developed for this work. The sixth and seventh techniques were not selected for full implementation or inclusion in the user studies to control the size of the studies.

The five techniques that were fully developed and evaluated are the following:

1. inter-surface distance mapped to surface color,
2. principal-curvature texture,
3. point-correspondence glyphs,
4. combining principal-curvature texture with cast shadows, and
5. combining principal-curvature texture with point-correspondence glyphs.

The two techniques that were not evaluated are the following:

6. technical illustration of the interior overlaid on a standard visualization of the exterior, and
7. systematic “carving” of the exterior surface down to the interior surface.

An initial implementation of the sixth technique was developed; the seventh technique was only proposed.

Section 4.1 describes the union/intersection refactoring technique. Section 4.2 describes the visualization techniques implemented and evaluated in this work. Section 4.3 describes the visualization techniques proposed, but not evaluated, for this work. Section 4.4 describes the implementation of the key algorithms used to produce the visualizations in this work.

4.1 Refactoring Intersecting Surfaces

This section presents the geometric refactoring that enables the use of existing and new techniques for nested-surface display on pairs of surfaces that may intersect. For a pair of nested surfaces, the exterior surface always occludes the interior surface. An algorithm for ameliorating the nested-surface occlusion problem need treat only the exterior surface. For a pair of intersecting surfaces, the surfaces swap interior/exterior roles at each intersection curve. For the tumor and molecular surface of interest to the scientists, each surface occludes the other in multiple regions, and multiple complex intersections are apparent from any viewpoint. The approach to ameliorating the intersecting-surface occlusion problem is to refactor the two intersecting surfaces into an interior, nested surface and an exterior, surrounding surface (I previously published this algorithm as [WTI05]).

Consider two closed, intersecting surfaces **A** and **B** enclosing respective, overlapping volume regions A and B. The boundary of $A \cap B$ is the desired interior surface and the boundary of $A \cup B$ is the desired exterior surface. See Figure 4.1.

To apply refactoring techniques to open surface patches as well as closed surfaces an interior/exterior classification must be made that does not rely on closed volume boundaries. This is easily accomplished by partitioning the intersecting surfaces along the intersection curves. Surface-surface intersections and the interior/exterior classification can be determined using geometric or image-based algorithms.

Geometric algorithms can accurately compute the classification for a fixed scene. Geometric al-

gorithms exist to compute triangle-triangle intersections [MÖ97, GD03], to compute spatial hierarchies that accelerate triangle-triangle testing [GLM96, vdB97, Ben75, Mea82, LGLM00] and to compute signed distance from a triangle mesh [BA05]. These algorithms together can be used to classify interior/exterior regions of intersecting surfaces. Section 4.4 describes the algorithms used in this work.

Image-based algorithms can compute the classification in an interactive environment (as long as the view-dependent depth complexity remains sufficiently low). A variety of image-based techniques exist that can perform the intersection and classification computations [Eve01, DWE02, GMTF89, NT00], and several can utilize the graphics processor for improved, interactive performance. Section 4.4.1 describes the algorithms used in this work.

Once refactored, the surface regions can be rendered with different perceptual cues labeling the different regions. The perceptual labeling should convey interior/exterior classification and source data set for each region [RR05].

Figure 4.2 shows two data sets (a pair of random heightfields and a pair of tumor surfaces from real MRI data) and their interior surfaces. These data sets will be used as examples throughout the

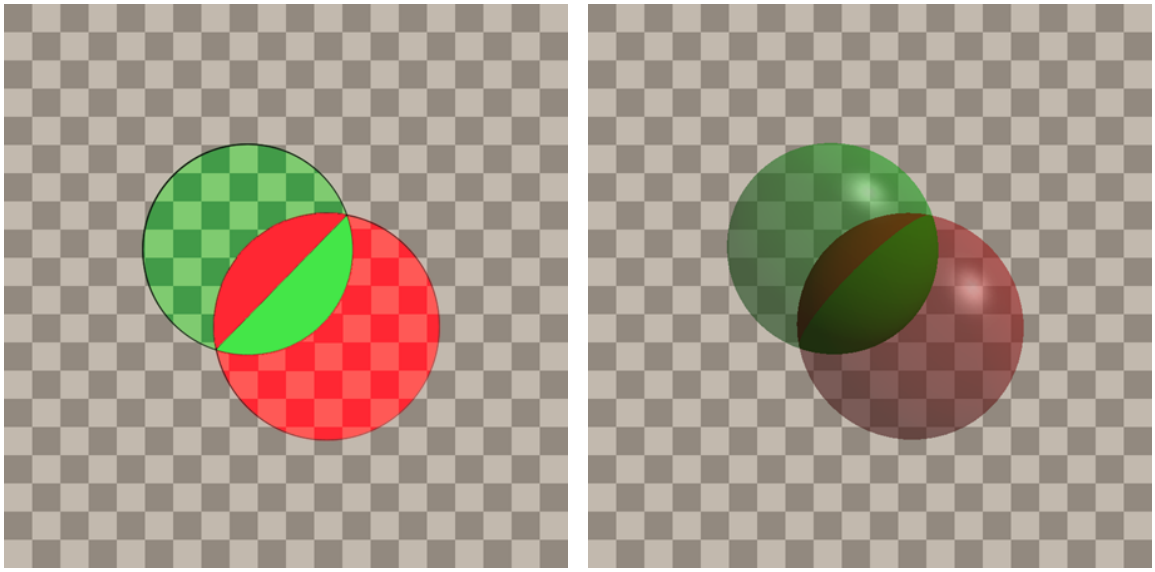

Figure 4.1: On the left, two circles intersect in 2D. The area inside the intersection ($A \cap B$) is opaque. The remaining area, the union minus the intersection ($A \cup B - A \cap B$) is translucent. A 3D version is shown on the right.

following section.

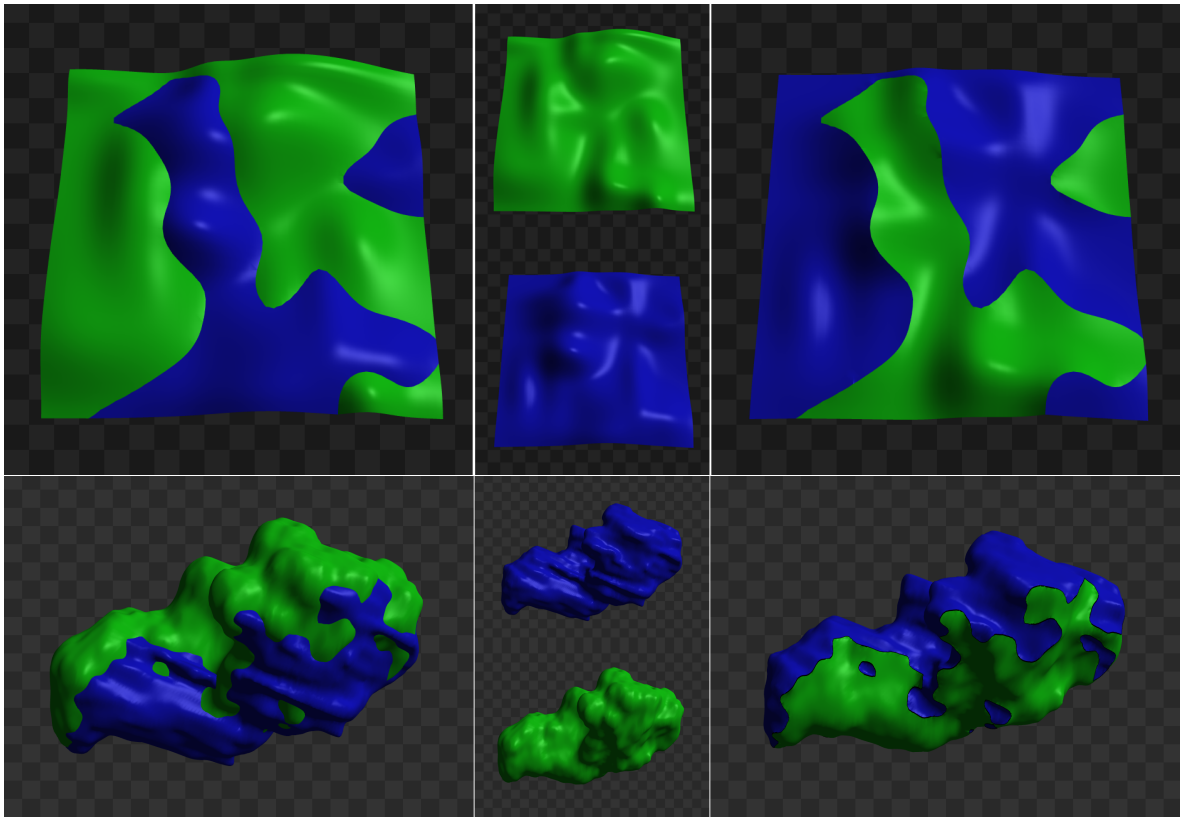

Figure 4.2: This image shows data sets and their interior and exterior surfaces as computed by the union/intersection refactoring algorithm. The top images show random surface patches. The bottom data sets are real tumors segmented from the same MRI volume; the blue tumor segmented by hand and the green tumor segmented by automatic algorithm. The left column is the exterior surface and the right column is the interior surface.

4.2 Evaluated Display Techniques

This section describes the display techniques included in the user studies discussed in Chapter 5. The descriptions are broken into three parts. The first part describes two existing techniques that are frequently used to display layered surfaces but do not completely meet the needs set out in Chapter 2. The second part describes an existing nested-surface technique adapted to general layered-surfaces by use of the refactoring algorithm. The third part describes two novel techniques that extend the technique of part two to better convey distance between layered surfaces.

4.2.1 Existing techniques

This section describes existing techniques used for comparison with the novel techniques in this study; pseudo-color mapping and line glyphs. These techniques are quite appropriate for displaying scalar information on a surface. These techniques are often used for layered-surface display because more effective techniques are relatively new and not generally available in visualization libraries. These frequently-used techniques serve as baselines for comparison.

Pseudo-color mapping

Pseudo-color mapping recolors a surface, usually at the vertices of the geometric representation, to display metric information through mapping to a color scale. In general, the metric may be any scalar field sampled on the surface. For layered surfaces the metric is typically distance between surfaces. This distance is often Euclidean shortest distance, which is asymmetric (see Figure 3.3).

Choosing the correct perceptual color scale is a critical design step when using color maps. Any color scale used to convey secondary metric information on a curved surface should be isoluminant[1] so that it does not interfere with the perception of the surface's shape [War88]. The remaining perceptual color channels for encoding metric information on a surface are the red-green and blue-yellow color channels. They may be combined to produce color scales varying in hue, saturation, or both, but care must be taken that the color scale remains isoluminant.

Because the surfaces of interest to this work intersect each other, the metric data to be encoded by color has positive, negative, and zero values (often referred to as *ratio* data). The positive and negative values should be clearly distinguishable. This rules out broad spectrum color scales such as the hot-body spectrum or those employed by Ware for metric encoding [War88].

In the first set of experiments (see Section 5.3), the color scale used was red-grey-blue. This color scale encodes sign with hue and magnitude with saturation. Red denotes a positive distance (the displayed geometry is on the exterior) and blue a negative distance (the displayed geometry is on the interior). Unsaturated grey denotes the intersection itself. See Figure 4.3 for an example. This scale

[1] An *isoluminant* color scale has a single fixed luminance throughout the scale.

is perceptible to those with red-green colorblindness (about 10% of the male population, and about 1% of the female population [War04]). It also uses a natural hot-cold encoding of the two ends of the color scale, making interpretation of the color scale easily remembered, if not intuitive.

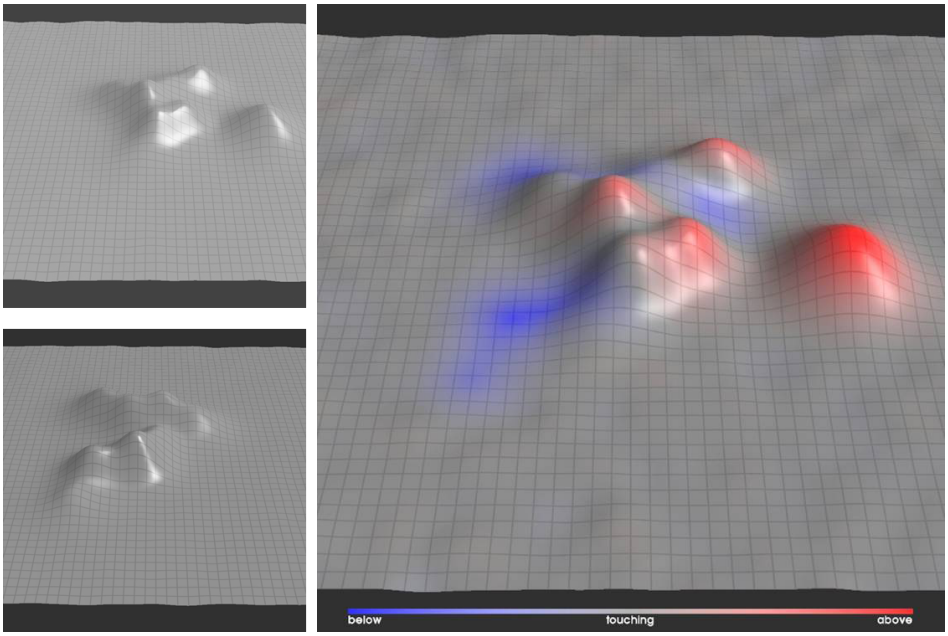

Figure 4.3: Two surfaces visualized using the red-grey-blue version of the color mapping technique. Blue indicates that the visible geometry is inside the second surface, red that the geometry is outside, and grey that the two surfaces are in contact.

In the third set of experiments (see Section 5.5), the color scale used was red-yellow-green. This color scale encodes both sign and magnitude with hue. Red denotes a positive distance (the displayed geometry is on the exterior) and green a negative distance (the displayed geometry is on the interior). Yellow denotes the intersection itself (see Figure 4.4). This scale uses only the most sensitive of the chromatic perceptual color channels (red-green).

Why the switch in color scales? When publishing the results of the first experiments (those using red-grey-blue), reviewers repeatedly commented that the red-grey-blue color scale probably underperformed relative to a red-yellow-green scale due to limited sensitivity for saturation and the sensitivity mismatch between the red and blue ends of the scale. The third set of user study experiments showed that the reviewers predictions were true for one task but not for the other (see Chapter 5, Section 5.5).

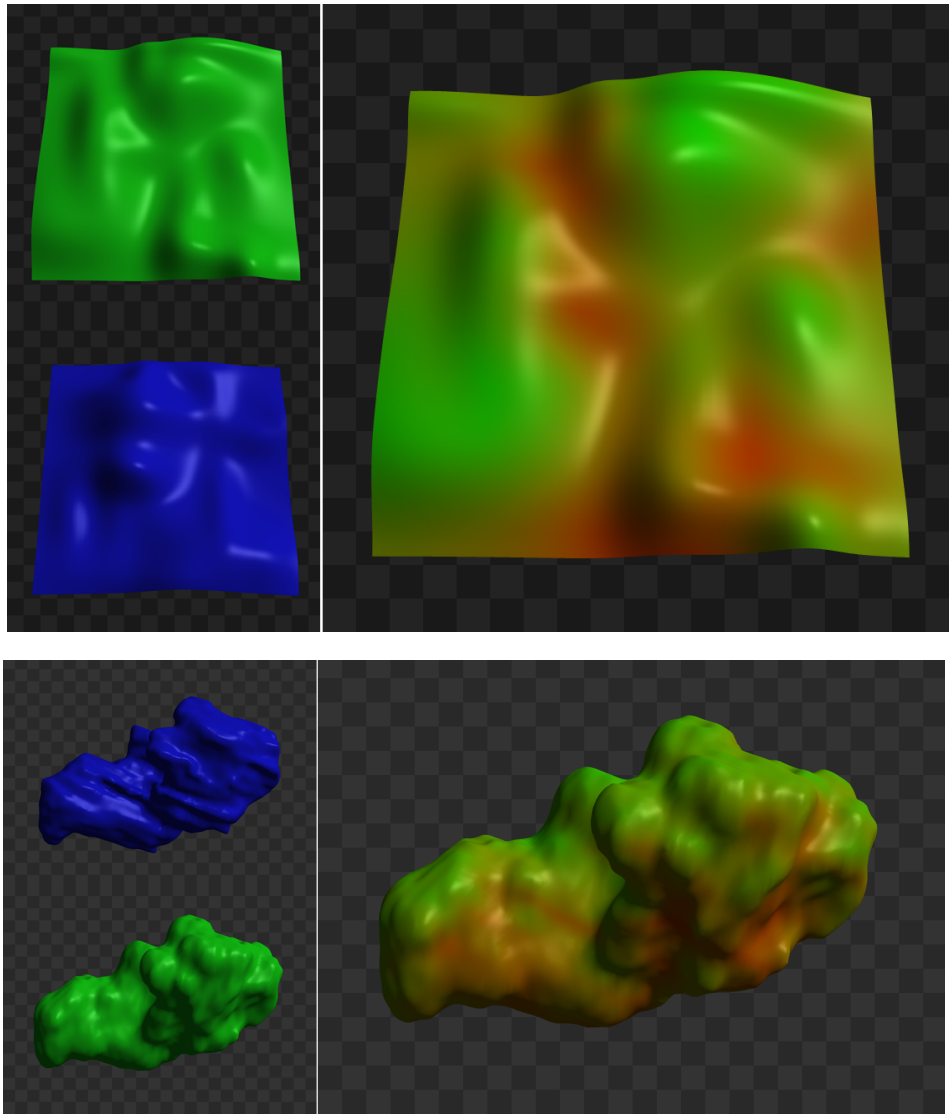

Figure 4.4: The hill and tumor data sets visualized using the red-yellow-green version of the color mapping technique. Red indicates that the visible geometry is inside the second surface, green that the geometry is outside, and yellow that the two surfaces are in contact.

Line glyphs

Line glyphs[2] are frequently used to display scalar data on a surface. In some cases, such as uncertainty magnitude in uncertainty visualization, the line glyphs may carry geometric information as well; if the "free" end of the glyphs rests on the error boundary, the glyphs effectively sample the

[2] *Line glyphs* are line segments attached at one end to the surface and extending for a distance related to the magnitude of the scalar field at the point of attachment. When used for scalar display, they typically extend in the direction of the surface normal at the point of attachment.

surface of the error.

Line glyphs may be used to show correspondence between two surfaces, and they are used to do so in this work (see Figure 4.5). Line glyphs used to show point correspondence will be referred to as point-correspondence glyphs throughout this work. To show correspondence between surfaces, the ends of each point-correspondence glyph rest on one of the two different surfaces. Although the distance between the two endpoints can be inferred, it is not necessarily computed when determining correspondence. Nor is distance necessarily directly displayed. For instance, the point-correspondence glyphs studied here do not follow the shortest paths between corresponding points, but instead follow smoothly curved paths. These curved paths are the trajectories of the corresponding points for a distortion-minimizing animation from one surface to the other.

For two arbitrary surfaces there may be no *a priori* correspondence information between the surfaces. If the surfaces are the result of a statistical model, there may exist a closed-form solution to a point-correspondence map between surfaces. If the two surfaces are described only by their geometry, the correspondence must be approximated. The desired property for a correspondence mapping between two surfaces is that the mapping be a bijection (both one-to-one and onto). One common method for computing a bijective map between surfaces is to solve Laplace's equation using the two surfaces as boundaries. Following an integral path of the gradient of the heat diffusion from one surface to another then yields the geometry of the point-correspondence glyph between those two points. Computing correspondence between arbitrary surfaces is discussed in more detail in Section 4.4.3.

Point-correspondence glyphs appear in two techniques in this work. The first of these is described here. This technique displays the interior of a pair of layered surfaces, as computed by the refactoring algorithm. The interior pieces are colored to show to which of the potentially intersecting layered surfaces each piece originally belonged. Point-correspondence glyphs are computed between the interior and exterior surfaces. The correspondence-glyph endpoints on the exterior surface are spread over the surface such that the geodesic distance between endpoints follows a Poisson law distribution. Where the point-correspondence glyphs terminate on the interior surface, an additional proximity glyph is placed. The proximity glyph approximates shadowing on the interior surface by the point-correspondence glyph due to global illumination. This enhances the perception that the interior surface

and point-correspondence glyphs do indeed contact [TSS+98]. See Figure 4.5.

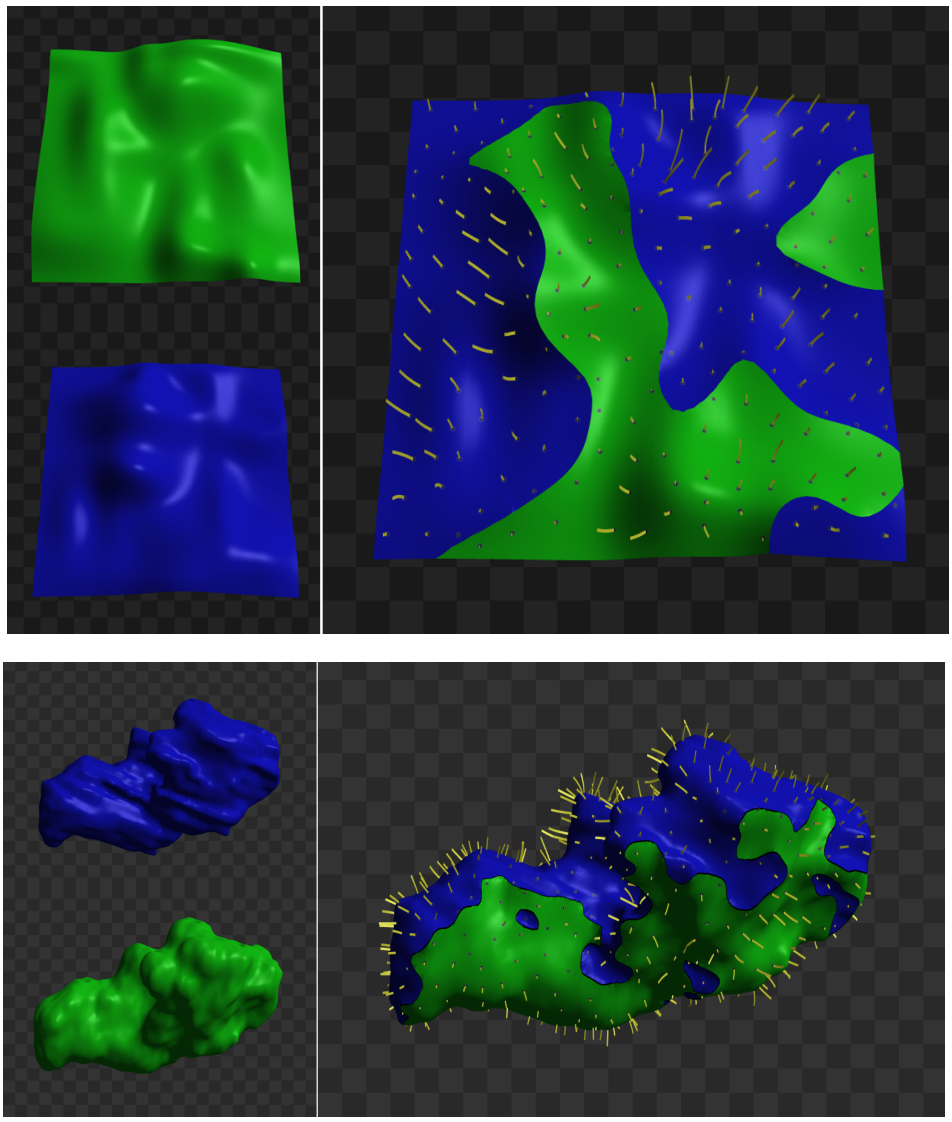

Figure 4.5: The hill and tumor data sets visualized using the point-correspondence technique. The correspondence glyphs connect points on the (hidden) exterior surface to their corresponding points on the (visible) interior surface.

4.2.2 Adapting a Nested-Surface Technique

This section describes an adaptation of an existing nested-surface technique to the visualization of general layered surfaces. The nested-surface technique is based on Interrante's principal-curvature driven strokes [IFP96, IFP97]. Interrante's textures paint a translucent exterior surface with strokes

that follow integral curves in the direction of first principal curvature where they are well defined[3]. The length of the strokes varies, with shorter strokes in regions of low curvature (where undulations due to noise would be more perceptible).

Principal curvature texture

For this work, the potentially intersecting surfaces are refactored into interior and exterior parts. Color is used to label to which original surface the interior and exterior parts belong. The exterior parts are also textured with a principal-curvature texture composed of discrete glyphs. The glyphs are cross shaped, such that the long axis follows the direction of first principal curvature and the short axis follows the direction of second principal curvature. The glyphs sample the estimated curvature only at their center; they do not attempt to follow the changes in curvature direction as they extend out from their center. See Figure 4.6.

The glyph centers are laid out in a Poisson-like distribution, covering the surface relatively sparsely such that the interior is easily visible. As the user studies described in Chapter 5 will show, the exterior surface shape is still readily perceived. This work does not attempt to find the ideal balance of density for understanding both interior and exterior surface shape. The glyphs applied in the user study experiments in Chapter 5 represent approximately 16 units of surface area each.

4.2.3 Novel Techniques

This section describes the two novel techniques developed for this work. The two techniques combine principal-curvature texture with additional cues to the inter-surface distance; cast shadows and point-correspondence glyphs.

[3]The principal curvature directions for a point on a surface are the directions of minimum and maximum curvature. These directions are not always well defined. Both planar and spherical regions on the surface have the same curvature in all directions, thus these regions have no unique principal curvature directions. A technique using principal curvature directions to texture the surface may use an arbitrary choice of direction in such cases or attempt to avoid texturing these locations entirely.

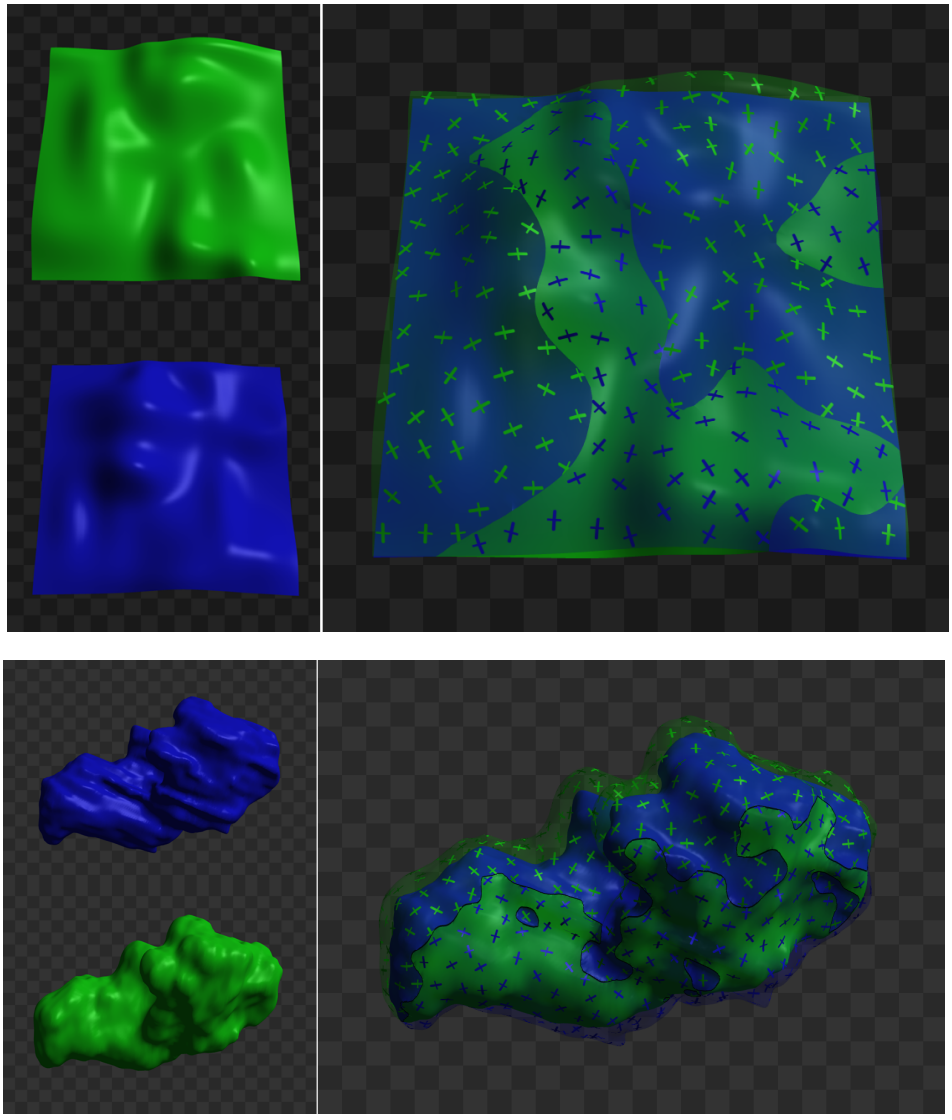

Figure 4.6: The hill and tumor data sets visualized using principal curvature texture. The exterior surface is textured with cross glyphs locally aligned with the directions of principal curvature.

Principal-curvature texture with cast shadows

By casting shadows of the exterior surface curvature glyphs onto the interior surface, this technique conveys additional cues to the distance between the interior and exterior surfaces. The distance between the image of the glyph and the image of its shadow reveals information about the distance between these regions of surface. See Figure 4.7.

It is important to note that the use of principal curvature texture, as opposed to a repeating regular

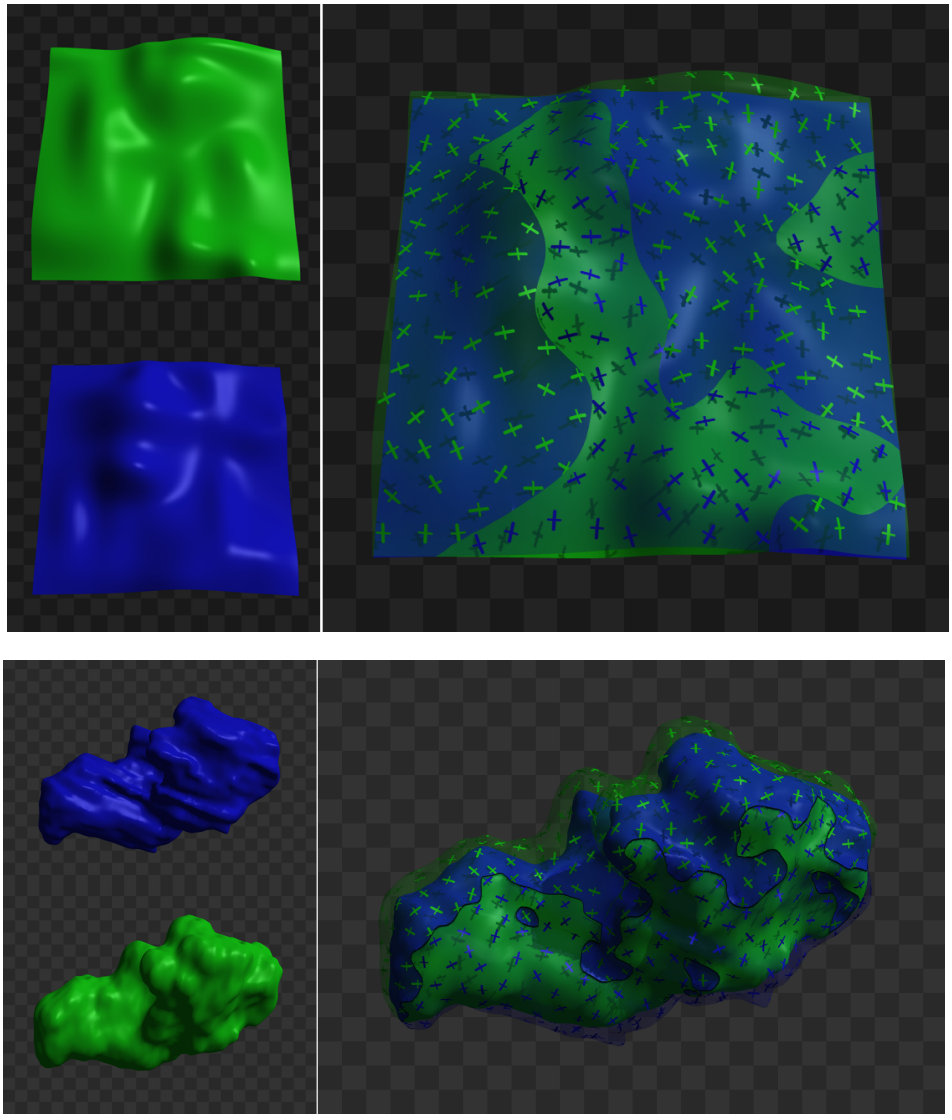

Figure 4.7: The hill and tumor data sets visualized using principal curvature texture with cast shadows. The exterior surface is textured with cross glyphs locally aligned with the directions of principal curvature. The glyphs cast shadows onto the interior surface.

pattern such as a grid, is not a requirement for conveying the shape of two surfaces. Principal curvature texture does provide an irregular texture enabling users to quickly match glyphs to their corresponding cast shadows, thereby getting an estimate on surface shape and inter-surface distance. However, the same could be accomplished with other irregular texture patterns. Regular texture patterns also allow the same perception, though they may require a search for easy correspondences before arbitrary sections of the pattern and shadow can be visually matched.

Principal-curvature texture with point-correspondence glyphs

Casting shadows from one surface to another does give an additional cue to the distance between surfaces, but it has limited application. If texture patterns on the outer surface cast the shadows, as they do for the principal-texture technique employed herein, then the pattern must not be everywhere regular or it may be too difficult to discern which shadows are cast from which parts of the texture. Similar difficulties arise in using cast-shadow information when the surfaces are significantly distant from each other. For closed surfaces, regions of the textured outer surface cannot cast shadows onto the interior without multiple light sources (as might be used in non-photorealistic, technical illustrations [LHV04, LHV05]) or warping the shadow geometry.

Geometric glyphs[4] can be used to show the distance between two surfaces and can do so without the limitations of cast shadows. In this work, line glyphs show point correspondence between the two surfaces. Additionally, these point-correspondence glyphs show an upper bound on the local distance between the two surfaces. It is an upper bound on distance because the correspondence glyphs follow energy-minimizing paths rather than following the shortest paths between corresponding points. Section 4.4.3 discusses the computation of the correspondence glyphs in more detail.

The visualization technique combining principal-curvature texture and point-correspondence glyphs does so in a straightforward manner. The point correspondences are computed between exterior and interior surfaces, using the center of each principal-curvature glyphs as the end point on the exterior. As in the previous technique to use point-correspondence glyphs, the point of contact between interior surface and glyph is marked with a proximity glyph. The point of contact between the exterior surface and point-correspondence glyphs is usually hidden, so no proximity glyph is attached. See Figure 4.8.

Early implementations of this technique did not use principal-curvature texture. This technique was conceived to look similar to the "plasma lamp" novelty toy, where arcing electricity excites gases trapped between two glass globes. The ends of each glowing arc in the plasma lamp spread out slightly at the points of contact with each globe. This technique initially used a simple disc texture on the exterior surface as the arc terminator. The arc terminators were expected to provide a local surface

[4] *Geometric glyphs* are geometric probes typically attached to surface geometry to visualize associated data. The visual properties of the glyph (color, texture, orientation, height, width, twist, etc.) are related to the data.

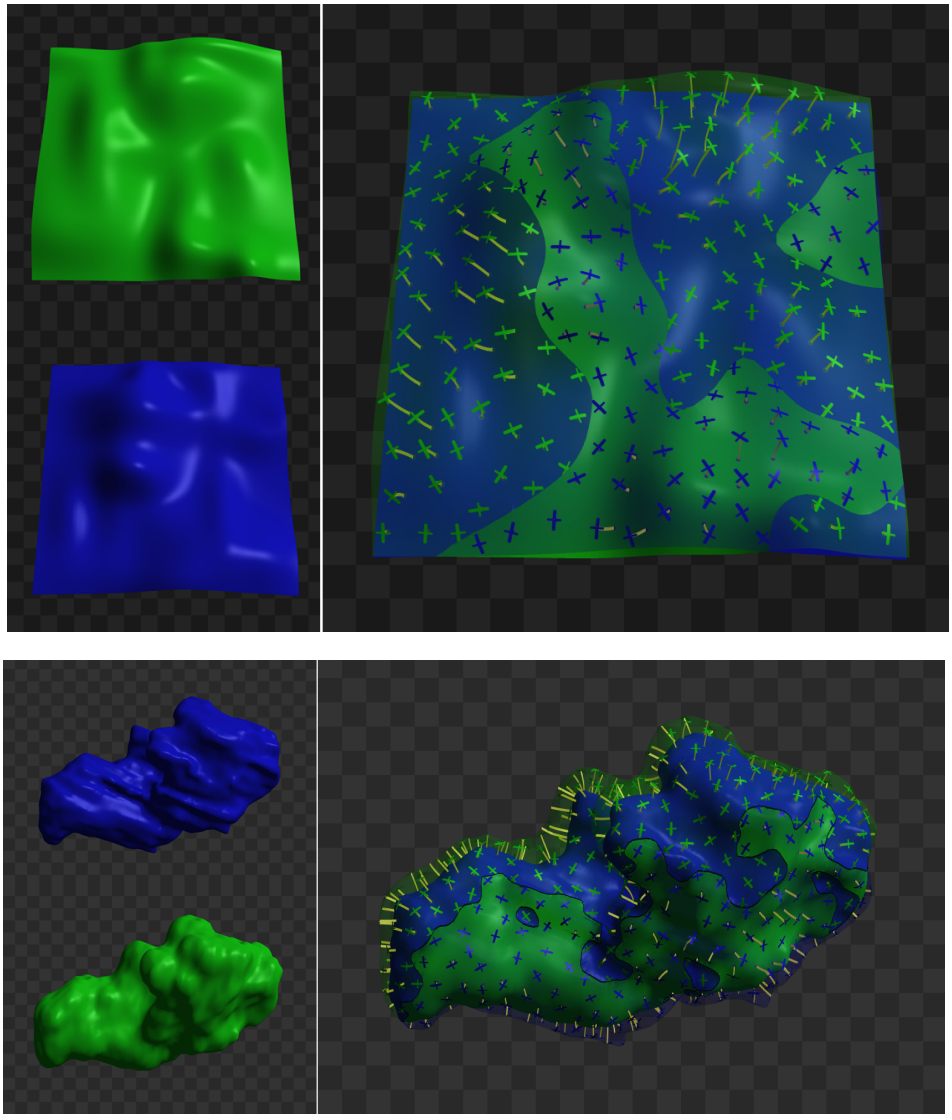

Figure 4.8: The hill and tumor data sets visualized using the principal curvature texture with point-correspondence glyphs. The exterior surface is textured with cross glyphs locally aligned with the directions of principal curvature. The glyphs cast shadows onto the interior surface.

patch whose eccentricity and illumination would reveal the local surface orientation. Surprisingly, the cross glyphs seemed to provide much better shape cues when the two implementations were compared side by side (see Figure 4.9), so they were chosen for the user study. The discs were on the same scale as the crosses are in the final implementation, and also obscured the point-correspondence glyphs. The scale and density of the cross glyphs was believed to be near enough to an optimal balance that it was decided to use the crosses instead of finding parameters that better matched the discs.

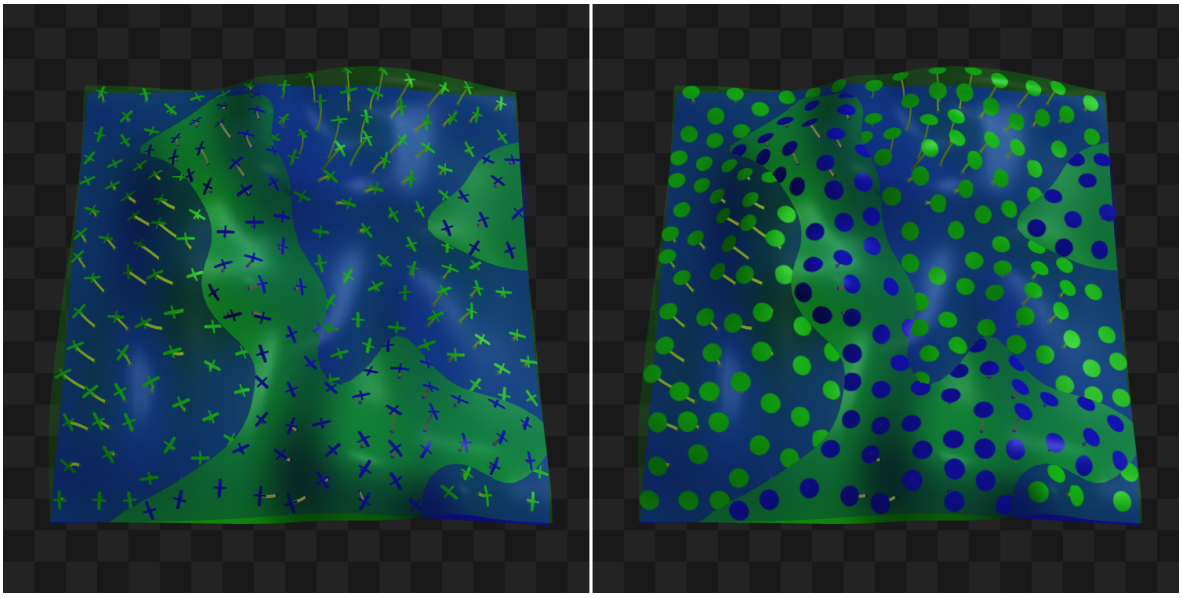

Figure 4.9: The hills data set visualized using texture with point-correspondence glyphs. On the left, the texture is the cross glyph showing local principal curvature direction. On the right, the texture is a simple disc.

4.3 Proposed Display Techniques

This section briefly describes two techniques originally proposed for this work. User study size was the primary reason these techniques were not developed for evaluation.

4.3.1 Interior overlaid on exterior

In this proposed technique a technical illustration of the interior surface is generated but not displayed. The illustration makes use of principal-curvature hatching [PHWF01], silhouette rendering [RC99], and depth-cueing [NM00, WE02]. The density of the silhouettes and hatching would be used to indicate depth, with further features appearing thinner and sparser. This image of the interior is then overlaid onto a standard, opaque surface visualization of the exterior. The overlay might be accomplished by projective texturing [SKvW$^+$92]. Figure 4.10 is an early implementation of this technique before it was decided not to include it in the evaluations.

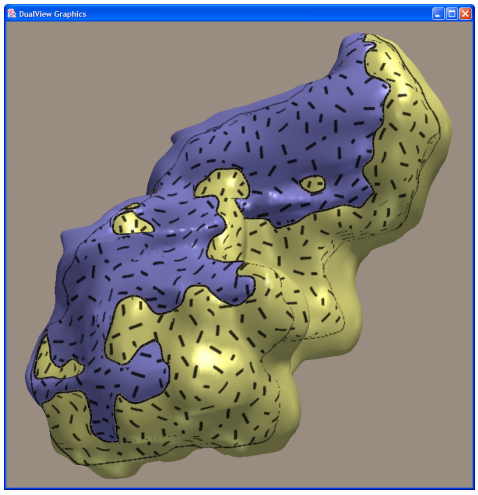

Figure 4.10: This is an example of overlaying a technical illustration of the interior onto a standard exterior visualization.

4.3.2 Surface carving

In this proposed technique the exterior surface is cut away to expose the interior surface. The cuts might follow valley lines in a manner used by some sculptors to depict translucent materials (Figure 4.11). New geometry would be computed to connect the remaining exterior to the interior surface, giving the visualization the appearance of a carved solid. The visualization might benefit from some form of global illumination, perhaps shadowing or accessibility shading [Mil94]. Without the new geometry, this proposed technique is similar in some respects to work by Bauer-Kirpes *et al.* that displays only ribbon-like regions of the exterior surface (called "barrel-loops") to expose the interior [BKSBL87].

Figure 4.11: In "The Veiled Maiden" (A. Filli), the sculptor carved away valleys in the veil to expose the surface of the maiden's face beneath, creating the illusion of a translucent veil.

4.4 Implementation Details

This section describes the implementation of the key algorithms used to produce the visualizations evaluated in this work. These algorithms include intersecting-surface refactoring, signed-distance computation, principal curvature computation, texture coordinate computation, point-correspondence computation, and shadows.

4.4.1 Refactoring algorithms

In the following two sections, two algorithms for refactoring intersecting surfaces, one image-based and one geometric, will be outlined.

The purpose of refactoring intersecting surfaces is to be able to treat them as nested surfaces for visualization. Because effective techniques for nested surface display already exist, refactoring intersecting surfaces immediately enables those techniques to be applied to intersecting surfaces. Further, new visualization techniques developed with intersecting surfaces in mind but relying on refactoring also apply to visualizing nested surfaces.

Both the image-based and geometric algorithms determine the classification (interior or exterior) of parts of the surfaces. The image-based algorithm manipulates the surfaces as image elements, while the geometric algorithm manipulates the surfaces as polygons.

Image-based algorithm

An image-based algorithm for refactoring intersecting surfaces was implemented for the first set of user studies. It is described in Chapter 5. The algorithm relies heavily on *depth peeling* [DWE02], a view-dependent, image-based technique for separating the geometry of a scene into layers of depth according to the depth complexity of the scene. The *depth complexity* of a scene is the maximum number of graphics primitives rendered in a given pixel over all views. The *view-dependent depth complexity* of a scene is the maximum number of graphics primitives rendered in a given pixel for the

current view. Each layer of depth produced by the depth peeling algorithm is stored in a depth image[5]. Each new pass of the depth peeling algorithm can then access previous depth values by texture lookup into the stored depth images.

Depth peeling rejects fragments[6] according to standard depth-buffer hidden-surface removal and a second depth test that rejects fragments included in previous depth images. The second test is performed by comparing the current fragment's depth to its counterpart in the previous (nearer) depth image. If the current fragment has a greater depth, it passes the test and can be considered for inclusion in the current depth image.

Complete depth peeling requires rendering a scene of depth complexity n in up to n passes, each pass creating a depth image. The exact number of passes depends on the view-dependent depth complexity. In practice, graphics techniques utilizing depth peeling do not compute all depth images. One common termination criteria is to use an occlusion test to determine when the number of graphics fragments not yet in a depth image is below some threshold. Another common termination criteria is simply to limit the number of passes actually computed.

Computing each depth image required for the full depth peeling requires rendering of the entire scene. Therefore, the total cost of image-based refactoring is dependent on the depth complexity of the scene and on the number of geometric primitives used to represent the surfaces in the scene. The total cost greatly limits the situations where image-based refactoring can be used to produce interactive visualizations (dynamically controlled by the user while producing at least 15 images per second).

The image-based refactoring algorithm proceeds as Algorithm 1. The complete 3D scene is processed in multiple passes in this algorithm. Each pass relies on standard graphics rendering operations to convert the geometric representations (triangles) into fragments (containing image coordinates, depth, RGB color used as an object identification, and a fourth color channel used as a interior/exterior label). These fragments are then operated on to perform a secondary depth test, comparing against the result of the previous pass. The secondary depth test only passes if the fragment depth is greater

[5] A *depth image* is an image containing only depth values instead of color intensity

[6] A *fragment* is the most basic graphics rendering primitive. For this discussion, a fragment has properties of at least image coordinates, color and depth and may be viewed as a candidate pixel that will be written to the final image if it passes a series of tests comparing its properties to other fragments that are also candidates for the same pixel in the final image.

than that recorded for the previous pass at the same image coordinate. If the fragment passes the secondary depth test then its interior/exterior labeling is determined by object parity. The algorithm assumes objects do not self intersect. The first fragment found for any image coordinate is labeled an exterior fragment. Any fragment appearing deeper than another fragment from the same object is also labeled an exterior fragment. Any fragment appearing deeper than a fragment from a different object is labeled an interior fragment. Any fragment appearing deeper than a fragment already labeled interior is also labeled interior (it will not be visible when the depth layers are composited). Once a fragment is labeled, the standard graphics pipeline continues and applies the standard depth test, possibly rejecting the fragment. Once all fragments have been operated on, a depth image has been constructed that contains a single peel or layer of the scene. The depth values in this new image are all greater or equal to those in all previous depth image. This image can now be used as an input to the next pass over the complete scene. Once all depth images are created, they can be processed in order from last to first, compositing the layers such that, at each image coordinate, translucent exterior pixels are blended with opaque interior pixels.

Geometric algorithm

A geometric algorithm for refactoring intersecting surfaces was implemented for the second set of user studies (described in Chapter 5). The algorithm relies on triangle-triangle intersection and signed-distance field computations.

The triangle-triangle intersection computation first determines if two triangles intersect. The computation begins by testing the points of one triangle against the plane equation of a second triangle. If the two triangles do intersect, the point or line-segment of intersection are computed. Computing the intersection between two triangle models then proceeds by computing all possible triangle intersections between the two models. For models of n and m triangles, this requires $O(mn)$ intersection tests. This work uses the algorithm of Guigue and Devillers [GD03]. Although this test is capable of detecting coplanar triangles (with allowances for floating-point roundoff), it does not return the region of overlap. Coplanar triangles do not occur in the user study data or in the representative data sets given to me by the scientists, so I did not address this shortcoming.

Algorithm 1 Image-Based Refactoring

{a fragment p has fields of $imagecoordinate$, $depth$, $color$, and $label$}
{p_i is a fragment potentially to be written into the current pixel of the current depth layer}
{p_{i-1} is the corresponding pixel in the previous depth layer. p_i and p_{i-1} have the same $imagecoordinate$.}

Require: $p_i.color \neq 0$
  repeat
    for all fragments p generated by rendering the complete scene **do**
      if $p_i.depth < p_{i-1}.depth$ **then**
        discard this fragment
      end if
      if $p_{i-1}.color = 0$ **then**
        $out.color \leftarrow p_i.color$
        $out.label \leftarrow exterior$
      else if $p_{i-1}.color = p_i.color$ **then**
        $out.color \leftarrow 0$
        $out.label \leftarrow 0$
      else
        $out.color \leftarrow p_i.color$
        $out.label \leftarrow interior$
      end if
      if $out.depth$ passes normal depth test **then**
        write out to current depth layer
      end if
    end for
  until count of $fragments$ failing normal depth test < 500

Spatial hierarchies are commonly used to accelerate geometric computations, especially proximity and intersection testing [Ben75, Mea82, GLM96, vdB97, LGLM00]. Instead of performing the desired test over all pairs of primitives, nodes in the hierarchy can be tested for overlap. If two nodes do not overlap, a significant number of tests between primitives may be avoided. If overlapping nodes are not leaf nodes, it may still be possible to cull many tests depending on the results of overlap tests between child nodes.

Spatial hierarchies construct a tree structure of boundary nodes. Nodes contain links to the model primitives (for instance, triangles) that fall within the bounded region. If the node contains more than some threshold of primitives the node will also contain links to child nodes bounding a smaller region of space, typically with fewer primitives. Spatial hierarchies generally differ in the type of boundary geometry, making trade-offs between wasted space in the boundary hierarchy and the cost of the overlap test.

This work uses the vtkOBBTree class from the Visualization ToolKit library (VTK) [SML98], which provides a hierarchy of oriented boundary boxes (OBB) [GLM96]. OBBs compute boundary geometry from eigenanalysis of the bounded primitives, splitting nodes in such that each child node bounds roughly half the number of primitives as the parent node.

Once the intersection geometry is found, the intersecting triangles are retriangulated with respect to the intersection. This is accomplished by constrained Delaunay triangulation using the vtkDelaunay2D class form the VTK library. The signed distances of each vertex of one surface to the other surface are then computed. The magnitude and sign of the distances at the vertices are used to label which triangles are on the interior surface and which are on the exterior surface. The algorithms for computing signed distance are described in Section 4.4.2.

The geometric refactoring algorithm proceeds as Algorithm 2.

Two input surfaces, A and B, are represented by triangle meshes. An OBB tree is computed for each input surface. The two OBB trees are then used to accelerate the computation of I, the intersection of surfaces A and B. Each input surface is retriangulated such that their triangle meshes contain the geometry of the intersection I. In my implementation, this is accomplished by constrained

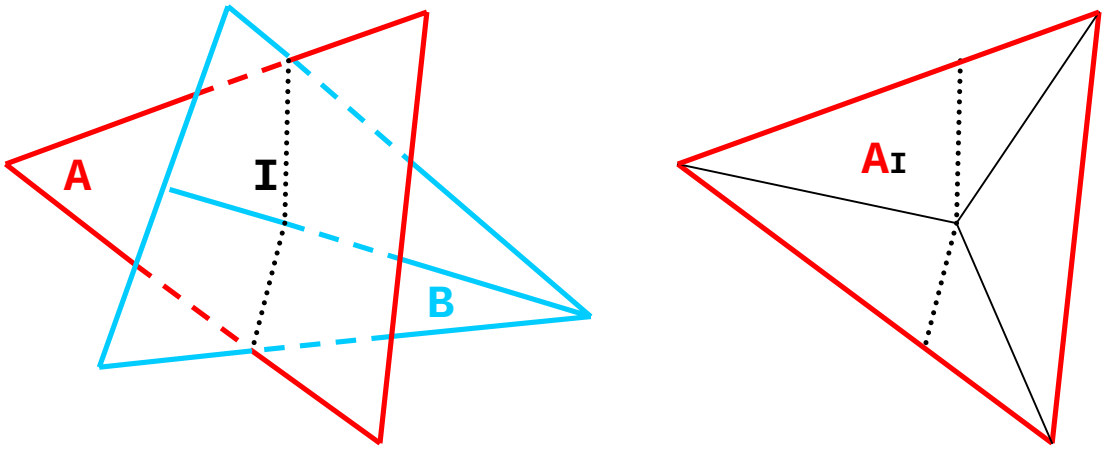

Figure 4.12: This figure shows the process of retriangulating a single intersected triangle. The triangle of A intersects the two triangles of B. The intersection curve I is composed of two line segments. The intersected triangle from A can be retriangulated with the constraint the line segments of I must be edges in the new triangulation. One possible such retriangulation is shown as A_I – it is a constrained Delaunay triangulation of the geometry of A and I.

Delaunay triangulation of each intersected triangle with the associated geometry of I, as illustrated in Figure 4.12. The signed distances between the new meshes A_I and B_I are computed, and the signs are used to classify mesh geometry as interior (negative signed distance) or exterior (positive signed distance). Once classified, it is a simple matter to produce a mesh containing only the interior or exterior geometry.

Algorithm 2 Geometric Refactoring

{given surfaces A and B}
{construct OBB trees to accelerate intersection tests}
$I \leftarrow$ line segments from intersecting A with B
$A_I \leftarrow A$ retriangulated with respect to I
$B_I \leftarrow B$ retriangulated with respect to I
$\{dist(X,Y)$ labels the each vertex in X with its signed distances to the geometry of $Y\}$
$\{interior(X)$ returns all triangles in X with vertex distances $<= 0\}$
$\{exterior(X)$ returns all triangles in X with vertex distances $>= 0\}$
$AB_{int} \leftarrow interior(A_I, dist(A_I, B_I)) + interior(B_I, dist(B_I, A_I))$
$AB_{ext} \leftarrow exterior(A_I, dist(A_I, B_I)) + exterior(B_I, dist(B_I, A_I))$
return AB_{int} and AB_{ext}

Image-based versus geometric

The image-based and geometric algorithms best address different needs in a refactoring algorithm. These needs may be accuracy, interactivity, or ease of further computation.

The image-based algorithm is better for situations where user control is more important than intersection accuracy. The accuracy of the image-based algorithm is limited by the resolution of the images used in the computation. User control may be more important in situations where a user needs to position or orient one or more of the intersecting surfaces. However, the image-based algorithm is a poor choice for visualization techniques that compute new geometry based on the refactored surfaces (such as point-correspondence glyphs between the interior and exterior surfaces). Further, because the image-based algorithm performance is dependent on scene depth complexity, it may not be able to deliver interactive visualizations even when the scene is not dynamically changing.

The geometric algorithm is better for situations where accuracy is more important than the ability to interactively reposition the surface geometry. The geometric algorithm implemented in this dissertation is not fast enough to use interactively. Instead it is best used to pre-compute the refactoring of surfaces given fixed positions and orientations. Because the refactoring is computed geometrically, it is available as input to further computation. With refactoring precomputed, visualization and exploration may proceed at interactive rates.

The image-based algorithm was implemented first because it appeared to be faster to implement, enabling the shadow-casting technique to be developed and evaluated quickly. The image-based algorithm was used for the first two sets of experiments.

The implementation of point-correspondence requires the geometry of the refactored surfaces, so the geometric algorithm was implemented as well. All images for the third set of experiments were generated using the geometric algorithm.

4.4.2 Computing signed distance

The geometric refactoring algorithm used in this work relies on computing the signed distance from an arbitrary point in space to the closest point on a surface. For many surface representations (implicit surfaces, medial representations, and others) signed-distance computation is a relatively simple task. For triangle meshes it is more difficult.

Computing distance fields from triangle meshes has received a great deal of attention [Set96, BS97, GPRJ00, Gib98, KS98b, BA05] as many important computational algorithms depend on fast, accurate distance computations. Not all of these algorithms are appropriate for computing the distances between the vertices of one mesh and the vertices of a second mesh, or even between a single point and a mesh. Most distance field algorithms are designed to compute a regular (or perhaps adaptive) volume of distance samples around a triangle mesh. Their speed and accuracy comes from adopting a form of fast-marching method [Set96, BS97, KS98b] to propagate the distance field from the initial mesh to the encompassing volume.

For a single triangle, the triangle normal can be used to determine whether a given point is on one side or the other of the triangle. For a give point p in space, and an arbitrary point r on the triangle, the side (or equivalently the sign of the distance) of the point p with respect to the triangle can be determined from the dot product of the triangle normal and the vector $r - p$. However, this does not extend immediately to the triangle mesh because the triangle mesh is not C^1 continuous. The triangle mesh itself does not define surface normals at its edges or vertices.

In computer graphics it is typical to compute additional surface normals at vertices but not at the edges. Though the common algorithms used to compute vertex normals from triangle-face normals can be extended to compute edge normals as well, they do not produce correct signs for computing signed distance. Instead, the angle-weighted pseudonormal should be used to compute edge and vertex normals from triangle normals [BA05].

The angle-weighted pseudonormal generalizes the idea of a surface normal over the triangle mesh. For the triangle face, the angle-weighted pseudonormal is exactly the face normal. For the edge between two triangles, the angle-weighted pseudonormal is the average of the incident face normals.

For the vertex, the angle-weighted pseudonormal is $\frac{\sum_i \alpha_i \vec{n_i}}{||\sum_i \alpha_i \vec{n_i}||}$, where $\vec{n_i}$ are the normals of the incident faces and α_i are the angles at the vertex for each face.

Combined with a hierarchical structure to efficiently locate the closest triangle faces to a given point, the angle-weighted pseudonormal yields a method for fast and accurate computation of the signed distance from a triangle mesh to a point. The Visualization Tool-Kit library (VTK) provides an appropriate hierarchy in the vtkKDTree class, and a class to locate the point of closest approach between a point and a triangle in the vtkTriangle class [SML98]. The angle-weighted pseudonormal algorithm was implemented for this work.

The full algorithm for computing signed distance is given as Algorithm 3. Two surfaces meshes, A and B, are input. A hierarchical search structure is constructed from input B (in my implementation, a kD-tree is used) and used for all proximity queries. For each vertex v in A, a proximity query returns the closest point p on the mesh B. The unsigned distance between v and p is trivially computed. The sign is then computed from the dot product of the direction vector $d = p - v$ and the pseudonormal at p. If the point p lies inside a single face of B then the pseudonormal is the face normal. If the point p lies on an edge of B then the pseudonormal is the average of the adjacent face normals. If the point p is a vertex of B then the pseudonormal is the angle-weighted pseudonormal at that vertex (which weights and normalizes the contribution of each adjacent face normal by the interior angle of that face at the vertex p).

4.4.3 Computing point-correspondence glyphs

In computer graphics, point correspondence is often computed in terms of surface morphing, smoothly animating from one surface to another [DYT05, TO02b, SAPH04, DM06, BW01, COSL98, GSL$^+$98, KSK00]. Surface morphing computes the geometry for surfaces at a time t, where $t = C_0$ returns the geometry of one surface and $t = C_1$ returns the geometry of the second surface. The point-correspondence properties of many surface-morphing techniques have been used previously to transfer or animate texture coordinates from one surface to another [DYT05, GSL$^+$98].

Algorithm 3 Computing Signed Distance

```
{given surfaces A and B}
build a hierarchical data structure for surface B to accelerate proximity queries
for all vertices v ∈ B do
  p ← the closest point on surface B to point v
  dist ← ||p − v||
  if p is interior to a triangle of B then
    sign ← sign of dist using the face normal at p
  else if p is on an edge of B then
    collect the triangles adjacent to the edge
    sign ← sign of dist using the angle-weighted pseudonormal of the edge
  else
    {p is a vertex of B}
    collect the triangles adjacent to the vertex
    sign ← sign of dist using the angle-weighted pseudonormal at p
  end if
end for
return sign and dist
```

Laplace's equation

To compute point correspondence between two surfaces, it is necessary to compute a bijective map[7] between the two surfaces. It is also desirable that this mapping be a smooth function over the domain so that the path from any given point to its corresponding point is also smooth.

One common technique for surface morphing is to find an approximate solution to the scalar form of Laplace's equation $\nabla^2\psi = 0$ (a linear elliptic partial differential equation) given Dirichlet boundary conditions. The two surfaces define the boundary of the computational domain, with $\psi = C_0$ over one surface and $\psi = C_1$ over the second surface. Solutions to Laplace's equation are commonly used for surface morphing and point correspondence because, if certain conditions are met, they yield bijective maps from one surface to the other. The Dirichlet form of Laplace's equation also represents the energy in some physical system (such as heat flow between boundaries), and its solution represents a minimum energy, equilibrium state.

The conditions under which solutions to Laplace's equation are also bijections are given below.

[7] A *bijective map* is both one-to-one and onto. It takes each individual member of one set and maps them uniquely to individual members of a second set such that all set members are mapped. This mapping is also invertible, such that if $Fa = b$ then $F^{-}1(b) = a$.

In this case the solution ψ is a scalar field smoothly interpolating the boundary values between the two surfaces. For surface morphing, a surface at any time $C_0 < t < C_1$ can be found by computing the level set $\psi = t$. One way to find corresponding points is to start with a point on one surface, then follow the gradient of ψ to a second point on the other surface. Since ψ is a bijection, the second point is guaranteed to be unique.

A solution ψ to Laplace's equation is a also harmonic function[8] and therefore has two properties desirable for surface morphing and point correspondence. The solution ψ has no minimum or maximum except on the boundaries; that is it has no local minimum or maxima interior to the domain. The solution ψ obeys the mean value property that for any epsilon ball within the domain, the value of ψ at the center of the ball is the average of the values of ψ on the boundary of the ball and also the average of the values of ψ in the interior of the ball, so the function ψ is smooth.

One of the most common methods for finding a solution to Laplace's equation is the finite element method (FEM). FEM finds solutions to Laplace's equation by solving a linear system for the unknown interior variables given the boundary conditions. The connectivity between variables (equivalently, the kind of mesh used to represent the domain) determines the form of the linear system, and the solution operator (i.e. umbrella) determines the coefficients of the linear system. In general, the linear system takes the form $\sum_{j \in N_i} w_{ij}(\psi(v_j) - \psi(v_i)) = 0$ for each vertex v_i and its adjacent vertices N_i. As long as the edge weights w_{ij} are positive, the solution ψ will also be a bijection. The coefficient matrix of the linear system is typically large, sparse, and symmetric, and approximate solutions are efficiently found by iterative solvers such as conjugate gradient methods.

Using FEM to solve Laplace's equation between two surfaces requires a volumetric mesh to represent the interior, unknown values of ψ. For surfaces represented by triangle meshes, the most convenient volume representation is the tetrahedral mesh. The surface triangles then correspond to boundary faces of the tetrahedral mesh. FEM over triangular or tetrahedral meshes typically employ the discrete Laplace-Beltrami operator to compute the weights w_{ij} for the linear system because it removes the solution's dependence on the local coordinates of the mesh. However, use of the discrete Laplace-Beltrami operator places a restriction on the mesh. The form of the Laplace-Beltrami

[8] A *harmonic function* is any function of the form $\frac{d^2x}{dt} + \alpha^2 x = 0$, which is the equation describing harmonic motion.

operator for simplical meshes (triangles, tetrahedra, and extensions to arbitrary dimension) requires computing the cotangents of the interior angles of the simplices. Specifically, for triangle meshes, the operator is $w_{ij} = \cot\alpha_{ij} + \cot\beta_{ij}$, where α_{ij} and β_{ij} are the angles opposite the edge (v_i, v_j). This restricts the mesh angles to those between 0 and $\frac{\pi}{2}$ (or 90 degrees) where the cotangent is both positive and finite.

Although there are algorithms for guaranteeing acute triangle surface meshes, there are none for tetrahedral volume meshes. Most libraries for constructing tetrahedral meshes do not make angle guarantees at all, but instead make volume or edge-ratio guarantees. Some libraries make Delaunay guarantees as long as the input is a piecewise linear complex (i.e. a closed mesh). Plaza and Rivara published an algorithm to iteratively reduce the number of obtuse tetrahedra by bisecting such tetrahedra along their long edges first [PR03]. Each pass improves the mesh quality, but no guarantee about the number of iterations required can be made.

Mean value coordinates

Recently, mean values coordinates were introduced as a generalization of barycentric coordinates[9] [Flo03, FKR05]. The derivation of mean value coordinates was motivated by the mean value theorem for harmonic functions, and the linear system used to solve for mean value coordinates takes the same form as that of solving Laplace's equation by FEM. Though mean value coordinates are not guaranteed to yield a harmonic function, the coordinates possess the same properties that made solutions to Laplace's equation desirable for computing point correspondence. Importantly, the weights w_{ij} are all positive so long as the mesh angles are between 0 and π, or 180 degrees, so for any well formed mesh the solution is guaranteed to be a bijection.

Mean value coordinates were introduced for surface parameterization[10] of triangle meshes [Flo03] and later extended to tetrahedra [FKR05].

[9] The *barycentric coordinates* of a point p inside some triangle describe the masses m_a, m_b, and m_c placed at the vertices such that the point p is the center of mass. They are defined uniquely for any triangle if $m_a + m_b + m_c = 1$.

[10] *Surface parameterization* is concerned with computing texture coordinates for arbitrary triangular meshes from the mesh geometry. Desirable properties of a good surface parameterization are that the parameterization be efficient to compute and produce coordinates that are smooth and have low distortion.

The most important aspect of mean value coordinates for this work is that they do not require meshes with only acute angles. The trade-off is that the matrix of coefficients is not symmetric, so more complex solvers are required. A stabilized bi-conjugate gradient solver is able to efficiently find solutions to the linear system, though they are not guaranteed to be optimal solutions (the solution may be a local minimum in the solution space).

Recently, a different formulation of barycentric coordinates, called harmonic coordinates, has been proposed [DM06] that is additionally a solution to Laplace's equation. Harmonic coordinates have an advantage over mean value coordinates for surface morphing; mean value coordinates may produce some undesirable interpolations for animating characters that harmonic coordinates do not. However, solving for harmonic coordinates is more computationally expensive than solving for mean value coordinates. Harmonic coordinates may provide better point correspondence than mean value coordinates when the boundary surfaces are far apart.

Mean value coordinates are used to find point correspondences in this work.

Topological changes

Neither solving Laplace's equation nor computing barycentric coordinates handles topological differences between the two surface without additional effort. For instance, Dinh and Turk describe a solution to finding point correspondences by FEM when the two surfaces are topologically different [DYT05]. They construct their mesh in 4D and solve a 4D heat diffusion. By projecting the solution back to 3D, their technique handles the topological changes smoothly.

For the user studies in this work, and for the real data collected from scientists, the two surfaces are not topologically different. Therefore, no additional effort was put into formulations that could handle topological changes. For more general treatment of layered surfaces with arbitrary topology, the approach of Dinh and Turk (or an equivalent approach for mean value coordinates) is required.

Implementation

A number of libraries are used to complete the point-correspondence algorithm. The TetGen library is used to construct the initial tetrahedral mesh [Si06]. SparseLib++ [DPRL04b] and IML++ [DPRL04a] are the libraries used for representing sparse matrices and for solving linear systems by iterative conjugate gradient methods. Several VTK classes are used [SML98], but vtkStreamTracer is the most important; it is used to find the geometry of the point-correspondence glyphs once the solution to the linear system is found by following the gradient of the solution (using a 4th order adaptive Runge-Kutta integrator).

The algorithm to compute correspondence glyphs for this work proceeds as Algorithm 4. Given two input surfaces, A and B, a tetrahedral mesh is constructed from the vertices v of both meshes such that the tetrahedral mesh lies between the two input surfaces, e.g. the mesh is bounded on one side by the surface A and on the other side by the surface B. In my implementation this tetrahedral mesh is constructed by first constructing a Delaunay tetrahedralization of the input vertices v (which covers the convex hull of the input vertices), then removing individual tetrahedra that lie completely inside both surfaces or completely outside both surfaces. The vertices v are assigned scalar values based on membership in the boundary surfaces A and B. The tetrahedral mesh is then subdivided along edges spanning between surface A and B, with new vertices labeled as unknowns. This refined mesh is used to construct a linear system with coefficients determined by the mean value coordinates representation of each unknown vertex [FKR05]. The linear system is solved using a stabilized bi-conjugate gradient method. This solution approximates a smooth function mapping surface A to surface B. The gradient of this solution gives correspondence trajectories that can be integrated from a point on surface A to find the corresponding point (according to the approximated mapping function) on surface B, and vice versa.

4.4.4 Principal-curvature texture

Several techniques in this work employ principal-curvature texture for display of an outer surface. Previous research in curvature computation [Des04, MDSB02, FJ89, IFP96, SM97, Tau95, GI04]

Algorithm 4 Computing Point-Correspondence

{given surfaces A and B, and optionally their intersection curve I}
{given seed vertices $S \in A$ to start each point-correspondence glyph}
$CHtets \leftarrow$ Delaunay tetrahedral mesh of the input vertices {computed by the TetGen library}
$tets \leftarrow CHtets-$ tetrahedra not between the boundary surfaces
unlabeled vertices of $tets$ from I are labeled .5
unlabeled vertices of $tets$ from A are labeled 0
unlabeled vertices of $tets$ from B are labeled 1
$mesh \leftarrow tets$ split along non-boundary edges to introduce new vertices labeled as $UNKNOWN$
construct linear system from *mesh* according to mean value coordinates
solve for unknowns using stabilized bi-conjugate gradient method
compute gradient of solution
for all $s \in S$ **do**
  trace along gradient starting at s to find path p and endpoint e
  $output \leftarrow output + (s, p, e)$
end for
return $output$

and surface parameterization [EDT+95, Lev01, LPRM02, DMA02, LSS+98, Flo97, FKR05, Flo03, MLBD02] leads to several options in how to texture surfaces with principal-curvature information. It should be kept in mind that the principal-curvature texture applied in this work is sparse. Because the texture elements are far apart, more error is tolerable than if the curvature information needed to be continuous across texture seams.

Computing principal curvature

For a continuous smooth surface, the curvatures at any point can be computed exactly from the second fundamental form. For discrete representations of surfaces, the curvatures can usually only be approximated.[11] Curvatures are typically approximated by differential geometry or fitting some local parameterization, then approximating the second fundamental form at each vertex of the triangle mesh.

There are three commonly used general methods for estimating principal curvature on a polygonal mesh. Goldfeather and Interrante [GI04] refer to these as

[11] Surfaces with explicit mathematical descriptions (parametric surfaces, etc.) may have closed-form expressions for curvature.

1. normal curvature approximation,

2. quadratic surface approximation, and

3. adjacent-normal approximation.

The first two methods are second order approximations. The approximation order of the adjacent-normal method [GI04] depends on the mesh connectivity, but it can be at least third order for triangle meshes. Although higher-order approximations produce less error in general, the error of any approximation depends on the quality of the input. In particular, these approximation methods can all produce large errors when the input meshes are irregular.

All three methods begin by approximating the normal at each vertex by the sum of weighted adjacent face normals[12]. Then, for each vertex v_i in turn, other vertices v_j in some neighborhood are visited (the neighborhood typically includes at least the adjacent vertices), and their contribution is computed.

Normal curvature methods use the distance between each neighbor v_j and the projection of v_j onto the tangent plane at v_i. Individual contributions of the vertices v_j are used to construct a matrix M that can be diagonalized to yield the second fundamental form. Quadratic surface methods use the vertices v_j to fit an approximate parabolic patch to the neighborhood about v_i. The local curvature can then be determined directly from the parameters of the least-squares parabola. Finally, adjacent-normal approximation uses the normals at the vertices v_j to find a least-squares fit for a smooth third-order (or higher if the mesh connectivity supports it) patch.

This work implements a variant on the normal curvature approximation method of Taubin [Tau95]. Taubin weights the contribution of the neighbors v_j based on the surface area of the triangles adjacent to the edge (v_i, v_j). The implementation in this work enables the neighborhood to include vertices v_j that are not adjacent to v_i but that are within a specified radius. The vertices v_j in the radius are weighted according to the surface area of adjacent triangles and the inverse of their distance from v_i. Also, vertices are not included in v_j if the local surface normal differs from the normal at v_i by more

[12]Goldfeather and Interrante show that the type of weighting does not have a significant impact on the result [GI04]

than some angle threshold (180 degrees was used here). These modifications reduce error in regions with irregular triangulations, at sharp features, and near boundaries.

Computing texture coordinates

Although techniques for computing a global parameterization of a triangle mesh exist [GY03, Flo03, DMA02, Flo97], they do not generally produce low distortion coordinates over the entire mesh. Techniques that divide the surface into many local patches achieve far more consistent distortion over the whole surface [Tur91, BVI91, PFH00, PC05, LPRM02, SWG$^+$03]. Recently, techniques have been proposed that divide a triangle mesh into a minimum of patches to achieve low distortion [ZMT05, EHP02]. Many of these techniques entail topological analysis of the surface to select minimum required surface cuts.

Surface patching

This work uses an algorithm that produces many patches, one for each texture glyph indicating principal curvature. In particular, a greedy geodesic algorithm is used to select seed vertices for patches similar to that of Peyré and Cohen [PC05]. The remaining, non-seed, vertices are then grouped into patches with the nearest (by geodesic distance) seed vertex. This produces a Poisson-like distribution of seed vertices, and Voronoi-cell like patches.

Many algorithms have been proposed for computing geodesic distances on surfaces [AE98, Axe99, KS98a, SSK$^+$05]. Several methods for computing geodesic distances on a mesh use front propagation, similar to Dijkstra's single source shortest path (SSSP) algorithm. The algorithm proceeds by visiting the vertex with the smallest distance from a *front* of vertices that are being updated. The visited vertex is marked as having a final distance value, and all non-final vertices adjacent to it are updated and added to the front. The front is usually kept in a priority queue with insertion time $O(logn)$, and every point in the mesh is visited at most a constant number of times. From this the time complexity of running this scheme on a mesh with N vertices is $O(NlogN)$.

The accuracy of a direct application of Dijkstra's SSSP (using the most obvious weight, Euclidean

length of the edges of the mesh) is relatively poor. The accuracy can be improved, at a computational cost, by using the law of cosines to compute distances across adjacent triangles where possible instead of using only distances along mesh edges. The most accurate means of computing geodesic distance on a triangle mesh is to use the fast marching method of Sethian [Set96, KS98a]. Fast marching methods formulate the problem as one of solving the Hamilton-Jacobi equation $|\nabla T|F = 1$ for the travel time T given a front propagation speed $F > 0$. Kimmel's implementation is $O(NlogN)$ [KS98a], though Yatziv et. al recently introduced an $O(N)$ implementation [Yat06] for regular grids.

Because the geodesic distance is being used only to cut the surface into patches, the accuracy of the method is not critical. Instead, ease of implementation led to using Dijkstra's SSSP with the law of cosines distance computation.

Texture coordinates

To display principal-curvature-aligned textures on each patch, a texture coordinate system must be computed such that it is aligned with principal curvature. This work only aligns the texture with the curvature at the seed vertex for the patch, which greatly simplifies the coordinate computation. Also, the computation is done in two steps, the first computing texture coordinates with essentially arbitrary axes and the second rotating the coordinates to align with the principal-curvature directions.

The initial texture coordinates for each patch are computed by locally linear embedding (LLE) [RS00]. The LLE algorithm is a manifold-learning technique for discovering low dimensional structure in high dimensional data. To compute texture coordinates for the patch, LLE uses a matrix of all-pairs distances between the vertices in the patch to compute the eigenvectors of the patch geometry. The first two eigenvectors then give an orthogonal coordinate system.

4.4.5 Shadows

The shadow implementation used in this work is standard hardware shadow mapping [Wil78, RSC87, ERC02]. A depth image of the scene is captured from the point of view of the light source. Then the display image is captured from the point of view of the camera. While generating the

display image, geometry is transformed into light space, and its depth from the camera is compared to the corresponding position in the previous depth image. Geometry that is further away from the light than the corresponding pixel in the depth image is in shadow. All other geometry is in light.

Chapter 5

Evaluation

This chapter describes the user studies I ran to evaluate the general layered-surface visualization techniques developed as part of this work.

The user studies drew from three tasks identified through interviews with scientists (see Chapter 2). The three tasks evaluate and compare a set of visualization techniques' effectiveness at conveying shape by asking participants to perform the following:

1. compare distances between surfaces (the *distance* task),
2. compare local surface shapes (the *local shape* task), and
3. recognize global surface shapes (the *global shape* task).

Section 5.1 introduces the tasks, describes what they present to the participant, and describes what they measure. Section 5.2 describes implementation details that are common to multiple user studies. Sections 5.3, 5.4, and 5.5 discuss the user studies in detail.

A total of six user studies were performed. The user studies were performed in three experiment groups, one group evaluating a set of visualization techniques for a set of tasks. The composition of the experiment groups is summarized in Table 5.1.

Experiment 1 (Section 5.3) included color mapping and principal curvature texture techniques,

Table 5.1: List of user study experiments

Experiment	User Study	Task	Visualization Techniques
1	1	distance	color mapping principal curvature texture principal curvature texture with cast shadows
1	2	local shape	color mapping principal curvature texture principal curvature texture with cast shadows
2	1	distance	**rocking versus shadows** (principal curvature texture)
3	1	distance	color mapping principal curvature texture principal curvature texture with cast shadows point-correspondence principal curvature texture with point-correspondence
3	2	local shape	color mapping principal curvature texture principal curvature texture with cast shadows point-correspondence principal curvature texture with point-correspondence
3	3	global shape	color mapping principal curvature texture principal curvature texture with cast shadows point-correspondence principal curvature texture with point-correspondence

introduced one novel layered-surface technique, principal curvature texture with shadows, and evaluated performance on the distance and local shape tasks. Experiment 2 (Section 5.4) included principal curvature texture with and without shadows, evaluated performance on the distance task only, and addressed the issue of surface motion overpowering the effects of shadows in Experiment 1. Experiment 3 (Section 5.5) included the visualization techniques from Experiment 1, introduced the second novel layered-surface technique, principal curvature texture with correspondence glyphs, included a fifth technique (correspondence glyphs on a single surface) for comparison, and evaluated performance on all three tasks.

Results across the three experiment groups are not immediately comparable. The number of visualization techniques increases with each experiment group, and the number of trials per visualization is reduced (by removing trials found to elicit responses at chance or at plateau) to keep the user study session time approximately the same. Experiments 1 and 2 are essentially pilot studies used to de-

termine the statistical power of the user study tasks and to isolate confounding conditions. However, Experiments 1 and 2 produced significant results and are already published [WTI05], showing that intersecting surfaces can be visualized as nested surfaces and that shadows can be beneficial for performing the distance task.

The experiment groups build on each other, so there is a great deal of commonality in their design and implementation. The common elements among the three experiments are described in Section 5.2.

A Note on Human Subject Research

All studies performed for this work were reviewed by the Office of Human Research Ethics (OHRE) at UNC-CH. All participant recruitment, screening, and renumeration were approved by OHRE. All participants were asked for, and gave, informed consent. All user study procedures were determined to put participants at minimal risk, and were approved by the OHRE.

5.1 User study tasks

Three tasks are used to evaluate how well the visualizations convey the shape of intersecting surfaces. This section will describe the most general aspects of each task (i.e. the wording of the question, the nature of the possible responses). Descriptions of the visualizations or the trial data are discussed in later sections.

The first task (*distance*) asks the participant to estimate and compare distances between two surfaces. The second task (*local shape*) asks the participant to estimate and compare local shape between two surfaces. The third task (*global shape*) asks the participant to recognize individual shapes in a pair of intersecting shapes.

These user study tasks were chosen in consultation with scientists, as described in Chapter 2. The tasks needed to satisfy the following requirements:

- satisfy the scientists that the study tasks related to their research questions,

- use shape tasks commonly employed in the literature (adapted as necessary for two intersecting surfaces), and
- facilitate fast, simple judgments from the participants.

Because the scientists are interested in both the distance between intersecting surfaces and the shape of intersecting surfaces, the user studies include tasks evaluating performance for estimating and comparing both distances between surfaces and local surface shape. Typically, either a distance task or a local shape task alone would be considered sufficient to determine the effectiveness of a visualization technique at conveying surface shape[1]. I include both of these tasks to directly address scientists' questions about layered-surface data. As will be shown, these two tasks (as implemented here) produced different rankings of the evaluated visualization techniques.

The scientists' questions are predominantly about comparing the two surfaces, so I decided that the tasks should involve comparisons between two surfaces. To facilitate quick responses from the participants, the tasks are of a forced-choice design with two possible responses to each trial. Forced choice also removes the need to train participants to manipulate direct-measurement widgets to respond to tasks (i.e. the orientation probe developed by Koenderink and van Doorn [KVD95]). Because one of the visualization techniques included in the studies renders only one surface (color mapping), forced choice also avoids the problem of indicating where on the invisible surface the participant should estimate local shape. With forced-choice tasks, participants could perform many trials in a relatively short amount of time (compared to manipulating widgets). However, these tasks yield only binary responses instead of metric errors.

5.1.1 Distance

The *distance* task evaluates how well a visualization technique conveys surface shape by asking participants to compare distance between intersecting surface at two points. Participants make judgements about the relative distances, reporting which distance appears shorter. The distance task

[1] Langer and Bülthoff list the most commonly used shape perception tasks and weigh their advantages and disadvantages [LB00]

evaluates how effectively a visualization technique can be utilized to explore questions like *Where are the two surfaces separated by more or less than some threshold?* (see Section 2.3 for a discussion of scientists' questions about distances between intersecting surfaces).

The distance task presents the participant with a forced choice between two regions in a display of intersecting surfaces. Participants are shown a display of two intersecting surfaces with two distinct regions indicated by perceptually distinguishable markers. The participant is presented with the following question:

In which circled region do the two surfaces appear to be closer together?

The participant compares the relative distances and responds with the region containing the smaller distance.

5.1.2 Local shape

The *local shape* task evaluates how well a visualization technique conveys surface shape by asking participants to estimate local surface orientation. An estimate of local surface orientation is equivalent to an estimate of the local surface geometry (specifically, the surface normal at that point). Accurately estimating the local surface normal is an indication that the participant understands the shape of the surface in that region. Participants make judgements about relative differences in local surface orientation, reporting which differences appear smaller.

The local shape task evaluates how effectively a visualization technique can be utilized to explore questions like *Are the apparent differences between surfaces consistent with some missing features?* (see Section 2.3 for a discussion of scientists' questions about distances between intersecting surfaces). Additionally, the local shape task evaluates how effectively a visualization technique enables the participant to estimate local shape on one of the pair of intersecting surfaces.

This task presents the participant with a forced choice between two regions in a display of intersecting surfaces. Participants are shown a display of two intersecting surfaces with two distinct regions indicated by perceptually distinguishable markers. The participant is presented with the fol-

lowing question:

In which circled region do the two surfaces appear to be more similarly oriented or parallel?

The participant compares the local surface orientations for both surfaces in each region, then compares the orientation differences between regions, then responds with the region containing the smaller difference.

5.1.3 Global shape

The *global shape* task evaluates how well a visualization techniques conveys surface shape by asking participants to recognize objects. Participants determine if a pair of intersecting objects includes a target object, reporting the target object's presence or absence from the pair. The global shape task evaluates how effectively a visualization technique enables the participant to understand each of the intersecting surfaces as an individual object.

This task presents the participant with a forced choice between the presence or absence of a target object in a display of intersecting objects. Participants are shown a display of two intersecting objects that when displayed alone would be easily recognizable (e.g. fruit, vegetables, domestic animals). The participant is presented with the following question:

Is the *target* present in this pair of objects?

The participant reconstructs the shape of each object as if displayed individually, determines if either displayed object is the target object, then responds if the target object is absent or present in the pair.

5.2 Common Implementation Details

Many of the details of the user studies (e.g. data sets used, viewing parameters, and the user interface) are common across all instances in the three experiment groups. The common details are described here.

5.2.1 Common data for distance and local shape tasks

Recall that the three experiment groups contain a total of six user studies. Of the six user studies, five ask the participants to perform distance or local shape tasks. The distance task appears in all three experiment groups, and the local shape task appears in Experiments 1 and 3. In all instances, these two tasks draw trials from the same collection of synthetic intersecting surface data.

The surfaces generated for the distance and local shape tasks were limited to height fields. The geometry for all surfaces was computed on a 100x100 grid. Inter-surface distances were computed at 10 times that resolution to ensure accurate data for the color mapping technique. Each surface was constructed from eight Gaussian bumps. The bumps have random centers, maxima, and sigmas, and are allowed to overlap. Noise is also included in each surface; the noise is one third the scale of the bumps. Figure 5.1 shows several examples. Although the described set of surfaces does not at first appear representative of all possible real-world data, it should be noted that typical shape features (e.g. bumps, saddles, ridges, valleys, etc.) are present.

Limiting the investigation to height fields is not uncommon in studies of surface shape. Height fields greatly simplify the demands on the participants. The inclusion of closed surfaces in our evaluation of the perceptual effects of shadows would require participants to have interactive control of the light source or the objects (or both).

5.2.2 Viewing Parameters

Surfaces were pre-rendered from a vantage point 45 degrees above the plane of the grid (rotation about the horizontal axis). The initial renderings were generated at 1500x1500, filtered, and re-sampled at the final display resolution (750x750 pixels) to reduce aliasing artifacts. Participants were seated such that their distance from a 21-inch monitor was approximately 53 cm[2]. Participants viewed the images binocularly, but images were not generated for stereoscopic display. At the center of view, the surfaces extend horizontally just beyond the viewport. The viewport is 22 cm square and

[2]Participants were not forced to maintain this distance. This is the distance from which a typical participant would view the monitor and comfortably reach the keyboard and mouse.

subtends 24 degrees visual angle (given the 53 cm viewing distance). These view parameters display the surfaces such that, assuming the surfaces lie immediately behind the monitor screen, the distance between samples of the 100x100 grid of the surface geometry are approximately 2.5 mm at the center of view.

Illumination was from an infinite point source with a direction vector $(\frac{\sqrt{3}}{3}, \frac{\sqrt{3}}{3}, \frac{\sqrt{3}}{3})$, effectively over the viewer's right shoulder. The infinite point-source light was also used for all shadow calculations. Per-pixel Phong illumination [Pho75] was employed instead of typical Gouraud interpolation of per-vertex Blinn-Phong illumination [Bli77]. Per-pixel Phong illumination produces more realistic specularities on the surfaces, particularly by properly capturing the peak intensity of the specularity.

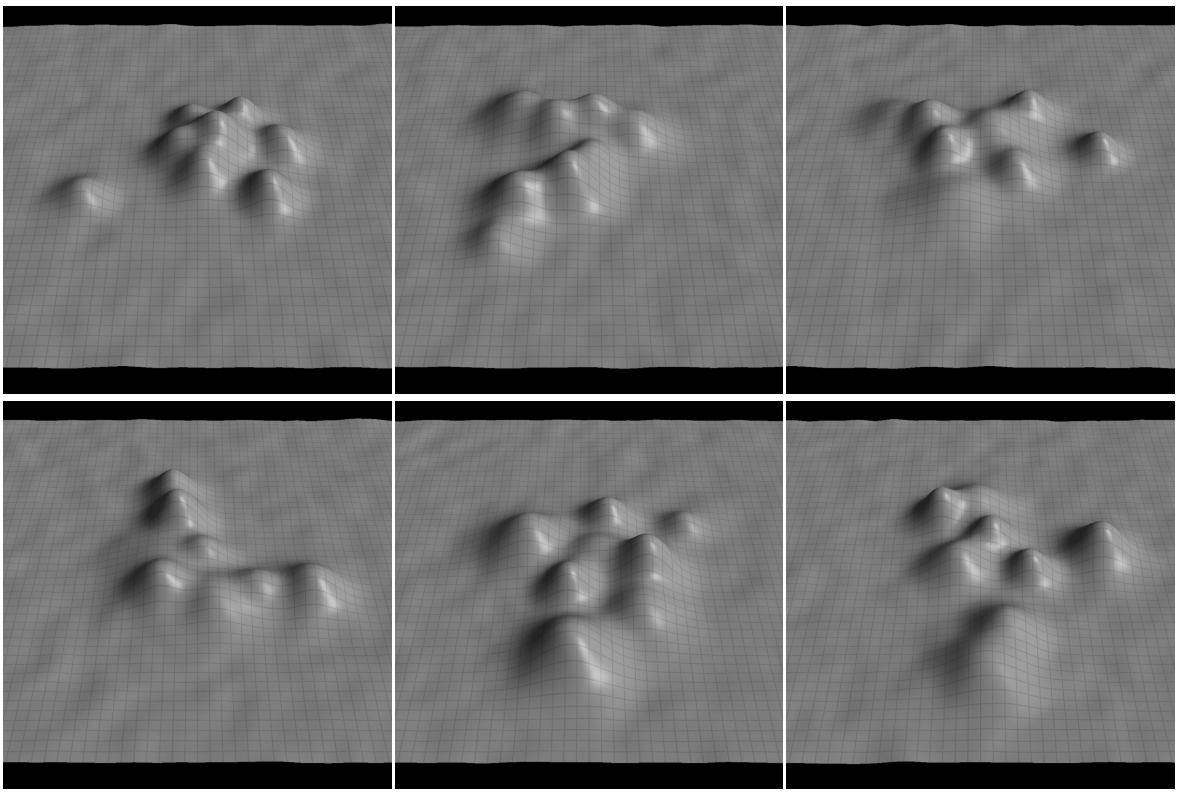

Figure 5.1: This figure presents examples of the random surfaces created for the distance and local shape tasks. The example surfaces consist of random Gaussian bumps on a background of noise.

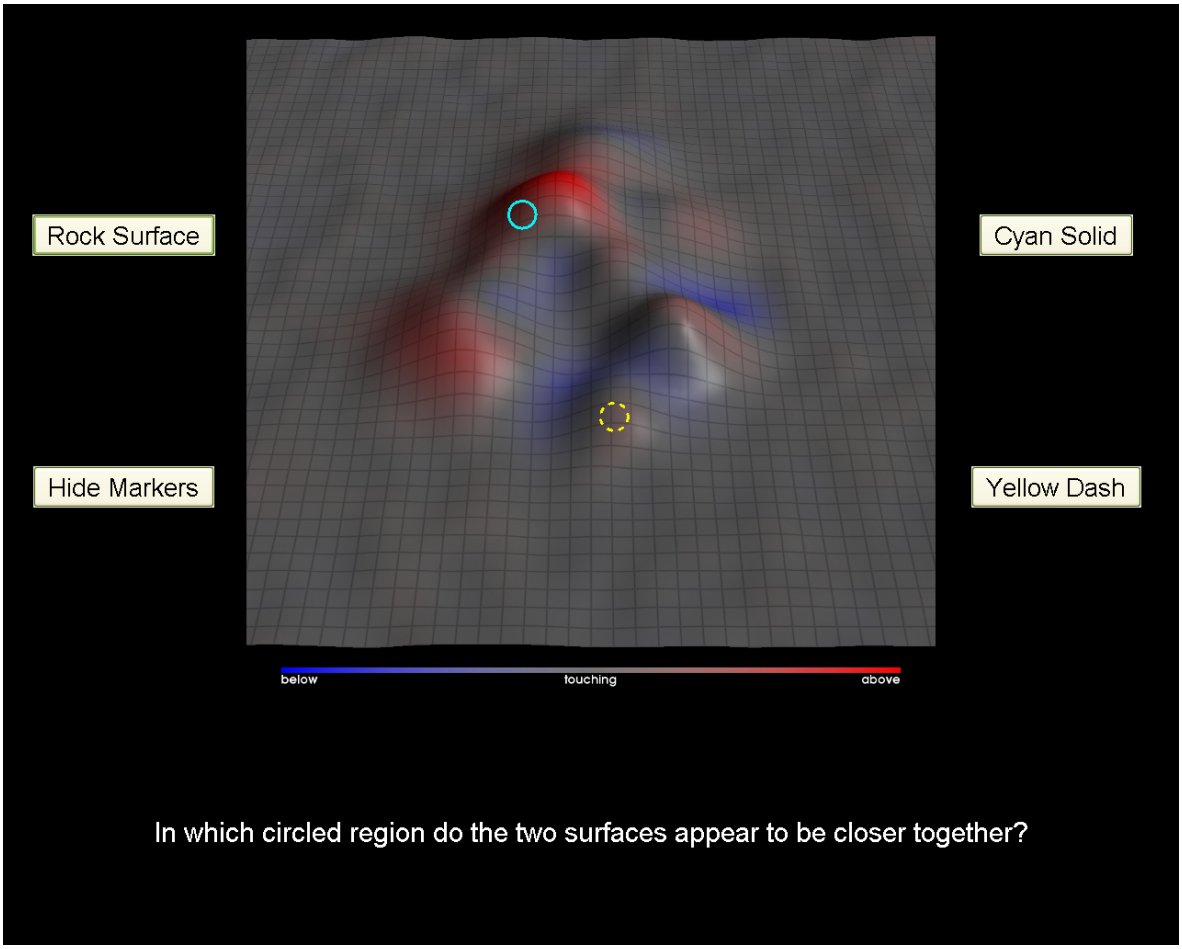

Figure 5.2: This is an example of a single trial from the user studies. This example shows the distance task. Two regions are marked with circles, and participants are asked to choose the marked region that appears to be the correct response to the question. Participants can also hide the region markers and, in this case, animate the surfaces with a torsion pendulum rocking motion.

5.2.3 User Interface

All three tasks shared a common user interface. A 750x750 pixel image is displayed at the top center of the screen. To the right of the image are two buttons that can be used to indicate one of two choices (all tasks use forced-choice responses). To the left of the image are zero to two buttons, as appropriate, allowing the participant to initiate short pre-determined animations. Below the image is the text of the task question to which the participant responds. See Figure 5.2 for an example.

For the distance and local shape tasks, the participants are asked to estimate some shape metric

at two distinct locations, compare the metrics, and report the smaller metric. Regions were labeled by overlaying unfilled circles with a radius of 15 pixels, one solid and the other dashed. The circles were also distinguishable by their color, and the colors were chosen to contrast with the color mapping condition.

5.3 Experiment 1

This section describes the first group of experiments, consisting of two user studies. The two studies evaluate the relative effectiveness of color mapping versus principal curvature texture (with and without cast shadows), the first with the distance task and the second with the local shape tasks. The studies were run simultaneously using the same trial data and the same visualization techniques but with half the participants performing the distance task and half performing the local shape task.

This experiment serves as a pilot study to isolate confounding factors in the user study designs and to ensure that the tasks can measure the effectiveness of the visualization techniques.

5.3.1 Conditions: Visualization techniques

The following sections describe the three visualization techniques included in this experiment: color mapping, principal curvature texture, and principal curvature texture with shadows.

Color mapping

The color mapping technique displays the geometry of one of the two intersecting surfaces. That surface's color is mapped to the Euclidean signed shortest distance between the two intersecting surfaces (Figure 5.3). A double-ended saturation scale, blue through grey to red, classifies inside, touching, and outside as hue while also encoding distance as saturation. This scale is suggested by Ware as a possible scale for conveying ratio data, though Ware notes that conveying ratio data in color is "a tall order" [War04]. This color scale is also perceptible by those with deuteroanomaly, deuteropia, protoanomlay, or protopia, which are the most common forms of color blindness. Additionally, a

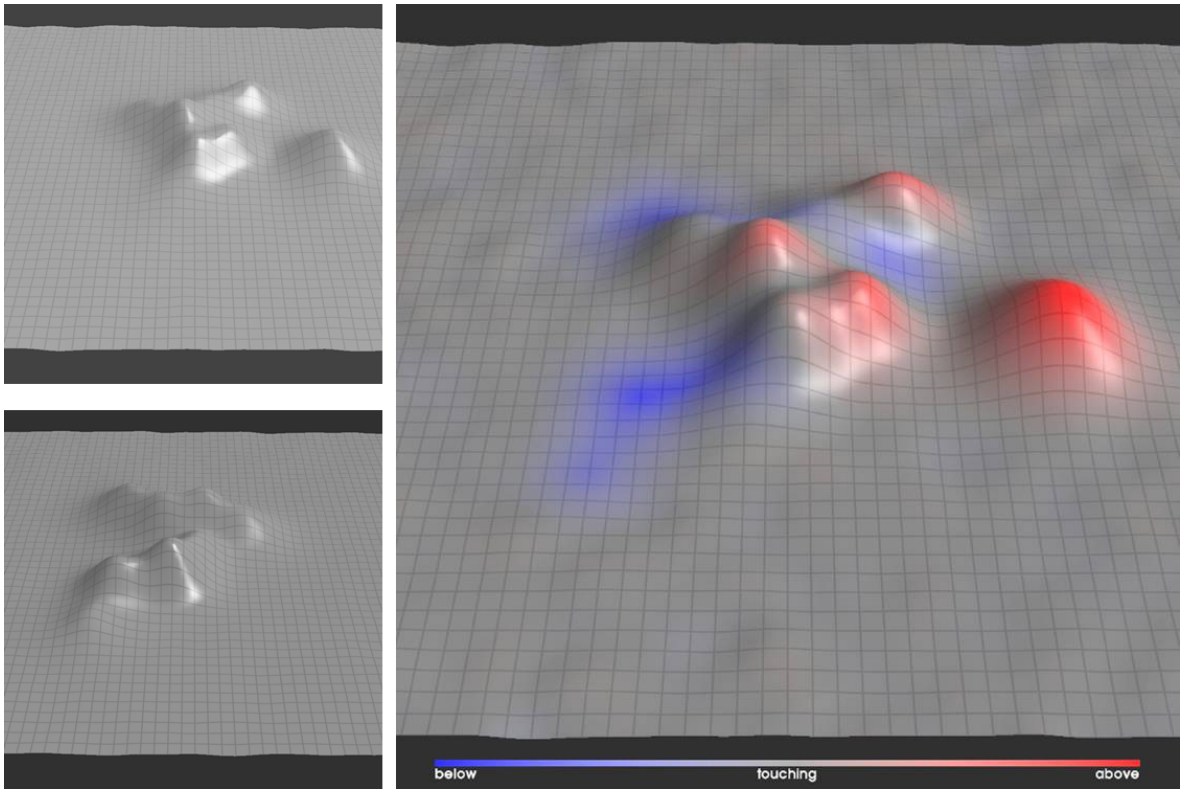

Figure 5.3: This is an example of the color mapping technique. The two surfaces on the left are used to produce the visualization on the right. The top left image is used as geometry, and the bottom left image is used to compute the distances mapped to the color scale.

simple grid texture projected orthogonally onto the surface along the Z axis appears on the visible surface to provide stronger shape cues. The color scale is normalized such that the range of the color scale maps to the range of values $(-m, m)$ where m is the maximum (unsigned) distance between the two surfaces. This maximizes the available perceptual precision in the saturation scale and would be expected practice if such a scale were applied to real data.

Color mapping is a frequently used visualization technique for displaying scalar values on surfaces – a task for which it is well suited when used appropriately [Hea96, War88]. Applying a color scale to a surface can be quite effective for classification or metric estimation but is not a good perceptual technique for conveying geometric information. The color scale can only depict the values of a scalar-valued function at every point on a surface, but an arbitrary geometry can not necessarily be represented as a function over the surface. A color mapping technique is included because it is

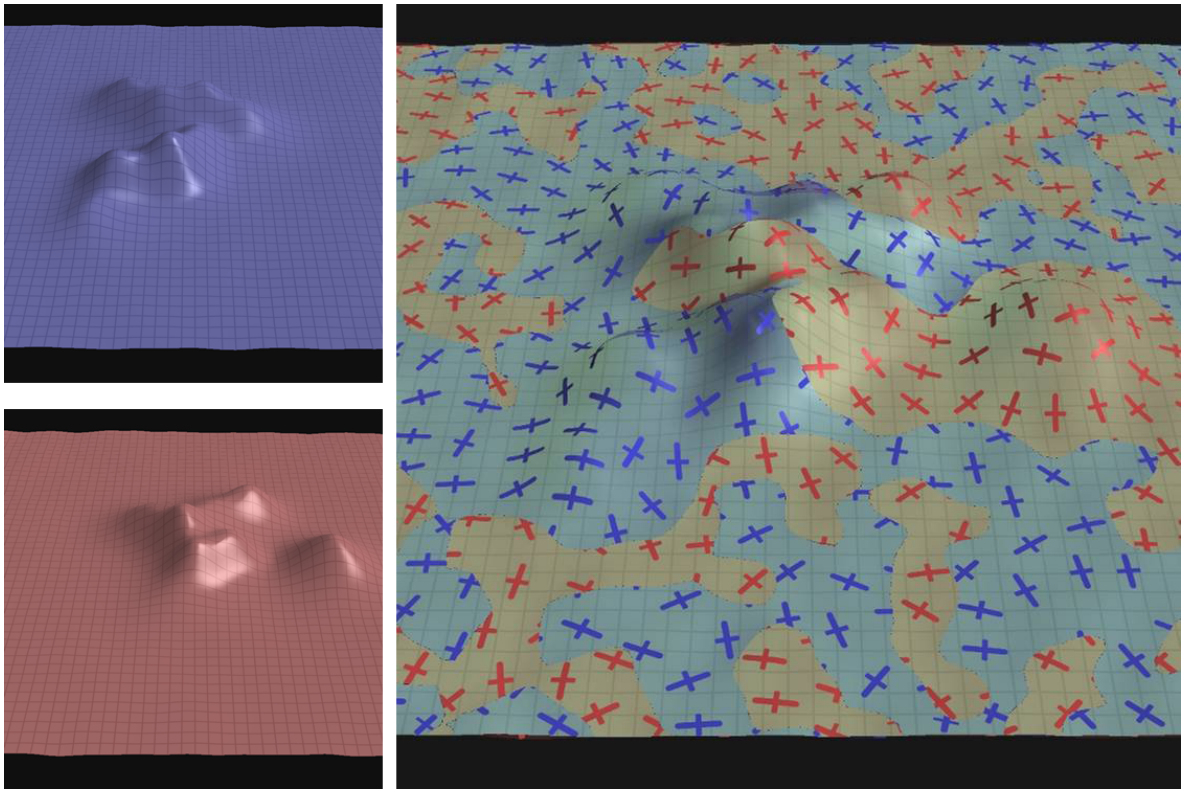

Figure 5.4: This is an example of the principal curvature texture technique. The two surfaces on the left are used to produce the visualization on the right, and appear in the same colors. Regions of the surfaces labeled *interior* appear colored by the exterior, but are visualized as a neutral grey material with a regular-grid texture. Regions of the surfaces labeled *exterior* appear as principal-curvature glyphs textured onto a translucent surface.

a typically employed approach for comparing two surfaces. Though it conveys no perceptual shape information about one of the surfaces, the color scale directly encodes the metric for comparison in the distance task, and the gradient of the color scale encodes the metric for comparison in the local shape task (the magnitude of the color gradient tells how fast the local surface normals diverge).

Principal curvature texture

The second visualization technique is an adaptation of existing nested surface techniques. It is based on Interrante's curvature-directed strokes [IFP96]. The technique employs textured glyphs which conform to both principal curvature directions, as suggested by Kim *et al.* [KHSI03], and

modulate translucency (Figure 5.4). The glyph is a elongated plus – the long axis indicates an estimate of the first principal curvature direction at the glyph center. Recall that the data includes noise, so the surface does not have significant regions with undefined principal directions (e.g. flat regions). Though one could replace the anisotropic glyph with an isotropic glyph to signify regions where the principal directions were undefined, this was not done here.

Red and blue are used to denote ownership of the exterior surface regions. Red regions belong to surface *A*, and blue regions belong to surface *B*. Though the apparent color is modified by the translucent exterior regions, the interior regions are rendered as a neutral grey. Neutral grey was chosen to minimize differences between this technique and the next, where I felt it important that the interior coloring provide better contrast for shadows than the red and blue color coding would. The interior is also textured with a simple grid to enhance shape perception.

Principal curvature texture with cast shadows

The third visualization technique adds cast shadows to the principal curvature texture (Figure 5.5). Again, red and blue denote ownership of the exterior regions of the two surfaces, while the interior is a neutral grey (tinted by the translucent exterior). Neutral grey provides better contrast for the cast shadows than would red or blue, helping the cast shadows to stand out against the interior and to be perceptually separable from the principal curvature glyph texture itself. The interior is also textured with a simple grid to enhance shape perception. Recall that the light source is fixed, thus when the surfaces undergo the rocking motion, the shadows move appropriately. I expected the cast shadows to enhance the ability to perceive inter-surface distance because cast shadows have been reported to help fix the frame of reference between caster and receiver [CL89].

5.3.2 Questionnaire

As part of this set of user studies, participants completed a short questionnaire. The questionnaire consisted of two questions, one asking about clarity of display and the other about preference.

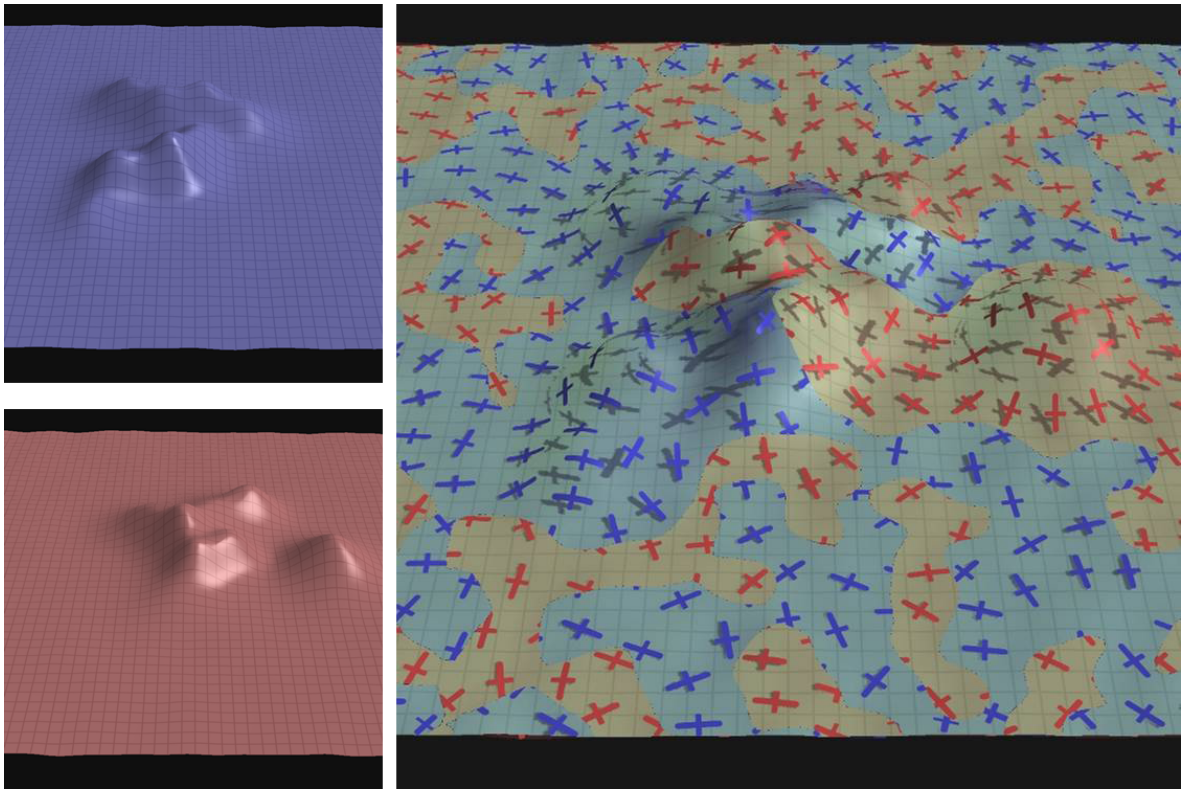

Figure 5.5: This is an example of the principal curvature texture with cast shadows technique. The two surfaces on left are used to produce the visualization on the right, and appear in the same colors. Regions of the surfaces labeled *interior* appear colored by the exterior, but are visualized as a neutral grey material with a regular-grid texture. Regions of the surfaces labeled *exterior* appear as principal-curvature glyphs textured onto a translucent surface. All opaque surface elements cast shadows.

1. On a scale of 1 to 9, how clearly did each display technique convey the information you needed to complete the task?

2. If you were to perform this task again using these display techniques, what would be your order of preference?

These are essentially both preference questions, the second more explicitly so than the first. I expected responses to the two questions to be correlated, with the display scoring highest for clarity also being most preferred. I intended the clarity question to allow some flexibility in the participants' response while the preference question would force a strict ordering (and break ties in scoring for clarity).

5.3.3 Rocking animation

When surfaces are first presented, they rock five degrees to either side of center around the vertical axis. The motion is that of a torsion pendulum with a period of two seconds. The pendulum motion accelerates the surfaces from their initial rest position (facing the participant), decelerates into and accelerates out of direction changes, then finally decelerates to rest back at the initial position. The apparent light source remains fixed. Participants may also repeat the rocking animation as they desire during trials. The region markers (the two circles) fade out before the rocking animation begins and fade in after the animation ends. The inclusion of the rocking animation turned out to be a critical design factor in this experiment group.

5.3.4 User Study 1.1: Distance task

Methods

Subjects: Six undergraduate and graduate students performed the distance task. All participants had normal or corrected-to-normal vision and reported normal color sensitivity but were not tested. Participants were compensated for their time.

Stimuli: The participants viewed images of the bump data under the following visualization techniques: color mapping, principal curvature texture, and principal curvature texture with shadows.

Design: This user study compares the three visualization techniques for enabling the distance task. Each participant viewed 60 unique, random surface pairs for each of the three visualization techniques for a total of 180 trials.

Participants estimated how closely the two surfaces approached each other within each of a pair of indicated regions and reported which of the pair of regions contained the closer approach (the smaller distance). The region locations were precomputed to guarantee that bumps were present in both surfaces (instead of the background noise) and that the surface intersections themselves were excluded from the regions. The distances between surfaces at the regions were distributed between 0.5 and 12 grid units (approximately 1 mm to 30 mm). The pairs of regions were selected such that differences in

closest approach were uniformly distributed between 0 and 5.5 grid units (approximately 0 mm to 14 mm) in 0.5 grid unit steps. Region locations were otherwise random. Trials were randomly ordered for each participant.

Participants were asked to respond to the following question:

In which circled region do the two surfaces appear to be closer together?

Each session began with a short training exercise. Participants were introduced to the user interface, each visualization technique, marking of regions for comparison, and the current task. Participants were then shown 6 example trials, 2 for each visualization technique. Participants were challenged to perform each training task as they would during the recorded trials, then given the correct response to the training trial, and then allowed to further study the trial image.

Hypothesis

The hypothesis is that the percentage of correct participant responses depends on the visualization technique and on the difference between the region distances.

Independent variables: The design directly manipulates two independent variables – the distance difference between regions and the visualization technique. Also recorded are the following predictor variables: a random unique identifier for each participant, the participant's gender, and the participant's response time.

Dependent variable: The dependent variable in this experiment is the percentage of correct responses.

I expected participants would be able to compare distance correctly with the color mapping technique because it directly encodes the necessary information. I expected the cast shadows would enhance the perception of separation between surfaces, yielding better task performance than for the curvature technique without shadows.

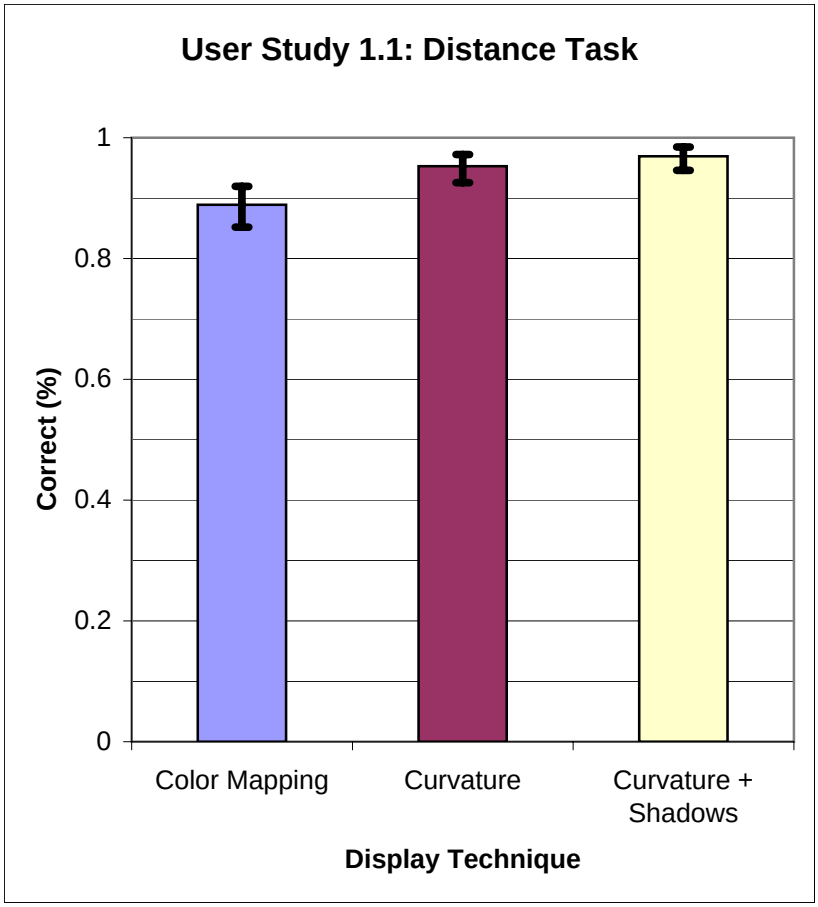

Figure 5.6: This figure shows the overall percentages of correct responses and their 95% confidence intervals for the distance task. Tukey's HSD test finds that the two principal curvature texture techniques are statistically different from the color mapping technique, but not from each other.

Results

Unless otherwise noted, independent variables have no statistical significance ($p > .05$).

Analysis: ANOVA analysis finds significant main effects for the distance difference between marked regions ($p < .01$), the visualization technique ($p < .001$), the participant ($p < .001$), and participant response time ($p < .001$). As the distance difference increases, participants give more correct responses. In fact, at a distance difference of 0 participant responses are at chance (as they should be), and the responses eventually plateau (larger differences in distances no longer produce an increased number of correct responses). Longer response times correlated to higher percentages of correct responses; this effect could be from participants rocking the surface to understand the shape,

but no count of the number of times participants' rocked the surface was recorded so it can not be tested.

Figure 5.6 shows the percentages of correct responses and the 95% confidence intervals by visualization technique. Figure 5.6 also shows that the performance of the participants is better than chance. A Tukey's Honestly Separable Difference (HSD) test[3] finds that participants are correct more often with the two curvature techniques than with direct color mapping. The two curvature techniques are not separable from each other.

Responses to the questionnaire show that the average participant found color mapping and principal curvature texture with cast shadows to show distance with equal clarity and with greater clarity than principal curvature texture alone. However, the average participant preferred principal curvature with shadows over the other two techniques. This is an interesting result, as it shows the participants' judgment of the strength of the techniques does not match the study findings. The results did not show the expected improvement in perception due to cast shadows for the principal curvature texture technique.

Discussion: The user study results show the principal curvature texture techniques enabled more correct responses to the distance task than directly mapping distance to color. It should be noted that these results do not reveal the precision with which a single estimation of distance could be made, only that the relative magnitudes of distance can be effectively compared.

That the curvature techniques are better at all for distance is somewhat surprising to note because the color mapping visualization directly encodes that information while the curvature techniques present two shapes from which the distances must be inferred.

An interesting result of this experiment comes from the questionnaires. Subjective preference does not reflect objective performance. Participants expressed a preference for color mapping or principal curvature texture with shadows over curvature texture without shadows and a preference for color mapping over curvature with shadows for the distance task. Neither of these preferences can be

[3]In the context of Tukey's Honestly Separable Difference test, *separable* means that the parameter estimates or each level of the factor was found to have statistically significant differences that can be used to group the factor levels into categories. In these experiments, the *factor* is the visualization technique.

supported by the performance results. In particular, it is interesting that participants preferred direct encoding of the metric to be estimated over a technique which enabled better task performance.

Shadows showed no benefit. At this point, I believed the effect of shadows to be masked by the rocking animation. This will be discussed further, after considering the results of the other user study in this experiment group.

5.3.5 User Study 1.2: Local shape task

Methods

Subjects: Seven undergraduate and graduate students performed the local shape task. None of the seven took part in User Study 1.1. All had normal or corrected-to-normal vision and reported normal color sensitivity but were not tested. Participants were compensated for their time.

Stimuli: The participants viewed images of the bump data under the following visualization techniques: color mapping, principal curvature texture, and principal curvature texture with shadows.

Design: This user study compares the three visualization techniques for enabling the distance task. Each participant viewed 180 trials, as in User Study 1.1.

Participants estimated the local shape of each surface within indicated pairs of regions and reported which of the pair of regions contained the smallest orientation difference (the smaller angle difference between surface normals). The regions were selected such that the orientation differences for the intersecting surfaces within each region ranged from 0 to 70 degrees. The region pairs were selected such that the differences of orientation differences between two regions were uniformly distributed between 0 and 45 degrees at 5 degree steps. The region locations were otherwise determined as in User Study 1.1. Trials were randomly ordered for each participant.

Participants were asked to respond to the following question:

In which circled region do the two surfaces appear to be more similarly oriented or parallel?

Subjects received training as in Experiment 1.

Hypothesis

The hypothesis is that the percentage of correct participant responses depends on the visualization technique and on the difference between the region orientation differences.

Independent variables: The design directly manipulates two independent variables – the difference between region orientation differences and the visualization technique. Also recorded are the following predictor variables: a random unique identifier for each participant, the participant's gender, and the participant's response time.

Dependent variable: The dependent variable in this experiment is the percentage of correct responses.

I expected the percentage of correct participant responses to depend on the difference between the two region orientation differences and on the visualization technique. I expected that participants would be able to compare orientation differences in the color mapping technique by comparing color gradients in the marked regions. Because the distance between the two surfaces changes where the two surfaces have different orientations, the color changes there also. I expected cast shadows to enhance the perception of shape, especially on the interior surface. Finally, I expected the principal curvature techniques to enable better performance than the color mapping technique because they present geometry of both surfaces.

Results

Unless otherwise noted, independent variables have no statistical significance ($p > .05$).

Analysis: ANOVA analysis finds significant main effects for orientation difference between marked regions ($p < .001$), the visualization technique ($p < .01$), the participant ($p < .01$) and participant response time ($p < .01$). As the orientation difference increases, participants give more correct responses. In fact, at a orientation difference of 0 participant responses are at chance, and the responses eventually plateau (larger differences in distances no longer produce an increased number of correct responses). Longer response times correlated to higher percentages of correct responses; this effect

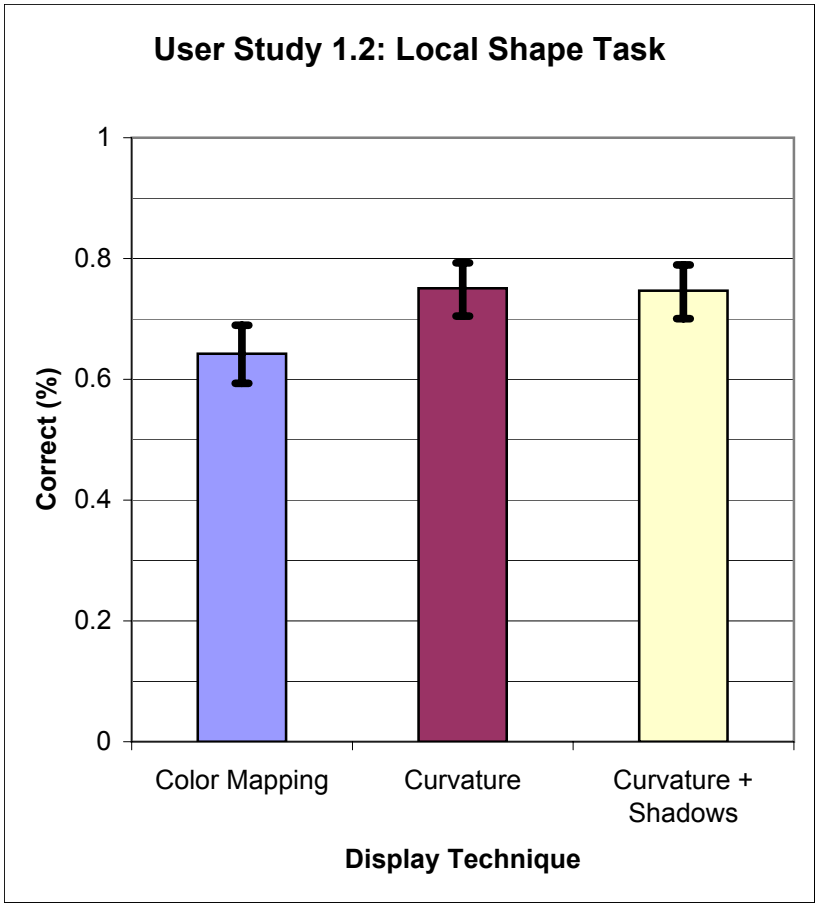

Figure 5.7: This figure shows the overall percentages of correct responses and their 95% confidence intervals for the local shape task. Tukey's HSD test finds that the two principal curvature texture techniques are statistically different from the color mapping technique, but not from each other.

could be from participants rocking the surface to understand the shape, but no count of the number of times participants' rocked the surface was recorded so it can not be tested.

Figure 5.7 shows the overall percentages of correct responses and 95% confidence intervals by visualization technique; the figure also shows that the performance of participants is better than chance. A Tukey's HSD test finds that the two principal curvature texture techniques are better than direct color mapping but are not separable from each other.

Responses to the questionnaire show that the average participant found the principal curvature texture with shadows marginally clearer than color and either clearer than curvature texture alone. No preference was reported between color or curvature with shadows, but either was preferred over

curvature alone. As in the distance task, participants' judgment of the ranking of the techniques does not match the study findings. Also, the results did not show the expected improvement in perception due to cast shadows for the two curvature techniques.

Discussion: The user study results show the principal curvature texture techniques enabled more correct responses to the local shape task than directly mapping distance to color. Principal curvature texture clearly enables better performance for the local shape task.

Again, the questionnaires show that subjective preference does not reflect objective performance. Participants expressed a preference for color mapping or principal curvature texture with shadows over curvature texture without shadows for the local shape tasks. This preferences can be supported by the performance results. In particular, it is interesting that participants preferred direct encoding of the metric to be estimated over a technique which enabled better task performance.

Again, shadows showed no benefit.

5.3.6 Experiment discussion

The combination of statistically better performance for both distance and local shape tasks suggests that a curvature texture technique would be a better overall visualization for our collaborators.

A reasonable question is whether another color scale would have enabled better performance than the red-grey-blue scale. In fact, this is the case for the distance task, as will be shown in Experiment 3 (see Section 5.5). It should not be a surprise that there exists some color scale that enables metric estimation more accurately than principal curvature texture enables shape estimation. However, I claim that no color scale will enable perception of the shape of the hidden surface. That the curvature techniques are comparable to some direct encoding of the shape metrics suggests that they are better techniques than color mapping for exploratory visualization. Although a color-mapped surface can be used to encode shape metric information about the difference between two surfaces, it should not be said to convey the shape of two surfaces.

One might question why color still represents distance in the local shape task. Mapping an es-

timate of the difference in orientation would seem more effective for enabling the local shape task. However, the goal is to find a technique that can be used effectively for all three tasks evaluated in this dissertation. Mapping distance to color also encodes orientation differences in the surface color gradient, but mapping angle differences to color does not encode distances in any way.

There are a number of possible reasons why adding cast shadows to the principal curvature texture technique did not have a measurable effect. One reason may be that shadows make no difference. Another reason may be a lack of statistical power – it may require many more participants to statistically differentiate the two techniques. A related reason may be that the techniques do not enable participants to perceive the estimated metrics with sufficient precision to find differences between them. I hypothesize that, in fact, the rocking animation reveals too much of the shape for the shadows to have any effect. The static images of the two curvature techniques certainly seem to suggest that shadows do have some effect, and they theoretically should help ground the location of the curvature above the interior surfaces. I designed a second experiment to test the theory that allowing participants to rock the surfaces masked any benefits of cast shadows; this experiment is described in Section 5.4.

5.4 Experiment 2

The second experiment consisted of one user study designed to test whether adding cast shadows to the principal curvature texture technique had any benefit and whether allowing limited animation (surface rocking) in Experiment 1 masked that benefit. I expected that the rocking animation did, in fact, mask the benefits of cast shadows because the kinetic depth effect is triggered by the object motion and produces a very strong perception of surface shape.

This experiment used only the distance task. Including only one task deviates from the previous decision to accommodate our collaborators and perform two shape perception evaluations. The distance task is the one for which I expected principal curvature texture to realize the most benefit from cast shadows. It was also more expedient to run only the one study in this experiment.

5.4.1 User Study 2.1: Distance task

Methods

Subjects: Seven undergraduate and graduate students performed the distance task. Two participants also took part in User Study 1.2. All participants had normal or corrected-to-normal vision and reported normal color sensitivity but were not tested. Participants were compensated for their time.

Stimuli: The bump data sets from Experiment 1 were re-used for this experiment. The interface and view parameters were also the same as Experiment 1.

Design: The principal curvature texture technique was the basis for all techniques in this experiment. This study used a two-by-two factorial design for the display technique with the presence of cast shadows and the availability of rocking as the two factors. When rocking was part of the technique, participants were allowed to initiate the torsion-pendulum animation at will after its initial occurrence. When rocking was not part of the technique, it did not ever occur.

For this study, only the distance task was considered. It was presented in exactly the same manner as in User Study 1.1 (with allowances for rocking). The range of differences between region distances was restricted to 0.5 grid units through 3 grid units (approximately 1 mm through 8 mm) in 0.5 grid unit increments. The analysis of User Study 1.1 found that at the short-distance end participants performed near chance and at the long-distance end participants percentage of correct responses plateaued. Because this experiment involved four visualization techniques, reducing the number of trials also helped control the time to complete a session.

Each participant viewed 33 trials for each of the four visualization techniques for a total of 132 trials. Other aspects of each session were as in User Study 1.1. Trials were randomly ordered for each participant. Training was similar to Experiment 1.

Participants were asked to respond to the following question:

In which circled region do the two surfaces appear to be closer together?

This experiment group does not include a questionnaire.

Hypothesis

The hypothesis is that the percentage of correct participant responses depends on the presence or absence of shadows but that the presence of rocking can mask the effect.

Independent variables: The design directly manipulates three independent variables – the distance difference between regions, the presence of shadows, and the presence of rocking. Also recorded are the following predictor variables: a random unique identifier for each participant, the participant's gender, the participant's response time, and the number of times the rocking animation is triggered.

Dependent variable: The dependent variable in this experiment is the percentage of correct responses.

I expected shadows without rocking to enable better task performance than principal curvature texture with no shadows and no rocking. I expected rocking to provide more benefit than shadows, thus explaining why Experiment 1 showed no benefit for shadows.

Results

Unless otherwise noted, independent variables have no statistical significance ($p > .05$).

Analysis: Two-way ANOVA analysis finds significant main effects for rocking ($p < .001$) and response time ($p < .01$). Rocking can be said to have an overall impact on task performance, but the same can not be said for shadows. A significant interaction effect was also found between shadows and rocking ($p < .001$). The interaction can not be interpreted without a *post hoc* test. Figure 5.8 shows the overall percentages of correct responses and 95% confidence intervals by visualization technique; the figure also shows that the performance of participants is better than chance. A Tukey's HSD test finds the following:

- using any combination of rocking and shadows is better than using none,
- combining shadows and rocking is not separable from using either alone, and
- using only rocking is better than using only shadows.

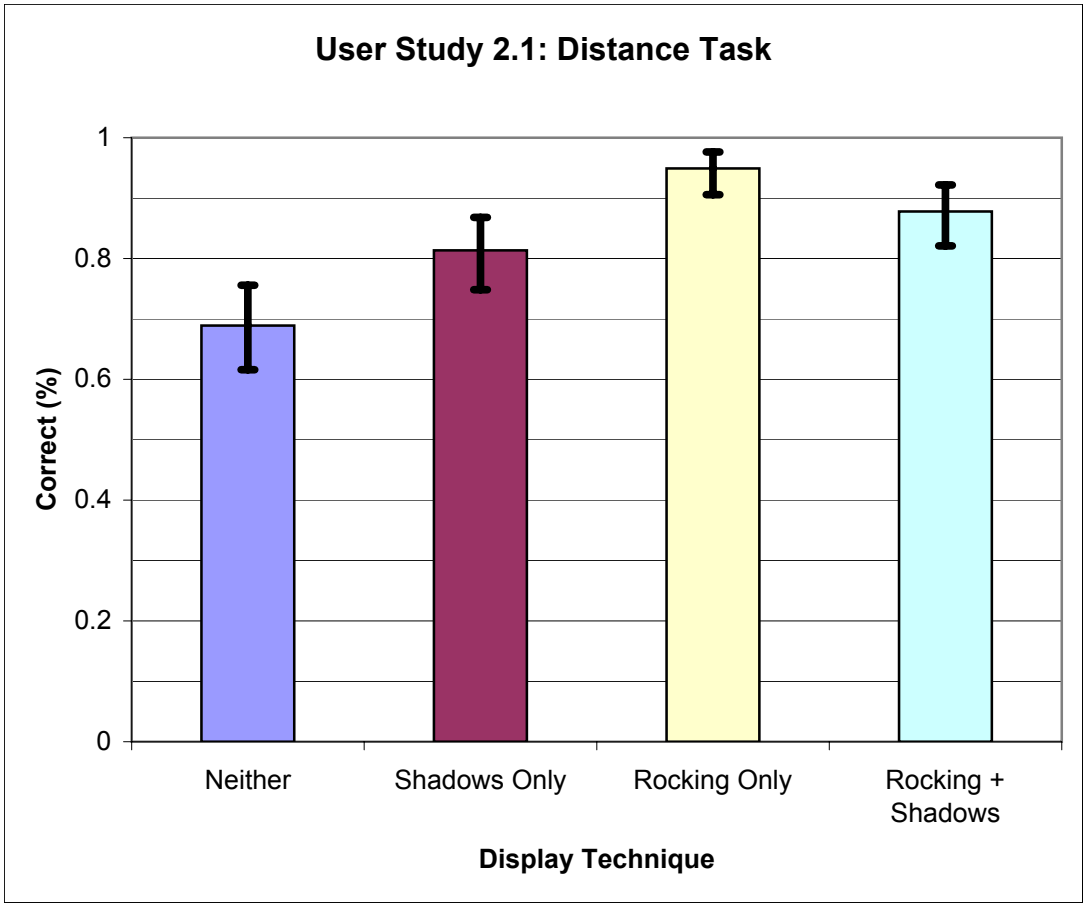

Figure 5.8: This figure shows the overall percentages of correct responses and their 95% confidence intervals for the distance task while comparing the effects of rocking and shadows applied to the principal curvature texture technique. Tukey's HSD test finds that introducing shadows or rocking to the curvature texture technique conveys inter-surface shape better the texture alone.

Given the *post hoc* Tukey's HSD test, it can be said that shadows provide a benefit in the absence of rocking.

The fact that response time is a predictor of correct responses but animation count is not a predictor suggests that response times may not be lengthened solely by triggering the animation, as I suggested in Experiment 1. However, it is still the case that participants provide more correct responses the longer the response time.

Discussion: Experiment 2 appears to support my claim that including a rocking animation in the first experiment masked any benefit shadows would have provided. This strongly suggests removing the animation component from further user studies to better control the experiments. Of more general

interest, it can be said that adding shadows to the principal curvature texture technique is beneficial for comparing inter-surface distances in static images (like those intended for print publication). If prioritizing between animation and shadows, animation should be added to the visualization first.

On the other hand, I claim a potential benefit of including shadows even in interactive visualizations (such as the exploratory visualization of interest to the scientists). Consider the perception of shape from animated point samples and how quickly the perception of shape fades once the motion stops. I claim a similar perceptual loss for principal curvature texture is possible. Cast shadows could help minimize the difference.

5.5 Experiment 3

The third experiment group consists of three user studies, comparing five visualization techniques for effectiveness with three tasks. The group uses the three visualization techniques from the previous two experiment groups with minor changes. The group adds an additional baseline technique for comparison, point-correspondence glyphs. The group also introduces one novel layered-surface visualization technique, principal curvature texture with correspondence glyphs. The experiment group uses three tasks, the distance and local shape tasks used in the previous two experiment groups, and a global shape task. The global shape task uses surface data not included in the previous experiments.

5.5.1 Data

The data sets for the distance and local shape tasks are the same as in Experiments 1 and 2.

The global shape task asks participants to indicate the presence or absence of recognizable shapes, so a class of familiar objects was chosen. Six different fruit shapes were chosen; apple, banana, cherry, grape, orange, and pear (see Figure 5.9). The fruit data are not to scale, instead they are all rescaled to be approximately the same size.

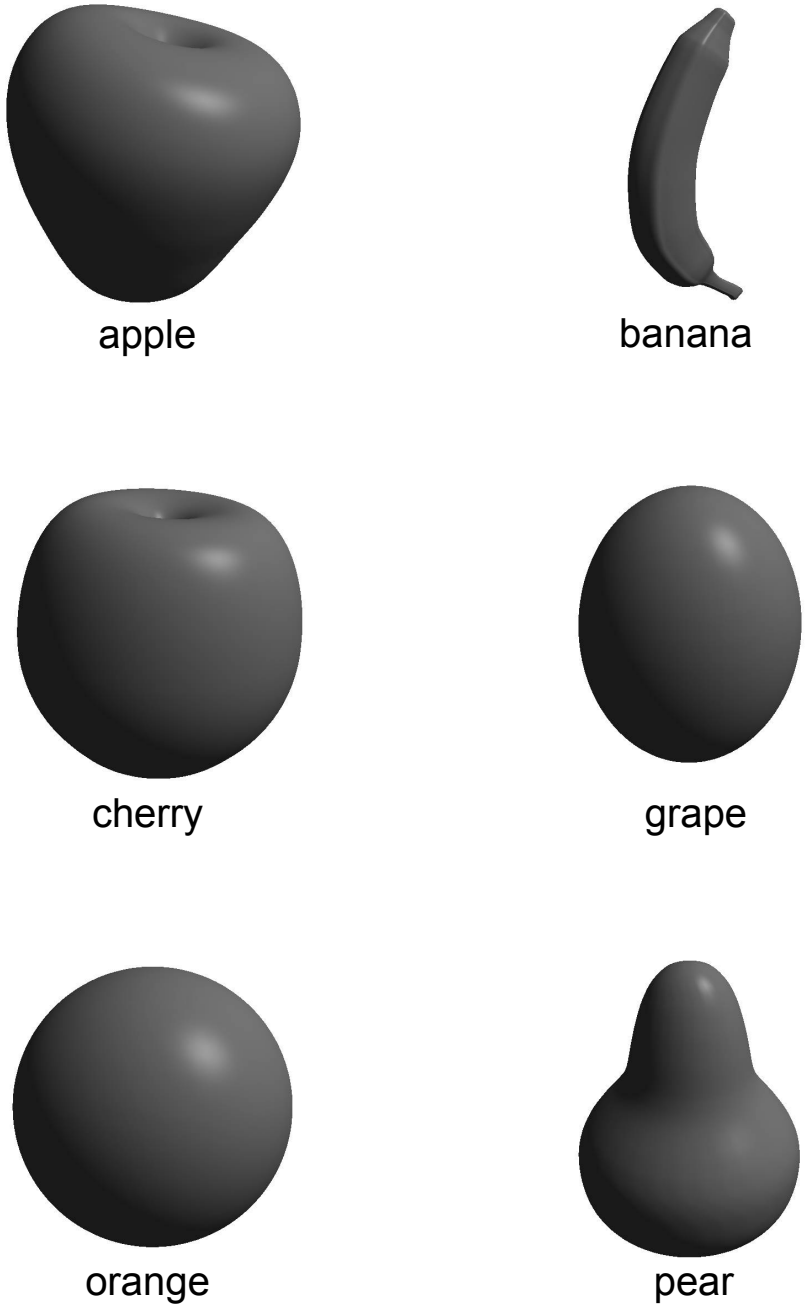

Figure 5.9: This image shows the complete set of data used for the global shape task of Experiment 3. The data were chosen to be easily recognizable.

5.5.2 Conditions: Visualization techniques

Experiments 1 and 2 use red and blue colors, including a red-grey-blue saturation scale. In the process of publishing and presenting the first two experiments, the red-grey-blue color scale was frequently questioned. In particular, some reviewers asked whether a hue only red-yellow-green color scale would lead to better performance. To answer these questions, the color scale in the color mapping technique for Experiment 3 is changed to red-yellow-green. For consistency, red and blue are changed to red and green throughout Experiment 3. Although this change does make a difference for the distance task, it does not appear to make a significant difference for the local shape task.

The visualizations in Experiments 1 and 2 utilize a regular grid for parts of the display. Texturing a height-field with a low-distortion regular grid is simple. Texturing arbitrary surfaces with a low-distortion regular grid is more difficult. In fact, the regular grid texture is commonly used to show the limitations of automatic surface parameterization techniques. Instead of implementing a technique that could texture the fruit surfaces with a low-distortion regular grid, the regular grid texture is removed from all visualizations in Experiment 3. In the techniques using principal curvature texture, the grid texture on the interior surface is replaced with a procedural noise texture which serves to help distinguish the interior from the exterior. In the remaining two techniques, which do not display interior and exterior surfaces simultaneously, neither noise nor grid texture was used.

Color mapping

As already mentioned, the color scale used for the color mapping technique is red-yellow-green. Also, the regular grid present in Experiment 1 is removed. Figure 5.10 shows examples of the implementation of the color map visualization for this experiment group. Note that now red indicates that the visible surface geometry is below (or inside) the second surface geometry, yellow indicates the intersection, and green indicates that the visible surface geometry is above (or outside) the second surface geometry.

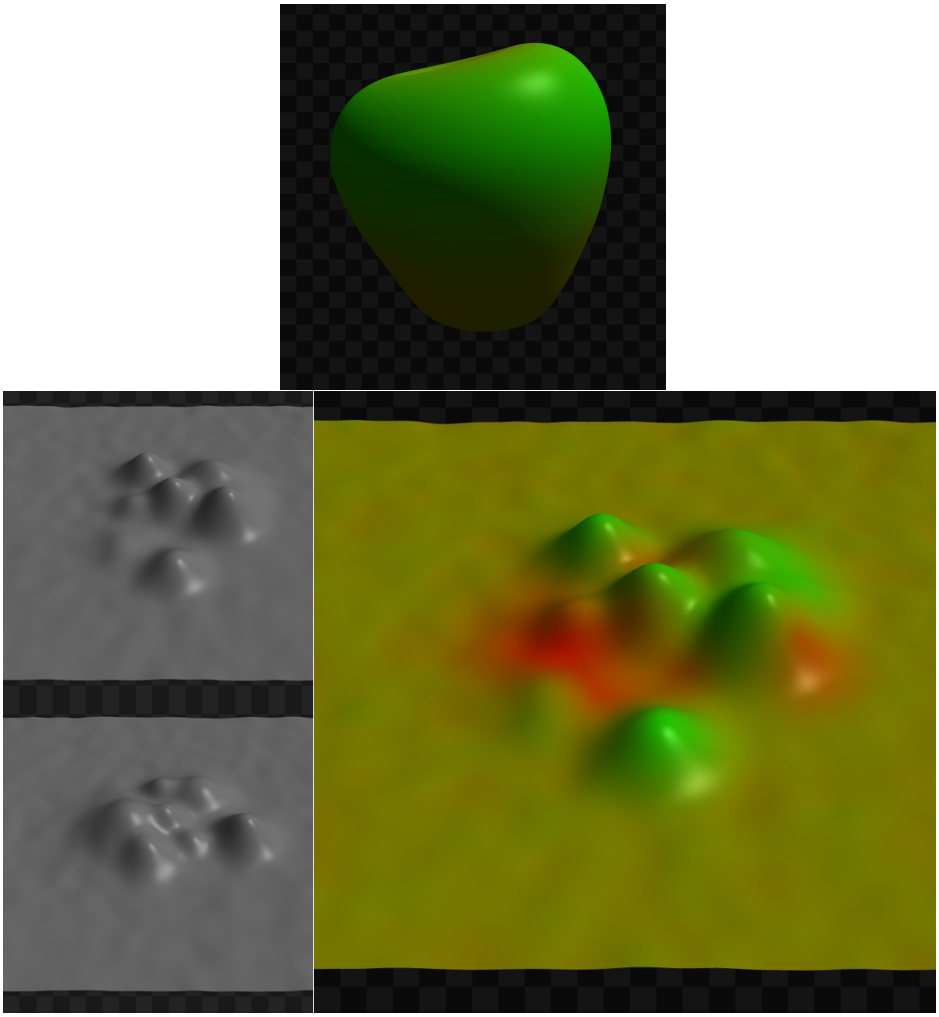

Figure 5.10: Examples of the color mapping technique. The top image uses the fruit data. The visualization is of the apple and the pear. The two surfaces on bottom left are used to produce the visualization on the bottom right.

Principal curvature texture

There are two changes from the version in Experiments 1 and 2. First, the colors are changed. Second, and more significantly, the regular grid texture on the interior has been replaced with procedural noise [Ola05]. The noise texture is more easily applied to arbitrary closed surfaces (e.g. fruit shapes) than is the regular grid. Figure 5.11 shows examples of trials used in this set of experiments.

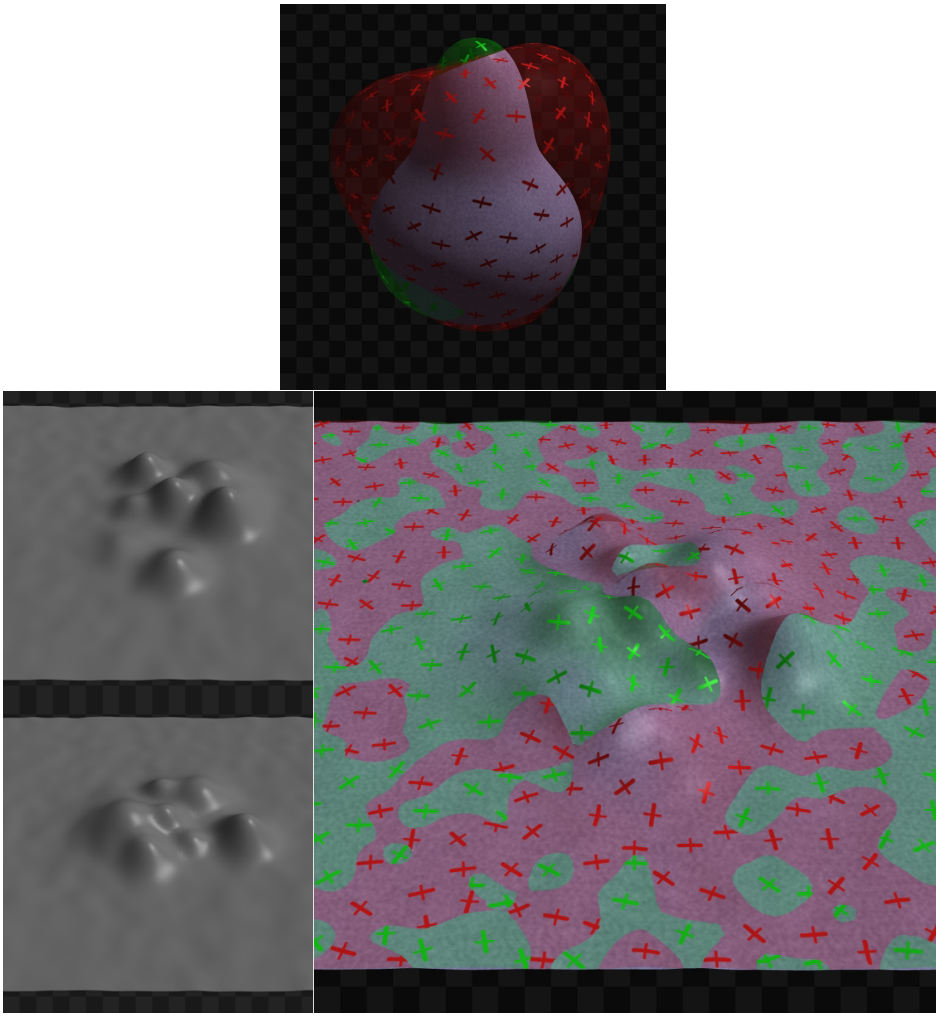

Figure 5.11: Examples of the principal curvature texture technique. The top image uses the fruit data. The visualization is of the apple and the pear. The two surfaces on the bottom left are used to produce the visualization on the bottom right.

Principal curvature texture with cast shadows

Again, the only changes as compared to Experiments 1 and 2 is color and interior texture. See Figure 5.12.

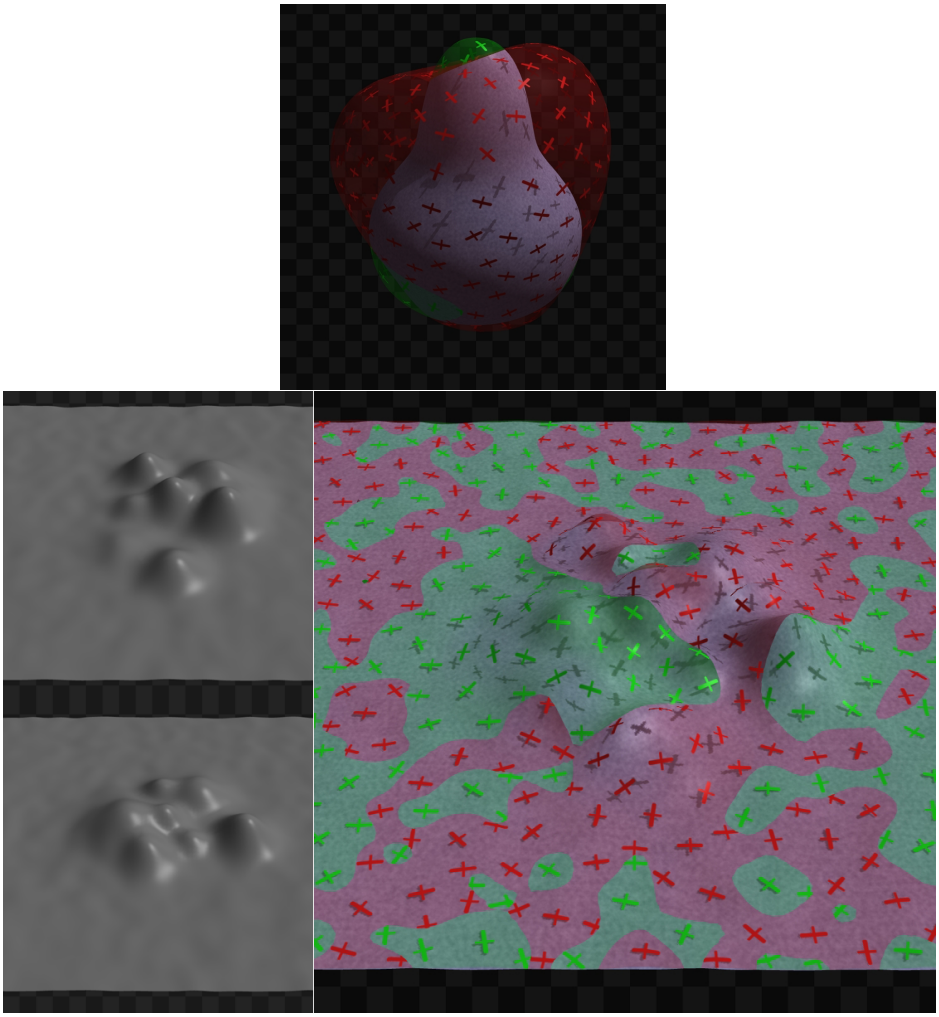

Figure 5.12: Examples of the principal curvature texture with cast shadows technique. The top image uses the fruit data. The visualization is of the apple and the pear. The two surfaces on the bottom left are used to produce the visualization on the bottom right.

Point-correspondence glyphs

This set of user studies uses an additional baseline comparison technique, point-correspondence glyphs. Line glyphs[4] on surfaces are commonly used to show a scalar field on a surface. They are also frequently used in uncertainty visualization to show the error or uncertainty in the local surface position. When used for uncertainty, they effectively sample the "error" surface and connect a point on the visible surface to its corresponding "error" point. It is this property that makes them attractive

[4]Recall that *line glyphs* are line segments attached at one end to the surface and extending for a distance related to the magnitude of the scalar field at the point of attachment.

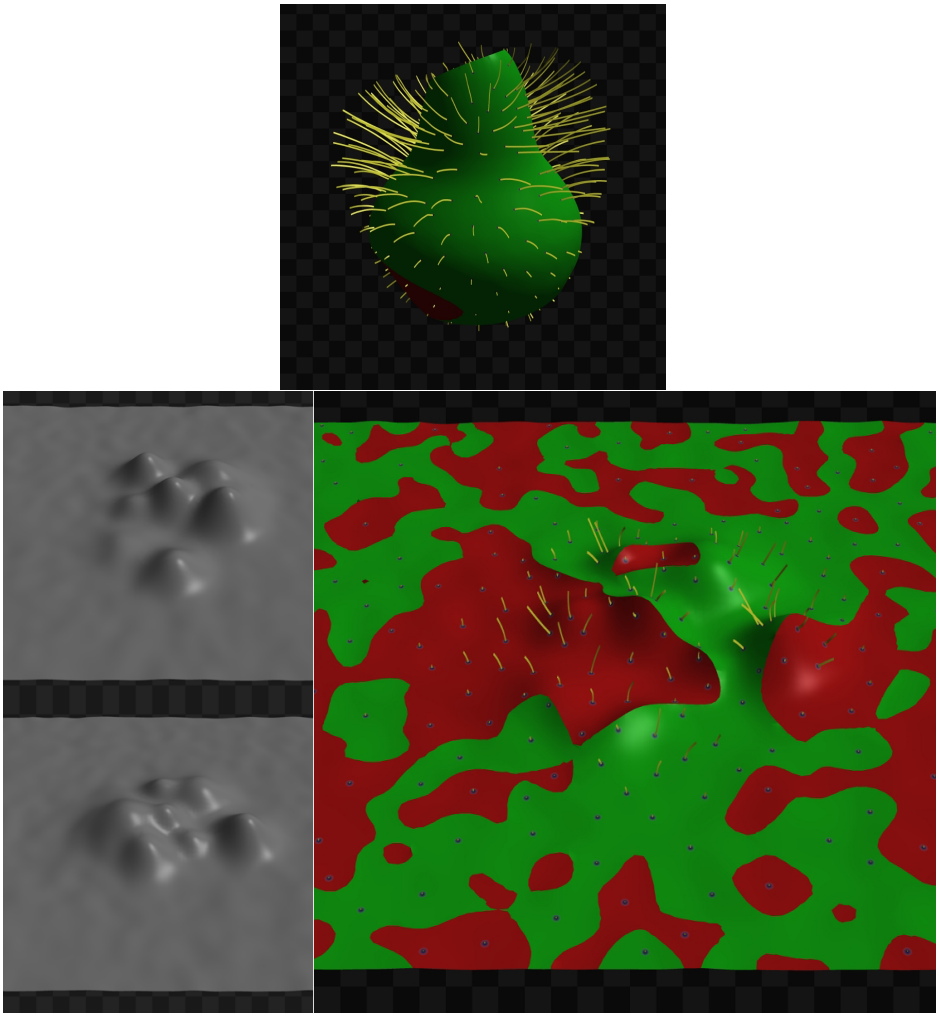

Figure 5.13: Examples of the point-correspondence glyphs technique. The top image uses the fruit data. The visualization is of the apple and the pear. The two surfaces on the bottom left are used to produce the visualization on the bottom right.

for layered-surface visualization.

In this technique, instead of the line glyph indicating error it indicates the position of the corresponding point on the second surface. Here the visible surface is the *interior* of the refactored intersecting surfaces with color used to label the original data source. The second surface, the one sampled by the unattached end of the point-correspondence glyphs, is the *exterior* of the refactored intersecting surfaces. The sampling of the exterior surface by the point correspondence glyphs is Poisson-like and relatively sparse. The sampling rate is the same as that used for the principal curvature texture techniques. See Figure 5.13. The intersecting surfaces are refactored because the correspondence glyphs

would be inside the visible surface in some regions otherwise and would not be of any benefit.

Principal curvature texture with correspondence glyphs

This visualization technique combines principal curvature texture with point-correspondence glyphs. The interior and exterior surfaces are displayed as in the other curvature texture techniques; the interior is grey with a noise texture and the exterior is translucent with curvature-glyph texture using color as a data label. Additionally, yellow point-correspondence glyphs connect the center of each curvature-glyph texture to its corresponding interior point. See Figure 5.14.

5.5.3 Tasks

The distance task and local shape tasks are included in this set of experiments. They are presented as they were in Experiment 1 except for the number of visualization techniques and the number of distinct trials. Because there are now 5 visualization techniques for evaluation, the range of differences to compare is smaller than in Experiment 1 (as in Experiment 2, by removing the extreme ends of the ranges) to keep the total number of trials about the same.

The third user study in this set is the global shape task. One reason for the inclusion of some global shape task is that the scientists indicated interest in questions about global trends (i.e. percentage of inter-surface distance below some threshold). These questions were very difficult to design shape perception task around but could be touched on with a global task. Further, because of the complexity of the visualizations, it seemed expedient to include a task that might show that individual global shapes could still be understood.

I decided to make the global shape task fit into the framework of the other tasks (forced choice between two options). I considered many versions of the global shape task of the form, "Does one of the two surfaces depicted in this image *possess some property*?" For instance, one of the rejected versions included expressive faces. Expressive faces (e.g. surprised, sad, happy, etc.) were rejected because of the perceptual machinery in the human visual system specifically tuned to recognizing faces [KMC97]; there was concern that the results would come into question due to the unquantifi-

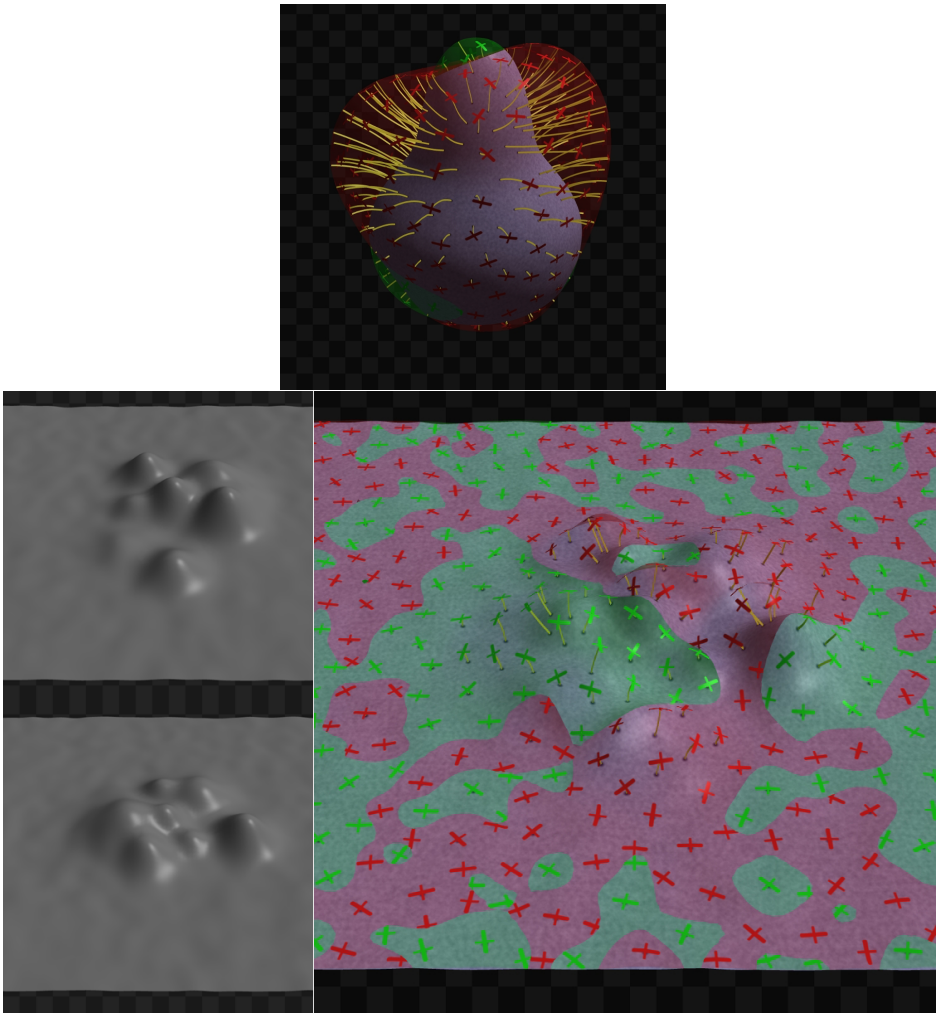

Figure 5.14: Examples of the principal curvature with point-correspondence glyphs technique. The top image uses the fruit data. The visualization is of the apple and the pear. The two surfaces on the bottom left are used to produce the visualization on the bottom right.

able contribution of this machinery. Other potential sets of data were rejected for not being easily recognized by a naive population or for not clearly requiring perception of the global shape.

The global shape task uses a small set of recognizable fruit as data. In fact, most types of fruit have many common varieties, so participants are given a set of images showing each fruit model rendered alone to avoid confusion due to preferred varieties[5] (see Figure 5.9). Participants are shown a random pairing of fruit (same-same pairings do not occur) and asked if one of the six types of fruit is present

[5]For example, one participant questioned the shape of the pear until I explained that it was an European pear not an Asian pear.

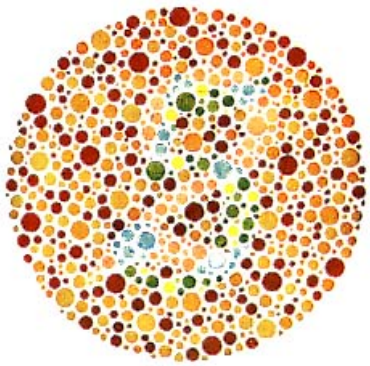

Figure 5.15: A color-sensitivity test in the style of Ishihara [Ish94]. An individual with normal color vision will see the number 5. An individual with red/green color blindness will see the number 2.

or not.

5.5.4 Questionnaire

This set of user studies included a questionnaire. The questionnaire consisted of two questions:

1. On a scale of 1 to 9, how well did each display present the information you needed to perform the task?

2. How would you rank the effectiveness of each display?

These are essentially the same questions asked in Experiment 1.

5.5.5 Screening

The visualizations in this experiment group use the colors red and green extensively. The most common forms of anomalous color sensitivity fall in the red-green perceptual color channel. Potential participants are therefore screened for normal color perception before they begin their trial. I used the standard Ishihara test for color blindness (see Figure 5.15) [Ish94].

5.5.6 User Study 3.1: Distance task

Methods

Subjects: Twelve graduate students performed the distance task. All participants had normal or corrected-to-normal vision and were screened for normal color sensitivity using the standard Ishihara test for color blindness. Participants were compensated for their time.

Stimuli: The participants viewed images of the bump data under the following visualization techniques: color mapping, point-correspondence glyphs, principal curvature texture, principal curvature texture with shadows, principal curvature texture with point-correspondence glyphs. The rocking animation present in the previous experiment groups is not included in this user study.

Design: This user study compares the five visualization techniques for enabling the distance task. Each participant viewed 25 unique, random surface pairs per visualization technique for a total of 125 trials.

Participants estimated how closely the two surfaces approached each other within each of a pair of indicated regions and reported which of the pair of regions contained the closer approach (the smaller distance). The regions were selected such that differences in closest approach were uniformly distributed between 0.5 and 2.5 grid units (approximately 1 mm to 6 mm) in 0.5 grid unit steps. Trials were randomly ordered for each participant. All other parameters were as in Experiment 1.

Participants were asked to respond to the following question:

In which circled region do the two surfaces appear to be closer together?

Each session began with a short training exercise, as in Experiment 1.

Hypothesis

The hypothesis is that the percentage of correct participant responses depends on the visualization technique and on the difference between the region distances.

Independent variables: The design directly manipulates two independent variables – the distance difference between regions and the visualization technique. Also recorded are the following predictor variables: a random unique identifier for each participant, the participant's gender, and the participant's response time.

Dependent variable: The dependent variable in this experiment is the percentage of correct responses.

I expected the percentage of correct responses to depend on the difference between the compared distances and on the visualization technique. I expected participants would be able to compare distance effectively with the color mapping technique because it directly encodes the necessary information. I expected participants would be able to compare distance somewhat less well with the point-correspondence technique because it encodes only a rough upper bound on the distance information. I expected participants would perform better with principal curvature texture with shadows or point-correspondence than without either.

Results

Unless otherwise noted, independent variables have no statistical significance ($p > .05$).

Analysis: ANOVA analysis finds significant main effects for the distance difference between marked regions ($p < .05$) and the visualization technique ($p < .02$). Again, the correlation between correct responses and the relative distance difference is not surprising. Figure 5.16 shows the overall percentages of correct responses and 95% confidence intervals by visualization technique; the figure also shows that the performance of participants is better than chance. A Tukey's HSD test finds that the principal curvature texture technique was the worst performer with participants performing significantly better when using any of the other techniques. On other statistical differences can be found.

Responses to the questionnaire showed that participants also selected principal curvature texture as the lest effective technique. However, the participants did distinguish between the other techniques, greatly preferring the two techniques with point-correspondence glyphs over the others and preferring

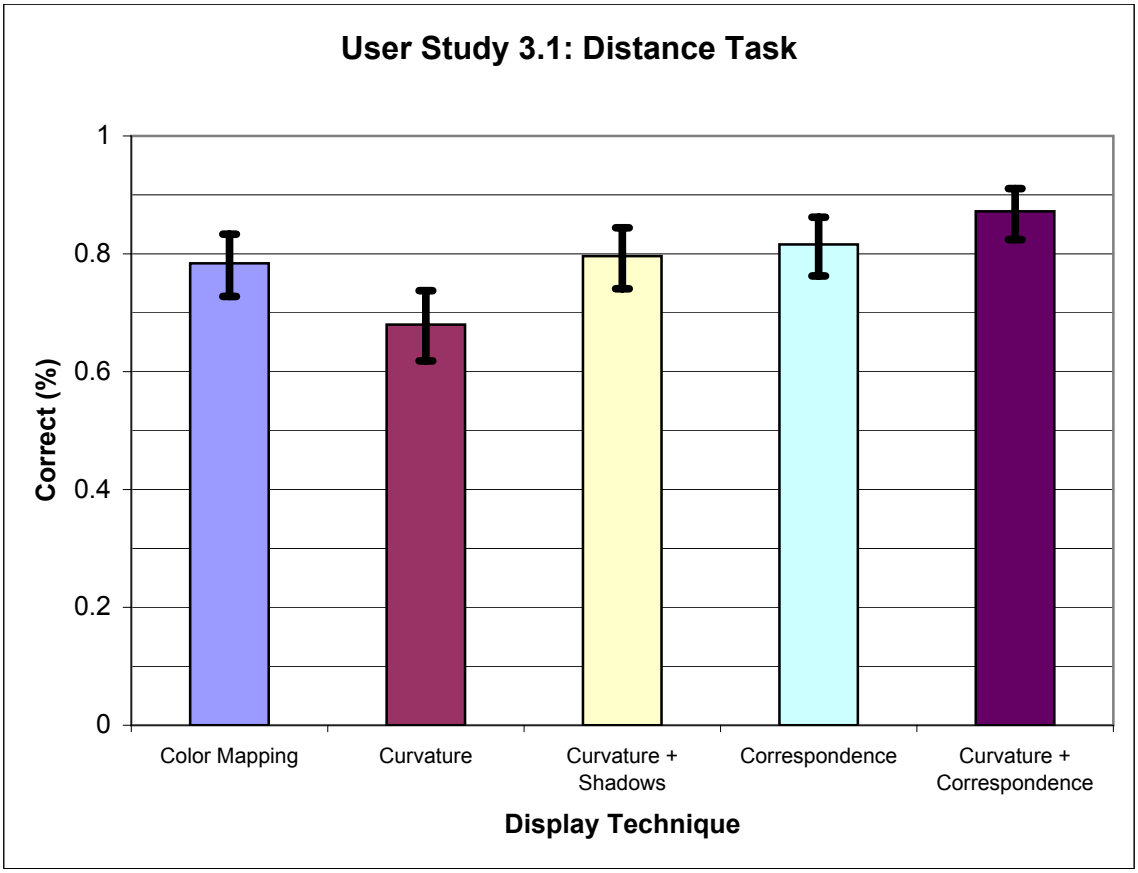

Figure 5.16: This figure shows the overall percentages of correct responses and their 95% confidence intervals for the distance task. Tukey's HSD test finds that the principal curvature texture technique is statistically different from all the other techniques.

principal curvature texture with point-correspondence glyphs most of all. On average, the participants did not distinguish between the color map visualization and the principal curvature texture with shadows.

Discussion: The user study results show principal curvature texture alone to provide the worst task performance. All other techniques are statistically tied. Principal curvature texture with correspondence glyphs shows the highest percent correct, though it is only statistically different from principal curvature alone.

The change in color scale (red-grey-blue changes to red-yellow-green) does appear to improve the performance of the color mapping visualization relative to principal curvature alone and principal curvature with shadows. In User Study 1.1, the color mapping technique performed worse than either

of these principal curvature texture techniques. Also note that response time dose not appear to predict the percentage of correct responses as it did in Experiments 1 and 2.

5.5.7 User Study 3.2: Local shape task

Methods

Subjects: Thirteen graduate students performed the local shape task. All participants had normal or corrected-to-normal vision and were screened for normal color sensitivity using the standard Ishihara test for color blindness. Participants were compensated for their time.

Stimuli: The participants viewed images of the bump data under the following visualization techniques: color mapping, point-correspondence glyphs, principal curvature texture, principal curvature texture with shadows, principal curvature texture with point-correspondence glyphs. The rocking animation present in the previous experiment groups is not included in this user study.

Design: This user study compares the five visualization techniques for enabling the local shape task. Each participant viewed 30 unique, random surface pairs per visualization condition, for a total of 150 trials.

Participants estimated the local shape of each surface within indicated pairs of regions and reported which of the pair of regions contained the smallest orientation difference (the smaller angle difference between surface normals). The region pairs were selected such that differences in local orientation between pairs were uniformly distributed between 10 and 30 degrees in 5 degree steps. Trials were randomly ordered for each participant. All other parameters were as in Experiment 1.

Participants were asked to respond to the following question:

In which circled region do the two surfaces appear to be more similarly oriented or parallel?

Subjects received training as in Experiment 1.

Hypothesis

The hypothesis is that the percentage of correct participant responses depends on the visualization technique and on the difference between the region orientation differences.

Independent variables: The design directly manipulates two independent variables – the difference between region orientation differences and the visualization technique. Also recorded are the following predictor variables: a random unique identifier for each participant, the participant's gender, and the participant's response time.

Dependent variable: The dependent variable in this experiment is the percentage of correct responses.

I expected the percentages of correct responses to depend on the magnitude of the difference between the compared local orientations and on the visualization technique. I expected participants would be able to compare local shape least well with the color mapping technique. I expected participants would be able to compare local shape better with principal curvature texture alone and with point correspondence. I expected participants would be able to compare local shape best with principal curvature texture combined with either shadows or point-correspondence.

Results

Unless otherwise noted, independent variables have no statistical significance ($p > .05$).

Analysis: ANOVA analysis finds significant main effects for the local shape difference between marked regions ($p < .01$), the visualization technique ($p < .001$), and the participant ($p < .001$). The meaning of the significance of difference between regions and the participant identifier is as in previous user studies. Figure 5.17 shows the overall percentages of correct responses and 95% confidence intervals by visualization technique; the figure also shows that the performance of participants is better than chance. A Tukey's HSD test finds that the color mapping technique, the principal curvature texture technique, and the point-correspondence technique performed worse than principal curvature texture with either shadows or point-correspondence glyphs. No statistical differences can be found

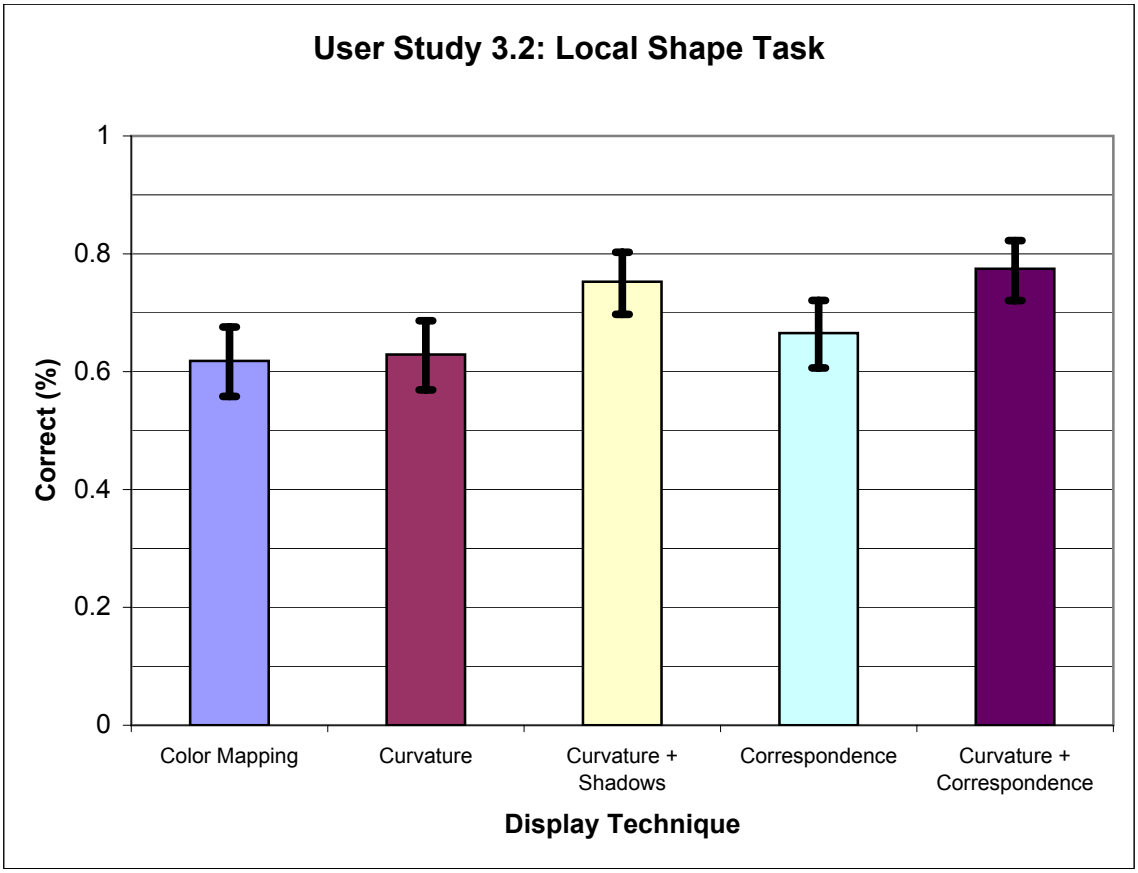

Figure 5.17: This figure shows the overall percentages of correct responses and their 95% confidence intervals for the local shape task. Tukey's HSD test finds that the techniques fall into two statistically different groups. Principal curvature texture with either shadows or point-correspondence are in the higher percentage correct group.

within these two groups.

Responses to the questionnaire showed that participants again selected principal curvature texture as the lest effective technique. The participants also selected the two correspondence techniques as the best performing. On average, participants ranked the performance of principal curvature texture with shadows above color mapping.

Discussion: The user study results show principal curvature with either shadows or point-correspondence glyphs to provide the best task performance. All other techniques are statistically tied. Principal curvature texture with correspondence glyphs shows the highest percent correct, though it is not statistically different from principal curvature with shadows.

The change in color scale (red-grey-blue changes to red-yellow-green) does not appear to provide a benefit for the color mapping visualization with the local shape task. Also note that response time dose not appear to predict the percentage of correct responses as it did in Experiments 1 and 2.

5.5.8 User Study 3.3: Global shape task

Methods

Subjects: Five graduate students performed the local shape task. All participants had normal or corrected-to-normal vision and were screened for normal color sensitivity using the standard Ishihara test for color blindness. Participants were compensated for their time.

Stimuli: The participants viewed images of the fruit data under the following visualization techniques: color mapping, point-correspondence glyphs, principal curvature texture, principal curvature texture with shadows, principal curvature texture with point-correspondence glyphs. The rocking animation present in the previous experiment groups is not included in this user study.

Design: This user study compares the five visualization techniques for enabling the global shape task. Each participant viewed 25 surface pairs per visualization technique, for a total of 125 trials.

Participants estimated the global shape of the intersecting objects and determined if either was a specified target object. Trials were randomly ordered for each participant.

Participants were asked to respond to the following question:

Is the *fruit* present in this pair of objects?

The text *fruit* is replaced with the name of one of the 6 types of fruit in the data set.

Training was similar to the other user studies in this experiment group.

Hypothesis

The hypothesis is that the percentage of correct participant responses depends on the visualization technique.

Independent variables: The design directly manipulates one independent variable – the visualization technique. Also recorded are the following predictor variables: a random unique identifier for each participant, the participant's gender, and the participant's response time.

Dependent variable:

For the color mapping technique, I expected participants to perform the task well in the case where the target fruit was the visible surface (8 of 25 trials). I further expected participants to perform at chance if the target fruit was not visible, either as the hidden surface (5 of 25 trials) or not present (12 of 25 trials). I expected an 66 percent correct responses for the color mapping technique. For the remaining techniques, I expected participants to perform well as the techniques would show the fruit silhouettes, which is sufficient to recognize the fruit in most cases.

Results

Unless otherwise noted, independent variables have no statistical significance ($p > .05$).

Analysis: ANOVA analysis finds significant main effects for the visualization technique ($p < .001$). Figure 5.18 shows the overall percentages of correct responses and 95% confidence intervals by visualization technique; the figure also shows that the performance of participants is better than chance. A Tukey's HSD test finds that the color mapping technique produced the worst performance, the point-correspondence technique produced better performance, and the principal curvature texture techniques produced the best performance. No statistical differences can be found within the group of texture techniques.

Responses to the questionnaire agreed with the performance analysis. Participants indicated a marginal overall preference for the principal curvature texture with point-correspondence glyphs technique.

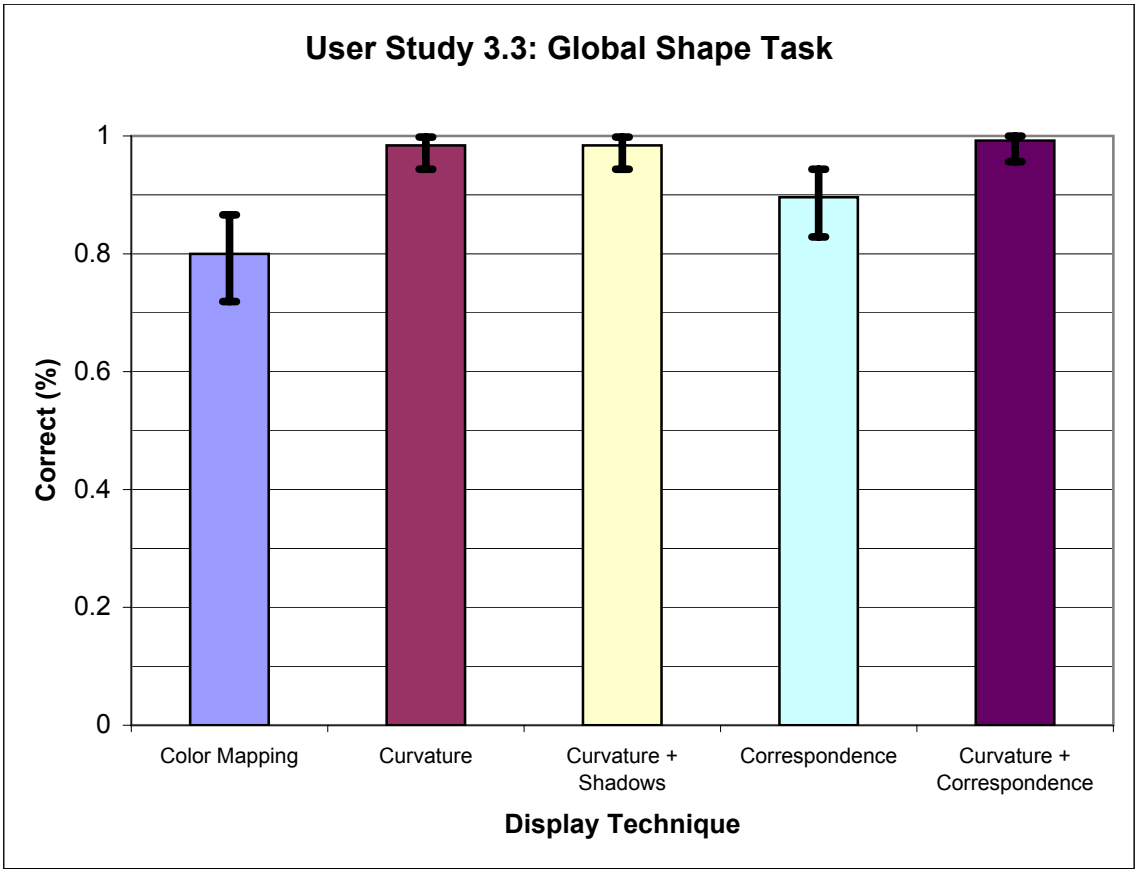

Figure 5.18: This figure shows the overall percentages of correct responses and their 95% confidence intervals for the global shape task. Tukey's HSD test finds that the techniques fall into three statistically different groups. Principal curvature texture techniques make up the highest performing group. The color mapping technique is the lowest performing technique. The point-correspondence technique falls between the other two groups.

Discussion: The principal texture based techniques provided the best performance. The color mapping technique provided the worst performance. The point-correspondence technique provided performance between these two extremes. Again, principal curvature texture with point-correspondence produced the most correct responses but did not show a statistically significant difference from the next best performer.

The color mapping technique did perform better than expected (66 percent correct responses expected). Further analysis shows that the participants responded as expected in the cases where the specified fruit was present whether it was hidden or not but outperformed expectation when the specified fruit was not present in the visualization. One possible explanation is that certain fruits (such as

the banana) produced easily recognizable color patterns, so it would be relatively easy to determine that it was not present.

5.5.9 Experiment discussion

The red-yellow-green color scale does appear to perform better, at least for directly reading a distance metric from the color scale, than the red-grey-blue color scale. The red-yellow-green scale made no significant difference for the local shape task. The color map visualization also enabled the poorest performance for the global shape task. This is not surprising because the technique shows only a single surface, and the second surface must be inferred from the pattern of color. Those color patterns are often ambiguous, making it difficult to determine the shape of the second surface.

Principal curvature texture alone appears to be a relatively poor technique overall. Although it was in the best performing group for the global shape task, it was in the worst performing group for the other two tasks. Its performance in the global shape task may be entirely attributable to showing the silhouettes of both objects.

Point-correspondence alone performed as expected overall. It was surprising that it was not in the best performing group for the global shape task, but this is more likely attributed to the density of the correspondence glyphs along the interior surface interfering with silhouette completion. The intersection-refactored variant of point-correspondence in this study performed better overall than would an non-refactored version because the line glyphs would not be a useful shape cue in regions where they lie inside the non-refactored surface.

Principal curvature texture with shadows continued to perform at least as well if not better than curvature texture alone. The shadowed version of the technique was also preferred over the unshadowed version by participants.

Principal curvature texture with point-correspondence glyphs proved to be both the best overall performer and the participant favorite. Participant performance with the technique was in the best performing group for all tasks, and it received the highest scores and ranking in the questionnaire for all tasks.

5.6 Summary of Evaluation Results

The results of Experiment 1 show that refactoring intersecting surfaces into non-intersecting surfaces does enable for the effective application of nested-surface visualization to a broader range of layered surfaces. I would expect other nested-surface techniques, such as Rheingans', to also produce effective visualizations on refactored surfaces.

The results of Experiment 2 show that there is a benefit to including cast shadows, but that the benefit can be overpowered by motion. I claim that shadows are still beneficial in interactive applications, and are especially useful for presentation of static visualizations. Therefore, cast shadows should not be excluded from visualization tools just because the kinetic depth effect proves a stronger shape cue. Indeed, reinforcing shape perception with multiple cues is generally considered good visualization practice.

The results of Experiment 3 show that the two novel techniques developed for this dissertation, principal curvature texture with cast shadows and principal curvature texture with point-correspondence glyphs, provided the best combined performance. These two techniques are both recommendable for exploratory visualization of general layered surfaces. Although the cast shadows may be difficult to interpret for more regular textures, such as Rheingans', the point-correspondence glyphs should provide similar benefit if combined with techniques beyond principal curvature texture.

Of the published layered-surface techniques (Interrante [IFP96], Rheingans [Rhe96], and Bair *et al.* [BHW05]) only Interrante and Bair *et al.* conducted user studies, and they both used stereo display. Further, only Interrante compared her technique against other techniques; Bair *et al.* was exploring a large parameter space of textures by steering genetic algorithms according to participant responses to shape perception tasks. It is therefore difficult to compare these results with the other existing techniques or to use such comparison to draw conclusions about techniques tested by others.

Although the performance difference between principal curvature texture with point-correspondence glyphs and principal curvature texture with shadows is not statistically significant, texture with correspondence did consistently provide the highest percentage of correct responses for all tasks. For that reason, if I were to recommend only one technique on the basis of perception alone, it would

be texture with correspondence. However, if computation cost were also a consideration, I would recommend texture with shadows instead.

Chapter 6

Conclusions

I have introduced a novel refactoring of intersecting surfaces that enables existing nested-surface techniques to be applied more broadly to intersecting surfaces. By refactoring geometry at the surface intersections, regions of the intersecting-surface geometry can be categorized as *interior* or *exterior*. The refactored intersecting surface can then be visualized with nested-surface techniques.

I have introduced two novel general layered-surface visualization techniques. The techniques build on a variation of an existing nested-surface technique, principal curvature textures, and the novel refactoring algorithm. The first novel technique adds cast shadows and is shown to improve shape perception task performance over principal curvature texture alone. The second novel technique adds point-correspondence glyphs (instead of shadows) and is shown to improve the shape perception task performance over principal curvature texture alone and over the shadow technique.

I have interviewed five scientists about their potential use for general layered-surface visualization techniques, and from these interviews constructed a set of user study tasks for evaluating such techniques. The set of techniques specifically addresses the shape perception issues common to the five scientists and their data exploration needs. I have used these user study tasks to develop and evaluate two novel general layered-surface visualization techniques.

I expect that other nested-surface visualizations can benefit from one or both of shadows and point-correspondence glyphs. For instance Rheingans' opacity-modulating triangle textures [Rhe96] might not be a good fit for shadows – because it might be difficult to infer the correspondence between

the regular texture on the exterior surface and its cast shadow – but it should work well with point-correspondence glyphs.

6.1 Thesis Statement

My thesis statement consists of three claims, all of them supported by the results of the user studies.

Claim 1: *Union/intersection refactoring of intersecting surface geometry into non-intersecting components enables the effective application of existing nested-surface visualization techniques to general layered-surface data.*

The union/intersection refactoring converts intersecting surfaces into nested surfaces. This enables a number of existing nested surface techniques to be applied in a straightforward manner to a larger class of layered surfaces. In particular, this has enabled nested surface techniques to be applied to surface data that a group of scientists care about. The user study results bolster this claim; the principal-curvature texture technique has been shown to be moderately effective at enabling participants to perform shape perception tasks on intersecting surfaces.

Claim 2: *Two novel layered-surface display techniques, relying on the refactoring algorithm and utilizing (1) cast shadows or (2) point-correspondence glyphs, enable better shape perception for a pair of general layered surfaces than a set of previous techniques.*

Color mapping, point-correspondence glyphs (alone), and principal curvature texture (alone) are all considered previous techniques. In all of the six studies participants perform the tasks as well or better with the two novel techniques than they do with the previous techniques. Thus the user studies establish this claim as true.

Claim 3: *The novel techniques also preserve the ability to comprehend the shape of the individual surfaces.*

In User Study 3.3, the novel techniques, as well as the others, are evaluated with a global shape task. Participants are asked to determine the presence or absence of particular fruit shape in a visual-

ization of two intersecting fruit shapes. Both novel techniques enabled very high accuracy at this task. Thus result of User Study 3.3 establishes this claim.

6.2 Do the techniques satisfy user needs?

Recall from Section 2.3 that six questions were identified for specifying tasks in the evaluation studies. Also recall that question five, which pertained to volume estimation, was excluded from the evaluation studies.

Question 1 asks *Where are the two surfaces separated by more or less than some threshold?* Question 2 asks *How far apart are the two surfaces here?* Question 3 asks *What percent of the two surfaces are separated by more or less than some threshold?* All three questions pertain to estimating or comparing distance between intersection surfaces. The evaluation studies show that users could correctly perform a distance estimation and comparison task most often with the recommended visualizations.

Question 6 asks *Where are the surface intersections?*, and is answerable from these visualizations. Both recommended visualizations display the two objects as different colors, so the intersections can be identified as the change from one color to another.

Question 4 appears in three related parts, *Are the apparent differences consistent with* ***some hypothesis****?* The three hypotheses are *misalignment*, *missing features*, and *feature distortion*. All three hypotheses are concerned with estimating and comparing the shape of the two surfaces. Users provided the most correct responses to tasks evaluating local and global shape perception with the recommended visualizations.

Considering these questions and the evaluation study results, I would claim that the recommended techniques are the most capable (of those techniques compared) at answering scientists questions.

6.3 Recommendations and Limitations

It has been shown in this dissertation that principal curvature texture combined with either shadows or correspondence provides the best intersecting-surface visualization (of the techniques evaluated). This dissertation contains the most comprehensive comparitive evaluation yet performed of techniques for display of intersecting surfaces. As such, these two techniques (texture plus shadows or texture plus correspondence) are the *de facto* recommended techniques for visualization of layered surfaces.

I do not believe that the use of texture that indicates principal curvature information on the surface is of critical importance to the effectiveness of the techniques. The important aspects of the exterior surface texture are that it contains both translucent and opaque regions and that the opaque regions are dense enough to reveal exterior surface shape while simultaneously sparse enough to reveal interior surface shape. Indeed, Interrante found that a regular grid texture in some cases outperformed principal curvature texture for a shape task identifying closest approach between nested surfaces [IFP97].

In general, either of these two techniques can be recommended for visualizing nested or intersecting surfaces. Specifically, when point correspondence information is important or available it is recommended that the texture with correspondence technique be employed. If the correspondence information is not available and not important to the exploration of the surfaces, it is recommended that the texture with shadows technique be employed. The computation of a suitable point correspondence mapping from two surfaces with no *a priori* correspondence relationship is to expensive to justify (recall that no statistical difference exists between the two techniques for performance of the evaluated tasks).

Neither of these two techniques can be said to solve all visualization problems for intersecting surfaces. The following sections will lay out the limitations of the two techniques and, where possible, recommendations of the best way to handle facing those limitations.

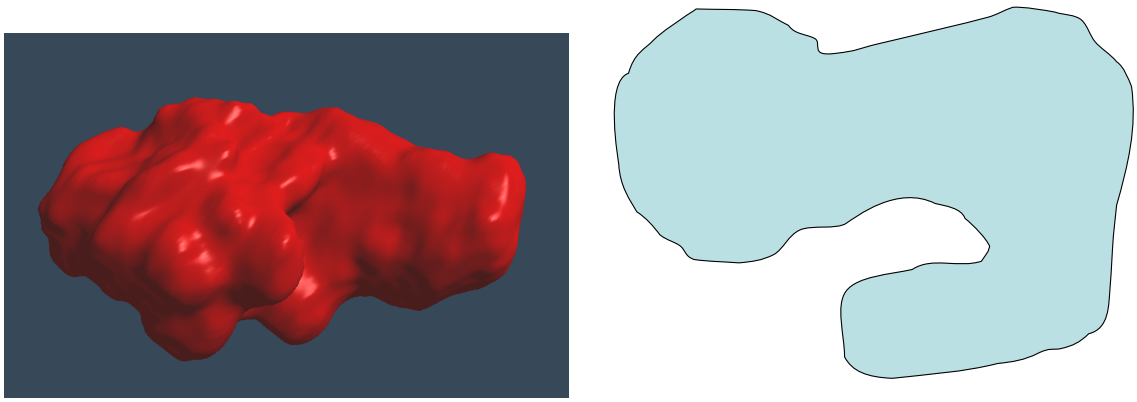

Figure 6.1: The image on the left is of a tumor surface. Note the protuberance on the left side of the tumor which folds back toward the right occluding a significant portion of the tumor. The image on the right is a 2D sketch of an oppositely folded surface.

6.3.1 Self-occluding surfaces

Many real world objects (such as the examples in Figure 6.1) have complex geometries that fold over such as to occlude other regions of the object when viewed from certain directions. For instance, the fingers of the relaxed human hand curl so as to "fold" over the palm. Fully exploring such surfaces usually relies on interactive visualization tools where the user controls the position and orientation of the view.

One should expect the same – interactive control – in a tool for exploring nested or intersecting surfaces. Indeed, because the most effective techniques for displaying nested or intersecting surfaces display portions of the occluding surface opaquely (via opacity-modulating texture), interactive control is necessary to explore the interior surface to the fullest. Also, interactive control greatly increases the understanding of the readily viewable shapes because of the kinetic depth effect, so such control is beneficial even when objects are not self-occluding.

6.3.2 Shape at scale

The techniques shown through human-subjects experiments (in this dissertation and other works) to effectively convey shape for nested or intersecting surfaces use opacity-modulating texture. Opacity-

modulating texture uses surface texture to alternate the occluding surface between opaque and translucent, enabling portions of both surfaces to be visible. The density of the opaque regions (equivalently, the frequency of the modulation) is critical to understanding both surface shapes simultaneously. The frequency of opaque regions in the texture pattern determines the texture's sampling of the occluding surface, but the surface may contain features at higher frequency than the texture's modulation frequency.

A common solution to sampling domains with varying frequency content is adaptive sampling. In adaptive sampling, some local metric on the domain is used to determine the local sampling rate within the domain. Adaptive sampling can be applied to adjust the sampling rate of the texture in an effort to capture significant high-frequency features. One method for accomplishing this is to vary the sampling frequency proportional to the magnitude of the local surface curvature. The resulting texture will be irregular unless the underlying surface has uniformly distributed frequency characteristics, so it generally will not be possible to produce regular texture as in Rheingans work [Rhe96]. However, localized irregularities in an otherwise regular texture will draw attention to higher-curvature regions, which may itself be a desirable effect of the visualization.

6.3.3 Small regions of intersection

Often, two intersecting objects may share a very small volume of overlap relative to their own volumes. Such cases are very different from those studied in this dissertation, and the techniques developed herein assume a large amount of object overlap. The two recommended techniques are developed around cases where the two objects are relatively close in volume as well as close in "registration" (i.e. their common features are relatively close in space).

When the two intersecting surfaces are not close in volume (i.e. one is significantly smaller than the other), neither of the two recommended techniques may provide a better understanding of the two surfaces than texture alone. The addition of shadows in such a case is unlikely to hinder understanding but correspondence glyphs may. When the two intersecting surfaces a not close in registration, it may be that it is sufficient simply to highlight the intersection without applying any of the techniques in

this dissertation. If the penetration depth between the two surfaces is important, one solution might be to use texture on both surfaces in the vicinity of their intersection, and use the point correspondence glyphs within the penetration.

6.3.4 Obvious versus non-obvious correspondences

The bump surfaces used in the evaluation studies in this dissertation were generally in close registration with each other – meaning their obvious features were in close proximity to each other. The data collected from domain scientists for this work also have the property that pairs of surfaces are in close registration. However, real data from other application areas may not have this property. In particular, objects that have obvious correspondences that are not closely registered with each other may pose special problems for visualizing with these techniques.

As an example of objects with obvious correspondence, suppose we had two statistical models of some recognizable object, say a human hand in a relaxed pose. Assume the difference between the two models has to do with some condition that effects the curl of the fingers in a relaxed pose. So the features of each hand are the same, but they are not all in close registration. Assuming the correspondence mapping is the expected or obvious one, it is helpful to display in the sense that it reinforces the expected correspondence.

Examples of non-obvious correspondences include shape features of one surface (i.e. bumps, dimples, vortices, folds, cusps) that correspond to very different features of the other surface. Assuming the correspondence mapping is not the expected or obvious one, it is helpful to show the true correspondence if the correspondence information itself is of importance. I claim it is also helpful to show the non-obvious correspondences when domain specific questions pertain to the evolution of one surface into the other, such changes in an object over time or changes in a model due to modification of model parameters.

Many of these shape features of interest may have a critical or extremal point that is especially useful to denote. Finding these points to best approximation and including them in the sampling of both the exterior surface (through use of opaque texture) and as an end point for correspondence

glyphs would also be of significant value in depicting the surfaces and their correspondences.

6.3.5 More than two surfaces

The evaluations in this dissertation focus on a pair of intersecting surfaces. Real science often requires the exploration of more than a pair of surfaces. For example, radiation treatment planning can involve the three common tumor volumes (Gross Tumor Volume, Clinical Target Volume, Planning Target Volume), level sets of radiation dosage, and surrounding healthy tissues. Displaying all these potential surfaces (or more usefully, enabling the clinician to select arbitrary combinations of these) can result in complex surface layerings.

Color and texture can be used to label object surfaces in the scene. Color alone may be used to distinctly label seven or more surfaces, and texture may be used to extend or reinforce the color labelings. Different texture shapes (i.e. the cross used throughout this work) could be used on different surface layers to disambiguate the layers (i.e. interior, middle, exterior), while color is used to disambiguate the objects.

It is an open question how effective the shadows would be at enhancing the perception of depth between more than two surfaces. Though not physically accurate, it may be that restricting shadows to fall only on the "next" innermost surface would yield the strongest benefit to pair-wise depth perception. For example, assuming for simplicity nested surfaces A containing B containing C; shadows from the texture on surface A fall onto B but not onto C, and shadows from the texture on surface B fall onto C. Thus, the shadows from A onto B would enhance the depth perception between surfaces A and B while minimally interfering with the shadows cast by B onto C.

Labeling the different layers of the surfaces now becomes more complex. Obviously interior/exterior alone is not generally sufficient. Further, there is a combinatorial explosion of possible regions to label. Two closed, intersecting surfaces A and B partition space into four (2^2) regions, $A \cap B$, $A \cap \bar{B}$, $\bar{A} \cap B$, and $\bar{A} \cap \bar{B}$. Similarly, three closed, intersecting surfaces potentially partition space into eight (2^3) regions, and n closed, intersecting surfaces potentially partition space into 2^n regions. Finding and labeling the layers of surface separating space interior to m surfaces from space interior to $m-1$

surfaces is complex computationally and perceptually.

6.4 Future Work

This work represents the first few steps toward the ultimate goal for general layered-surface visualization. This section describes many potential directions for future work.

6.4.1 Dissemination

There are effective layered-surface techniques in the visualization literature, but they are not widely available as full, ready to apply techniques in common visualization libraries or systems. The Visualization ToolKit includes a class to compute texture coordinates appropriate for Rheingans' technique [Rhe96], but I am not aware of a complementary class that can guarantee the appropriate retiling of a triangle mesh. I have developed my techniques using open or free libraries (VTK, SparseLib++, IML++, MV++, TetGen) with the aim of freely distributing the source.

6.4.2 New Techniques

One area of future work is to perform the same studies for other techniques commonly used for layered surfaces. This includes those specifically designed for such use, like Rheingans [Rhe96] and Bair *et al.* [BHW05]. It also includes those employed instead of specifically designed techniques, like wireframe rendering of one surface.

Another area of future work is to develop new techniques. There were more techniques originally proposed for this work, but the number of included techniques was curtailed so that the user studies would be practical. Some of these techniques include the use of animation, of illustrative techniques, or of natural phenomena rendering.

6.4.3 New Evaluations

The tasks in this work aimed at determining how accurately tasks could be performed with a set of techniques. Follow-on work should look at how precisely these tasks can be performed with the best techniques.

For the distance task this could be accomplished by asking participants to draw lines connecting the points of closest approach between the two surfaces. For the local shape task this could be accomplished by adapting the local shape probe of Koenderink and van Doorn [KVD95] to two surfaces, or by simply using two of them.

6.4.4 New Domains

Scientists interested in other domains than those included here could benefit from this work. An obvious question is whether the general questions synthesized for this work continue to cover other uses of layered-surface display. Would the same questions cover exploring uncertainty visualization of fossil fuel deposits, for instance?

Another area of interest is extension to more than 2 surfaces and multiple families of surfaces. For instance, can a technique like principal curvature texture with point-correspondence glyphs be extended to compare the boundaries of two statistical shape families (essentially visualizing 4 intersecting surfaces)?

Appendix A

User Study Response Tables

The tables beginning on the next page include all data included in the analysis of the six user studies. The following list defines the table headers and gives the associated data values.

`ID` - participant identifier
`TR` - trial number
`TECH` - visualization technique
    `0` = color mapping
    `1` = principal curvature texture
    `2` = texture with shadows
    `3` = point-correspondence
    `4` = texture with correspondence
`SHD` - shadows
    `3` = no
    `4` = yes
`RCK` - rocking animation
    `0` = no
    `1` = yes
`DIFF` - region difference
    grid units or degrees
`TIME` - time of response
    `gettimeofday()`
`RCKN` - count of participant triggered animation
`RESP` - response
    `0` = incorrect
    `1` = correct

Table A.1: Participant responses from User Study 1.1

ID	TR	TECH	DIFF	RESP	TIME
0	065	2	4	1	1095789052172
0	162	3	1	0	1095789139433
0	176	2	0.5	1	1095789158401
0	035	2	0	1	1095789199181
0	161	2	1.5	0	1095789234773
0	002	2	1	0	1095789256819
0	076	1	5	0	1095789310738
0	212	2	2.5	1	1095789342909
0	284	2	1.5	1	1095789365205
0	156	3	1	1	1095789378813
0	285	3	0	0	1095789412749
0	071	2	2	1	1095789440404
0	095	2	1.5	1	1095789484184
0	256	1	1	0	1095789529963
0	066	3	1.5	1	1095789558508
0	053	2	0	0	1095789575430
0	155	2	2	1	1095789594085
0	166	1	3.5	1	1095789631318
0	113	2	2	1	1095789647754
0	103	1	2.5	0	1095789685175
0	252	3	4	1	1095789695705
0	011	2	1	1	1095789720173
0	185	2	1.5	1	1095789745156
0	163	1	1	0	1095789756703
0	112	1	3	0	1095789773983
0	124	1	1.5	1	1095789782998
0	232	1	2.5	1	1095789793857
0	243	3	4	1	1095789811028
0	031	1	0.5	0	1095789831262
0	231	3	1	1	1095789851745
0	075	3	3.5	1	1095789867916
0	093	3	0	1	1095789891150
0	255	3	0.5	0	1095789910571
0	044	2	5	1	1095789936116
0	296	2	4	1	1095789952506
0	005	2	3.5	1	1095789970240
0	205	1	3.5	0	1095789995504
0	233	2	0.5	1	1095790027112
0	014	2	0.5	0	1095790049393
0	056	2	2	1	1095790079938
0	222	3	0.5	1	1095790099328
0	224	2	3	1	1095790110296
0	064	1	0.5	1	1095790138357
0	236	2	0	1	1095790154935
0	225	3	1	0	1095790166809
0	131	2	3.5	1	1095790182637
0	061	1	3	1	1095790195058
0	125	2	1	1	1095790213745
0	111	3	0	1	1095790237494
0	074	2	4	1	1095790250243
0	214	1	3.5	1	1095790259899
0	196	1	4.5	1	1095790296600
0	175	1	5.5	0	1095790316912
0	096	3	3	1	1095790333005
0	083	2	2	1	1095790351410
0	034	1	0	1	1095790359457
0	023	2	2.5	1	1095790389159
0	072	3	1.5	0	1095790415126
0	221	2	3	1	1095790435625
0	202	1	4.5	1	1095790443984
0	032	2	4.5	1	1095790458249
0	003	3	1.5	1	1095790471921
0	134	2	4	1	1095790484311
0	275	2	0.5	1	1095790501544
0	063	3	1.5	1	1095790518981
0	001	1	1	0	1095790532996
0	016	1	3.5	0	1095790553448
0	105	3	2	1	1095790571791
0	152	2	5	1	1095790583447
0	106	1	0	1	1095790593587
0	154	1	0	1	1095790602571
0	082	1	1.5	0	1095790615742
0	261	3	2	1	1095790630085
0	081	3	1	1	1095790644288
0	004	1	2	0	1095790657240
0	286	1	3	0	1095790712785
0	084	3	1.5	1	1095790732393
0	251	2	2	1	1095790748564
0	036	3	4.5	1	1095790763267
0	253	1	1	0	1095790778844
0	226	1	1	1	1095790816858
0	172	1	1.5	0	1095790830248
0	126	3	3.5	1	1095790842841
0	101	2	0.5	1	1095790860466
0	273	3	1	1	1095790874715
0	051	3	1.5	1	1095790889855
0	043	1	3.5	0	1095790918135
0	235	1	2.5	0	1095790928588
0	186	3	1.5	1	1095790948696
0	026	2	2	1	1095790967586
0	054	3	1.5	1	1095790979507
0	052	1	2.5	0	1095790997241
0	262	1	1.5	0	1095791007990
0	062	2	0.5	1	1095791027974
0	195	3	2.5	1	1095791038036
0	204	3	3	1	1095791049035
0	085	1	2.5	0	1095791075722
0	153	3	3.5	0	1095791106111
0	121	1	1.5	1	1095791130938
0	122	2	0	0	1095791143469
0	042	3	1.5	1	1095791159859
0	264	3	2	1	1095791174530
0	292	1	0	1	1095791189435
0	151	1	3.5	1	1095791203138
0	194	2	4.5	1	1095791216231
0	272	2	4	1	1095791229480
0	133	1	0.5	0	1095791248151
0	265	1	2.5	0	1095791260745
0	143	2	4	1	1095791272385
0	091	1	2	1	1095791280291
0	173	2	0.5	1	1095791298180
0	135	3	2.5	1	1095791312914
0	192	3	1.5	1	1095791332195
0	294	3	3	1	1095791345850
0	045	3	2	1	1095791365084
0	041	2	2	1	1095791379974
0	114	3	0	1	1095791396348
0	104	2	1.5	1	1095791414207
0	174	3	2.5	1	1095791428597
0	293	2	1.5	1	1095791443471
0	213	3	0	1	1095791543919
0	073	1	1	0	1095791552497
0	182	2	3.5	1	1095791563809
0	274	1	1.5	1	1095791571356
0	203	2	4.5	1	1095791581980
0	276	3	3	1	1095791592511
0	245	2	0.5	1	1095791603901
0	146	2	1.5	1	1095791618416
0	021	3	2	1	1095791631619
0	234	3	3	1	1095791643446
0	171	3	0	0	1095791655946
0	263	2	3.5	1	1095791670351
0	116	2	2.5	1	1095791681991
0	244	1	2	1	1095791691616
0	094	1	1	1	1095791703850
0	282	3	2	1	1095791716943
0	123	3	3.5	1	1095791727739
0	181	1	1.5	0	1095791742161
0	215	2	4	1	1095791753191
0	241	1	3	0	1095791761019
0	254	2	1	0	1095791771956
0	015	3	3	1	1095791782331
0	183	3	2.5	1	1095791793268
0	025	1	0.5	0	1095791800705
0	144	3	5.5	1	1095791812157
0	211	1	0.5	1	1095791821298
0	055	1	3	0	1095791832438
0	006	3	2	1	1095791845906
0	246	3	1	1	1095791858218
0	193	1	2	0	1095791866608
0	136	1	1.5	0	1095791883795

ID	TR	TECH	DIFF	RESP	TIME
0	022	1	0.5	0	1095791891560
0	216	3	5.5	1	1095791903825
0	012	3	2.5	1	1095791922371
0	283	1	1.5	1	1095791934056
0	102	3	0.5	1	1095791978165
0	115	1	1	0	1095791989337
0	165	3	4	1	1095791999540
0	145	1	4.5	0	1095792011227
0	024	3	0	1	1095792028024
0	201	3	0.5	1	1095792039899
0	291	3	3.5	1	1095792053915
0	164	2	4	1	1095792064602
0	271	1	4.5	1	1095792075133
0	206	2	4	1	1095792086024
0	046	1	4.5	1	1095792095711
0	086	2	1.5	1	1095792110946
0	223	1	1	1	1095792120742
0	295	1	3.5	1	1095792128227
0	141	3	3	1	1095792143586
0	142	1	3	0	1095792152086
0	132	3	3.5	1	1095792164023
0	013	1	2.5	1	1095792178570
0	281	2	4	1	1095792194273
0	033	3	2.5	1	1095792205757
0	266	2	0.5	1	1095792217289
0	242	2	0.5	0	1095792227976
0	092	2	1.5	1	1095792246101
0	184	1	3.5	1	1095792257804
0	191	2	5.5	1	1095792269132
5	132	2	3.5	1	1095865212899
5	071	1	2	1	1095865222242
5	134	1	4	1	1095865236945
5	164	1	3.5	1	1095865249008
5	203	1	5	1	1095865258430
5	011	1	1	1	1095865268789
5	185	1	1.5	1	1095865277070
5	095	1	1.5	1	1095865286976
5	023	1	1.5	1	1095865297867
5	233	1	0.5	0	1095865307336
5	183	2	2.5	1	1095865328304
5	144	2	5.5	1	1095865349585
5	193	3	3	1	1095865365398
5	072	2	1.5	1	1095865385913
5	116	1	2.5	1	1095865395304
5	022	3	0	0	1095865414069
5	186	2	1.5	1	1095865434600
5	152	1	5	1	1095865442647
5	153	2	3.5	1	1095865459491
5	103	3	3	1	1095865510147
5	143	1	2.5	1	1095865521490
5	296	1	4	1	1095865529147
5	166	3	3.5	1	1095865541506
5	212	1	2.5	1	1095865549443
5	284	1	1.5	1	1095865560740
5	172	3	1.5	1	1095865581771
5	065	1	3.5	1	1095865589537
5	123	2	3.5	1	1095865604599
5	056	1	1.5	1	1095865613740
5	136	3	2	1	1095865652349
5	113	1	1.5	1	1095865664161
5	236	1	0	0	1095865672255
5	196	3	3.5	1	1095865700005
5	295	3	3.5	1	1095865719833
5	146	1	1.5	1	1095865729130
5	084	2	1.5	1	1095865762364
5	111	2	0	0	1095865770458
5	281	1	3	1	1095865781270
5	173	1	0.5	1	1095865794832
5	105	2	2	1	1095865808614
5	165	2	4	1	1095865817004
5	115	3	1	1	1095865828551
5	001	3	1	1	1095865853082
5	251	1	2.5	1	1095865860598
5	081	2	1	1	1095865872738
5	082	3	1.5	0	1095865898738
5	042	2	1.5	1	1095865911238
5	145	3	4.5	1	1095865925941

ID	TR	TECH	DIFF	RESP	TIME
5	041	1	1.5	1	1095865935613
5	272	1	4	1	1095865943019
5	254	1	2	1	1095865958394
5	086	1	1.5	1	1095865968222
5	126	2	3.5	1	1095865982019
5	005	1	3.5	1	1095865989894
5	223	3	1	1	1095866005909
5	083	1	2.5	1	1095866013831
5	252	2	4	1	1095866033268
5	096	2	3	1	1095866048315
5	162	2	1	1	1095866068909
5	151	3	2.5	1	1095866090690
5	206	1	3.5	1	1095866099065
5	205	3	3.5	1	1095866129737
5	101	1	0.5	1	1095866138721
5	195	2	2.5	1	1095866160221
5	131	1	3	1	1095866167768
5	294	2	3	1	1095866187986
5	114	2	0	0	1095866199580
5	032	1	4.5	1	1095866207502
5	002	1	1	1	1095866220783
5	014	1	0.5	0	1095866240892
5	263	1	3.5	1	1095866250064
5	243	2	4	1	1095866266908
5	182	1	3.5	1	1095866276939
5	211	3	0.5	1	1095866315657
5	276	2	3	1	1095866329845
5	012	2	2.5	1	1095866344360
5	235	3	2.5	1	1095866363501
5	066	2	1.5	1	1095866382016
5	031	3	0.5	1	1095866402563
5	034	3	0	1	1095866420375
5	174	2	2.5	1	1095866435422
5	102	2	0.5	1	1095866452031
5	161	1	1.5	1	1095866462734
5	232	3	1.5	1	1095866476109
5	045	2	2	1	1095866503328
5	121	3	1.5	1	1095866533031
5	264	2	2	1	1095866548281
5	241	3	3	1	1095866560624
5	194	1	4	1	1095866569218
5	244	3	2	1	1095866583296
5	122	1	0	1	1095866598546
5	292	3	0	0	1095866630405
5	225	2	1	1	1095866640593
5	176	1	0	0	1095866652139
5	026	1	2.5	1	1095866669108
5	063	2	1.5	1	1095866687592
5	253	3	1	1	1095866703530
5	184	3	3.5	1	1095866716577
5	112	3	3	1	1095866725436
5	035	1	0	1	1095866743373
5	163	3	1	1	1095866766342
5	246	2	1	1	1095866781311
5	204	2	3	1	1095866795217
5	221	1	3.5	1	1095866804295
5	256	3	1	1	1095866814388
5	051	2	1.5	1	1095866826373
5	053	1	0.5	1	1095866837857
5	055	3	3	1	1095866858982
5	156	2	1	1	1095866876904
5	274	3	1.5	1	1095866895357
5	231	2	1	0	1095866906716
5	062	1	1	1	1095866915997
5	213	2	0	0	1095866931950
5	104	1	1.5	0	1095866943122
5	061	3	4.5	1	1095866955278
5	074	1	4	1	1095866964122
5	275	1	0.5	1	1095866979231
5	075	2	3.5	1	1095866999887
5	273	2	1	1	1095867017450
5	093	2	0	1	1095867034825
5	282	2	2	1	1095867073215
5	191	1	5.5	1	1095867081684
5	262	3	2	1	1095867097527
5	015	2	3	1	1095867117699
5	043	3	3	1	1095867135808

ID	TR	TECH	DIFF	RESP	TIME
5	141	2	3	1	1095867150730
5	106	3	0	0	1095867167574
5	261	2	2	1	1095867181464
5	283	3	1	1	1095867203636
5	224	1	3	1	1095867211698
5	024	2	0	1	1095867232636
5	085	3	2.5	1	1095867253042
5	046	3	4.5	1	1095867265573
5	202	3	5	1	1095867278323
5	135	2	2.5	1	1095867291573
5	154	3	0	0	1095867311463
5	215	1	4	1	1095867319448
5	255	2	0.5	0	1095867331104
5	285	2	0	1	1095867350979
5	201	2	0.5	1	1095867371682
5	133	3	0.5	1	1095867391713
5	044	1	5	1	1095867400557
5	004	3	2	1	1095867424385
5	091	3	2	1	1095867438603
5	006	2	2	0	1095867446213
5	052	3	3	1	1095867463806
5	125	1	1	1	1095867473790
5	003	2	1.5	1	1095867491072
5	076	3	4.5	1	1095867511290
5	142	3	3	1	1095867526728
5	155	1	2	1	1095867535087
5	226	3	1	1	1095867554790
5	094	3	0.5	1	1095867566868
5	265	3	2.5	1	1095867595321
5	036	2	4.5	1	1095867609665
5	286	3	3	1	1095867623899
5	092	1	1.5	1	1095867638961
5	175	3	5.5	1	1095867647883
5	245	1	1	1	1095867660539
5	222	2	0.5	1	1095867674055
5	293	1	1.5	1	1095867682883
5	171	2	0	0	1095867698133
5	242	1	0.5	0	1095867716695
5	266	1	0.5	1	1095867726992
5	291	2	3.5	1	1095867743992
5	016	3	3	1	1095867757257
5	271	3	4.5	1	1095867771148
5	216	2	5.5	1	1095867785398
5	234	2	3	1	1095867801788
5	033	2	2.5	1	1095867816007
5	021	2	2	1	1095867828382
5	124	3	2	1	1095867840835
5	054	2	1.5	1	1095867853929
5	073	3	1	1	1095867869085
5	214	3	3.5	1	1095867889163
5	013	3	3	1	1095867901710
5	192	2	1.5	1	1095867917569
5	025	3	0	0	1095867934241
5	181	3	1	0	1095867957053
5	064	3	0.5	0	1095867988037
10	293	2	1.5	0	1095963904940
10	222	3	0.5	1	1095963921393
10	226	1	1	1	1095963934033
10	104	2	1.5	0	1095963951049
10	174	3	2.5	1	1095963971502
10	172	1	1.5	1	1095963980330
10	131	2	3.5	1	1095964002158
10	121	1	1.5	0	1095964026783
10	243	3	4	1	1095964047064
10	191	2	5.5	1	1095964068704
10	214	1	3.5	1	1095964081892
10	296	2	4	1	1095964101189
10	034	1	0	1	1095964109642
10	044	2	5	1	1095964128970
10	221	2	3	1	1095964148204
10	134	2	4	1	1095964167626
10	196	1	4.5	1	1095964176641
10	195	3	2.5	1	1095964200313
10	261	3	2	1	1095964220219
10	056	2	2	1	1095964240078
10	026	2	2	1	1095964257203
10	194	2	4.5	1	1095964273734

ID	TR	TECH	DIFF	RESP	TIME
10	141	3	3	1	1095964287656
10	153	3	3.5	1	1095964312797
10	013	1	2.5	1	1095964326781
10	124	1	1.5	0	1095964337984
10	073	1	1	1	1095964347656
10	102	3	0.5	1	1095964369374
10	014	2	0.5	0	1095964388124
10	192	3	1.5	1	1095964411437
10	041	2	2	1	1095964427827
10	106	1	0	0	1095964437108
10	164	2	4	1	1095964454030
10	101	2	0.5	1	1095964475561
10	276	3	3	0	1095964508686
10	133	1	0.5	1	1095964521733
10	046	1	4.5	1	1095964530030
10	011	2	1	1	1095964566717
10	275	2	0.5	1	1095964596889
10	132	3	3.5	1	1095964614045
10	062	2	0.5	1	1095964639888
10	152	2	5	1	1095964665138
10	256	1	1	0	1095964685435
10	271	1	4.5	1	1095964696482
10	206	2	4	1	1095964716060
10	082	1	1.5	1	1095964723497
10	255	3	0.5	0	1095964785028
10	031	1	0.5	1	1095964793137
10	012	3	2.5	0	1095964818981
10	036	3	4.5	1	1095964837668
10	186	3	1.5	1	1095964869559
10	086	2	1.5	1	1095964890262
10	155	2	2	1	1095964913824
10	272	2	4	1	1095964933464
10	125	2	1	1	1095964950230
10	061	1	3	1	1095964958433
10	251	2	2	1	1095964974917
10	204	3	3	1	1095964985949
10	181	1	1.5	1	1095964995620
10	171	3	0	0	1095965025948
10	215	2	4	1	1095965041401
10	064	1	0.5	0	1095965055026
10	241	1	3	1	1095965062464
10	081	3	1	1	1095965081495
10	254	2	1	0	1095965102807
10	224	2	3	1	1095965118182
10	004	1	2	1	1095965126323
10	055	1	3	1	1095965135276
10	212	2	2.5	1	1095965154260
10	083	2	2	1	1095965179791
10	126	3	3.5	1	1095965195760
10	022	1	0.5	1	1095965205463
10	096	3	3	1	1095965218510
10	066	3	1.5	1	1095965234838
10	286	1	3	1	1095965243119
10	163	1	1	1	1095965260619
10	173	2	0.5	1	1095965285353
10	023	2	2.5	1	1095965311087
10	274	1	1.5	1	1095965322462
10	091	1	2	1	1095965329431
10	282	3	2	1	1095965348477
10	103	1	2.5	1	1095965357227
10	161	2	1.5	1	1095965376634
10	184	1	3.5	1	1095965386087
10	076	1	5	1	1095965398477
10	253	1	1	1	1095965411446
10	095	2	1.5	1	1095965441789
10	005	2	3.5	1	1095965465180
10	183	3	2.5	1	1095965483742
10	182	2	3.5	1	1095965502164
10	235	1	2.5	1	1095965513476
10	135	3	2.5	1	1095965526476
10	092	2	1.5	1	1095965546586
10	072	3	1.5	0	1095965581835
10	284	2	1.5	0	1095965598070
10	001	1	1	1	1095965613679
10	113	2	2	1	1095965636351
10	094	1	1	1	1095965651366
10	145	1	4.5	1	1095965661413

ID	TR	TECH	DIFF	RESP	TIME
10	093	3	0	0	1095965677882
10	146	2	1.5	1	1095965696038
10	202	1	4.5	1	1095965704006
10	143	2	4	1	1095965721178
10	003	3	1.5	1	1095965743116
10	273	3	1	1	1095965755037
10	042	3	1.5	0	1095965790459
10	156	3	1	1	1095965810084
10	165	3	4	1	1095965825584
10	193	1	2	1	1095965840021
10	052	1	2.5	1	1095965848459
10	201	3	0.5	0	1095965866599
10	266	2	0.5	1	1095965891833
10	045	3	2	1	1095965910083
10	234	3	3	1	1095965922021
10	245	2	0.5	1	1095965937333
10	116	2	2.5	1	1095965952192
10	236	2	0	1	1095965974020
10	223	1	1	1	1095965983489
10	071	2	2	0	1095966005270
10	242	2	0.5	1	1095966020348
10	292	1	0	0	1095966041254
10	054	3	1.5	1	1095966067285
10	051	3	1.5	1	1095966082504
10	002	2	1	1	1095966098395
10	203	2	4.5	1	1095966109535
10	263	2	3.5	1	1095966126847
10	144	3	5.5	1	1095966138566
10	244	1	2	1	1095966146816
10	211	1	0.5	0	1095966167785
10	111	3	0	1	1095966188753
10	142	1	3	1	1095966196222
10	262	1	1.5	1	1095966207269
10	162	3	1	1	1095966233972
10	233	2	0.5	0	1095966263018
10	252	3	4	1	1095966276893
10	053	2	0	1	1095966298393
10	291	3	3.5	1	1095966317971
10	176	2	0.5	0	1095966333862
10	295	1	3.5	1	1095966341924
10	175	1	5.5	1	1095966354955
10	033	3	2.5	1	1095966380596
10	216	3	5.5	1	1095966391705
10	294	3	3	1	1095966404018
10	151	1	3.5	1	1095966414142
10	265	1	2.5	1	1095966423767
10	075	3	3.5	1	1095966435783
10	115	1	1	1	1095966452189
10	264	3	2	1	1095966465111
10	285	3	0	1	1095966481126
10	281	2	4	1	1095966495829
10	074	2	4	1	1095966511689
10	185	2	1.5	1	1095966523314
10	114	3	0	0	1095966539939
10	166	1	3.5	1	1095966547657
10	024	3	0	1	1095966568798
10	123	3	3.5	1	1095966582391
10	136	1	1.5	1	1095966592329
10	016	1	3.5	1	1095966607641
10	105	3	2	1	1095966624297
10	085	1	2.5	1	1095966631985
10	065	2	4	1	1095966646157
10	015	3	3	1	1095966657657
10	246	3	1	1	1095966676172
10	025	1	0.5	1	1095966689719
10	032	2	4.5	1	1095966704359
10	213	3	0	1	1095966719391
10	283	1	1.5	1	1095966730750
10	225	3	1	0	1095966749937
10	231	3	1	1	1095966765406
10	084	3	1.5	1	1095966783406
10	006	3	2	1	1095966802015
10	232	1	2.5	1	1095966809577
10	122	2	0	0	1095966830530
10	021	3	2	1	1095966847780
10	035	2	0	0	1095966863311
10	043	1	3.5	1	1095966871843

ID	TR	TECH	DIFF	RESP	TIME
10	063	3	1.5	1	1095966885968
10	205	1	3.5	1	1095966895718
10	112	1	3	1	1095966904092
10	154	1	0	0	1095966922452
11	245	2	0.5	1	1096038208852
11	285	3	0	0	1096038219133
11	291	3	3.5	1	1096038240024
11	142	1	3	1	1096038249571
11	132	3	3.5	1	1096038263805
11	244	1	2	1	1096038272008
11	271	1	4.5	1	1096038286477
11	042	3	1.5	1	1096038303148
11	182	2	3.5	1	1096038315492
11	123	3	3.5	1	1096038325226
11	026	2	2	1	1096038337445
11	191	2	5.5	1	1096038349054
11	286	1	3	1	1096038358429
11	035	2	0	0	1096038378976
11	146	2	1.5	1	1096038397960
11	046	1	4.5	1	1096038405242
11	202	1	4.5	1	1096038414726
11	255	3	0.5	0	1096038437116
11	095	2	1.5	0	1096038449116
11	292	1	0	1	1096038458366
11	053	2	0	1	1096038471804
11	185	2	1.5	1	1096038486382
11	143	2	4	1	1096038501163
11	263	2	3.5	0	1096038521788
11	193	1	2	1	1096038533725
11	172	1	1.5	1	1096038541475
11	131	2	3.5	1	1096038560303
11	253	1	1	1	1096038570881
11	215	2	4	1	1096038593194
11	175	1	5.5	1	1096038606131
11	232	1	2.5	1	1096038613334
11	114	3	0	0	1096038632412
11	092	2	1.5	1	1096038644240
11	002	2	1	1	1096038655896
11	213	3	0	1	1096038664334
11	284	2	1.5	0	1096038678099
11	221	2	3	1	1096038690193
11	085	1	2.5	1	1096038697630
11	236	2	0	1	1096038710005
11	163	1	1	1	1096038719490
11	212	2	2.5	1	1096038730880
11	272	2	4	1	1096038743349
11	014	2	0.5	0	1096038766583
11	052	1	2.5	1	1096038777677
11	116	2	2.5	1	1096038790192
11	295	1	3.5	1	1096038797083
11	216	3	5.5	1	1096038810536
11	126	3	3.5	1	1096038820161
11	214	1	3.5	1	1096038828114
11	004	1	2	1	1096038836879
11	006	3	2	1	1096038850520
11	083	2	2	0	1096038862739
11	242	2	0.5	1	1096038875223
11	093	3	0	1	1096038888942
11	102	3	0.5	1	1096038902629
11	041	2	2	1	1096038915941
11	161	2	1.5	1	1096038931223
11	045	3	2	0	1096038944285
11	241	1	3	1	1096038951441
11	104	2	1.5	0	1096038966300
11	266	2	0.5	0	1096038985253
11	166	1	3.5	1	1096038995597
11	022	1	0.5	0	1096039006035
11	101	2	0.5	1	1096039018097
11	152	2	5	1	1096039029316
11	156	3	1	1	1096039038378
11	033	3	2.5	1	1096039051550
11	243	3	4	1	1096039061097
11	136	1	1.5	1	1096039069112
11	226	1	1	1	1096039080300
11	064	1	0.5	0	1096039090643
11	162	3	1	1	1096039102815
11	135	3	2.5	1	1096039110456

ID	TR	TECH	DIFF	RESP	TIME
11	094	1	1	1	1096039121471
11	056	2	2	0	1096039137190
11	196	1	4.5	1	1096039144877
11	076	1	5	1	1096039152565
11	005	2	3.5	1	1096039166284
11	072	3	1.5	0	1096039182455
11	096	3	3	1	1096039194237
11	201	3	0.5	0	1096039204393
11	043	1	3.5	1	1096039212283
11	151	1	3.5	1	1096039220236
11	274	1	1.5	1	1096039230096
11	122	2	0	0	1096039243299
11	211	1	0.5	1	1096039251346
11	234	3	3	1	1096039263002
11	051	3	1.5	1	1096039274330
11	106	1	0	0	1096039282517
11	296	2	4	1	1096039297064
11	044	2	5	1	1096039309142
11	176	2	0.5	0	1096039318564
11	223	1	1	1	1096039326454
11	164	2	4	1	1096039338876
11	111	3	0	0	1096039349126
11	081	3	1	1	1096039363376
11	275	2	0.5	0	1096039380173
11	065	2	4	1	1096039391767
11	121	1	1.5	0	1096039399204
11	183	3	2.5	1	1096039411157
11	113	2	2	1	1096039422954
11	195	3	2.5	0	1096039432298
11	055	1	3	1	1096039439829
11	256	1	1	1	1096039449282
11	075	3	3.5	1	1096039458469
11	184	1	3.5	1	1096039467063
11	133	1	0.5	0	1096039477172
11	073	1	1	1	1096039485766
11	115	1	1	1	1096039492610
11	224	2	3	1	1096039508047
11	276	3	3	1	1096039515688
11	204	3	3	1	1096039528344
11	084	3	1.5	1	1096039537750
11	105	3	2	1	1096039547297
11	262	1	1.5	1	1096039556187
11	023	2	2.5	1	1096039572875
11	283	1	1.5	0	1096039588468
11	154	1	0	0	1096039597593
11	054	3	1.5	1	1096039605828
11	141	3	3	1	1096039615874
11	294	3	3	1	1096039627437
11	071	2	2	1	1096039641452
11	282	3	2	1	1096039649327
11	231	3	1	1	1096039660280
11	233	2	0.5	1	1096039677827
11	225	3	1	0	1096039693077
11	021	3	2	1	1096039703421
11	293	2	1.5	1	1096039719030
11	153	3	3.5	1	1096039729639
11	062	2	0.5	0	1096039743546
11	251	2	2	1	1096039756233
11	235	1	2.5	1	1096039764014
11	181	1	1.5	1	1096039775639
11	155	2	2	1	1096039789951
11	016	1	3.5	1	1096039798436
11	171	3	0	0	1096039812733
11	281	2	4	1	1096039823154
11	034	1	0	1	1096039834123
11	066	3	1.5	1	1096039846889
11	165	3	4	1	1096039854732
11	192	3	1.5	1	1096039865107
11	013	1	2.5	0	1096039877857
11	012	3	2.5	1	1096039888263
11	173	2	0.5	1	1096039903341
11	063	3	1.5	1	1096039911185
11	086	2	1.5	1	1096039928607
11	125	2	1	0	1096039942482
11	194	2	4.5	1	1096039966232
11	273	3	1	1	1096039977638
11	252	3	4	1	1096039986341

ID	TR	TECH	DIFF	RESP	TIME
11	186	3	1.5	1	1096039999513
11	003	3	1.5	1	1096040011153
11	206	2	4	1	1096040028262
11	024	3	0	1	1096040045903
11	091	1	2	1	1096040054184
11	032	2	4.5	1	1096040068731
11	061	1	3	1	1096040077278
11	174	3	2.5	1	1096040088871
11	124	1	1.5	1	1096040096559
11	265	1	2.5	1	1096040105324
11	082	1	1.5	1	1096040114778
11	011	2	1	1	1096040127731
11	203	2	4.5	1	1096040140137
11	264	3	2	1	1096040148324
11	103	1	2.5	1	1096040158543
11	025	1	0.5	1	1096040170058
11	112	1	3	1	1096040180230
11	205	1	3.5	1	1096040188277
11	036	3	4.5	1	1096040196980
11	134	2	4	1	1096040215667
11	015	3	3	1	1096040232574
11	074	2	4	1	1096040244495
11	254	2	1	0	1096040257042
11	144	3	5.5	1	1096040264839
11	261	3	2	1	1096040280026
11	001	1	1	1	1096040288308
11	222	3	0.5	0	1096040306073
11	145	1	4.5	1	1096040313682
11	246	3	1	1	1096040326839
11	031	1	0.5	1	1096040333964

Table A.2: Participant responses from User Study 1.2

ID	TR	TECH	DIFF	RESP	TIME
17	091	2	10	0	1098972746343
17	075	1	50	1	1098972767687
17	044	3	5	1	1098972790609
17	283	2	5	0	1098972804968
17	015	1	20	1	1098972822046
17	164	3	0	0	1098972842234
17	266	3	10	0	1098972867281
17	202	2	35	1	1098972888218
17	243	1	10	0	1098972902500
17	285	1	50	0	1098972926078
17	085	2	20	1	1098972944312
17	296	3	0	0	1098972967359
17	295	2	5	0	1098972991140
17	273	1	50	1	1098973005968
17	195	1	30	1	1098973019828
17	193	2	40	1	1098973042343
17	094	2	10	1	1098973077578
17	071	3	50	1	1098973108906
17	174	1	10	1	1098973134781
17	134	3	25	1	1098973151578
17	165	1	30	1	1098973165031
17	276	1	35	0	1098973177531
17	104	3	25	1	1098973200859
17	154	2	5	0	1098973215500
17	234	1	10	1	1098973227234
17	262	2	0	1	1098973254578
17	025	2	20	1	1098973277765
17	281	3	35	1	1098973303171
17	155	3	5	0	1098973336156
17	026	3	15	1	1098973368187
17	076	2	45	1	1098973384937
17	153	1	5	1	1098973400906
17	204	1	30	1	1098973419984
17	293	3	5	0	1098973437656
17	122	3	20	0	1098973457703
17	002	3	20	1	1098973478953
17	275	3	40	1	1098973502515
17	073	2	20	1	1098973518046
17	101	3	20	1	1098973534421
17	175	2	0	1	1098973554640
17	231	1	20	0	1098973572015
17	124	2	15	0	1098973599750
17	024	1	35	0	1098973612671
17	082	2	10	0	1098973635906
17	053	3	30	1	1098973651859
17	103	2	20	1	1098973677750
17	196	2	30	0	1098973707765
17	016	2	30	1	1098973736937
17	135	1	25	0	1098973756093
17	035	3	25	1	1098973785390
17	173	3	30	1	1098973811031
17	203	3	40	1	1098973847625
17	294	1	20	1	1098973859953
17	162	1	30	0	1098973879406
17	166	2	25	1	1098973905656
17	096	1	20	1	1098973917468
17	111	1	0	1	1098973941281
17	034	2	15	0	1098973966609
17	185	3	30	1	1098973981078
17	081	1	0	0	1098973992281
17	161	3	20	0	1098974037953
17	156	1	0	0	1098974052171
17	013	2	45	1	1098974080203
17	205	2	35	1	1098974098687
17	041	3	5	0	1098974130375
17	236	3	10	0	1098974147687
17	066	1	20	0	1098974169312
17	274	2	50	1	1098974184250
17	084	1	10	0	1098974203375
17	172	2	35	1	1098974225390
17	225	1	40	1	1098974236828
17	235	2	0	1	1098974252000
17	112	2	20	1	1098974274171
17	183	1	5	1	1098974286750
17	163	2	0	1	1098974310328
17	254	3	45	1	1098974332437
17	222	1	5	1	1098974350343
17	125	3	15	1	1098974374937
17	106	2	20	1	1098974395843
17	051	1	0	1	1098974408843
17	223	2	5	1	1098974423656
17	132	1	15	1	1098974436359
17	006	1	10	1	1098974449484
17	052	2	10	0	1098974497968
17	146	3	25	1	1098974513125
17	245	3	5	1	1098974532062
17	213	1	40	1	1098974545046
17	242	3	0	1	1098974568015
17	211	2	10	1	1098974587625
17	232	2	5	1	1098974600875
17	093	1	0	0	1098974621046
17	042	1	10	1	1098974653296
17	005	3	35	1	1098974666781
17	264	1	30	1	1098974684156
17	121	2	20	1	1098974706500
17	291	1	15	0	1098974717468
17	113	3	20	1	1098974742421
17	253	2	15	1	1098974757734
17	241	2	30	0	1098974781375
17	114	1	5	0	1098974797312
17	212	3	0	0	1098974811859
17	181	2	50	1	1098974827609
17	282	1	35	1	1098974837046
17	021	1	15	0	1098974851000
17	144	1	5	0	1098974867875
17	192	1	5	0	1098974880796
17	014	3	45	1	1098974896562
17	043	2	20	0	1098974912515
17	151	2	5	1	1098974930750
17	004	2	25	1	1098974944296
17	182	3	5	1	1098974963734
17	224	3	15	1	1098974982171
17	184	2	25	1	1098974996703
17	032	3	20	1	1098975011375
17	255	1	0	0	1098975025093
17	011	3	10	1	1098975039765
17	244	2	15	1	1098975055500
17	064	2	35	1	1098975070015
17	031	2	10	0	1098975090921
17	284	3	40	1	1098975107078
17	126	1	15	0	1098975147250
17	065	3	25	1	1098975169781
17	256	2	60	1	1098975181750
17	012	1	25	1	1098975194687
17	105	1	25	1	1098975206390
17	233	3	0	1	1098975221140
17	003	1	25	1	1098975234671
17	194	3	35	1	1098975254656
17	062	3	15	1	1098975279843
17	055	2	25	1	1098975293687
17	265	2	5	1	1098975322109
17	221	3	15	1	1098975336609
17	186	1	0	0	1098975358593
17	152	3	15	1	1098975373390
17	171	1	35	1	1098975395718
17	201	1	20	0	1098975413609
17	086	3	20	0	1098975436781
17	136	2	30	1	1098975450843
17	022	2	20	1	1098975476000
17	191	3	0	1	1098975491656
17	261	1	30	1	1098975505156
17	292	2	50	1	1098975520718
17	102	1	10	0	1098975531359
17	061	2	25	1	1098975545468
17	046	2	20	1	1098975559109
17	023	3	30	0	1098975588843
17	271	2	20	0	1098975610906
17	116	3	15	0	1098975632609
17	252	1	30	1	1098975656312
17	056	3	40	1	1098975678609
17	272	3	40	1	1098975690437

ID	TR	TECH	DIFF	RESP	TIME
17	216	1	35	1	1098975700765
17	142	2	30	1	1098975719156
17	123	1	25	1	1098975730625
17	074	3	35	1	1098975747171
17	001	2	15	1	1098975767312
17	215	3	35	1	1098975781015
17	072	1	40	1	1098975792078
17	176	3	10	1	1098975806656
17	214	2	30	1	1098975820703
17	145	2	25	1	1098975834843
17	141	1	25	1	1098975852187
17	226	2	35	1	1098975869078
17	095	3	25	1	1098975885062
17	092	3	15	0	1098975903531
17	054	1	0	1	1098975915703
17	133	2	20	1	1098975940578
17	206	3	35	1	1098975954968
17	143	3	30	1	1098975972078
17	083	3	15	1	1098975987000
17	286	2	10	1	1098976001890
17	115	2	55	1	1098976017546
17	036	1	45	0	1098976035859
17	131	3	10	1	1098976052718
17	251	3	30	1	1098976072484
17	033	1	15	0	1098976085609
17	246	1	10	1	1098976096312
17	045	1	10	1	1098976109296
17	063	1	30	1	1098976124578
17	263	3	5	0	1098976140171
18	246	3	10	1	1098991166468
18	154	1	5	0	1098991190734
18	121	1	20	0	1098991204343
18	112	1	20	0	1098991213359
18	084	3	10	0	1098991256781
18	025	1	20	0	1098991276546
18	293	2	5	1	1098991305984
18	252	3	30	1	1098991321296
18	172	1	35	1	1098991332484
18	261	3	30	1	1098991353281
18	045	3	10	0	1098991425312
18	215	2	35	1	1098991440421
18	175	1	0	1	1098991453328
18	136	1	30	1	1098991474750
18	074	2	35	0	1098991483968
18	142	1	30	1	1098991495375
18	222	3	5	0	1098991515781
18	111	3	0	0	1098991524218
18	131	2	10	0	1098991555437
18	113	2	20	1	1098991586687
18	233	2	0	1	1098991612437
18	141	3	25	1	1098991628750
18	023	2	30	1	1098991659031
18	184	1	25	1	1098991671375
18	276	3	35	1	1098991701687
18	104	2	25	1	1098991717109
18	014	2	45	1	1098991731828
18	143	2	30	1	1098991746640
18	103	1	20	1	1098991774953
18	134	2	25	1	1098991803625
18	002	2	20	1	1098991822765
18	094	1	10	1	1098991832171
18	163	1	0	1	1098991840890
18	206	2	35	1	1098991859531
18	013	1	45	0	1098991871468
18	294	3	20	1	1098991885171
18	156	3	0	0	1098991908984
18	232	1	5	1	1098991917203
18	283	1	5	1	1098991928562
18	211	1	10	0	1098991942109
18	231	3	20	1	1098991968375
18	153	3	5	1	1098992000796
18	275	2	40	1	1098992017156
18	063	3	30	0	1098992028656
18	071	2	50	1	1098992038062
18	176	2	10	1	1098992045843
18	054	3	0	0	1098992063218
18	011	2	10	1	1098992080359

ID	TR	TECH	DIFF	RESP	TIME
18	082	1	10	1	1098992107140
18	262	1	0	1	1098992114593
18	073	1	20	1	1098992130406
18	253	1	15	0	1098992139328
18	264	3	30	1	1098992150093
18	061	1	25	1	1098992159640
18	174	3	10	1	1098992168187
18	044	2	5	1	1098992177890
18	254	2	45	1	1098992194671
18	213	3	40	1	1098992208718
18	224	2	15	1	1098992227812
18	173	2	30	1	1098992243171
18	263	2	5	0	1098992268546
18	282	3	35	1	1098992276625
18	223	1	5	1	1098992290015
18	005	2	35	1	1098992307546
18	015	3	20	1	1098992322187
18	255	3	0	0	1098992336468
18	055	1	25	1	1098992347734
18	101	2	20	1	1098992364109
18	161	2	20	1	1098992384687
18	132	3	15	1	1098992396468
18	056	2	40	1	1098992407578
18	024	3	35	0	1098992432421
18	201	3	20	1	1098992453609
18	216	3	35	1	1098992480296
18	214	1	30	1	1098992489484
18	285	3	50	1	1098992506843
18	036	3	45	1	1098992522890
18	114	3	5	0	1098992546484
18	186	3	0	1	1098992569281
18	221	2	15	1	1098992585078
18	096	3	20	1	1098992597343
18	051	3	0	1	1098992609328
18	065	2	25	1	1098992632984
18	162	3	30	1	1098992647140
18	244	1	15	1	1098992654765
18	042	3	10	1	1098992669593
18	052	1	10	1	1098992677390
18	296	2	0	0	1098992694531
18	086	2	20	1	1098992709671
18	235	1	0	1	1098992718734
18	256	1	60	1	1098992726718
18	202	1	35	1	1098992737843
18	205	1	35	1	1098992754765
18	181	1	50	1	1098992763312
18	003	3	25	1	1098992779468
18	093	3	0	0	1098992798656
18	271	1	20	0	1098992806156
18	146	2	25	1	1098992824718
18	266	2	10	1	1098992840187
18	191	2	0	1	1098992855640
18	041	2	5	0	1098992880250
18	242	2	0	1	1098992902906
18	012	3	25	1	1098992915968
18	195	3	30	1	1098992932781
18	085	1	20	0	1098992940406
18	166	1	25	1	1098992955562
18	075	3	50	1	1098992972609
18	241	1	30	0	1098992984812
18	034	1	15	0	1098993013546
18	105	3	25	1	1098993026187
18	021	3	15	0	1098993041328
18	295	1	5	0	1098993048781
18	133	1	20	1	1098993058437
18	284	2	40	1	1098993076515
18	243	3	10	0	1098993091078
18	116	2	15	1	1098993115406
18	033	3	15	1	1098993137093
18	152	2	15	1	1098993154312
18	076	1	45	0	1098993162953
18	234	3	10	0	1098993199515
18	095	2	25	1	1098993253359
18	066	3	20	0	1098993265953
18	273	3	50	1	1098993274953
18	203	2	40	1	1098993293859
18	265	1	5	0	1098993311046

ID	TR	TECH	DIFF	RESP	TIME
18	292	1	50	1	1098993319718
18	135	3	25	1	1098993337687
18	062	2	15	1	1098993352968
18	046	1	20	1	1098993364031
18	274	1	50	1	1098993371453
18	212	2	0	0	1098993390328
18	053	2	30	1	1098993405390
18	185	2	30	1	1098993422265
18	155	2	5	0	1098993438781
18	291	3	15	1	1098993458187
18	043	1	20	0	1098993466531
18	083	2	15	1	1098993482828
18	236	2	10	0	1098993506593
18	183	3	5	0	1098993527484
18	115	1	55	1	1098993536562
18	072	3	40	1	1098993555718
18	125	2	15	1	1098993571171
18	031	1	10	0	1098993584265
18	196	1	30	0	1098993601875
18	006	3	10	1	1098993618468
18	144	3	5	0	1098993626187
18	004	1	25	1	1098993636546
18	192	3	5	1	1098993668046
18	091	1	10	1	1098993676000
18	225	3	40	1	1098993688453
18	035	2	25	1	1098993706000
18	081	3	0	0	1098993721500
18	126	3	15	1	1098993745687
18	286	1	10	1	1098993762312
18	145	1	25	1	1098993770203
18	123	3	25	1	1098993789765
18	204	3	30	1	1098993809859
18	026	2	15	1	1098993829250
18	245	2	5	0	1098993863671
18	164	2	0	1	1098993884406
18	226	1	35	1	1098993893796
18	016	1	30	0	1098993901234
18	122	2	20	0	1098993925687
18	194	2	35	1	1098993941703
18	182	2	5	1	1098993958796
18	165	3	30	1	1098993967093
18	032	2	20	1	1098993980593
18	001	1	15	0	1098993993500
18	272	2	40	1	1098994007218
18	092	2	15	0	1098994019062
18	171	3	35	1	1098994031156
18	106	1	20	0	1098994041593
18	151	1	5	0	1098994067531
18	251	2	30	1	1098994084031
18	193	1	40	0	1098994092000
18	102	3	10	0	1098994121484
18	064	1	35	1	1098994133421
18	281	2	35	1	1098994148484
18	022	1	20	1	1098994155531
18	124	1	15	0	1098994173468
1	176	2	10	1	1095793837388
1	052	1	10	1	1095793848122
1	144	3	5	0	1095793863637
1	085	1	20	0	1095793872684
1	225	3	40	1	1095793901668
1	136	1	30	1	1095793913200
1	166	1	25	0	1095793920965
1	005	2	35	1	1095793939934
1	044	2	5	1	1095793973137
1	081	3	0	0	1095793993543
1	066	3	20	1	1095794015480
1	265	1	5	0	1095794025308
1	003	3	25	1	1095794074417
1	174	3	10	1	1095794088995
1	254	2	45	1	1095794136292
1	204	3	30	1	1095794154651
1	125	2	15	1	1095794182089
1	053	2	30	1	1095794201088
1	084	3	10	1	1095794234869
1	041	2	5	0	1095794259557
1	142	1	30	1	1095794272088
1	155	2	5	0	1095794295510

ID	TR	TECH	DIFF	RESP	TIME
1	236	2	10	0	1095794367259
1	276	3	35	1	1095794414087
1	131	2	10	1	1095794439071
1	181	1	50	1	1095794450837
1	261	3	30	0	1095794488555
1	072	3	40	1	1095794505336
1	205	1	35	1	1095794526524
1	275	2	40	1	1095794546133
1	106	1	20	1	1095794567149
1	165	3	30	1	1095794578008
1	161	2	20	1	1095794593648
1	035	2	25	1	1095794608133
1	141	3	25	1	1095794642914
1	015	3	20	1	1095794668085
1	184	1	25	1	1095794691210
1	076	1	45	0	1095794699023
1	206	2	35	1	1095794740960
1	134	2	25	1	1095794773600
1	133	1	20	1	1095794782413
1	093	3	0	1	1095794802444
1	022	1	20	1	1095794822381
1	021	3	15	0	1095794844616
1	253	1	15	1	1095794854037
1	272	2	40	1	1095794876022
1	241	1	30	1	1095794886115
1	251	2	30	1	1095794914724
1	295	1	5	0	1095794936427
1	151	1	5	1	1095794960115
1	132	3	15	1	1095794978787
1	104	2	25	1	1095794992193
1	183	3	5	1	1095795032021
1	014	2	45	1	1095795056208
1	113	2	20	0	1095795070520
1	042	3	10	1	1095795091458
1	266	2	10	1	1095795112364
1	291	3	15	0	1095795148832
1	182	2	5	0	1095795173676
1	152	2	15	1	1095795194723
1	025	1	20	1	1095795215707
1	095	2	25	1	1095795240301
1	071	2	50	1	1095795252597
1	243	3	10	0	1095795283144
1	032	2	20	1	1095795298425
1	244	1	15	0	1095795312253
1	061	1	25	1	1095795328503
1	273	3	50	1	1095795344519
1	063	3	30	1	1095795364628
1	194	2	35	1	1095795384612
1	154	1	5	0	1095795406143
1	094	1	10	1	1095795423721
1	153	3	5	1	1095795442034
1	185	2	30	1	1095795463065
1	075	3	50	1	1095795481565
1	172	1	35	1	1095795497315
1	036	3	45	1	1095795524346
1	016	1	30	0	1095795544845
1	073	1	20	1	1095795557752
1	264	3	30	1	1095795580095
1	116	2	15	0	1095795596876
1	062	2	15	1	1095795624204
1	163	1	0	0	1095795633314
1	054	3	0	0	1095795660376
1	231	3	20	1	1095795682141
1	115	1	55	1	1095795692891
1	294	3	20	1	1095795722094
1	285	3	50	1	1095795739329
1	162	3	30	1	1095795758735
1	012	3	25	1	1095795769953
1	211	1	10	1	1095795777781
1	045	3	10	1	1095795794703
1	293	2	5	0	1095795840922
1	002	2	20	1	1095795865047
1	175	1	0	0	1095795874562
1	135	3	25	1	1095795914343
1	221	2	15	1	1095795931343
1	171	3	35	1	1095795956343
1	242	2	0	1	1095795993077

ID	TR	TECH	DIFF	RESP	TIME
1	105	3	25	1	1095796009999
1	274	1	50	1	1095796022108
1	213	3	40	1	1095796048827
1	124	1	15	1	1095796064202
1	252	3	30	1	1095796077780
1	056	2	40	1	1095796092514
1	051	3	0	1	1095796103826
1	263	2	5	0	1095796131951
1	281	2	35	1	1095796158310
1	024	3	35	1	1095796180545
1	096	3	20	1	1095796206013
1	193	1	40	1	1095796214435
1	065	2	25	1	1095796251153
1	286	1	10	1	1095796259138
1	196	1	30	1	1095796281247
1	004	1	25	1	1095796294013
1	271	1	20	1	1095796315841
1	262	1	0	1	1095796367918
1	112	1	20	0	1095796377793
1	011	2	10	1	1095796397262
1	122	2	20	0	1095796412027
1	203	2	40	1	1095796709822
1	156	3	0	1	1095796730853
1	091	1	10	1	1095796739416
1	283	1	5	1	1095796754400
1	043	1	20	1	1095796767463
1	195	3	30	1	1095796792478
1	215	2	35	1	1095796812806
1	086	2	20	1	1095796830712
1	033	3	15	1	1095796861040
1	023	2	30	1	1095796887118
1	226	1	35	1	1095796897618
1	232	1	5	1	1095796905759
1	121	1	20	0	1095796929352
1	186	3	0	0	1095796947227
1	146	2	25	1	1095796957711
1	055	1	25	1	1095796973664
1	222	3	5	0	1095796999211
1	192	3	5	1	1095797025336
1	233	2	0	1	1095797045101
1	083	2	15	1	1095797061117
1	173	2	30	1	1095797079164
1	046	1	20	1	1095797091179
1	001	1	15	1	1095797099867
1	296	2	0	0	1095797124898
1	255	3	0	0	1095797142195
1	006	3	10	1	1095797169507
1	102	3	10	1	1095797196179
1	201	3	20	1	1095797216538
1	103	1	20	1	1095797233788
1	292	1	50	1	1095797249553
1	074	2	35	1	1095797275600
1	282	3	35	1	10957973070 37
1	235	1	0	1	1095797320256
1	191	2	0	1	1095797341287
1	256	1	60	1	1095797356240
1	234	3	10	0	1095797380115
1	114	3	5	0	1095797420896
1	145	1	25	1	1095797429193
1	013	1	45	0	1095797436958
1	034	1	15	0	1095797455083
1	224	2	15	1	1095797471474
1	082	1	10	1	1095797483114
1	164	2	0	1	1095797503880
1	026	2	15	1	1095797521473
1	101	2	20	1	1095797539583
1	092	2	15	0	1095797557083
1	126	3	15	1	1095797579942
1	123	3	25	1	1095797599364
1	216	3	35	1	1095797615942
1	064	1	35	1	1095797626988
1	284	2	40	1	1095797667363
1	031	1	10	0	1095797682160
1	143	2	30	1	1095797715988
1	245	2	5	1	1095797730003
1	202	1	35	1	1095797737581
1	212	2	0	0	1095797751738

ID	TR	TECH	DIFF	RESP	TIME
1	111	3	0	0	1095797769081
1	214	1	30	1	1095797779831
1	223	1	5	0	1095797796519
1	246	3	10	1	1095797814331
6	031	2	10	1	1095882331508
6	076	2	45	1	1095882356226
6	104	3	25	1	1095882374336
6	005	3	35	1	1095882390789
6	151	2	5	1	1095882420179
6	246	1	10	0	1095882451195
6	092	3	15	1	1095882467991
6	112	2	20	1	1095882474804
6	245	3	5	1	1095882503241
6	012	1	25	0	1095882532210
6	011	3	10	1	1095882551241
6	214	2	30	1	1095882574100
6	091	2	10	0	1095882589366
6	241	2	30	0	1095882605131
6	283	2	5	0	1095882618834
6	002	3	20	1	1095882637865
6	254	3	45	1	1095882662646
6	083	3	15	1	1095882676771
6	213	1	40	1	1095882696662
6	074	3	35	1	1095882714615
6	085	2	20	1	1095882739208
6	014	3	45	1	1095882753865
6	191	3	0	1	1095882775552
6	182	3	5	1	1095882863504
6	152	3	15	1	1095882880692
6	164	3	0	1	1095882905192
6	224	3	15	1	1095882919051
6	135	1	25	1	1095882933988
6	015	1	20	1	1095882946270
6	045	1	10	0	1095882963066
6	093	1	0	1	1095882973191
6	173	3	30	1	1095882991082
6	174	1	10	1	1095883007316
6	272	3	40	1	1095883022582
6	102	1	10	0	1095883035519
6	034	2	15	0	1095883054894
6	055	2	25	1	1095883066613
6	256	2	60	1	1095883080081
6	255	1	0	1	1095883092487
6	145	2	25	1	1095883118253
6	023	3	30	1	1095883144128
6	071	3	50	1	1095883161206
6	056	3	40	1	1095883177299
6	184	2	25	1	1095883194190
6	064	2	35	1	1095883207174
6	294	1	20	1	1095883223127
6	202	2	35	1	1095883238565
6	013	2	45	1	1095883274627
6	051	1	0	1	1095883286924
6	165	1	30	0	1095883303017
6	132	1	15	1	1095883312142
6	113	3	20	1	1095883324861
6	095	3	25	1	1095883335658
6	204	1	30	1	1095883351126
6	262	2	0	0	1095883364954
6	261	1	30	1	1095883418907
6	176	3	10	1	1095883432985
6	066	1	20	1	1095883445923
6	024	1	35	0	1095883464532
6	183	1	5	0	1095883476001
6	063	1	30	0	1095883681765
6	136	2	30	1	1095883696968
6	106	2	20	1	1095883709452
6	061	2	25	1	1095883722624
6	223	2	5	0	1095883733374
6	114	1	5	1	1095883744624
6	242	3	0	1	1095883752827
6	244	2	15	1	1095883769967
6	094	2	10	0	1095883778592
6	251	3	30	1	1095883788124
6	253	2	15	1	1095883835029
6	054	1	0	0	1095883844701
6	103	2	20	0	1095883856404

ID	TR	TECH	DIFF	RESP	TIME
6	133	2	20	0	1095883868748
6	111	1	0	0	1095883884482
6	156	1	0	0	1095883895279
6	281	3	35	1	1095883909154
6	185	3	30	1	1095883925295
6	275	3	40	0	1095883939013
6	196	2	30	0	1095883949216
6	084	1	10	1	1095883964732
6	075	1	50	1	1095883973497
6	131	3	10	1	1095883987982
6	274	2	50	0	1095883997513
6	221	3	15	1	1095884009419
6	193	2	40	1	1095884024075
6	235	2	0	0	1095884037497
6	285	1	50	1	1095884046841
6	271	2	20	0	1095884060669
6	144	1	5	0	1095884068247
6	052	2	10	1	1095884078403
6	233	3	0	1	1095884093559
6	225	1	40	1	1095884101450
6	041	3	5	0	1095884115700
6	121	2	20	1	1095884132231
6	295	2	5	0	1095884144418
6	122	3	20	0	1095884156152
6	234	1	10	1	1095884164215
6	016	2	30	1	1095884180105
6	105	1	25	1	1095884191449
6	222	1	5	0	1095884204183
6	086	3	20	1	1095884212824
6	006	1	10	1	1095884222183
6	142	2	30	1	1095884235121
6	082	2	10	0	1095884247605
6	146	3	25	1	1095884260652
6	226	2	35	1	1095884272074
6	042	1	10	1	1095884285464
6	161	3	20	0	1095884298636
6	022	2	20	0	1095884305683
6	081	1	0	1	1095884316417
6	162	1	30	0	1095884326104
6	026	3	15	0	1095884347620
6	134	3	25	0	1095884368167
6	115	2	55	1	1095884384588
6	123	1	25	1	1095884391807
6	211	2	10	1	1095884404026
6	021	1	15	0	1095884416260
6	206	3	35	1	1095884427401
6	036	1	45	1	1095884435666
6	284	3	40	1	1095884462932
6	286	2	10	0	1095884474135
6	205	2	35	1	1095884484291
6	072	1	40	1	1095884494369
6	231	1	20	0	1095884503791
6	252	1	30	1	1095884511478
6	163	2	0	1	1095884525166
6	181	2	50	0	1095884544181
6	171	1	35	0	1095884554775
6	126	1	15	1	1095884567947
6	065	3	25	1	1095884588322
6	025	2	20	1	1095884599478
6	116	3	15	1	1095884608056
6	143	3	30	0	1095884618040
6	044	3	5	0	1095884628681
6	273	1	50	1	1095884639868
6	125	3	15	1	1095884647993
6	195	1	30	1	1095884661368
6	166	2	25	1	1095884670415
6	264	1	30	1	1095884678727
6	291	1	15	1	1095884689633
6	175	2	0	1	1095884697555
6	216	1	35	1	1095884706508
6	043	2	20	0	1095884715602
6	203	3	40	1	1095884728555
6	276	1	35	0	1095884736196
6	096	1	20	1	1095884749305
6	046	2	20	0	1095884764039
6	192	1	5	0	1095884771414
6	212	3	0	0	1095884782273

ID	TR	TECH	DIFF	RESP	TIME
6	153	1	5	1	1095884790680
6	201	1	20	1	1095884799086
6	236	3	10	1	1095884812883
6	265	2	5	1	1095884826383
6	263	3	5	1	1095884833336
6	001	2	15	0	1095884847726
6	033	1	15	0	1095884855007
6	004	2	25	1	1095884868257
6	035	3	25	1	1095884875835
6	194	3	35	1	1095884888648
6	215	3	35	1	1095884897070
6	073	2	20	1	1095884909288
6	053	3	30	1	1095884921366
6	292	2	50	1	1095884934538
6	154	2	5	1	1095884945679
6	186	1	0	0	1095884952975
6	232	2	5	0	1095884967272
6	296	3	0	0	1095884975413
6	101	3	20	1	1095884983944
6	141	1	25	0	1095884995163
6	266	3	10	1	1095885003772
6	003	1	25	0	1095885012522
6	124	2	15	1	1095885021913
6	243	1	10	0	1095885036866
6	172	2	35	0	1095885043412
6	062	3	15	1	1095885054631
6	282	1	35	1	1095885062178
6	293	3	5	1	1095885072256
6	032	3	20	0	1095885081850
6	155	3	5	0	1095885090131
11	245	2	5	1	1095968006710
11	285	3	50	1	1095968020382
11	291	3	15	0	1095968036491
11	142	1	30	1	1095968051445
11	132	3	15	1	1095968063038
11	244	1	15	1	1095968073929
11	271	1	20	0	1095968088476
11	042	3	10	0	1095968102913
11	182	2	5	1	1095968116553
11	123	3	25	1	1095968132616
11	026	2	15	0	1095968152491
11	191	2	0	1	1095968163241
11	286	1	10	1	1095968175444
11	035	2	25	1	1095968197584
11	146	2	25	1	1095968209897
11	046	1	20	1	1095968225584
11	202	1	35	1	1095968234803
11	255	3	0	0	1095968255162
11	095	2	25	1	1095968268834
11	292	1	50	1	1095968282990
11	053	2	30	0	1095968295771
11	185	2	30	1	1095968307099
11	143	2	30	1	1095968323490
11	263	2	5	0	1095968337161
11	193	1	40	0	1095968350161
11	172	1	35	0	1095968368489
11	131	2	10	1	1095968380177
11	253	1	15	0	1095968393661
11	215	2	35	1	1095968405567
11	175	1	0	1	1095968414020
11	232	1	5	1	1095968428098
11	114	3	5	1	1095968439442
11	092	2	15	1	1095968462192
11	002	2	20	1	1095968475395
11	213	3	40	1	1095968489004
11	284	2	40	0	1095968501176
11	221	2	15	1	1095968513035
11	085	1	20	0	1095968520801
11	236	2	10	0	1095968544316
11	163	1	0	1	1095968560644
11	212	2	0	0	1095968576144
11	272	2	40	1	1095968587332
11	014	2	45	0	1095968599957
11	052	1	10	1	1095968607957
11	116	2	15	1	1095968628753
11	295	1	5	0	1095968636097
11	216	3	35	1	1095968649816

ID	TR	TECH	DIFF	RESP	TIME
11	126	3	15	1	1095968665409
11	214	1	30	1	1095968677019
11	004	1	25	1	1095968686034
11	006	3	10	1	1095968697972
11	083	2	15	1	1095968717972
11	242	2	0	1	1095968736471
11	093	3	0	1	1095968753956
11	102	3	10	0	1095968773112
11	041	2	5	0	1095968788112
11	161	2	20	0	1095968822080
11	045	3	10	1	1095968850236
11	241	1	30	0	1095968862033
11	104	2	25	1	1095968883986
11	266	2	10	1	1095968898017
11	166	1	25	0	1095968913173
11	022	1	20	0	1095968928908
11	101	2	20	1	1095968960189
11	152	2	15	1	1095968971907
11	156	3	0	0	1095968987314
11	033	3	15	0	1095969006829
11	243	3	10	0	1095969019376
11	136	1	30	1	1095969038141
11	226	1	35	1	1095969046407
11	064	1	35	0	1095969070594
11	162	3	30	1	1095969087313
11	135	3	25	0	1095969104485
11	094	1	10	1	1095969118000
11	056	2	40	1	1095969129781
11	196	1	30	1	1095969145266
11	076	1	45	0	1095969153406
11	005	2	35	1	1095969169437
11	072	3	40	0	1095969183140
11	096	3	20	1	1095969199047
11	201	3	20	1	1095969209796
11	043	1	20	1	1095969220437
11	151	1	5	0	1095969234812
11	274	1	50	1	1095969247937
11	122	2	20	0	1095969263140
11	211	1	10	0	1095969274734
11	234	3	10	1	1095969286452
11	051	3	0	1	1095969298577
11	106	1	20	1	1095969310155
11	296	2	0	0	1095969323749
11	044	2	5	1	1095969334389
11	176	2	10	1	1095969349811
11	223	1	5	1	1095969357967
11	164	2	0	1	1095969376811
11	111	3	0	0	1095969389420
11	081	3	0	0	1095969405842
11	275	2	40	0	1095969417311
11	065	2	25	0	1095969431498
11	121	1	20	1	1095969462935
11	183	3	5	0	1095969475857
11	113	2	20	1	1095969487029
11	195	3	30	0	1095969498920
11	055	1	25	1	1095969507170
11	256	1	60	1	1095969516748
11	075	3	50	0	1095969531529
11	184	1	25	1	1095969539591
11	133	1	20	1	1095969551263
11	073	1	20	1	1095969562154
11	115	1	55	1	1095969574232
11	224	2	15	0	1095969589060
11	276	3	35	0	1095969620528
11	204	3	30	1	1095969631497
11	084	3	10	1	1095969644434
11	105	3	25	1	1095969661122
11	262	1	0	1	1095969669653
11	023	2	30	1	1095969691965
11	283	1	5	1	1095969700403
11	154	1	5	0	1095969714621
11	054	3	0	1	1095969727887
11	141	3	25	0	1095969740152
11	294	3	20	1	1095969757168
11	071	2	50	1	1095969773699
11	282	3	35	1	1095969785183
11	231	3	20	1	1095969807480

ID	TR	TECH	DIFF	RESP	TIME
11	233	2	0	0	1095969819433
11	225	3	40	1	1095969831558
11	021	3	15	0	1095969844855
11	293	2	5	0	1095969862355
11	153	3	5	0	1095969873198
11	062	2	15	1	1095969888745
11	251	2	30	1	1095969899339
11	235	1	0	1	1095969907167
11	181	1	50	1	1095969916698
11	155	2	5	0	1095969930042
11	016	1	30	0	1095969937542
11	171	3	35	1	1095969951417
11	281	2	35	1	1095969968932
11	034	1	15	1	1095969980838
11	066	3	20	1	1095969993416
11	165	3	30	1	1095970001120
11	192	3	5	1	1095970014276
11	013	1	45	0	1095970021994
11	012	3	25	1	1095970034557
11	173	2	30	0	1095970052479
11	063	3	30	0	1095970061291
11	086	2	20	1	1095970073650
11	125	2	15	1	1095970084510
11	194	2	35	1	1095970095963
11	273	3	50	1	1095970106275
11	252	3	30	1	1095970114806
11	186	3	0	0	1095970124759
11	003	3	25	1	1095970141744
11	206	2	35	1	1095970151822
11	024	3	35	0	1095970164822
11	091	1	10	1	1095970172634
11	032	2	20	1	1095970184650
11	061	1	25	1	1095970191650
11	174	3	10	1	1095970205603
11	124	1	15	0	1095970215259
11	265	1	5	0	1095970225806
11	082	1	10	0	1095970234181
11	011	2	10	1	1095970246524
11	203	2	40	1	1095970257696
11	264	3	30	1	1095970268493
11	103	1	20	0	1095970277696
11	025	1	20	1	1095970285211
11	112	1	20	0	1095970294211
11	205	1	35	0	1095970314118
11	036	3	45	0	1095970327180
11	134	2	25	1	1095970339602
11	015	3	20	1	1095970350242
11	074	2	35	1	1095970363211
11	254	2	45	1	1095970374914
11	144	3	5	0	1095970388820
11	261	3	30	1	1095970403133
11	001	1	15	0	1095970420601
11	222	3	5	0	1095970433632
11	145	1	25	1	1095970440976
11	246	3	10	1	1095970454398
11	031	1	10	0	1095970467804
14	046	3	20	1	1096049807059
14	236	1	10	0	1096049827559
14	241	3	30	0	1096049888793
14	112	3	20	0	1096049914324
14	166	3	25	0	1096049952027
14	194	1	35	0	1096049968089
14	163	3	0	1	1096049986886
14	056	1	40	1	1096049998871
14	004	3	25	1	1096050033855
14	085	3	20	0	1096050056370
14	145	3	25	1	1096050083823
14	224	1	15	0	1096050097526
14	204	2	30	1	1096050144870
14	141	2	25	1	1096050184010
14	036	2	45	0	1096050218994
14	051	2	0	1	1096050244306
14	142	3	30	0	1096050321150
14	053	1	30	1	1096050343868
14	094	3	10	1	1096050374056
14	243	2	10	0	1096050400743
14	134	1	25	0	1096050417571

ID	TR	TECH	DIFF	RESP	TIME
14	103	3	20	0	1096050436446
14	181	3	50	0	1096050500477
14	006	2	10	1	1096050518430
14	131	1	10	1	1096050533070
14	072	2	40	1	1096050552633
14	171	2	35	1	1096050574773
14	215	1	35	1	1096050591632
14	174	2	10	1	1096050617070
14	173	1	30	0	1096050631820
14	251	1	30	1	1096050650788
14	191	1	0	1	1096050680491
14	254	1	45	0	1096050704194
14	011	1	10	1	1096050715616
14	272	1	40	1	1096050730866
14	216	2	35	1	1096050750209
14	034	3	15	0	1096050795850
14	032	1	20	1	1096050808365
14	113	1	20	1	1096050822834
14	246	2	10	0	1096050855099
14	263	1	5	0	1096050868552
14	293	1	5	1	1096050886646
14	143	1	30	1	1096050899115
14	195	2	30	1	1096050918708
14	021	2	15	0	1096050945083
14	244	3	15	1	1096050961771
14	012	2	25	1	1096050980911
14	125	1	15	1	1096050998880
14	102	2	10	0	1096051017895
14	105	2	25	1	1096051037504
14	116	1	15	1	1096051053270
14	242	1	0	1	1096051064692
14	075	2	50	1	1096051080410
14	106	3	20	0	1096051120301
14	271	3	20	0	1096051143051
14	003	2	25	1	1096051174113
14	252	2	30	1	1096051192457
14	234	2	10	1	1096051211206
14	086	1	20	1	1096051229503
14	225	2	40	1	1096051246706
14	033	2	15	0	1096051265394
14	153	2	5	1	1096051280894
14	202	3	35	1	1096051311331
14	096	2	20	1	1096051329362
14	101	1	20	1	1096051343362
14	162	2	30	1	1096051362424
14	285	2	50	1	1096051406455
14	071	1	50	0	1096051428283
14	235	3	0	1	1096051444658
14	135	2	25	0	1096051478908
14	265	3	5	0	1096051501736
14	154	3	5	0	1096051520001
14	026	1	15	0	1096051532720
14	296	1	0	0	1096051546439
14	211	3	10	1	1096051590188
14	155	1	5	0	1096051600345
14	022	3	20	1	1096051618829
14	214	3	30	1	1096051635016
14	175	3	0	1	1096051653626
14	121	3	20	1	1096051677860
14	095	1	25	0	1096051696625
14	186	2	0	0	1096051754937
14	061	3	25	1	1096051774828
14	065	1	25	0	1096051787265
14	184	3	25	1	1096051826921
14	185	1	30	1	1096051836109
14	295	3	5	0	1096051857374
14	172	3	35	1	1096051880921
14	284	1	40	0	1096051894046
14	274	3	50	1	1096051916655
14	282	2	35	1	1096051936139
14	082	3	10	1	1096051983889
14	092	1	15	0	1096051995592
14	192	2	5	0	1096052016389
14	291	2	15	1	1096052040873
14	206	1	35	1	1096052052857
14	245	1	5	1	1096052068248
14	054	2	0	1	1096052085670

ID	TR	TECH	DIFF	RESP	TIME
14	152	1	15	1	1096052096904
14	205	3	35	0	1096052141904
14	222	2	5	0	1096052156341
14	264	2	30	1	1096052173232
14	273	2	50	1	1096052192606
14	024	2	35	0	1096052229887
14	231	2	20	1	1096052250903
14	132	2	15	1	1096052265653
14	014	1	45	1	1096052284950
14	111	2	0	1	1096052305840
14	081	2	0	0	1096052325074
14	201	2	20	0	1096052346230
14	223	3	5	1	1096052370168
14	062	1	15	1	1096052392027
14	074	1	35	1	1096052401230
14	005	1	35	1	1096052410355
14	064	3	35	1	1096052428792
14	292	3	50	1	1096052449589
14	213	2	40	1	1096052468652
14	001	3	15	1	1096052499698
14	151	3	5	0	1096052526292
14	266	1	10	0	1096052539260
14	133	3	20	1	1096052563245
14	002	1	20	1	1096052570557
14	294	2	20	1	1096052596401
14	045	2	10	1	1096052617682
14	212	1	0	0	1096052627088
14	276	2	35	1	1096052650197
14	093	2	0	1	1096052679916
14	043	3	20	1	1096052711025
14	226	3	35	1	1096052729119
14	182	1	5	1	1096052739900
14	283	3	5	1	1096052765947
14	052	3	10	1	1096052787446
14	156	2	0	0	1096052801962
14	193	3	40	0	1096052829477
14	275	1	40	0	1096052848087
14	066	2	20	1	1096052873821
14	063	2	30	1	1096052893133
14	013	3	45	0	1096052908696
14	091	3	10	1	1096052923930
14	221	1	15	1	1096052931211
14	196	3	30	1	1096052958539
14	255	2	0	0	1096052995789
14	253	3	15	0	1096053020539
14	123	2	25	1	1096053037789
14	023	1	30	1	1096053052132
14	281	1	35	1	1096053060226
14	183	2	5	1	1096053080195
14	262	3	0	1	1096053095601
14	031	3	10	0	1096053109788
14	042	2	10	1	1096053131694
14	122	1	20	0	1096053143304
14	016	3	30	0	1096053164444
14	084	2	10	1	1096053179335
14	025	3	20	1	1096053219412
14	083	1	15	1	1096053236194
14	176	1	10	1	1096053248318
14	144	2	5	0	1096053264162
14	233	1	0	0	1096053276521
14	015	2	20	1	1096053297599
14	261	2	30	1	1096053313162
14	203	1	40	0	1096053338349
14	044	1	5	1	1096053352521
14	115	3	55	1	1096053369302
14	286	3	10	1	1096053390505
14	161	1	20	1	1096053404661
14	256	3	60	1	1096053425567
14	104	1	25	1	1096053434755
14	164	1	0	1	1096053452911
14	232	3	5	1	1096053470723
14	035	1	25	1	1096053484879
14	076	3	45	1	1096053503520
14	126	2	15	0	1096053529879
14	055	3	25	1	1096053551973
14	041	1	5	0	1096053564363
14	073	3	20	1	1096053589285

ID	TR	TECH	DIFF	RESP	TIME
14	114	2	5	0	1096053621238
14	165	2	30	1	1096053633582
14	124	3	15	0	1096053648285
14	136	3	30	1	1096053661316
14	146	1	25	1	1096053675472
19	024	3	35	0	1099057196304
19	271	1	20	0	1099057219867
19	066	3	20	1	1099057251539
19	275	2	40	1	1099057281648
19	123	3	25	1	1099057301960
19	155	2	5	0	1099057317117
19	115	1	55	1	1099057363460
19	122	2	20	0	1099057390757
19	131	2	10	1	1099057407632
19	171	3	35	1	1099057426945
19	254	2	45	1	1099057448476
19	064	1	35	1	1099057462039
19	296	2	0	0	1099057477492
19	121	1	20	0	1099057493664
19	255	3	0	1	1099057522960
19	125	2	15	1	1099057538585
19	103	1	20	1	1099057561632
19	183	3	5	1	1099057595070
19	233	2	0	1	1099057610460
19	261	3	30	1	1099057624757
19	236	2	10	0	1099057642945
19	293	2	5	0	1099057673429
19	194	2	35	1	1099057695429
19	264	3	30	1	1099057715148
19	065	2	25	0	1099057753617
19	172	1	35	1	1099057765273
19	102	3	10	0	1099057788179
19	134	2	25	1	1099057808445
19	232	1	5	1	1099057825679
19	085	1	20	0	1099057835492
19	273	3	50	1	1099057851851
19	234	3	10	1	1099057876023
19	295	1	5	0	1099057888695
19	185	2	30	1	1099057903148
19	173	2	30	0	1099057917851
19	215	2	35	1	1099057933445
19	094	1	10	0	1099057950632
19	221	2	15	1	1099057974304
19	243	3	10	0	1099057992726
19	034	1	15	0	1099058007742
19	072	3	40	1	1099058032226
19	294	3	20	1	1099058047710
19	195	3	30	1	1099058063335
19	246	3	10	1	1099058087304
19	175	1	0	1	1099058097695
19	231	3	20	0	1099058114585
19	272	2	40	1	1099058129085
19	214	1	30	1	1099058141304
19	106	1	20	1	1099058157710
19	051	3	0	1	1099058172460
19	044	2	5	1	1099058187695
19	235	1	0	1	1099058208164
19	153	3	5	0	1099058235992
19	184	1	25	1	1099058253476
19	176	2	10	1	1099058269132
19	262	1	0	1	1099058284523
19	042	3	10	1	1099058301007
19	165	3	30	1	1099058312726
19	252	3	30	1	1099058329179
19	012	3	25	1	1099058344242
19	162	3	30	1	1099058382070
19	225	3	40	1	1099058398132
19	244	1	15	1	1099058417445
19	164	2	0	1	1099058433367
19	286	1	10	1	1099058445976
19	281	2	35	1	1099058461257
19	084	3	10	1	1099058485601
19	152	2	15	1	1099058508882
19	193	1	40	0	1099058520773
19	033	3	15	1	1099058545601
19	126	3	15	1	1099058560007
19	096	3	20	1	1099058574351

ID	TR	TECH	DIFF	RESP	TIME
19	002	2	20	1	1099058585054
19	263	2	5	0	1099058597164
19	062	2	15	1	1099058617054
19	071	2	50	1	1099058631023
19	211	1	10	1	1099058644085
19	144	3	5	0	1099058657210
19	202	1	35	1	1099058668601
19	226	1	35	1	1099058680367
19	201	3	20	1	1099058696726
19	112	1	20	0	1099058707945
19	276	3	35	1	1099058720101
19	192	3	5	1	1099058744914
19	182	2	5	1	1099058757007
19	061	1	25	1	1099058765367
19	075	3	50	1	1099058782335
19	141	3	25	1	1099058797851
19	156	3	0	0	1099058813054
19	073	1	20	1	1099058825914
19	163	1	0	1	1099058834132
19	016	1	30	0	1099058843585
19	274	1	50	1	1099058852507
19	054	3	0	1	1099058870664
19	143	2	30	1	1099058884898
19	003	3	25	1	1099058899960
19	093	3	0	0	1099058912414
19	213	3	40	1	1099058923976
19	241	1	30	0	1099058937023
19	216	3	35	1	1099058949335
19	181	1	50	1	1099058981164
19	041	2	5	0	1099058997101
19	205	1	35	1	1099059031960
19	045	3	10	1	1099059054132
19	204	3	30	1	1099059069867
19	191	2	0	1	1099059081398
19	266	2	10	1	1099059099632
19	135	3	25	1	1099059118882
19	004	1	25	1	1099059126710
19	186	3	0	1	1099059143570
19	001	1	15	1	1099059161367
19	046	1	20	1	1099059173054
19	283	1	5	1	1099059185570
19	081	3	0	0	1099059200898
19	151	1	5	1	1099059219210
19	253	1	15	1	1099059231601
19	043	1	20	0	1099059252695
19	021	3	15	1	1099059270148
19	284	2	40	1	1099059281210
19	023	2	30	1	1099059311554
19	166	1	25	0	1099059335679
19	142	1	30	1	1099059347273
19	146	2	25	1	1099059363132
19	105	3	25	1	1099059374039
19	013	1	45	0	1099059386695
19	005	2	35	1	1099059400117
19	242	2	0	0	1099059415148
19	265	1	5	0	1099059427617
19	196	1	30	0	1099059448382
19	063	3	30	1	1099059459617
19	154	1	5	1	1099059471601
19	133	1	20	1	1099059483617
19	222	3	5	1	1099059501226
19	086	2	20	1	1099059519945
19	292	1	50	1	1099059528867
19	145	1	25	1	1099059537007
19	092	2	15	0	1099059554023
19	136	1	30	1	1099059566132
19	111	3	0	0	1099059578320
19	056	2	40	1	1099059590054
19	101	2	20	1	1099059603789
19	022	1	20	1	1099059615679
19	116	2	15	1	1099059633914
19	076	1	45	0	1099059651132
19	011	2	10	1	1099059663179
19	032	2	20	1	1099059678617
19	245	2	5	0	1099059697804
19	291	3	15	1	1099059711492
19	036	3	45	1	1099059731304

ID	TR	TECH	DIFF	RESP	TIME
19	035	2	25	1	1099059748664
19	083	2	15	1	1099059768070
19	212	2	0	0	1099059782054
19	082	1	10	1	1099059793148
19	132	3	15	1	1099059804882
19	206	2	35	1	1099059816382
19	285	3	50	1	1099059832242
19	015	3	20	1	1099059843882
19	223	1	5	0	1099059857851
19	091	1	10	1	1099059865539
19	203	2	40	0	1099059889773
19	174	3	10	1	1099059901804
19	224	2	15	1	1099059923929
19	014	2	45	1	1099059939851
19	052	1	10	1	1099059947023
19	282	3	35	1	1099059985289
19	095	2	25	1	1099060005523
19	114	3	5	0	1099060024414
19	006	3	10	1	1099060036492
19	251	2	30	1	1099060047585
19	031	1	10	0	1099060059335
19	256	1	60	1	1099060067398
19	113	2	20	1	1099060081695
19	025	1	20	1	1099060092398
19	026	2	15	0	1099060110742
19	055	1	25	1	1099060118710
19	104	2	25	1	1099060139304
19	053	2	30	1	1099060152179
19	124	1	15	1	1099060163273
19	074	2	35	1	1099060176132
19	161	2	20	1	1099060195773

Table A.3: Participant responses from User Study 2.1

ID	TR	SHD	RCK	DIFF	RCKN	TIME	RESP
0	283	4	0	1.5	0	1110322563631	1
0	082	4	1	2	1	1110322579819	0
0	086	4	1	2	1	1110322596928	1
0	231	4	0	1.5	0	1110322605224	0
0	274	3	1	2	1	1110322621959	1
0	111	3	0	0.5	0	1110322632693	1
0	003	3	0	2	0	1110322638427	1
0	166	4	1	4	1	1110322655333	1
0	031	4	1	1	1	1110322679255	0
0	172	4	1	2	0	1110322692880	1
0	034	4	0	0.5	0	1110322702067	1
0	146	4	0	2	0	1110322708036	1
0	212	4	0	3	0	1110322712754	1
0	166	3	0	4	0	1110322718020	1
0	086	3	0	2	0	1110322724535	1
0	073	4	0	1.5	0	1110322730176	1
0	185	3	1	2	0	1110322742754	1
0	066	4	1	2	1	1110322760738	1
0	122	3	1	0.5	1	1110322777738	0
0	195	4	0	3	0	1110322787410	1
0	031	3	0	1	0	1110322792191	0
0	176	4	0	1	0	1110322797503	0
0	251	3	1	2.5	0	1110322810269	1
0	073	3	1	1.5	1	1110322828487	1
0	111	4	1	0.5	0	1110322841659	1
0	022	4	1	0.5	0	1110322857221	0
0	115	4	1	1.5	1	1110322877315	1
0	056	4	0	2.5	0	1110322884752	1
0	226	4	0	1.5	0	1110322889690	1
0	153	3	1	4	1	1110322908142	1
0	251	4	0	2.5	0	1110322913189	1
0	004	4	0	2.5	0	1110322919908	1
0	162	4	1	1.5	1	1110322936673	1
0	072	3	0	2	0	1110322947408	0
0	026	3	1	2.5	1	1110322967173	1
0	025	4	0	0.5	0	1110322971751	0
0	212	3	1	3	0	1110322984001	1
0	053	3	0	0.5	0	1110322989735	0
0	022	3	0	0.5	0	1110322995001	1
0	066	3	0	2	0	1110323001688	1
0	213	3	0	0.5	0	1110323011016	0
0	226	3	1	1.5	0	1110323024532	1
0	232	3	0	2	0	1110323032672	1
0	181	4	0	1.5	0	1110323040313	1
0	034	3	1	0.5	0	1110323056969	1
0	094	3	1	1	1	1110323084843	1
0	095	4	0	2	0	1110323101749	1
0	011	3	1	1.5	0	1110323118890	0
0	114	3	1	0.5	1	1110323135733	0
0	136	3	0	2.5	0	1110323152967	0
0	183	4	1	3	0	1110323167467	1
0	103	4	1	3.5	1	1110323184639	1
0	283	3	1	1.5	1	1110323203920	1
0	033	3	0	3	0	1110323212592	1
0	124	4	0	2.5	0	1110323219029	1
0	115	3	0	1.5	0	1110323225248	1
0	201	4	0	1	0	1110323231654	0
0	121	3	0	2	0	1110323239841	1
0	213	4	1	0.5	0	1110323254685	1
0	235	4	1	3	1	1110323271435	1
0	162	3	0	1.5	0	1110323278778	1
0	122	4	0	0.5	0	1110323284153	0
0	211	4	1	1	0	1110323298497	0
0	103	3	0	3.5	0	1110323304575	1
0	092	4	0	2	0	1110323310497	1
0	114	4	0	0.5	0	1110323315622	0
0	222	3	0	1	0	1110323322809	1
0	153	4	0	4	0	1110323331684	1
0	246	4	1	1.5	0	1110323345246	1
0	294	3	0	3.5	0	1110323354137	0
0	072	4	1	2	1	1110323372308	1
0	244	3	0	2.5	0	1110323379355	1
0	025	3	1	0.5	0	1110323393558	0
0	026	4	0	2.5	0	1110323398683	1
0	154	3	0	0.5	0	1110323403605	0
0	136	4	1	2.5	0	1110323416527	1
0	265	3	0	3	0	1110323423917	1
0	192	4	1	2	0	1110323440167	1
0	223	3	0	1.5	0	1110323446104	1
0	294	4	1	3.5	0	1110323459714	1
0	146	3	1	2	1	1110323479010	1
0	063	4	1	2	0	1110323495041	1
0	222	4	1	1	0	1110323511307	1
0	085	4	0	3	0	1110323517697	1
0	033	4	1	3	0	1110323534509	1
0	274	4	0	2	0	1110323540947	1
0	002	4	0	1.5	0	1110323556900	1
0	113	3	1	2.5	0	1110323570978	1
0	003	4	1	2	0	1110323587212	1
0	192	3	0	2	0	1110323596743	0
0	054	3	0	2	0	1110323603837	0
0	082	3	0	2	0	1110323609649	0
0	056	3	1	2.5	0	1110323623836	1
0	063	3	0	2	0	1110323630086	1
0	012	3	1	3	1	1110323648242	1
0	023	4	1	3	1	1110323667008	1
0	012	4	0	3	0	1110323676929	1
0	002	3	1	1.5	1	1110323701007	1
0	176	3	1	1	1	1110323722413	0
0	053	4	1	0.5	1	1110323741085	1
0	246	3	0	1.5	0	1110323750772	1
0	211	3	0	1	0	1110323755413	0
0	253	4	0	1.5	0	1110323763881	1
0	125	3	1	1.5	0	1110323777475	1
0	265	4	1	3	1	1110323794240	1
0	054	4	1	2	1	1110323815896	1
0	201	3	1	1	1	1110323838818	0
0	282	3	1	2.5	1	1110323855708	1
0	253	3	1	1.5	1	1110323871458	1
0	282	4	0	2.5	0	1110323880442	1
0	092	3	1	2	0	1110323894114	1
0	181	3	1	1.5	1	1110323909536	1
0	244	4	1	2.5	0	1110323922723	1
0	235	3	0	3	0	1110323928208	1
0	185	4	0	2	0	1110323939020	1
0	125	4	0	1.5	0	1110323949379	1
0	154	4	1	0.5	0	1110323963707	0
0	183	3	0	3	0	1110323970910	1
0	232	4	1	2	0	1110323984551	1
0	085	3	1	3	1	1110324001550	1
0	195	3	1	3	0	1110324015535	1
0	113	4	0	2.5	0	1110324024644	1
0	121	4	1	2	1	1110324043487	0
0	172	3	0	2	0	1110324048612	1
0	004	3	1	2.5	1	1110324067440	1
0	023	3	0	3	0	1110324080143	0
0	124	3	1	2.5	1	1110324096518	1
0	223	4	1	1.5	1	1110324115689	1
0	094	4	0	1	0	1110324122564	0
0	011	4	0	1.5	0	1110324127471	0
0	095	3	1	2	0	1110324142986	0
0	231	3	1	1.5	1	1110324158486	0
2	115	4	1	1.5	1	1110404030828	1
2	222	3	0	1	0	1110404039479	1
2	253	4	0	1.5	0	1110404057895	0
2	103	3	0	3.5	0	1110404072655	1
2	282	3	1	2.5	1	1110404089448	1
2	066	4	1	2	1	1110404104929	1
2	121	4	1	2	2	1110404145104	1
2	094	3	1	1	1	1110404162958	0
2	095	3	1	2	2	1110404183587	1
2	246	3	0	1.5	0	1110404192959	1
2	011	3	1	1.5	1	1110404215350	0
2	056	3	1	2.5	2	1110404237010	1
2	172	3	0	2	0	1110404246513	1
2	122	4	0	0.5	0	1110404268032	0
2	235	3	0	3	0	1110404287118	1
2	114	3	1	0.5	1	1110404309058	0
2	294	3	0	3.5	0	1110404328915	1
2	004	3	1	2.5	1	1110404346590	1
2	115	3	0	1.5	0	1110404358706	1

ID	TR	SHD	RCK	DIFF	RCKN	TIME	RESP
2	073	3	1	1.5	1	1110404375229	0
2	265	3	0	3	0	1110404387145	1
2	166	4	1	4	0	1110404399702	1
2	226	3	1	1.5	1	1110404419039	1
2	195	3	1	3	0	1110404432077	1
2	192	4	1	2	3	1110404457071	1
2	146	4	0	2	0	1110404470659	1
2	031	4	1	1	1	1110404489746	1
2	023	3	0	3	0	1110404499108	1
2	082	4	1	2	1	1110404518715	1
2	111	4	1	0.5	1	1110404536269	1
2	054	4	1	2	0	1110404548987	1
2	053	4	1	0.5	4	1110404584886	1
2	033	4	1	3	3	1110404610531	1
2	146	3	1	2	0	1110404623188	1
2	153	3	1	4	1	1110404645509	1
2	172	4	1	2	1	1110404663583	1
2	033	3	0	3	0	1110404672265	0
2	154	4	1	0.5	2	1110404693214	0
2	232	3	0	2	0	1110404702877	1
2	073	4	0	1.5	0	1110404713982	1
2	231	4	0	1.5	0	1110404734611	0
2	095	4	0	2	0	1110404745896	1
2	211	4	1	1	2	1110404766244	0
2	003	4	1	2	0	1110404778591	1
2	025	3	1	0.5	1	1110404798298	0
2	246	4	1	1.5	0	1110404818325	1
2	223	3	0	1.5	0	1110404829070	1
2	185	3	1	2	0	1110404840906	1
2	054	3	0	2	0	1110404852682	0
2	232	4	1	2	0	1110404864889	1
2	026	3	1	2.5	0	1110404877025	1
2	223	4	1	1.5	0	1110404889202	1
2	162	3	0	1.5	0	1110404898455	1
2	201	3	1	1	2	1110404926253	0
2	003	3	0	2	0	1110404937468	1
2	251	4	0	2.5	0	1110404946510	1
2	153	4	0	4	0	1110404957556	0
2	012	4	0	3	0	1110404970563	0
2	125	4	0	1.5	0	1110404986095	1
2	012	3	1	3	1	1110405003318	1
2	094	4	0	1	0	1110405031206	1
2	294	4	1	3.5	0	1110405043113	1
2	092	3	1	2	0	1110405055710	1
2	231	3	1	1.5	1	1110405073064	1
2	274	3	1	2	0	1110405085521	1
2	002	4	0	1.5	0	1110405096375	1
2	274	4	0	2	0	1110405108322	1
2	113	3	1	2.5	1	1110405124334	1
2	283	4	0	1.5	0	1110405141647	1
2	253	3	1	1.5	0	1110405154815	1
2	181	4	0	1.5	0	1110405166862	1
2	103	4	1	3.5	1	1110405187250	1
2	034	4	0	0.5	0	1110405197794	1
2	086	3	0	2	0	1110405212184	1
2	022	3	0	0.5	0	1110405225062	1
2	092	4	0	2	0	1110405245289	0
2	122	3	1	0.5	0	1110405257366	0
2	211	3	0	1	0	1110405267229	0
2	125	3	1	1.5	1	1110405284603	1
2	023	4	1	3	0	1110405298152	1
2	031	3	0	1	0	1110405311149	1
2	251	3	1	2.5	0	1110405323106	1
2	113	4	0	2.5	0	1110405333310	1
2	183	3	0	3	0	1110405350183	1
2	181	3	1	1.5	3	1110405380775	0
2	063	3	0	2	0	1110405390147	1
2	201	4	0	1	0	1110405402144	0
2	235	4	1	3	1	1110405420439	1
2	222	4	1	1	0	1110405435039	1
2	136	3	0	2.5	0	1110405447956	0
2	072	4	1	2	1	1110405467163	0
2	085	3	1	3	1	1110405485518	1
2	283	3	1	1.5	1	1110405504223	1
2	082	3	0	2	0	1110405530419	0
2	244	4	1	2.5	0	1110405543537	1
2	176	3	1	1	0	1110405554753	0

ID	TR	SHD	RCK	DIFF	RCKN	TIME	RESP
2	025	4	0	0.5	0	1110405568341	0
2	244	3	0	2.5	0	1110405576612	1
2	192	3	0	2	0	1110405593836	0
2	226	4	0	1.5	0	1110405601867	1
2	066	3	0	2	0	1110405610539	1
2	282	4	0	2.5	0	1110405616978	1
2	053	3	0	0.5	0	1110405627342	0
2	212	3	1	3	1	1110405643724	1
2	026	4	0	2.5	0	1110405655490	1
2	085	4	0	3	0	1110405664843	1
2	213	3	0	0.5	0	1110405675668	1
2	136	4	1	2.5	2	1110405697468	0
2	154	3	0	0.5	0	1110405714681	0
2	124	3	1	2.5	1	1110405734448	1
2	212	4	0	3	0	1110405743891	1
2	022	4	1	0.5	0	1110405755728	0
2	111	3	0	0.5	0	1110405764319	1
2	162	4	1	1.5	2	1110405785668	1
2	086	4	1	2	1	1110405803543	1
2	114	4	0	0.5	0	1110405821327	1
2	004	4	0	2.5	0	1110405834415	1
2	063	4	1	2	0	1110405847323	1
2	265	4	1	3	0	1110405860331	1
2	176	4	0	1	0	1110405869874	0
2	056	4	0	2.5	0	1110405879487	1
2	124	4	0	2.5	0	1110405890181	1
2	034	3	1	0.5	0	1110405901867	1
2	195	4	0	3	0	1110405923157	1
2	183	4	1	3	1	1110405940340	1
2	185	4	0	2	0	1110405948381	1
2	166	3	0	4	0	1110405961789	1
2	072	3	0	2	0	1110405970391	1
2	011	4	0	1.5	0	1110405981436	0
2	121	3	0	2	0	1110406006611	1
2	002	3	1	1.5	0	1110406018908	1
2	213	4	1	0.5	2	1110406038895	1
4	282	3	1	2.5	1	1110463448355	1
4	195	3	1	3	2	1110463470867	1
4	244	3	0	2.5	0	1110463499418	1
4	153	4	0	4	0	1110463519917	0
4	185	4	0	2	0	1110463529812	1
4	072	3	0	2	0	1110463543501	0
4	265	4	1	3	2	1110463570300	1
4	232	3	0	2	0	1110463588246	1
4	251	4	0	2.5	0	1110463598951	1
4	124	4	0	2.5	0	1110463612701	1
4	183	4	1	3	1	1110463642654	1
4	053	4	1	0.5	1	1110463663394	0
4	113	3	1	2.5	2	1110463686076	1
4	103	4	1	3.5	0	1110463700457	1
4	172	3	0	2	0	1110463732844	1
4	136	3	0	2.5	0	1110463764048	0
4	082	4	1	2	3	1110463792279	1
4	213	4	1	0.5	0	1110463805318	1
4	056	4	0	2.5	0	1110463821070	1
4	023	4	1	3	2	1110463848220	1
4	086	3	0	2	0	1110463885443	0
4	122	4	0	0.5	0	1110463896018	0
4	085	3	1	3	3	1110463922616	1
4	231	4	0	1.5	0	1110463930528	1
4	195	4	0	3	0	1110463938892	0
4	282	4	0	2.5	0	1110463945979	1
4	012	3	1	3	1	1110463962883	1
4	223	4	1	1.5	3	1110463989092	1
4	154	4	1	0.5	3	1110464017441	0
4	172	4	1	2	2	1110464038883	1
4	092	3	1	2	2	1110464061944	1
4	235	4	1	3	2	1110464090563	1
4	244	4	1	2.5	0	1110464103738	1
4	201	3	1	1	3	1110464131477	1
4	122	3	1	0.5	0	1110464143502	0
4	094	3	1	1	3	1110464169182	1
4	066	3	0	2	0	1110464182797	1
4	181	3	1	1.5	2	1110464204998	1
4	031	4	1	1	2	1110464227579	0
4	185	3	1	2	2	1110464247226	1
4	176	3	1	1	1	1110464264061	0

ID	TR	SHD	RCK	DIFF	RCKN	TIME	RESP
4	103	3	0	3.5	0	1110464275638	1
4	213	3	0	0.5	0	1110464296049	0
4	211	4	1	1	1	1110464313474	0
4	003	3	0	2	0	1110464337259	1
4	246	4	1	1.5	2	1110464481483	1
4	136	4	1	2.5	2	1110464504467	0
4	183	3	0	3	0	1110464516464	0
4	033	4	1	3	3	1110464541892	1
4	066	4	1	2	3	1110464567570	1
4	054	4	1	2	2	1110464592507	1
4	033	3	0	3	0	1110464603964	1
4	023	3	0	3	0	1110464611475	0
4	053	3	0	0.5	0	1110464634218	1
4	253	3	1	1.5	0	1110464645775	1
4	211	3	0	1	0	1110464654158	1
4	115	3	0	1.5	0	1110464678353	1
4	073	3	1	1.5	1	1110464695339	1
4	231	3	1	1.5	3	1110464719735	1
4	125	3	1	1.5	1	1110464737411	1
4	073	4	0	1.5	0	1110464746614	1
4	166	4	1	4	1	1110464763439	1
4	113	4	0	2.5	0	1110464776909	1
4	026	4	0	2.5	0	1110464784500	0
4	022	4	1	0.5	1	1110464803328	0
4	166	3	0	4	0	1110464829527	0
4	124	3	1	2.5	0	1110464841815	1
4	034	4	0	0.5	0	1110464862696	1
4	176	4	0	1	0	1110464908544	0
4	294	4	1	3.5	2	1110464928774	1
4	025	4	0	0.5	0	1110464938338	1
4	004	3	1	2.5	0	1110464950526	1
4	111	3	0	0.5	0	1110464968753	0
4	054	3	0	2	0	1110464984894	0
4	003	4	1	2	2	1110465006009	1
4	232	4	1	2	2	1110465027666	1
4	002	4	0	1.5	0	1110465034494	1
4	283	4	0	1.5	0	1110465044967	0
4	246	3	0	1.5	0	1110465057933	1
4	115	4	1	1.5	3	1110465082463	1
4	226	3	1	1.5	1	1110465098692	1
4	085	4	0	3	0	1110465109496	1
4	265	3	0	3	0	1110465117215	1
4	082	3	0	2	0	1110465136158	1
4	192	4	1	2	2	1110465157594	1
4	063	4	1	2	0	1110465169399	1
4	125	4	0	1.5	0	1110465181844	1
4	153	3	1	4	1	1110465199826	1
4	011	4	0	1.5	0	1110465209497	1
4	114	3	1	0.5	2	1110465324532	0
4	226	4	0	1.5	0	1110465342456	0
4	111	4	1	0.5	2	1110465366227	1
4	162	4	1	1.5	2	1110465388696	1
4	223	3	0	1.5	0	1110465405428	0
4	026	3	1	2.5	1	1110465424953	1
4	154	3	0	0.5	0	1110465445110	0
4	011	3	1	1.5	3	1110465480666	1
4	294	3	0	3.5	0	1110465503486	1
4	181	4	0	1.5	0	1110465519878	1
4	004	4	0	2.5	0	1110465538132	0
4	086	4	1	2	3	1110465562704	1
4	114	4	0	0.5	0	1110465572166	1
4	235	3	0	3	0	1110465595877	1
4	095	3	1	2	3	1110465619788	1
4	072	4	1	2	2	1110465642488	1
4	274	3	1	2	1	1110465659600	1
4	146	4	0	2	0	1110465670345	1
4	212	4	0	3	0	1110465676883	1
4	025	3	1	0.5	1	1110465692504	0
4	253	4	0	1.5	0	1110465716285	1
4	222	4	1	1	2	1110465736281	1
4	212	3	1	3	0	1110465749298	1
4	162	3	0	1.5	0	1110465760573	1
4	192	3	0	2	0	1110465769835	1
4	022	3	0	0.5	0	1110465786757	0
4	251	3	1	2.5	2	1110465808275	0
4	012	4	0	3	0	1110465817227	0
4	201	4	0	1	0	1110465826649	0

ID	TR	SHD	RCK	DIFF	RCKN	TIME	RESP
4	095	4	0	2	0	1110465836582	1
4	056	3	1	2.5	1	1110465852483	1
4	002	3	1	1.5	1	1110465869525	1
4	121	3	0	2	0	1110465883303	0
4	092	4	0	2	0	1110465892195	1
4	121	4	1	2	3	1110465916477	1
4	031	3	0	1	0	1110465928973	1
4	274	4	0	2	0	1110465947377	1
4	034	3	1	0.5	3	1110465972179	0
4	222	3	0	1	0	1110465983715	0
4	283	3	1	1.5	0	1110465997412	1
4	063	3	0	2	0	1110466006070	0
4	146	3	1	2	0	1110466018976	1
4	094	4	0	1	0	1110466027964	1
6	226	4	0	1.5	0	1110486782240	1
6	003	3	0	2	0	1110486804442	1
6	183	3	0	3	0	1110486839771	1
6	025	4	0	0.5	0	1110486860501	1
6	125	3	1	1.5	2	1110486882772	1
6	166	4	1	4	2	1110486903431	1
6	235	3	0	3	0	1110486930629	0
6	111	4	1	0.5	4	1110486957567	1
6	244	4	1	2.5	0	1110486971116	1
6	053	3	0	0.5	0	1110486987099	1
6	176	4	0	1	0	1110487011353	0
6	183	4	1	3	1	1110487029709	1
6	282	4	0	2.5	0	1110487043959	1
6	004	3	1	2.5	1	1110487065840	1
6	113	4	0	2.5	0	1110487078798	1
6	111	3	0	0.5	0	1110487090975	1
6	153	3	1	4	1	1110487108360	1
6	124	4	0	2.5	0	1110487123581	1
6	195	3	1	3	2	1110487142908	1
6	136	3	0	2.5	0	1110487154334	0
6	012	4	0	3	0	1110487162015	0
6	022	3	0	0.5	0	1110487177146	1
6	026	3	1	2.5	2	1110487196464	1
6	121	4	1	2	1	1110487211435	1
6	246	4	1	1.5	0	1110487224263	1
6	054	4	1	2	1	1110487239875	1
6	072	4	1	2	2	1110487259122	1
6	181	3	1	1.5	3	1110487283626	1
6	011	4	0	1.5	0	1110487302733	1
6	185	4	0	2	0	1110487309663	1
6	004	4	0	2.5	0	1110487332145	1
6	092	3	1	2	2	1110487351141	1
6	232	4	1	2	1	1110487366152	1
6	063	3	0	2	0	1110487385119	1
6	166	3	0	4	0	1110487398889	0
6	115	3	0	1.5	0	1110487413709	1
6	056	4	0	2.5	0	1110487431625	1
6	114	4	0	0.5	0	1110487448619	0
6	231	4	0	1.5	0	1110487464331	1
6	231	3	1	1.5	2	1110487483918	1
6	201	4	0	1	0	1110487498349	0
6	146	4	0	2	0	1110487507932	1
6	066	3	0	2	0	1110487523274	1
6	136	4	1	2.5	6	1110487557482	1
6	232	3	0	2	0	1110487568217	1
6	226	3	1	1.5	2	1110487602235	1
6	235	4	1	3	2	1110487622513	1
6	034	4	0	0.5	0	1110487635572	1
6	274	4	0	2	0	1110487658985	1
6	056	3	1	2.5	2	1110487683309	1
6	031	4	1	1	4	1110487709466	1
6	122	3	1	0.5	2	1110487729274	0
6	212	4	0	3	0	1110487740970	1
6	023	4	1	3	1	1110487756382	1
6	154	3	0	0.5	0	1110487765665	0
6	253	4	0	1.5	0	1110487777832	1
6	086	4	1	2	2	1110487797720	1
6	086	3	0	2	0	1110487818179	1
6	211	3	0	1	0	1110487830626	0
6	113	3	1	2.5	2	1110487851436	1
6	092	4	0	2	0	1110487866998	1
6	192	4	1	2	2	1110487886655	1
6	294	3	0	3.5	0	1110487910299	1

ID	TR	SHD	RCK	DIFF	RCKN	TIME	RESP
6	095	4	0	2	0	1110487919271	1
6	072	3	0	2	0	1110487930777	1
6	154	4	1	0.5	4	1110487959117	0
6	185	3	1	2	2	1110487979556	1
6	172	3	0	2	0	1110487994397	1
6	023	3	0	3	0	1110488007966	1
6	002	3	1	1.5	1	1110488022817	1
6	002	4	0	1.5	0	1110488034634	1
6	054	3	0	2	0	1110488042795	1
6	195	4	0	3	0	1110488058277	0
6	201	3	1	1	4	1110488086096	1
6	114	3	1	0.5	2	1110488106735	1
6	172	4	1	2	3	1110488133122	1
6	085	4	0	3	0	1110488141314	1
6	251	3	1	2.5	2	1110488161252	1
6	265	4	1	3	2	1110488180900	1
6	103	4	1	3.5	1	1110488196251	1
6	265	3	0	3	0	1110488211262	1
6	251	4	0	2.5	0	1110488218292	1
6	094	3	1	1	6	1110488252801	0
6	003	4	1	2	3	1110488276094	0
6	213	4	1	0.5	0	1110488287149	1
6	124	3	1	2.5	0	1110488299016	1
6	294	4	1	3.5	0	1110488310813	1
6	022	4	1	0.5	1	1110488327766	0
6	073	4	0	1.5	0	1110488338341	1
6	115	4	1	1.5	2	1110488364007	1
6	082	3	0	2	0	1110488377346	0
6	063	4	1	2	1	1110488394040	1
6	011	3	1	1.5	2	1110488415029	1
6	125	4	0	1.5	0	1110488422270	1
6	176	3	1	1	1	1110488440215	0
6	162	3	0	1.5	0	1110488459822	1
6	053	4	1	0.5	2	1110488480732	0
6	283	3	1	1.5	0	1110488493830	1
6	222	3	0	1	0	1110488518705	1
6	153	4	0	4	0	1110488527978	0
6	253	3	1	1.5	0	1110488540336	1
6	103	3	0	3.5	0	1110488549819	1
6	213	3	0	0.5	0	1110488570448	0
6	162	4	1	1.5	4	1110488597246	1
6	244	3	0	2.5	0	1110488609083	1
6	223	4	1	1.5	1	1110488624304	1
6	012	3	1	3	0	1110488636431	1
6	246	3	0	1.5	0	1110488652514	1
6	274	3	1	2	2	1110488673303	1
6	031	3	0	1	0	1110488694863	0
6	026	4	0	2.5	0	1110488709704	0
6	082	4	1	2	2	1110488728641	0
6	192	3	0	2	0	1110488740357	0
6	211	4	1	1	5	1110488771391	0
6	025	3	1	0.5	3	1110488795225	0
6	034	3	1	0.5	3	1110488821281	1
6	085	3	1	3	1	1110488837855	1
6	094	4	0	1	0	1110488870100	1
6	033	4	1	3	3	1110488892992	1
6	223	3	0	1.5	0	1110488904569	0
6	122	4	0	0.5	0	1110488913621	0
6	033	3	0	3	0	1110488923525	1
6	212	3	1	3	0	1110488935823	1
6	121	3	0	2	0	1110488946337	0
6	066	4	1	2	1	1110488965895	1
6	282	3	1	2.5	1	1110488981717	1
6	073	3	1	1.5	2	1110489000123	1
6	146	3	1	2	2	1110489019901	1
6	095	3	1	2	2	1110489041752	1
6	222	4	1	1	2	1110489060698	1
6	283	4	0	1.5	0	1110489070102	1
6	181	4	0	1.5	0	1110489092553	1
8	121	4	1	2	2	1110553537005	1
8	023	4	1	3	2	1110553559007	1
8	034	3	1	0.5	3	1110553585166	1
8	192	3	0	2	0	1110553605385	1
8	011	3	1	1.5	3	1110553633416	0
8	124	3	1	2.5	2	1110553659204	1
8	111	3	0	0.5	0	1110553671101	1
8	211	4	1	1	6	1110553710438	0

ID	TR	SHD	RCK	DIFF	RCKN	TIME	RESP
8	265	3	0	3	0	1110553722035	0
8	166	4	1	4	2	1110553746801	1
8	235	4	1	3	2	1110553769845	1
8	201	3	1	1	2	1110553793880	1
8	115	4	1	1.5	2	1110553820018	1
8	195	3	1	3	2	1110553842000	1
8	246	4	1	1.5	1	1110553860607	1
8	274	4	0	2	0	1110553878153	1
8	012	3	1	3	0	1110553890771	1
8	066	3	0	2	0	1110553907435	1
8	124	4	0	2.5	0	1110553919773	1
8	094	3	1	1	2	1110553940824	1
8	121	3	0	2	0	1110553960733	0
8	232	4	1	2	0	1110553973472	1
8	201	4	0	1	0	1110553995995	0
8	114	4	0	0.5	0	1110554014782	1
8	125	3	1	1.5	2	1110554035833	1
8	092	4	0	2	0	1110554045447	1
8	172	4	1	2	1	1110554063132	1
8	026	4	0	2.5	0	1110554073738	0
8	213	3	0	0.5	0	1110554092986	0
8	181	4	0	1.5	0	1110554102009	1
8	283	4	0	1.5	0	1110554120136	1
8	231	3	1	1.5	2	1110554142498	1
8	212	4	0	3	0	1110554150149	1
8	113	3	1	2.5	5	1110554186763	1
8	153	4	0	4	0	1110554204799	0
8	274	3	1	2	0	1110554218198	1
8	073	3	1	1.5	3	1110554241673	1
8	251	3	1	2.5	1	1110554258597	1
8	235	3	0	3	0	1110554270465	0
8	265	4	1	3	2	1110554291095	1
8	034	4	0	0.5	0	1110554301850	1
8	154	3	0	0.5	0	1110554313417	0
8	072	3	0	2	0	1110554323873	0
8	026	3	1	2.5	1	1110554339435	1
8	162	3	0	1.5	0	1110554348659	1
8	253	4	0	1.5	0	1110554419842	1
8	033	3	0	3	0	1110554437368	1
8	226	4	0	1.5	0	1110554450988	0
8	226	3	1	1.5	3	1110554474422	1
8	185	3	1	2	1	1110554492288	1
8	172	3	0	2	0	1110554500590	1
8	111	4	1	0.5	3	1110554527429	1
8	063	3	0	2	0	1110554537294	1
8	246	3	0	1.5	0	1110554544144	1
8	003	4	1	2	3	1110554570602	1
8	244	4	1	2.5	1	1110554587978	1
8	086	3	0	2	0	1110554595338	1
8	022	4	1	0.5	2	1110554616069	1
8	162	4	1	1.5	1	1110554633023	1
8	073	4	0	1.5	0	1110554639673	1
8	122	3	1	0.5	1	1110554656437	0
8	146	3	1	2	2	1110554676757	1
8	025	4	0	0.5	0	1110554686671	0
8	153	3	1	4	0	1110554698308	1
8	094	4	0	1	0	1110554711207	1
8	054	4	1	2	1	1110554727521	1
8	103	3	0	3.5	0	1110554736063	1
8	012	4	0	3	0	1110554746368	1
8	054	3	0	2	0	1110554761300	0
8	283	3	1	1.5	2	1110554780198	1
8	146	4	0	2	0	1110554788250	1
8	223	3	0	1.5	0	1110554795841	0
8	166	3	0	4	0	1110554810312	1
8	082	4	1	2	3	1110554838743	1
8	231	4	0	1.5	0	1110554849689	0
8	212	3	1	3	1	1110554865903	1
8	085	3	1	3	1	1110554880955	1
8	033	4	1	3	2	1110554901585	1
8	095	4	0	2	0	1110554911129	1
8	002	4	0	1.5	0	1110554919271	1
8	086	4	1	2	1	1110554935825	1
8	085	4	0	3	0	1110554944017	1
8	056	3	1	2.5	2	1110554964737	1
8	082	3	0	2	0	1110554978377	1
8	053	4	1	0.5	2	1110554998746	1

ID	TR	SHD	RCK	DIFF	RCKN	TIME	RESP
8	154	4	1	0.5	2	1110555019537	0
8	066	4	1	2	1	1110555036802	1
8	053	3	0	0.5	0	1110555044593	1
8	103	4	1	3.5	2	1110555073225	1
8	056	4	0	2.5	0	1110555170170	1
8	294	4	1	3.5	1	1110555186391	1
8	023	3	0	3	0	1110555193500	0
8	181	3	1	1.5	0	1110555205275	1
8	192	4	1	2	2	1110555227474	1
8	031	4	1	1	1	1110555242884	1
8	223	4	1	1.5	0	1110555255480	1
8	176	4	0	1	0	1110555263340	0
8	122	4	0	0.5	0	1110555272011	0
8	095	3	1	2	4	1110555301749	1
8	025	3	1	0.5	3	1110555327543	0
8	222	3	0	1	0	1110555338777	0
8	244	3	0	2.5	0	1110555345416	1
8	063	4	1	2	1	1110555361677	1
8	222	4	1	1	2	1110555382595	1
8	253	3	1	1.5	0	1110555395033	1
8	136	3	0	2.5	0	1110555402905	0
8	125	4	0	1.5	0	1110555420841	1
8	213	4	1	0.5	1	1110555436874	1
8	282	3	1	2.5	2	1110555458215	1
8	195	4	0	3	0	1110555471845	0
8	183	3	0	3	0	1110555478906	0
8	072	4	1	2	2	1110555500637	1
8	011	4	0	1.5	0	1110555508459	1
8	114	3	1	0.5	2	1110555530721	1
8	232	3	0	2	0	1110555538873	1
8	004	3	1	2.5	1	1110555556659	1
8	031	3	0	1	0	1110555563419	0
8	251	4	0	2.5	0	1110555569878	1
8	183	4	1	3	1	1110555586132	1
8	022	3	0	0.5	0	1110555594895	1
8	002	3	1	1.5	2	1110555615755	1
8	115	3	0	1.5	0	1110555629095	1
8	003	3	0	2	0	1110555635364	1
8	294	3	0	3.5	0	1110555641483	1
8	282	4	0	2.5	0	1110555652238	1
8	185	4	0	2	0	1110555658427	1
8	136	4	1	2.5	2	1110555678627	0
8	211	3	0	1	0	1110555684375	0
8	176	3	1	1	1	1110555700388	0
8	092	3	1	2	0	1110555712716	1
8	113	4	0	2.5	0	1110555723362	1
8	004	4	0	2.5	0	1110555732115	1

Table A.4: Participant responses from User Study 3.1

ID	TR	TECH	DIFF	TIME	RESP
92	614	3	2.0	1151287241645	1
92	216	5	1.0	1151287262427	1
92	409	3	0.5	1151287297552	1
92	625	5	1.0	1151287305505	1
92	217	2	1.5	1151287322942	1
92	208	2	1.5	1151287333520	1
92	116	1	1.5	1151287340005	1
92	228	2	2.5	1151287352786	1
92	217	1	1.5	1151287358864	1
92	510	1	2.0	1151287364020	1
92	614	4	2.0	1151287377270	1
92	217	3	1.5	1151287394724	1
92	622	5	1.0	1151287399599	1
92	523	3	2.5	1151287406817	1
92	400	3	2.5	1151287415505	1
92	625	1	1.0	1151287426895	1
92	523	2	2.5	1151287443270	1
92	210	3	0.5	1151287451145	1
92	400	5	2.5	1151287455739	1
92	622	4	1.0	1151287460333	0
92	216	2	1.0	1151287469349	1
92	102	4	2.0	1151287474724	1
92	316	2	1.0	1151287484942	0
92	310	3	2.5	1151287500692	1
92	401	1	0.5	1151287506520	0
92	228	3	2.5	1151287514224	1
92	401	4	0.5	1151287521786	0
92	310	4	2.5	1151287527474	1
92	409	4	0.5	1151287536333	1
92	222	2	0.5	1151287543395	1
92	116	3	1.5	1151287550567	1
92	510	3	2.0	1151287565286	1
92	504	3	2.0	1151287580208	1
92	427	2	1.5	1151287590052	1
92	528	3	0.5	1151287598114	0
92	302	2	2.5	1151287604770	0
92	210	1	0.5	1151287609677	0
92	208	3	1.5	1151287630864	1
92	400	1	2.5	1151287635833	1
92	409	1	0.5	1151287641536	1
92	523	4	2.5	1151287646942	1
92	208	5	1.5	1151287656567	1
92	410	4	1.5	1151287668755	1
92	523	5	2.5	1151287673692	1
92	401	5	0.5	1151287678661	1
92	102	5	2.0	1151287683583	1
92	210	4	0.5	1151287705317	1
92	216	1	1.0	1151287711427	1
92	222	5	0.5	1151287725020	1
92	316	4	1.0	1151287732974	1
92	228	5	2.5	1151287739645	1
92	102	3	2.0	1151287753052	1
92	210	5	0.5	1151287758395	1
92	100	1	1.0	1151287763989	1
92	614	2	2.0	1151287770286	0
92	310	5	2.5	1151287783349	1
92	608	4	2.0	1151287802208	1
92	208	1	1.5	1151287811661	1
92	504	1	2.0	1151287817724	0
92	409	5	0.5	1151287825114	1
92	622	2	1.0	1151287830802	0
92	302	4	2.5	1151287835911	1
92	400	2	2.5	1151287843224	1
92	400	4	2.5	1151287848177	1
92	510	5	2.0	1151287854708	1
92	302	3	2.5	1151287865520	0
92	528	4	0.5	1151287876505	0
92	116	2	1.5	1151287881364	1
92	116	4	1.5	1151287886020	1
92	622	1	1.0	1151287891505	1
92	100	4	1.0	1151287896020	0
92	410	3	1.5	1151287903286	1
92	216	4	1.0	1151287916177	1
92	410	2	1.5	1151287920786	1
92	222	3	0.5	1151287927958	0
92	316	1	1.0	1151287935599	1
92	504	2	2.0	1151287943489	1
92	427	4	1.5	1151287950395	1
92	622	3	1.0	1151287959317	1
92	625	4	1.0	1151287964302	1
92	625	3	1.0	1151287969333	1
92	427	3	1.5	1151287983286	1
92	210	2	0.5	1151287989255	0
92	216	3	1.0	1151288001770	1
92	410	5	1.5	1151288018739	1
92	504	5	2.0	1151288023927	1
92	310	1	2.5	1151288029177	1
92	608	2	2.0	1151288036317	1
92	310	2	2.5	1151288040724	1
92	528	2	0.5	1151288045395	0
92	316	5	1.0	1151288053817	1
92	528	5	0.5	1151288060880	0
92	510	2	2.0	1151288066302	1
92	401	3	0.5	1151288072349	1
92	608	5	2.0	1151288079552	0
92	614	5	2.0	1151288084864	1
92	410	1	1.5	1151288091927	0
92	608	1	2.0	1151288096192	1
92	528	1	0.5	1151288100974	0
92	228	4	2.5	1151288107036	1
92	102	1	2.0	1151288111724	1
92	100	3	1.0	1151288119067	1
92	401	2	0.5	1151288124599	0
92	614	1	2.0	1151288132317	0
92	427	5	1.5	1151288142411	1
92	222	4	0.5	1151288148911	1
92	102	2	2.0	1151288153364	1
92	625	2	1.0	1151288157364	1
92	510	4	2.0	1151288162364	1
92	228	1	2.5	1151288167786	1
92	608	3	2.0	1151288179849	1
92	523	1	2.5	1151288185145	1
92	217	5	1.5	1151288191552	1
92	409	2	0.5	1151288196583	1
92	100	2	1.0	1151288201989	0
92	217	4	1.5	1151288208567	1
92	504	4	2.0	1151288215083	1
92	316	3	1.0	1151288222645	1
92	222	1	0.5	1151288228067	1
92	302	5	2.5	1151288234489	1
92	208	4	1.5	1151288242177	1
92	100	5	1.0	1151288249974	1
92	302	1	2.5	1151288254411	1
92	116	5	1.5	1151288262724	0
92	427	1	1.5	1151288266880	1
93	316	2	1.0	1151350585332	0
93	216	5	1.0	1151350592348	1
93	316	5	1.0	1151350598348	1
93	614	1	2.0	1151350604363	0
93	116	2	1.5	1151350610848	1
93	622	2	1.0	1151350618207	1
93	622	1	1.0	1151350622317	1
93	210	2	0.5	1151350630629	1
93	102	3	2.0	1151350634598	1
93	523	3	2.5	1151350641301	0
93	216	1	1.0	1151350647707	1
93	302	2	2.5	1151350654676	1
93	208	2	1.5	1151350662285	1
93	504	4	2.0	1151350671223	1
93	100	5	1.0	1151350675035	0
93	510	4	2.0	1151350678770	1
93	427	4	1.5	1151350685395	1
93	409	3	0.5	1151350694660	1
93	510	3	2.0	1151350701817	1
93	102	2	2.0	1151350708004	1
93	528	3	0.5	1151350713145	1
93	523	1	2.5	1151350719082	1
93	400	2	2.5	1151350727973	1
93	228	5	2.5	1151350737426	1
93	614	2	2.0	1151350745926	0
93	400	1	2.5	1151350750004	1

ID	TR	TECH	DIFF	TIME	RESP
93	222	1	0.5	1151350755285	1
93	608	5	2.0	1151350761910	0
93	528	1	0.5	1151350768317	0
93	217	1	1.5	1151350776051	1
93	100	3	1.0	1151350782879	1
93	409	5	0.5	1151350790645	1
93	316	4	1.0	1151350795395	0
93	625	1	1.0	1151350798754	1
93	401	5	0.5	1151350808520	0
93	427	3	1.5	1151350815348	1
93	409	4	0.5	1151350822285	1
93	100	2	1.0	1151350827957	1
93	316	1	1.0	1151350832457	1
93	510	2	2.0	1151350842285	1
93	208	1	1.5	1151350850238	1
93	622	3	1.0	1151350859035	1
93	410	2	1.5	1151350865442	1
93	401	3	0.5	1151350870895	0
93	100	4	1.0	1151350876348	0
93	523	5	2.5	1151350880379	1
93	409	1	0.5	1151350893254	0
93	401	1	0.5	1151350898801	0
93	410	4	1.5	1151350904645	0
93	116	5	1.5	1151350912926	1
93	625	5	1.0	1151350918348	1
93	625	3	1.0	1151350921988	1
93	510	5	2.0	1151350929817	1
93	523	2	2.5	1151350941317	1
93	625	4	1.0	1151350946207	1
93	116	4	1.5	1151350950520	1
93	302	4	2.5	1151350954942	1
93	608	1	2.0	1151350958254	1
93	228	1	2.5	1151350961895	1
93	222	3	0.5	1151350967942	1
93	228	2	2.5	1151350976645	1
93	310	1	2.5	1151350982223	1
93	310	5	2.5	1151350988910	1
93	216	3	1.0	1151350998004	0
93	302	1	2.5	1151351001801	1
93	228	3	2.5	1151351006598	1
93	608	3	2.0	1151351016582	1
93	510	1	2.0	1151351020942	1
93	400	3	2.5	1151351033582	1
93	401	2	0.5	1151351037098	1
93	622	5	1.0	1151351041817	1
93	504	2	2.0	1151351051160	0
93	102	4	2.0	1151351057332	1
93	208	5	1.5	1151351063285	1
93	228	4	2.5	1151351067207	1
93	116	1	1.5	1151351073879	1
93	216	2	1.0	1151351083660	0
93	504	3	2.0	1151351093629	1
93	208	3	1.5	1151351098879	1
93	614	4	2.0	1151351104301	0
93	504	1	2.0	1151351119004	1
93	222	4	0.5	1151351124473	1
93	100	1	1.0	1151351133942	0
93	622	4	1.0	1151351138067	1
93	222	5	0.5	1151351144879	1
93	316	3	1.0	1151351149442	1
93	302	3	2.5	1151351157629	0
93	216	4	1.0	1151351164973	1
93	217	5	1.5	1151351169473	1
93	302	5	2.5	1151351174207	1
93	310	3	2.5	1151351180738	0
93	608	2	2.0	1151351195848	1
93	310	4	2.5	1151351199567	1
93	116	3	1.5	1151351204957	1
93	210	4	0.5	1151351208395	1
93	409	2	0.5	1151351218363	1
93	102	5	2.0	1151351225238	1
93	427	1	1.5	1151351231895	1
93	210	3	0.5	1151351237770	1
93	528	4	0.5	1151351242832	1
93	528	2	0.5	1151351254176	0
93	310	2	2.5	1151351261051	1
93	614	3	2.0	1151351267629	0

ID	TR	TECH	DIFF	TIME	RESP
93	427	2	1.5	1151351274692	0
93	625	2	1.0	1151351281707	1
93	208	4	1.5	1151351289301	0
93	400	4	2.5	1151351293473	1
93	410	3	1.5	1151351302707	1
93	400	5	2.5	1151351309582	1
93	504	5	2.0	1151351323613	1
93	410	5	1.5	1151351328988	1
93	608	4	2.0	1151351336567	1
93	528	5	0.5	1151351342832	1
93	217	4	1.5	1151351346504	1
93	523	4	2.5	1151351350567	1
93	210	5	0.5	1151351355348	1
93	222	2	0.5	1151351362129	1
93	614	5	2.0	1151351367348	1
93	210	1	0.5	1151351378129	1
93	217	2	1.5	1151351384129	1
93	102	1	2.0	1151351388285	1
93	401	4	0.5	1151351392129	1
93	217	3	1.5	1151351402957	1
93	427	5	1.5	1151351408082	1
93	410	1	1.5	1151351412613	1
99	222	5	0.5	1151366951082	1
99	216	1	1.0	1151366958629	1
99	302	3	2.5	1151366971801	0
99	116	1	1.5	1151366978879	1
99	401	5	0.5	1151366994582	1
99	228	5	2.5	1151367001098	1
99	310	4	2.5	1151367006973	1
99	409	1	0.5	1151367012754	1
99	210	4	0.5	1151367019629	1
99	622	1	1.0	1151367028535	1
99	608	1	2.0	1151367034238	1
99	102	2	2.0	1151367063254	1
99	400	1	2.5	1151367067379	1
99	625	2	1.0	1151367075879	1
99	316	5	1.0	1151367086348	1
99	210	2	0.5	1151367104160	0
99	217	4	1.5	1151367111567	1
99	228	2	2.5	1151367126145	1
99	400	2	2.5	1151367134535	1
99	310	2	2.5	1151367143457	0
99	400	3	2.5	1151367149082	1
99	410	1	1.5	1151367153145	1
99	528	3	0.5	1151367163067	1
99	210	1	0.5	1151367170004	0
99	614	1	2.0	1151367177551	0
99	401	4	0.5	1151367183098	0
99	116	5	1.5	1151367200535	1
99	427	4	1.5	1151367210535	0
99	228	4	2.5	1151367215801	1
99	622	2	1.0	1151367240832	0
99	523	1	2.5	1151367248457	1
99	217	2	1.5	1151367261676	1
99	222	4	0.5	1151367266504	1
99	401	3	0.5	1151367271254	0
99	409	4	0.5	1151367276707	1
99	216	2	1.0	1151367292473	0
99	316	4	1.0	1151367300738	0
99	316	1	1.0	1151367307973	1
99	409	5	0.5	1151367319426	1
99	523	4	2.5	1151367327379	1
99	116	3	1.5	1151367338223	1
99	302	1	2.5	1151367343379	1
99	427	3	1.5	1151367353707	1
99	427	2	1.5	1151367361723	1
99	100	5	1.0	1151367366848	0
99	222	2	0.5	1151367375332	0
99	216	5	1.0	1151367385692	1
99	302	5	2.5	1151367392254	1
99	625	5	1.0	1151367402535	1
99	510	4	2.0	1151367407254	1
99	208	5	1.5	1151367414645	1
99	504	2	2.0	1151367426817	1
99	614	4	2.0	1151367432629	1
99	622	4	1.0	1151367438285	1
99	410	2	1.5	1151367451020	1

ID	TR	TECH	DIFF	TIME	RESP
99	608	2	2.0	1151367457707	0
99	504	5	2.0	1151367473801	1
99	217	5	1.5	1151367480270	1
99	316	3	1.0	1151367488004	1
99	400	5	2.5	1151367497426	1
99	208	2	1.5	1151367514645	0
99	528	2	0.5	1151367531848	0
99	102	5	2.0	1151367543488	1
99	228	1	2.5	1151367548285	1
99	614	2	2.0	1151367555832	1
99	216	3	1.0	1151367562817	1
99	608	4	2.0	1151367570863	1
99	510	1	2.0	1151367575129	1
99	427	5	1.5	1151367582488	1
99	528	4	0.5	1151367594035	1
99	625	3	1.0	1151367603598	1
99	302	2	2.5	1151367612035	0
99	510	5	2.0	1151367617113	1
99	222	3	0.5	1151367628723	1
99	222	1	0.5	1151367635051	1
99	614	3	2.0	1151367648738	0
99	400	4	2.5	1151367655926	1
99	427	1	1.5	1151367660535	1
99	528	5	0.5	1151367674426	1
99	528	1	0.5	1151367682082	1
99	210	3	0.5	1151367688035	1
99	410	5	1.5	1151367703520	1
99	523	2	2.5	1151367715067	1
99	102	4	2.0	1151367721035	1
99	510	2	2.0	1151367729738	1
99	401	2	0.5	1151367738457	1
99	622	5	1.0	1151367743770	1
99	216	4	1.0	1151367756067	1
99	523	5	2.5	1151367761410	1
99	622	3	1.0	1151367776270	1
99	410	3	1.5	1151367781863	0
99	523	3	2.5	1151367792082	1
99	409	3	0.5	1151367804692	1
99	100	4	1.0	1151367811035	0
99	100	3	1.0	1151367818629	1
99	217	3	1.5	1151367832098	1
99	614	5	2.0	1151367837520	1
99	100	2	1.0	1151367850879	1
99	625	4	1.0	1151367861504	1
99	504	3	2.0	1151367884426	0
99	210	5	0.5	1151367889613	1
99	102	3	2.0	1151367894801	1
99	504	1	2.0	1151367899957	1
99	116	2	1.5	1151367909848	0
99	410	4	1.5	1151367918254	1
99	102	1	2.0	1151367923067	1
99	100	1	1.0	1151367931567	1
99	310	1	2.5	1151367936629	1
99	625	1	1.0	1151367942473	1
99	116	4	1.5	1151367948254	1
99	217	1	1.5	1151367957567	1
99	409	2	0.5	1151367965567	0
99	208	4	1.5	1151367973848	0
99	208	3	1.5	1151367983567	1
99	608	5	2.0	1151367993457	1
99	208	1	1.5	1151368006848	0
99	608	3	2.0	1151368013535	0
99	504	4	2.0	1151368021238	1
99	228	3	2.5	1151368026973	1
99	310	5	2.5	1151368034270	1
99	302	4	2.5	1151368039582	1
99	316	2	1.0	1151368054645	0
99	401	1	0.5	1151368059379	0
99	510	3	2.0	1151368065957	1
99	310	3	2.5	1151368074379	0
0	608	2	2.0	1150987529809	1
0	523	4	2.5	1150987534264	1
0	622	5	1.0	1150987538937	1
0	523	1	2.5	1150987543079	1
0	228	4	2.5	1150987549221	1
0	222	1	0.5	1150987554723	1
0	523	2	2.5	1150987567805	1

ID	TR	TECH	DIFF	TIME	RESP
0	116	4	1.5	1150987572728	1
0	210	4	0.5	1150987576573	1
0	310	4	2.5	1150987581043	1
0	625	1	1.0	1150987585716	1
0	510	2	2.0	1150987592155	1
0	625	3	1.0	1150987605597	1
0	410	3	1.5	1150987616694	1
0	102	2	2.0	1150987623618	1
0	622	2	1.0	1150987627775	0
0	504	4	2.0	1150987633323	1
0	222	5	0.5	1150987637981	1
0	614	3	2.0	1150987651844	1
0	427	3	1.5	1150987660191	1
0	208	1	1.5	1150987664536	1
0	316	1	1.0	1150987669084	1
0	427	5	1.5	1150987674632	1
0	400	4	2.5	1150987679227	1
0	510	3	2.0	1150987690527	1
0	528	4	0.5	1150987695560	0
0	427	4	1.5	1150987699624	1
0	216	2	1.0	1150987706501	1
0	614	1	2.0	1150987710721	1
0	401	5	0.5	1150987714285	1
0	228	2	2.5	1150987722506	1
0	316	3	1.0	1150987729337	0
0	217	4	1.5	1150987734776	0
0	401	2	0.5	1150987738918	1
0	116	5	1.5	1150987743716	1
0	210	1	0.5	1150987748202	0
0	302	5	2.5	1150987752344	1
0	622	1	1.0	1150987756424	1
0	216	1	1.0	1150987760613	1
0	217	2	1.5	1150987767099	1
0	100	1	1.0	1150987771335	0
0	216	4	1.0	1150987778853	1
0	116	2	1.5	1150987800860	1
0	102	1	2.0	1150987804330	1
0	302	3	2.5	1150987808957	1
0	409	4	0.5	1150987816693	1
0	410	2	1.5	1150987820692	1
0	222	4	0.5	1150987826529	1
0	102	3	2.0	1150987830992	1
0	310	2	2.5	1150987834815	1
0	217	1	1.5	1150987837827	1
0	504	5	2.0	1150987843258	1
0	316	5	1.0	1150987853230	1
0	216	3	1.0	1150987857194	1
0	528	3	0.5	1150987861875	1
0	228	1	2.5	1150987865792	1
0	116	1	1.5	1150987873501	1
0	614	2	2.0	1150987878917	0
0	228	3	2.5	1150987883739	1
0	228	5	2.5	1150987886672	1
0	504	1	2.0	1150987892805	1
0	401	1	0.5	1150987896285	0
0	316	4	1.0	1150987899594	1
0	409	3	0.5	1150987908052	1
0	208	2	1.5	1150987912874	1
0	528	1	0.5	1150987916760	1
0	410	1	1.5	1150987922019	1
0	116	3	1.5	1150987926716	1
0	102	4	2.0	1150987931913	1
0	608	3	2.0	1150987941604	1
0	614	4	2.0	1150987946301	0
0	302	2	2.5	1150987951310	0
0	310	3	2.5	1150987956304	1
0	400	2	2.5	1150987961033	1
0	409	1	0.5	1150987966651	0
0	410	5	1.5	1150987971832	1
0	222	3	0.5	1150987976857	1
0	625	4	1.0	1150987981257	1
0	400	1	2.5	1150987985003	1
0	208	4	1.5	1150987992540	0
0	625	5	1.0	1150987995911	1
0	409	5	0.5	1150988000312	1
0	401	4	0.5	1150988004697	0
0	217	3	1.5	1150988008583	1

ID	TR	TECH	DIFF	TIME	RESP
0	622	3	1.0	1150988017353	1
0	100	2	1.0	1150988021270	0
0	222	2	0.5	1150988027512	0
0	217	5	1.5	1150988032085	1
0	208	5	1.5	1150988036548	1
0	510	1	2.0	1150988040480	1
0	625	2	1.0	1150988044163	1
0	316	2	1.0	1150988048205	0
0	528	5	0.5	1150988052184	0
0	427	2	1.5	1150988056413	1
0	614	5	2.0	1150988061048	1
0	400	5	2.5	1150988064934	1
0	401	3	0.5	1150988069335	0
0	510	4	2.0	1150988073345	1
0	523	3	2.5	1150988077169	1
0	400	3	2.5	1150988080555	1
0	528	2	0.5	1150988084815	0
0	608	1	2.0	1150988088670	1
0	310	1	2.5	1150988091932	1
0	608	4	2.0	1150988095817	1
0	510	5	2.0	1150988100000	1
0	302	4	2.5	1150988103870	1
0	100	4	1.0	1150988107927	0
0	310	5	2.5	1150988112437	1
0	410	4	1.5	1150988116869	1
0	210	3	0.5	1150988122349	1
0	210	5	0.5	1150988125925	1
0	622	4	1.0	1150988129860	1
0	608	5	2.0	1150988137855	1
0	100	3	1.0	1150988142821	0
0	409	2	0.5	1150988146772	1
0	302	1	2.5	1150988150301	1
0	504	3	2.0	1150988157562	1
0	208	3	1.5	1150988162856	1
0	100	5	1.0	1150988166900	0
0	102	5	2.0	1150988170414	1
0	427	1	1.5	1150988173631	1
0	504	2	2.0	1150988178097	1
0	216	5	1.0	1150988185374	0
0	210	2	0.5	1150988191995	1
0	523	5	2.5	1150988196211	1
1	622	5	1.0	1151084436490	1
1	316	2	1.0	1151084467130	0
1	427	4	1.5	1151084498255	1
1	401	3	0.5	1151084511692	1
1	208	5	1.5	1151084526974	1
1	625	4	1.0	1151084534942	1
1	222	5	0.5	1151084543661	1
1	210	1	0.5	1151084551645	0
1	401	2	0.5	1151084561505	0
1	400	2	2.5	1151084572958	1
1	102	2	2.0	1151084587083	1
1	216	2	1.0	1151084595661	1
1	401	1	0.5	1151084605129	0
1	100	5	1.0	1151084618723	0
1	116	5	1.5	1151084624801	1
1	400	5	2.5	1151084630379	1
1	222	4	0.5	1151084638192	1
1	622	2	1.0	1151084657645	1
1	222	3	0.5	1151084672566	1
1	302	1	2.5	1151084678488	1
1	217	4	1.5	1151084687301	1
1	504	4	2.0	1151084692629	1
1	409	3	0.5	1151084704582	1
1	302	3	2.5	1151084718113	1
1	409	4	0.5	1151084735550	1
1	625	5	1.0	1151084745144	1
1	504	3	2.0	1151084767331	1
1	614	2	2.0	1151084800519	1
1	302	5	2.5	1151084807925	1
1	401	4	0.5	1151084817659	1
1	608	3	2.0	1151084834597	1
1	528	5	0.5	1151084843597	0
1	228	4	2.5	1151084849347	1
1	523	1	2.5	1151084854831	1
1	216	4	1.0	1151084865503	1
1	217	1	1.5	1151084876221	1

ID	TR	TECH	DIFF	TIME	RESP
1	410	5	1.5	1151084890799	1
1	523	2	2.5	1151084901065	1
1	614	5	2.0	1151084907127	1
1	316	4	1.0	1151084915112	1
1	100	4	1.0	1151084919502	0
1	316	3	1.0	1151084929190	1
1	208	1	1.5	1151084938268	1
1	427	1	1.5	1151084946705	1
1	528	1	0.5	1151084954018	1
1	510	1	2.0	1151084959455	1
1	210	2	0.5	1151084973439	1
1	310	2	2.5	1151084981080	1
1	116	4	1.5	1151084985658	1
1	608	4	2.0	1151084991408	0
1	210	4	0.5	1151084996596	1
1	208	3	1.5	1151085022830	0
1	217	5	1.5	1151085029798	1
1	216	1	1.0	1151085043205	1
1	614	3	2.0	1151085053376	1
1	528	2	0.5	1151085060251	1
1	302	2	2.5	1151085070158	0
1	228	5	2.5	1151085074501	1
1	216	5	1.0	1151085084454	1
1	102	4	2.0	1151085091111	1
1	102	1	2.0	1151085096611	1
1	625	3	1.0	1151085109704	1
1	510	2	2.0	1151085118985	1
1	410	3	1.5	1151085125188	1
1	504	1	2.0	1151085140563	0
1	310	5	2.5	1151085152657	1
1	410	2	1.5	1151085160329	1
1	217	3	1.5	1151085172610	0
1	208	2	1.5	1151085183813	0
1	510	5	2.0	1151085188032	1
1	614	4	2.0	1151085195391	0
1	622	3	1.0	1151085203594	1
1	510	4	2.0	1151085218719	1
1	427	5	1.5	1151085232141	1
1	228	2	2.5	1151085244781	1
1	409	5	0.5	1151085257625	1
1	400	1	2.5	1151085261469	1
1	410	1	1.5	1151085269813	0
1	504	2	2.0	1151085276641	1
1	228	1	2.5	1151085281203	1
1	228	3	2.5	1151085292328	1
1	427	2	1.5	1151085312531	0
1	400	4	2.5	1151085317531	1
1	625	2	1.0	1151085324781	1
1	210	5	0.5	1151085333062	1
1	310	3	2.5	1151085342515	1
1	116	1	1.5	1151085347109	1
1	410	4	1.5	1151085356234	1
1	523	4	2.5	1151085364046	1
1	622	1	1.0	1151085370765	0
1	608	5	2.0	1151085376312	1
1	409	2	0.5	1151085387343	1
1	102	3	2.0	1151085393781	1
1	222	1	0.5	1151085400405	1
1	316	5	1.0	1151085410171	1
1	622	4	1.0	1151085418530	1
1	523	3	2.5	1151085430108	1
1	401	5	0.5	1151085436280	1
1	100	1	1.0	1151085444530	0
1	116	3	1.5	1151085449686	1
1	100	3	1.0	1151085454811	0
1	310	1	2.5	1151085459921	1
1	528	4	0.5	1151085467764	1
1	116	2	1.5	1151085473233	1
1	217	2	1.5	1151085487749	1
1	100	2	1.0	1151085493061	0
1	625	1	1.0	1151085498342	1
1	528	3	0.5	1151085504952	1
1	608	1	2.0	1151085508780	1
1	216	3	1.0	1151085514483	1
1	102	5	2.0	1151085520967	1
1	608	2	2.0	1151085547061	1
1	427	3	1.5	1151085558436	1

ID	TR	TECH	DIFF	TIME	RESP
1	504	5	2.0	1151085566483	1
1	409	1	0.5	1151085572201	1
1	302	4	2.5	1151085577654	1
1	208	4	1.5	1151085609654	0
1	510	3	2.0	1151085617795	1
1	316	1	1.0	1151085623248	1
1	400	3	2.5	1151085627154	1
1	523	5	2.5	1151085631638	1
1	310	4	2.5	1151085638810	1
1	210	3	0.5	1151085645998	1
1	614	1	2.0	1151085651107	0
1	222	2	0.5	1151085658263	1
2	427	4	1.5	1151003523981	1
2	410	1	1.5	1151003531997	0
2	310	1	2.5	1151003538325	1
2	409	3	0.5	1151003550684	1
2	310	5	2.5	1151003570762	1
2	222	5	0.5	1151003578872	1
2	216	5	1.0	1151003591840	1
2	409	4	0.5	1151003608731	1
2	401	5	0.5	1151003626122	1
2	528	2	0.5	1151003649794	0
2	222	4	0.5	1151003657419	1
2	528	5	0.5	1151003677325	1
2	210	2	0.5	1151003693450	1
2	401	1	0.5	1151003699481	0
2	100	3	1.0	1151003708231	0
2	102	3	2.0	1151003715247	1
2	608	3	2.0	1151003724231	1
2	523	5	2.5	1151003737559	1
2	228	1	2.5	1151003742262	1
2	400	4	2.5	1151003747559	1
2	222	3	0.5	1151003753215	1
2	401	2	0.5	1151003762450	0
2	216	4	1.0	1151003779653	1
2	217	1	1.5	1151003785887	1
2	625	4	1.0	1151003791325	1
2	510	2	2.0	1151003796012	1
2	210	4	0.5	1151003803372	1
2	622	3	1.0	1151003818840	1
2	523	4	2.5	1151003824981	1
2	510	3	2.0	1151003838637	1
2	302	4	2.5	1151003843965	1
2	400	3	2.5	1151003849669	1
2	409	2	0.5	1151003864044	1
2	625	5	1.0	1151003873731	1
2	510	4	2.0	1151003879419	1
2	310	4	2.5	1151003884215	1
2	216	3	1.0	1151003895137	1
2	504	3	2.0	1151003905809	1
2	116	2	1.5	1151003913325	0
2	622	2	1.0	1151003919653	1
2	523	1	2.5	1151003924653	1
2	410	2	1.5	1151003929934	1
2	316	4	1.0	1151003949981	1
2	208	5	1.5	1151003959184	0
2	310	3	2.5	1151003973794	0
2	102	4	2.0	1151003983106	1
2	400	1	2.5	1151003987262	1
2	504	4	2.0	1151003998465	1
2	625	2	1.0	1151004007419	1
2	100	5	1.0	1151004025247	1
2	116	5	1.5	1151004032856	1
2	116	4	1.5	1151004039653	1
2	504	1	2.0	1151004052387	0
2	100	4	1.0	1151004062481	1
2	523	2	2.5	1151004073512	1
2	228	2	2.5	1151004078497	1
2	116	3	1.5	1151004084622	1
2	401	3	0.5	1151004090387	0
2	302	1	2.5	1151004095434	1
2	614	5	2.0	1151004102028	0
2	427	1	1.5	1151004106153	1
2	228	3	2.5	1151004114309	1
2	210	5	0.5	1151004121903	1
2	208	4	1.5	1151004128324	0
2	228	4	2.5	1151004136231	1

ID	TR	TECH	DIFF	TIME	RESP
2	222	2	0.5	1151004141981	1
2	100	2	1.0	1151004147606	1
2	217	5	1.5	1151004154965	1
2	608	2	2.0	1151004161855	0
2	410	4	1.5	1151004171199	0
2	102	1	2.0	1151004175512	1
2	504	5	2.0	1151004181527	1
2	625	1	1.0	1151004186621	1
2	102	2	2.0	1151004192230	1
2	216	1	1.0	1151004201465	1
2	208	2	1.5	1151004209558	1
2	614	3	2.0	1151004223855	1
2	608	1	2.0	1151004227933	1
2	608	4	2.0	1151004233043	1
2	400	5	2.5	1151004237839	1
2	208	1	1.5	1151004247089	1
2	427	5	1.5	1151004253292	1
2	504	2	2.0	1151004259152	1
2	208	3	1.5	1151004266839	1
2	622	4	1.0	1151004277605	1
2	427	2	1.5	1151004291933	1
2	116	1	1.5	1151004300776	1
2	228	5	2.5	1151004306636	1
2	401	4	0.5	1151004313464	0
2	310	2	2.5	1151004320620	1
2	614	4	2.0	1151004331823	0
2	410	3	1.5	1151004337542	1
2	316	5	1.0	1151004346589	1
2	316	2	1.0	1151004359323	0
2	608	5	2.0	1151004371151	1
2	523	3	2.5	1151004382963	1
2	210	1	0.5	1151004388792	0
2	302	2	2.5	1151004398713	0
2	510	1	2.0	1151004405870	1
2	614	1	2.0	1151004410682	0
2	217	2	1.5	1151004427338	1
2	210	3	0.5	1151004434197	1
2	622	1	1.0	1151004441916	1
2	302	5	2.5	1151004447979	1
2	400	2	2.5	1151004457229	1
2	217	3	1.5	1151004465666	1
2	100	1	1.0	1151004472025	0
2	410	5	1.5	1151004482838	1
2	409	1	0.5	1151004491135	1
2	102	5	2.0	1151004500369	1
2	625	3	1.0	1151004506369	1
2	528	4	0.5	1151004513791	1
2	222	1	0.5	1151004519338	1
2	217	4	1.5	1151004534791	1
2	622	5	1.0	1151004547103	1
2	528	1	0.5	1151004550681	1
2	316	3	1.0	1151004558369	1
2	409	5	0.5	1151004566415	1
2	510	5	2.0	1151004572431	1
2	316	1	1.0	1151004582556	1
2	216	2	1.0	1151004589415	1
2	528	3	0.5	1151004595665	1
2	302	3	2.5	1151004606337	1
2	427	3	1.5	1151004613056	1
2	614	2	2.0	1151004619587	0
3	409	3	0.5	1151011017280	1
3	510	5	2.0	1151011025124	1
3	310	3	2.5	1151011046218	0
3	608	1	2.0	1151011052187	1
3	614	5	2.0	1151011079093	0
3	608	4	2.0	1151011087249	1
3	410	5	1.5	1151011095765	1
3	208	5	1.5	1151011102547	1
3	116	2	1.5	1151011110625	1
3	217	5	1.5	1151011117734	1
3	625	5	1.0	1151011123391	1
3	100	5	1.0	1151011128641	0
3	228	1	2.5	1151011133703	1
3	608	5	2.0	1151011154922	1
3	409	1	0.5	1151011160625	1
3	528	5	0.5	1151011169282	0
3	228	5	2.5	1151011174032	1

ID	TR	TECH	DIFF	TIME	RESP
3	400	2	2.5	1151011188641	1
3	310	1	2.5	1151011193251	1
3	316	4	1.0	1151011201985	1
3	210	5	0.5	1151011239095	1
3	401	5	0.5	1151011247173	0
3	528	3	0.5	1151011276971	1
3	410	4	1.5	1151011281643	1
3	316	5	1.0	1151011289549	1
3	216	5	1.0	1151011299971	0
3	510	4	2.0	1151011308705	1
3	116	3	1.5	1151011313815	1
3	504	3	2.0	1151011323596	1
3	310	4	2.5	1151011327471	0
3	208	3	1.5	1151011374722	1
3	427	3	1.5	1151011385953	0
3	222	3	0.5	1151011392388	1
3	210	4	0.5	1151011397152	1
3	116	1	1.5	1151011405791	0
3	622	5	1.0	1151011410039	1
3	208	2	1.5	1151011442014	1
3	427	4	1.5	1151011446669	1
3	510	2	2.0	1151011456619	1
3	622	1	1.0	1151011466117	1
3	409	2	0.5	1151011479378	1
3	510	1	2.0	1151011484189	1
3	523	5	2.5	1151011500544	1
3	523	4	2.5	1151011505027	1
3	622	2	1.0	1151011516914	1
3	302	4	2.5	1151011521288	1
3	100	1	1.0	1151011531988	0
3	401	3	0.5	1151011539970	0
3	217	4	1.5	1151011545593	1
3	410	2	1.5	1151011550248	1
3	614	2	2.0	1151011555934	1
3	625	3	1.0	1151011570867	1
3	614	4	2.0	1151011579052	0
3	302	3	2.5	1151011589752	1
3	528	2	0.5	1151011600842	0
3	216	1	1.0	1151011605497	1
3	409	4	0.5	1151011613229	1
3	504	4	2.0	1151011618915	1
3	216	3	1.0	1151011625913	0
3	116	4	1.5	1151011655561	1
3	427	5	1.5	1151011660762	1
3	102	3	2.0	1151011668682	1
3	625	4	1.0	1151011673321	1
3	222	4	0.5	1151011682304	1
3	100	2	1.0	1151011691803	1
3	401	2	0.5	1151011712253	1
3	217	1	1.5	1151011717549	1
3	622	4	1.0	1151011722376	1
3	228	2	2.5	1151011733172	1
3	316	2	1.0	1151011744326	1
3	427	1	1.5	1151011756590	1
3	222	1	0.5	1151011761246	0
3	401	1	0.5	1151011766261	0
3	523	2	2.5	1151011772869	1
3	614	1	2.0	1151011777462	0
3	625	1	1.0	1151011785648	1
3	316	1	1.0	1151011796084	1
3	217	3	1.5	1151011804427	1
3	100	4	1.0	1151011811379	0
3	608	3	2.0	1151011817409	0
3	210	1	0.5	1151011822080	0
3	208	1	1.5	1151011831673	1
3	427	2	1.5	1151011838765	0
3	409	5	0.5	1151011846842	1
3	102	5	2.0	1151011899038	1
3	302	1	2.5	1151011903772	1
3	228	4	2.5	1151011909646	1
3	228	3	2.5	1151011915957	1
3	217	2	1.5	1151011923441	0
3	102	2	2.0	1151011932642	0
3	302	5	2.5	1151011937345	1
3	222	2	0.5	1151011965997	0
3	400	3	2.5	1151011980698	1
3	625	2	1.0	1151011985854	1

ID	TR	TECH	DIFF	TIME	RESP
3	510	3	2.0	1151011991760	1
3	310	2	2.5	1151011996978	1
3	316	3	1.0	1151012003868	1
3	116	5	1.5	1151012013117	1
3	216	2	1.0	1151012018601	1
3	400	4	2.5	1151012025444	1
3	102	4	2.0	1151012029850	1
3	614	3	2.0	1151012039817	1
3	100	3	1.0	1151012063268	0
3	216	4	1.0	1151012072986	1
3	210	3	0.5	1151012079017	1
3	102	1	2.0	1151012083063	1
3	222	5	0.5	1151012087688	1
3	523	1	2.5	1151012095281	1
3	210	2	0.5	1151012105389	0
3	504	1	2.0	1151012110483	1
3	208	4	1.5	1151012124497	1
3	528	1	0.5	1151012131121	0
3	504	2	2.0	1151012144167	1
3	410	3	1.5	1151012155181	1
3	504	5	2.0	1151012159884	1
3	400	5	2.5	1151012164102	1
3	528	4	0.5	1151012175914	1
3	410	1	1.5	1151012179976	0
3	302	2	2.5	1151012186803	1
3	401	4	0.5	1151012197505	0
3	400	1	2.5	1151012201989	1
3	310	5	2.5	1151012206973	1
3	523	3	2.5	1151012231424	1
3	622	3	1.0	1151012253297	1
3	608	2	2.0	1151012261765	1
12	302	1	2.5	1151348847519	1
12	528	3	0.5	1151348854800	1
12	228	2	2.5	1151348871550	1
12	410	3	1.5	1151348881660	0
12	316	2	1.0	1151348899628	1
12	100	3	1.0	1151348910535	0
12	400	4	2.5	1151348918800	1
12	523	2	2.5	1151348930738	0
12	116	1	1.5	1151348939628	1
12	302	4	2.5	1151348944332	1
12	102	5	2.0	1151348960707	1
12	401	1	0.5	1151348966128	0
12	222	3	0.5	1151348981285	1
12	116	5	1.5	1151348987160	1
12	410	2	1.5	1151348999753	0
12	409	2	0.5	1151349016769	0
12	222	2	0.5	1151349024050	1
12	100	5	1.0	1151349037441	0
12	116	4	1.5	1151349045847	1
12	427	1	1.5	1151349050410	1
12	504	4	2.0	1151349062332	1
12	523	3	2.5	1151349077050	1
12	217	1	1.5	1151349084847	1
12	228	3	2.5	1151349091347	1
12	504	3	2.0	1151349099972	1
12	622	4	1.0	1151349105878	1
12	400	1	2.5	1151349113207	1
12	409	4	0.5	1151349127941	1
12	208	4	1.5	1151349153941	1
12	102	2	2.0	1151349191363	1
12	409	3	0.5	1151349208472	1
12	427	5	1.5	1151349215347	1
12	302	2	2.5	1151349225800	1
12	614	5	2.0	1151349248550	1
12	316	4	1.0	1151349261269	0
12	210	5	0.5	1151349271050	1
12	100	2	1.0	1151349283441	0
12	608	5	2.0	1151349306363	1
12	528	5	0.5	1151349312378	0
12	608	4	2.0	1151349319863	0
12	222	5	0.5	1151349329175	1
12	504	2	2.0	1151349348425	0
12	216	2	1.0	1151349366722	1
12	510	5	2.0	1151349372878	1
12	217	3	1.5	1151349390363	1
12	427	4	1.5	1151349398894	1

ID	TR	TECH	DIFF	TIME	RESP
12	210	1	0.5	1151349409535	0
12	216	4	1.0	1151349430253	1
12	528	4	0.5	1151349439957	0
12	310	4	2.5	1151349447566	1
12	228	1	2.5	1151349453832	1
12	410	4	1.5	1151349461300	1
12	222	1	0.5	1151349477332	1
12	608	3	2.0	1151349487628	1
12	528	2	0.5	1151349500988	1
12	504	5	2.0	1151349508566	1
12	625	4	1.0	1151349514441	1
12	100	1	1.0	1151349520238	0
12	510	3	2.0	1151349534597	1
12	310	3	2.5	1151349552082	1
12	510	1	2.0	1151349565503	1
12	116	3	1.5	1151349580144	1
12	410	1	1.5	1151349594128	1
12	217	5	1.5	1151349605988	1
12	208	1	1.5	1151349623222	1
12	102	4	2.0	1151349629019	1
12	400	5	2.5	1151349637066	1
12	400	2	2.5	1151349644660	1
12	608	2	2.0	1151349664910	1
12	409	5	0.5	1151349678832	1
12	116	2	1.5	1151349701238	1
12	614	4	2.0	1151349706628	1
12	622	5	1.0	1151349713785	1
12	625	3	1.0	1151349727457	1
12	614	1	2.0	1151349735675	0
12	222	4	0.5	1151349745097	1
12	208	2	1.5	1151349757097	1
12	210	2	0.5	1151349774644	0
12	210	4	0.5	1151349785941	1
12	510	4	2.0	1151349791191	1
12	216	3	1.0	1151349814800	1
12	228	4	2.5	1151349821503	1
12	216	5	1.0	1151349844785	1
12	614	2	2.0	1151349866472	0
12	102	1	2.0	1151349875035	1
12	427	3	1.5	1151349890410	1
12	216	1	1.0	1151349900566	1
12	622	1	1.0	1151349931894	1
12	401	4	0.5	1151349938394	0
12	523	1	2.5	1151349948941	1
12	401	5	0.5	1151349981285	0
12	316	5	1.0	1151349997878	1
12	614	3	2.0	1151350012597	1
12	217	2	1.5	1151350028472	1
12	622	2	1.0	1151350045441	1
12	316	3	1.0	1151350061847	1
12	523	5	2.5	1151350069316	1
12	217	4	1.5	1151350075097	1
12	409	1	0.5	1151350088644	0
12	100	4	1.0	1151350117707	0
12	228	5	2.5	1151350126128	1
12	523	4	2.5	1151350132472	1
12	400	3	2.5	1151350138128	1
12	625	2	1.0	1151350153300	1
12	401	2	0.5	1151350176894	1
12	427	2	1.5	1151350188753	1
12	622	3	1.0	1151350213035	1
12	310	1	2.5	1151350221316	1
12	625	1	1.0	1151350228144	1
12	310	5	2.5	1151350258722	1
12	210	3	0.5	1151350274472	1
12	316	1	1.0	1151350280707	1
12	504	1	2.0	1151350293425	1
12	102	3	2.0	1151350303816	1
12	310	2	2.5	1151350312222	1
12	625	5	1.0	1151350327269	1
12	208	3	1.5	1151350342644	1
12	302	5	2.5	1151350347863	1
12	401	3	0.5	1151350360394	1
12	302	3	2.5	1151350372957	1
12	528	1	0.5	1151350378582	0
12	208	5	1.5	1151350394847	1
12	410	5	1.5	1151350408628	1

ID	TR	TECH	DIFF	TIME	RESP
12	608	1	2.0	1151350413988	1
12	510	2	2.0	1151350434753	1
15	100	2	1.0	1151354798863	0
15	210	5	0.5	1151354806269	1
15	523	5	2.5	1151354810441	1
15	217	1	1.5	1151354817675	1
15	427	2	1.5	1151354827222	0
15	222	4	0.5	1151354833660	0
15	116	2	1.5	1151354839988	1
15	614	1	2.0	1151354847300	0
15	401	1	0.5	1151354852300	1
15	302	4	2.5	1151354856941	1
15	116	3	1.5	1151354862925	1
15	427	5	1.5	1151354867519	1
15	622	5	1.0	1151354871394	1
15	608	2	2.0	1151354877722	1
15	100	3	1.0	1151354883957	0
15	528	1	0.5	1151354890175	1
15	217	2	1.5	1151354897003	0
15	427	1	1.5	1151354902144	1
15	228	3	2.5	1151354906832	1
15	102	4	2.0	1151354913441	1
15	400	2	2.5	1151354919441	1
15	401	2	0.5	1151354923519	0
15	302	5	2.5	1151354928207	1
15	510	2	2.0	1151354935128	1
15	316	5	1.0	1151354945675	0
15	216	4	1.0	1151354954191	1
15	102	5	2.0	1151354959394	1
15	310	2	2.5	1151354965332	1
15	625	2	1.0	1151354969550	1
15	614	4	2.0	1151354973847	1
15	116	1	1.5	1151354978222	1
15	316	3	1.0	1151354985050	1
15	228	1	2.5	1151354989691	1
15	614	3	2.0	1151354994800	0
15	310	5	2.5	1151355000347	1
15	504	3	2.0	1151355006738	1
15	208	3	1.5	1151355012535	0
15	316	1	1.0	1151355017753	1
15	410	4	1.5	1151355026128	1
15	116	4	1.5	1151355033910	1
15	100	5	1.0	1151355043363	0
15	208	4	1.5	1151355048628	1
15	102	1	2.0	1151355056097	1
15	625	5	1.0	1151355062878	1
15	217	3	1.5	1151355070832	0
15	222	1	0.5	1151355075160	1
15	302	1	2.5	1151355079207	1
15	401	3	0.5	1151355083644	1
15	523	3	2.5	1151355089050	1
15	217	5	1.5	1151355093941	1
15	410	2	1.5	1151355098363	1
15	216	3	1.0	1151355105191	0
15	217	4	1.5	1151355111660	1
15	401	5	0.5	1151355117050	1
15	400	5	2.5	1151355123019	1
15	608	3	2.0	1151355137863	0
15	528	5	0.5	1151355142691	1
15	102	2	2.0	1151355149472	0
15	210	1	0.5	1151355157175	1
15	316	4	1.0	1151355161816	0
15	208	1	1.5	1151355165847	1
15	427	3	1.5	1151355171582	0
15	504	1	2.0	1151355176441	1
15	410	1	1.5	1151355184878	1
15	608	4	2.0	1151355189660	1
15	614	5	2.0	1151355200894	0
15	625	3	1.0	1151355205082	1
15	523	1	2.5	1151355209160	1
15	316	2	1.0	1151355213753	0
15	302	3	2.5	1151355219550	1
15	528	4	0.5	1151355224925	0
15	222	5	0.5	1151355230019	1
15	510	1	2.0	1151355236066	1
15	102	3	2.0	1151355241847	1
15	504	5	2.0	1151355245910	1

ID	TR	TECH	DIFF	TIME	RESP
15	222	2	0.5	1151355254582	1
15	523	2	2.5	1151355260441	1
15	409	1	0.5	1151355266082	1
15	622	3	1.0	1151355270863	1
15	608	5	2.0	1151355275738	1
15	528	2	0.5	1151355284113	0
15	210	4	0.5	1151355289800	1
15	228	5	2.5	1151355294082	1
15	523	4	2.5	1151355298488	1
15	116	5	1.5	1151355304253	1
15	622	1	1.0	1151355310128	1
15	100	1	1.0	1151355316503	1
15	302	2	2.5	1151355324660	1
15	410	3	1.5	1151355330613	1
15	625	4	1.0	1151355334941	1
15	100	4	1.0	1151355339832	0
15	510	5	2.0	1151355344128	1
15	216	2	1.0	1151355356878	1
15	409	2	0.5	1151355367472	1
15	400	3	2.5	1151355372066	1
15	504	2	2.0	1151355380394	1
15	510	4	2.0	1151355384566	1
15	409	3	0.5	1151355389238	1
15	210	3	0.5	1151355405628	1
15	614	2	2.0	1151355409394	0
15	625	1	1.0	1151355414628	1
15	401	4	0.5	1151355418753	1
15	228	4	2.5	1151355423472	1
15	409	4	0.5	1151355428738	1
15	210	2	0.5	1151355432816	1
15	216	1	1.0	1151355439003	1
15	310	3	2.5	1151355444019	0
15	622	4	1.0	1151355448519	1
15	400	4	2.5	1151355452519	1
15	608	1	2.0	1151355461753	1
15	208	5	1.5	1151355470410	1
15	216	5	1.0	1151355476222	1
15	504	4	2.0	1151355480472	1
15	222	3	0.5	1151355484800	0
15	228	2	2.5	1151355489550	1
15	410	5	1.5	1151355494269	1
15	409	5	0.5	1151355499175	0
15	510	3	2.0	1151355504878	1
15	400	1	2.5	1151355509332	1
15	528	3	0.5	1151355515425	1
15	310	4	2.5	1151355520769	1
15	622	2	1.0	1151355525300	1
15	208	2	1.5	1151355530347	1
15	310	1	2.5	1151355536175	1
15	427	4	1.5	1151355540519	1
20	510	3	2.0	1151417630994	0
20	400	1	2.5	1151417637775	1
20	210	5	0.5	1151417642587	1
20	427	2	1.5	1151417653619	1
20	409	1	0.5	1151417665384	1
20	523	5	2.5	1151417671134	1
20	625	4	1.0	1151417677931	1
20	523	2	2.5	1151417692150	1
20	217	4	1.5	1151417698525	1
20	208	2	1.5	1151417704384	0
20	222	1	0.5	1151417725103	1
20	401	3	0.5	1151417734181	0
20	100	1	1.0	1151417739916	0
20	523	4	2.5	1151417744478	1
20	410	2	1.5	1151417750962	0
20	504	1	2.0	1151417757337	1
20	222	5	0.5	1151417762087	1
20	302	4	2.5	1151417766119	1
20	608	5	2.0	1151417773337	1
20	427	4	1.5	1151417777744	1
20	625	1	1.0	1151417783869	1
20	208	4	1.5	1151417798462	0
20	400	2	2.5	1151417820697	1
20	625	3	1.0	1151417829431	1
20	102	4	2.0	1151417833744	1
20	410	5	1.5	1151417838712	0
20	614	3	2.0	1151417858025	0

ID	TR	TECH	DIFF	TIME	RESP
20	116	4	1.5	1151417863603	1
20	622	2	1.0	1151417878431	0
20	608	4	2.0	1151417891087	1
20	210	1	0.5	1151417902181	0
20	510	5	2.0	1151417906619	1
20	100	2	1.0	1151417916978	0
20	102	5	2.0	1151417923916	1
20	222	2	0.5	1151417930916	0
20	523	3	2.5	1151417945056	1
20	400	4	2.5	1151417950384	1
20	310	5	2.5	1151417955806	1
20	310	2	2.5	1151417963384	0
20	210	3	0.5	1151417976119	1
20	216	2	1.0	1151417990681	0
20	302	3	2.5	1151417996494	1
20	427	3	1.5	1151418006228	1
20	410	1	1.5	1151418031166	1
20	401	1	0.5	1151418045712	1
20	608	1	2.0	1151418049978	1
20	622	4	1.0	1151418054931	1
20	622	5	1.0	1151418060087	1
20	528	2	0.5	1151418072322	0
20	116	1	1.5	1151418080134	1
20	217	1	1.5	1151418086353	1
20	510	4	2.0	1151418090400	1
20	614	4	2.0	1151418095041	0
20	302	1	2.5	1151418100822	1
20	100	4	1.0	1151418104775	0
20	116	3	1.5	1151418109494	1
20	614	5	2.0	1151418114181	1
20	310	3	2.5	1151418118681	1
20	401	5	0.5	1151418142025	0
20	510	1	2.0	1151418146572	1
20	316	5	1.0	1151418155634	0
20	208	1	1.5	1151418163259	0
20	216	1	1.0	1151418169103	1
20	410	4	1.5	1151418180244	1
20	400	3	2.5	1151418185228	1
20	528	3	0.5	1151418197447	0
20	409	5	0.5	1151418208650	0
20	302	2	2.5	1151418218603	1
20	228	5	2.5	1151418223150	1
20	622	1	1.0	1151418231353	0
20	228	4	2.5	1151418237572	1
20	608	3	2.0	1151418243775	0
20	302	5	2.5	1151418248369	1
20	100	5	1.0	1151418252291	0
20	222	3	0.5	1151418271853	1
20	608	2	2.0	1151418279041	1
20	614	2	2.0	1151418306119	1
20	310	4	2.5	1151418310884	1
20	427	5	1.5	1151418314947	1
20	523	1	2.5	1151418323400	1
20	625	5	1.0	1151418327369	1
20	409	3	0.5	1151418342712	0
20	504	5	2.0	1151418347978	1
20	614	1	2.0	1151418355197	0
20	400	5	2.5	1151418362478	1
20	100	3	1.0	1151418368837	0
20	102	1	2.0	1151418373244	1
20	116	2	1.5	1151418380431	0
20	401	2	0.5	1151418399634	0
20	622	3	1.0	1151418404509	1
20	310	1	2.5	1151418409400	1
20	116	5	1.5	1151418413994	1
20	222	4	0.5	1151418425025	1
20	504	4	2.0	1151418433322	1
20	228	3	2.5	1151418438181	1
20	528	1	0.5	1151418443150	0
20	316	2	1.0	1151418450759	0
20	316	4	1.0	1151418472212	0
20	210	4	0.5	1151418477400	1
20	316	1	1.0	1151418482197	0
20	409	2	0.5	1151418488556	1
20	217	2	1.5	1151418501462	1
20	504	3	2.0	1151418512072	1
20	216	5	1.0	1151418522759	1

ID	TR	TECH	DIFF	TIME	RESP
20	102	2	2.0	1151418559837	1
20	208	3	1.5	1151418573275	1
20	625	2	1.0	1151418585744	0
20	217	5	1.5	1151418591119	1
20	102	3	2.0	1151418597259	1
20	410	3	1.5	1151418614166	0
20	427	1	1.5	1151418618712	1
20	217	3	1.5	1151418632791	1
20	210	2	0.5	1151418647337	1
20	216	4	1.0	1151418655119	1
20	409	4	0.5	1151418669712	1
20	510	2	2.0	1151418686916	0
20	208	5	1.5	1151418715978	0
20	504	2	2.0	1151418730228	1
20	528	5	0.5	1151418743322	1
20	401	4	0.5	1151418747884	0
20	528	4	0.5	1151418757806	1
20	228	1	2.5	1151418762806	1
20	216	3	1.0	1151418780494	0
20	316	3	1.0	1151418792291	1
20	228	2	2.5	1151418799259	1

Table A.5: Participant responses from User Study 3.2

ID	TR	TECH	DIFF	TIME	RESP
1	206	5	15	1151000379868	0
1	512	2	15	1151000393040	0
1	123	4	20	1151000406056	1
1	617	3	10	1151000418947	0
1	609	5	20	1151000425947	0
1	122	4	15	1151000431947	1
1	409	5	10	1151000439932	0
1	210	1	10	1151000446166	0
1	617	2	10	1151000461964	0
1	619	2	30	1151000472245	0
1	506	2	25	1151000480855	0
1	102	2	15	1151000494636	1
1	617	1	10	1151000500683	1
1	325	5	15	1151000505855	1
1	116	5	20	1151000512746	1
1	619	5	30	1151000524512	1
1	409	4	10	1151000530528	0
1	206	2	15	1151000537106	0
1	409	3	10	1151000544231	0
1	225	1	30	1151000551966	1
1	604	4	20	1151000559576	1
1	400	4	25	1151000565076	1
1	109	3	10	1151000575732	1
1	225	3	30	1151000587451	1
1	109	4	10	1151000592233	0
1	122	5	15	1151000598186	1
1	400	3	25	1151000609202	1
1	505	2	25	1151000620265	1
1	225	5	30	1151000629671	1
1	617	4	10	1151000635031	0
1	503	3	25	1151000642734	1
1	113	5	10	1151000648156	1
1	420	4	30	1151000653328	1
1	124	1	30	1151000660797	1
1	102	4	15	1151000666860	1
1	604	1	20	1151000675391	1
1	304	5	20	1151000680282	0
1	124	2	30	1151000689657	1
1	505	5	25	1151000694767	1
1	512	4	15	1151000700157	0
1	325	4	15	1151000705157	1
1	512	3	15	1151000714939	1
1	609	1	20	1151000727471	1
1	123	1	20	1151000732955	0
1	113	1	10	1151000740268	0
1	510	1	25	1151000745018	1
1	210	2	10	1151000750518	0
1	314	2	30	1151000757096	0
1	116	4	20	1151000762815	1
1	503	4	25	1151000768565	1
1	210	4	10	1151000775128	0
1	609	3	20	1151000782253	1
1	604	5	20	1151000787988	1
1	102	1	15	1151000795285	0
1	505	3	25	1151000808223	1
1	113	2	10	1151000813988	1
1	225	2	30	1151000820660	1
1	420	5	30	1151000825645	1
1	102	5	15	1151000831395	0
1	506	4	25	1151000848458	1
1	506	1	25	1151000853099	1
1	122	3	15	1151000859849	1
1	510	2	25	1151000867255	1
1	304	3	20	1151000876396	0
1	400	1	25	1151000881740	0
1	314	5	30	1151000888287	1
1	304	2	20	1151000895240	0
1	604	3	20	1151000905163	0
1	609	2	20	1151000909053	0
1	510	5	25	1151000914600	1
1	505	4	25	1151000920632	1
1	206	3	15	1151000926413	0
1	510	4	25	1151000932601	1
1	123	5	20	1151000938320	1
1	420	2	30	1151000943304	1
1	109	5	10	1151000948617	1
1	619	1	30	1151000955179	0
1	304	1	20	1151000961336	1
1	400	2	25	1151000967727	0
1	420	1	30	1151000972977	1
1	420	3	30	1151000978539	1
1	123	2	20	1151000988087	0
1	619	4	30	1151001006993	1
1	122	2	15	1151001012165	0
1	210	5	10	1151001018884	0
1	314	3	30	1151001026791	0
1	116	1	20	1151001031697	1
1	304	4	20	1151001035510	0
1	124	4	30	1151001042682	1
1	206	1	15	1151001047651	0
1	503	5	25	1151001052479	1
1	109	2	10	1151001058557	0
1	506	3	25	1151001066901	1
1	409	1	10	1151001077417	0
1	512	5	15	1151001092558	0
1	206	4	15	1151001097621	0
1	124	3	30	1151001103527	1
1	617	5	10	1151001112105	0
1	325	1	15	1151001118402	0
1	116	3	20	1151001123996	1
1	325	3	15	1151001129731	1
1	314	1	30	1151001135871	0
1	113	4	10	1151001139698	1
1	116	2	20	1151001144495	1
1	604	2	20	1151001150822	0
1	325	2	15	1151001156227	1
1	122	1	15	1151001160836	0
1	113	3	10	1151001166101	1
1	503	1	25	1151001170288	1
1	102	3	15	1151001178130	1
1	506	5	25	1151001187332	0
1	503	2	25	1151001193863	0
1	123	3	20	1151001200471	0
1	400	5	25	1151001205220	1
1	109	1	10	1151001209985	0
1	225	4	30	1151001214313	0
1	609	4	20	1151001221078	0
1	510	3	25	1151001225749	0
1	512	1	15	1151001230217	0
1	619	3	30	1151001235247	0
1	124	5	30	1151001239606	1
1	314	4	30	1151001244777	1
1	210	3	10	1151001249230	0
1	505	1	25	1151001258338	1
1	409	2	10	1151001262744	0
91	325	1	15	1151285328599	1
91	124	4	30	1151285339770	1
91	116	3	20	1151285352099	1
91	503	4	25	1151285363864	1
91	409	4	10	1151285372474	0
91	206	3	15	1151285380458	1
91	225	5	30	1151285392411	0
91	409	1	10	1151285402317	0
91	619	5	30	1151285415161	0
91	619	1	30	1151285432411	1
91	116	1	20	1151285444770	0
91	609	1	20	1151285451864	1
91	325	5	15	1151285462927	1
91	314	2	30	1151285494177	0
91	619	2	30	1151285515692	1
91	113	1	10	1151285523239	1
91	512	5	15	1151285533286	1
91	225	1	30	1151285548911	1
91	123	2	20	1151285573739	1
91	506	2	25	1151285581208	1
91	503	3	25	1151285600036	1
91	503	5	25	1151285610130	1
91	123	1	20	1151285627692	0
91	604	1	20	1151285638692	1
91	225	4	30	1151285655364	1
91	314	3	30	1151285673567	1

ID	TR	TECH	DIFF	TIME	RESP
91	206	1	15	1151285689505	1
91	122	1	15	1151285694286	1
91	512	1	15	1151285701317	1
91	123	4	20	1151285721302	1
91	116	4	20	1151285730255	1
91	210	4	10	1151285748224	0
91	123	5	20	1151285761755	1
91	210	2	10	1151285783645	0
91	124	5	30	1151285791083	1
91	123	3	20	1151285809770	1
91	304	3	20	1151285814645	1
91	505	5	25	1151285820958	1
91	420	5	30	1151285827833	1
91	617	5	10	1151285834286	1
91	109	3	10	1151285846395	1
91	505	3	25	1151285859395	1
91	124	2	30	1151285882208	1
91	304	1	20	1151285893583	1
91	210	3	10	1151285899505	0
91	510	1	25	1151285907255	1
91	304	2	20	1151285916567	0
91	400	1	25	1151285920755	1
91	122	3	15	1151285927411	1
91	609	5	20	1151285934224	1
91	506	4	25	1151285941942	1
91	506	1	25	1151285951177	0
91	604	4	20	1151285959427	1
91	116	2	20	1151285983317	1
91	124	1	30	1151286004724	1
91	102	5	15	1151286028942	1
91	102	2	15	1151286034239	0
91	325	2	15	1151286040145	1
91	505	1	25	1151286044255	1
91	206	5	15	1151286054520	1
91	619	3	30	1151286068239	1
91	304	4	20	1151286087364	0
91	400	3	25	1151286094895	1
91	113	5	10	1151286102458	1
91	325	3	15	1151286122005	1
91	124	3	30	1151286131192	1
91	113	3	10	1151286143614	1
91	510	5	25	1151286149161	1
91	400	4	25	1151286156520	1
91	512	4	15	1151286162958	1
91	116	5	20	1151286183411	0
91	109	4	10	1151286193364	0
91	400	5	25	1151286197208	1
91	604	5	20	1151286212145	0
91	314	5	30	1151286226208	1
91	506	5	25	1151286236661	1
91	512	2	15	1151286246927	1
91	210	5	10	1151286272005	1
91	122	5	15	1151286277192	1
91	109	2	10	1151286287270	0
91	102	1	15	1151286292895	0
91	409	5	10	1151286302114	0
91	409	2	10	1151286306192	0
91	619	4	30	1151286318989	0
91	113	2	10	1151286335349	0
91	109	5	10	1151286352599	1
91	304	5	20	1151286357692	0
91	505	4	25	1151286363911	1
91	420	2	30	1151286371927	1
91	617	1	10	1151286376833	1
91	505	2	25	1151286381036	1
91	225	3	30	1151286389895	1
91	609	4	20	1151286394177	1
91	609	3	20	1151286402567	1
91	512	3	15	1151286412974	1
91	506	3	25	1151286432849	1
91	210	1	10	1151286436739	0
91	503	2	25	1151286443817	1
91	604	2	20	1151286448302	0
91	604	3	20	1151286451411	1
91	510	3	25	1151286455599	1
91	109	1	10	1151286459849	1
91	420	1	30	1151286465474	0

ID	TR	TECH	DIFF	TIME	RESP
91	122	2	15	1151286470864	1
91	122	4	15	1151286474349	1
91	206	2	15	1151286479692	0
91	314	1	30	1151286484255	1
91	409	3	10	1151286490286	0
91	503	1	25	1151286496927	1
91	617	3	10	1151286507177	1
91	206	4	15	1151286515036	1
91	325	4	15	1151286523802	1
91	609	2	20	1151286533333	0
91	102	3	15	1151286537458	0
91	420	4	30	1151286543083	1
91	225	2	30	1151286548505	0
91	510	4	25	1151286551974	1
91	617	2	10	1151286557958	1
91	400	2	25	1151286570708	1
91	102	4	15	1151286574833	0
91	420	3	30	1151286584536	1
91	617	4	10	1151286589395	1
91	113	4	10	1151286593161	1
91	510	2	25	1151286596864	1
91	314	4	30	1151286602599	1
99	409	5	10	1151363433332	0
99	102	1	15	1151363442645	1
99	225	3	30	1151363451692	1
99	116	1	20	1151363464723	1
99	617	5	10	1151363481551	1
99	420	5	30	1151363506535	1
99	314	4	30	1151363523567	1
99	109	1	10	1151363535676	1
99	210	4	10	1151363548129	1
99	206	1	15	1151363574004	0
99	503	1	25	1151363600004	1
99	506	2	25	1151363617113	1
99	619	1	30	1151363633707	1
99	122	2	15	1151363657535	0
99	512	5	15	1151363667942	1
99	210	2	10	1151363703692	1
99	604	4	20	1151363713817	1
99	420	2	30	1151363737785	0
99	619	2	30	1151363767067	1
99	314	2	30	1151363790707	1
99	619	3	30	1151363808426	1
99	304	1	20	1151363826035	1
99	113	3	10	1151363836004	1
99	210	1	10	1151363848817	0
99	505	1	25	1151363877801	1
99	617	4	10	1151363890488	1
99	116	5	20	1151363909145	0
99	123	4	20	1151363921488	0
99	420	4	30	1151363929504	1
99	206	2	15	1151363947567	1
99	124	1	30	1151363970551	1
99	604	2	20	1151363999910	1
99	409	4	10	1151364013567	0
99	617	3	10	1151364028160	1
99	109	4	10	1151364045988	1
99	102	2	15	1151364066238	1
99	512	4	15	1151364080363	1
99	512	1	15	1151364092988	1
99	109	5	10	1151364111332	1
99	124	4	30	1151364132754	1
99	116	3	20	1151364151613	1
99	225	1	30	1151364161348	1
99	123	3	20	1151364183348	0
99	123	2	20	1151364203317	0
99	325	5	15	1151364224738	0
99	409	2	10	1151364247254	0
99	102	5	15	1151364265223	1
99	225	5	30	1151364280457	1
99	122	5	15	1151364295348	0
99	510	4	25	1151364310957	1
99	609	5	20	1151364328973	1
99	400	2	25	1151364341598	0
99	505	4	25	1151364363410	0
99	206	4	15	1151364380051	1
99	304	2	20	1151364408004	1

ID	TR	TECH	DIFF	TIME	RESP
99	503	2	25	1151364431317	0
99	400	5	25	1151364440270	1
99	604	5	20	1151364457910	0
99	512	3	15	1151364475020	1
99	619	5	30	1151364488129	1
99	609	2	20	1151364504957	0
99	113	2	10	1151364519207	1
99	506	5	25	1151364550567	1
99	420	1	30	1151364568942	0
99	505	2	25	1151364580723	1
99	102	3	15	1151364607348	1
99	503	4	25	1151364622020	1
99	510	1	25	1151364632160	0
99	123	5	20	1151364655457	1
99	113	4	10	1151364663645	1
99	122	3	15	1151364672895	1
99	225	2	30	1151364690035	1
99	510	5	25	1151364698832	1
99	409	3	10	1151364731442	0
99	409	1	10	1151364741942	1
99	505	3	25	1151364772363	1
99	619	4	30	1151364785613	1
99	123	1	20	1151364804692	0
99	113	5	10	1151364825348	1
99	113	1	10	1151364830848	1
99	210	3	10	1151364844535	1
99	304	5	20	1151364857457	1
99	124	2	30	1151364877707	1
99	506	4	25	1151364892035	0
99	510	2	25	1151364906817	1
99	617	2	10	1151364917254	1
99	206	5	15	1151364927520	1
99	102	4	15	1151364948363	0
99	124	5	30	1151364961707	1
99	206	3	15	1151364976692	0
99	304	3	20	1151365000098	0
99	124	3	30	1151365014660	1
99	109	3	10	1151365037957	1
99	325	4	15	1151365050598	1
99	325	3	15	1151365063207	1
99	604	3	20	1151365073692	1
99	505	5	25	1151365088785	1
99	325	2	15	1151365100363	1
99	122	4	15	1151365109113	1
99	400	3	25	1151365131598	1
99	210	5	10	1151365141051	1
99	506	3	25	1151365162145	1
99	400	1	25	1151365170192	1
99	116	2	20	1151365191567	1
99	304	4	20	1151365206785	0
99	506	1	25	1151365224223	0
99	325	1	15	1151365245020	1
99	314	1	30	1151365251238	1
99	122	1	15	1151365260629	1
99	116	4	20	1151365276488	1
99	604	1	20	1151365282098	1
99	109	2	10	1151365312363	0
99	609	4	20	1151365329035	0
99	609	3	20	1151365340270	0
99	503	5	25	1151365352582	1
99	609	1	20	1151365362738	1
99	503	3	25	1151365372973	1
99	400	4	25	1151365383723	1
99	420	3	30	1151365411723	1
99	314	5	30	1151365430629	1
99	225	4	30	1151365445863	1
99	512	2	15	1151365476785	0
99	617	1	10	1151365482598	1
99	510	3	25	1151365497192	1
99	314	3	30	1151365512863	1
0	503	2	25	1150988787869	1
0	124	4	30	1150988794820	0
0	206	5	15	1150988802115	1
0	124	1	30	1150988807754	0
0	420	4	30	1150988818501	0
0	409	1	10	1150988826546	0
0	124	2	30	1150988832435	1

ID	TR	TECH	DIFF	TIME	RESP
0	116	4	20	1150988846589	1
0	210	4	10	1150988874023	0
0	314	4	30	1150988882199	1
0	122	1	15	1150988886200	1
0	510	2	25	1150988890484	1
0	122	3	15	1150988895642	1
0	304	3	20	1150988900050	0
0	506	2	25	1150988912368	1
0	206	2	15	1150988916620	1
0	400	4	25	1150988920372	1
0	409	5	10	1150988925218	1
0	505	3	25	1150988936613	1
0	123	3	20	1150988941850	1
0	609	1	20	1150988947024	1
0	512	1	15	1150988950917	1
0	123	5	20	1150988963094	1
0	619	4	30	1150988969909	0
0	510	3	25	1150988974286	1
0	113	4	10	1150988977928	1
0	123	4	20	1150988981790	0
0	102	2	15	1150988985119	1
0	505	1	25	1150988989011	1
0	617	5	10	1150988995342	1
0	420	2	30	1150989000079	1
0	512	3	15	1150989013819	1
0	604	4	20	1150989021073	1
0	617	2	10	1150989025324	1
0	116	5	20	1150989030514	1
0	210	1	10	1150989034266	1
0	225	5	30	1150989045021	1
0	206	1	15	1150989050148	1
0	102	1	15	1150989054962	0
0	604	2	20	1150989059980	1
0	325	1	15	1150989063560	1
0	102	4	15	1150989071782	0
0	116	2	20	1150989079489	1
0	506	1	25	1150989083631	0
0	225	3	30	1150989089853	1
0	109	4	10	1150989094871	0
0	304	2	20	1150989098091	0
0	409	4	10	1150989102483	1
0	506	3	25	1150989108080	0
0	314	2	30	1150989111847	0
0	604	1	20	1150989115677	1
0	400	5	25	1150989119444	1
0	512	5	15	1150989123774	1
0	102	3	15	1150989129105	0
0	113	3	10	1150989133810	1
0	420	1	30	1150989139343	0
0	116	1	20	1150989143392	0
0	505	2	25	1150989147986	1
0	420	3	30	1150989152831	1
0	420	5	30	1150989156956	1
0	400	1	25	1150989160801	0
0	617	1	10	1150989165114	1
0	512	4	15	1150989173474	0
0	109	3	10	1150989179584	1
0	609	2	20	1150989183804	1
0	113	1	10	1150989187195	1
0	304	1	20	1150989191461	0
0	116	3	20	1150989195696	1
0	506	4	25	1150989199243	1
0	503	3	25	1150989203306	1
0	505	4	25	1150989207729	1
0	225	2	30	1150989211839	0
0	314	3	30	1150989218855	0
0	619	2	30	1150989222809	1
0	109	1	10	1150989226606	1
0	304	5	20	1150989230404	0
0	409	3	10	1150989235514	1
0	122	4	15	1150989239405	1
0	619	1	30	1150989243218	1
0	609	4	20	1150989248547	1
0	122	5	15	1150989253032	1
0	109	5	10	1150989261080	1
0	617	4	10	1150989265362	1
0	604	3	20	1150989269815	1

ID	TR	TECH	DIFF	TIME	RESP
0	206	3	15	1150989280020	0
0	325	2	15	1150989284208	1
0	409	2	10	1150989288193	0
0	604	5	20	1150989292178	1
0	609	5	20	1150989298413	1
0	510	1	25	1150989304148	0
0	122	2	15	1150989309008	1
0	512	2	15	1150989312915	1
0	113	5	10	1150989316931	1
0	123	2	20	1150989321432	1
0	505	5	25	1150989325495	1
0	619	5	30	1150989330042	0
0	617	3	10	1150989335184	1
0	510	4	25	1150989338637	1
0	124	3	30	1150989344950	1
0	619	3	30	1150989350420	1
0	113	2	10	1150989354327	1
0	503	1	25	1150989358046	0
0	314	1	30	1150989361875	1
0	503	4	25	1150989368469	1
0	510	5	25	1150989372532	1
0	225	4	30	1150989381924	1
0	325	4	15	1150989385643	1
0	314	5	30	1150989391988	0
0	304	4	20	1150989397551	0
0	210	3	10	1150989402396	1
0	210	5	10	1150989406224	1
0	206	4	15	1150989411709	1
0	503	5	25	1150989415710	1
0	325	3	15	1150989422930	1
0	109	2	10	1150989427243	1
0	225	1	30	1150989430509	1
0	400	3	25	1150989435384	1
0	609	3	20	1150989440010	1
0	325	5	15	1150989445245	1
0	506	5	25	1150989453230	0
0	123	1	20	1150989457792	1
0	400	2	25	1150989463589	0
0	102	5	15	1150989470214	0
0	210	2	10	1150989476074	1
0	124	5	30	1150989480262	1
2	123	4	20	1151075956048	0
2	304	1	20	1151075966282	1
2	314	1	30	1151075977329	1
2	109	3	10	1151075984329	1
2	314	5	30	1151076000500	1
2	409	5	10	1151076014625	1
2	102	5	15	1151076031047	0
2	109	4	10	1151076037484	1
2	617	5	10	1151076047953	1
2	113	2	10	1151076074656	0
2	409	4	10	1151076085312	0
2	113	5	10	1151076092640	1
2	210	2	10	1151076098218	1
2	617	1	10	1151076109640	1
2	325	3	15	1151076127483	0
2	506	3	25	1151076138983	1
2	503	3	25	1151076149686	1
2	124	5	30	1151076171826	0
2	420	1	30	1151076176529	0
2	619	4	30	1151076186045	0
2	409	3	10	1151076197388	1
2	617	2	10	1151076220138	1
2	102	4	15	1151076225341	0
2	604	1	20	1151076230263	1
2	122	4	15	1151076236825	1
2	510	2	25	1151076249028	1
2	210	4	10	1151076267247	1
2	206	3	15	1151076295434	0
2	124	4	30	1151076300403	0
2	510	3	25	1151076312543	1
2	225	4	30	1151076320856	1
2	619	3	30	11510763306 21	1
2	109	2	10	1151076338746	1
2	122	5	15	1151076344887	1
2	510	4	25	1151076354121	0
2	314	4	30	1151076361199	1

ID	TR	TECH	DIFF	TIME	RESP
2	102	3	15	11510763708 55	1
2	400	3	25	1151076381511	1
2	116	2	20	1151076386245	1
2	206	2	15	1151076393745	1
2	124	1	30	1151076404886	0
2	304	2	20	1151076419183	1
2	512	4	15	1151076438479	1
2	609	5	20	1151076468573	0
2	314	3	30	1151076478994	1
2	506	4	25	1151076490010	0
2	619	1	30	1151076498791	0
2	400	4	25	1151076504166	1
2	122	2	15	1151076510634	0
2	325	5	15	1151076521962	1
2	116	5	20	1151076531572	1
2	116	4	20	1151076536665	1
2	400	1	25	1151076541415	1
2	325	4	15	1151076549087	1
2	124	2	30	1151076554337	1
2	420	2	30	1151076565196	1
2	116	3	20	1151076572821	0
2	617	3	10	1151076584321	1
2	225	1	30	1151076590196	1
2	505	5	25	1151076602602	1
2	123	1	20	1151076613508	1
2	420	3	30	1151076622289	1
2	210	5	10	1151076631586	0
2	609	4	20	1151076637211	1
2	420	4	30	1151076643008	1
2	409	2	10	1151076651773	0
2	325	2	15	1151076669398	0
2	604	5	20	1151076679632	0
2	503	2	25	1151076687398	1
2	304	4	20	1151076698710	1
2	506	1	25	1151076704960	0
2	400	5	25	1151076713335	1
2	122	1	15	1151076717319	1
2	506	2	25	1151076727491	0
2	102	1	15	1151076731663	0
2	609	2	20	1151076749335	0
2	505	3	25	1151076768850	1
2	503	1	25	1151076773100	1
2	503	4	25	1151076779600	1
2	619	5	30	1151076793740	1
2	609	1	20	1151076797584	1
2	123	5	20	1151076811006	1
2	400	2	25	1151076817740	1
2	609	3	20	1151076828177	1
2	206	4	15	1151076853693	1
2	123	2	20	1151076859161	1
2	116	1	20	1151076862458	0
2	420	5	30	1151076872114	1
2	617	4	10	1151076880583	1
2	314	2	30	1151076887333	1
2	505	4	25	1151076905412	1
2	304	3	20	1151076917040	1
2	512	5	15	1151076923447	1
2	512	2	15	1151076928073	0
2	503	5	25	1151076951672	1
2	124	3	30	1151076962127	1
2	210	1	10	1151076966018	0
2	225	2	30	1151076970582	0
2	510	1	25	1151076977442	1
2	505	1	25	1151076982037	1
2	604	2	20	1151076987772	1
2	210	3	10	1151077001431	1
2	206	1	15	1151077005667	0
2	225	5	30	1151077010808	1
2	619	2	30	1151077017872	0
2	604	3	20	1151077023029	1
2	325	1	15	1151077027968	0
2	304	5	20	1151077044002	1
2	109	1	10	1151077047925	1
2	506	5	25	1151077065100	0
2	122	3	15	1151077076165	0
2	113	4	10	1151077080853	1
2	409	1	10	1151077085089	1

ID	TR	TECH	DIFF	TIME	RESP
2	604	4	20	1151077096528	0
2	206	5	15	1151077104233	1
2	113	1	10	1151077109109	1
2	512	3	15	1151077122862	1
2	109	5	10	1151077129785	1
2	510	5	25	1151077149461	1
2	512	1	15	1151077152961	1
2	102	2	15	1151077158775	1
2	113	3	10	1151077163417	1
2	225	3	30	1151077168183	1
2	123	3	20	1151077179639	0
2	505	2	25	1151077187593	1
4	314	5	30	1151007640418	1
4	512	5	15	1151007664091	1
4	225	2	30	1151007677763	1
4	116	3	20	1151007715202	0
4	109	2	10	1151007736484	0
4	617	2	10	1151007757890	1
4	510	5	25	1151007772016	1
4	116	2	20	1151007793001	1
4	420	2	30	1151007810001	1
4	113	3	10	1151007817424	1
4	123	2	20	1151007845315	1
4	619	3	30	1151007857831	1
4	604	5	20	1151007888254	1
4	400	5	25	1151007896207	1
4	210	2	10	1151007929098	0
4	314	2	30	1151007944270	0
4	124	4	30	1151007969927	1
4	420	3	30	1151008000600	1
4	102	2	15	1151008013334	1
4	619	5	30	1151008024459	0
4	506	2	25	1151008038178	1
4	617	1	10	1151008048288	1
4	225	3	30	1151008058804	1
4	124	1	30	1151008068695	1
4	123	3	20	1151008117289	1
4	210	3	10	1151008137430	0
4	505	5	25	1151008171290	1
4	116	4	20	1151008180275	1
4	400	3	25	1151008191462	1
4	314	4	30	1151008205384	1
4	210	5	10	1151008217385	1
4	420	5	30	1151008227775	1
4	503	5	25	1151008236166	1
4	325	4	15	1151008242119	1
4	505	3	25	1151008252416	1
4	109	4	10	1151008262526	1
4	604	2	20	1151008275307	1
4	206	4	15	1151008287995	0
4	210	4	10	1151008306995	0
4	400	4	25	1151008313183	1
4	124	3	30	1151008328527	1
4	109	3	10	1151008340058	1
4	325	1	15	1151008368199	1
4	512	4	15	1151008375527	1
4	124	2	30	1151008382355	1
4	506	4	25	1151008394262	0
4	304	5	20	1151008401965	1
4	609	3	20	1151008429622	1
4	325	2	15	1151008458919	1
4	409	5	10	1151008469216	0
4	225	4	30	1151008478044	1
4	102	3	15	1151008499498	1
4	206	3	15	1151008513576	0
4	206	1	15	1151008521232	0
4	304	4	20	1151008537732	0
4	503	1	25	1151008559045	0
4	420	1	30	1151008564827	1
4	619	4	30	1151008576155	0
4	609	4	20	1151008586592	1
4	503	4	25	1151008593218	1
4	206	2	15	1151008602983	0
4	304	1	20	1151008608124	1
4	400	2	25	1151008624999	0
4	619	2	30	1151008637031	0
4	113	4	10	1151008643265	1

ID	TR	TECH	DIFF	TIME	RESP
4	304	3	20	1151008657312	1
4	506	5	25	1151008674203	0
4	122	1	15	1151008683672	1
4	512	1	15	1151008690063	1
4	123	1	20	1151008705578	0
4	210	1	10	1151008719032	0
4	124	5	30	1151008729626	1
4	409	1	10	1151008737485	0
4	122	2	15	1151008755063	1
4	609	5	20	1151008776579	1
4	325	5	15	1151008788017	1
4	409	2	10	1151008803814	0
4	503	2	25	1151008823455	1
4	113	2	10	1151008833361	1
4	123	4	20	1151008847096	1
4	102	4	15	1151008856299	0
4	604	3	20	1151008866799	1
4	409	3	10	1151008905472	0
4	512	2	15	1151008912503	1
4	122	4	15	1151008940409	1
4	109	5	10	1151008945316	1
4	225	1	30	1151008950722	0
4	122	5	15	1151008956628	1
4	604	1	20	1151008969175	0
4	506	3	25	1151008997426	1
4	505	1	25	1151009020442	1
4	510	3	25	1151009025723	1
4	604	4	20	1151009038848	0
4	619	1	30	1151009046255	0
4	116	5	20	1151009055020	1
4	109	1	10	1151009067630	1
4	409	4	10	1151009076661	1
4	503	3	25	1151009087724	1
4	506	1	25	1151009094021	1
4	512	3	15	1151009108865	1
4	206	5	15	1151009118943	0
4	113	1	10	1151009123974	1
4	325	3	15	1151009153147	1
4	617	5	10	1151009159147	1
4	505	4	25	1151009186616	0
4	420	4	30	1151009199553	0
4	510	2	25	1151009218616	1
4	122	3	15	1151009229585	1
4	314	3	30	1151009237866	0
4	314	1	30	1151009246820	1
4	617	4	10	1151009251492	1
4	225	5	30	1151009259617	1
4	400	1	25	1151009270711	1
4	510	1	25	1151009275242	1
4	102	1	15	1151009279351	1
4	123	5	20	1151009288305	1
4	617	3	10	1151009299336	1
4	116	1	20	1151009303539	1
4	304	2	20	1151009314039	1
4	113	5	10	1151009321305	1
4	510	4	25	1151009326649	1
4	505	2	25	1151009339102	1
4	609	2	20	1151009351837	1
4	102	5	15	1151009366634	1
4	609	1	20	1151009378228	1
10	609	2	20	1151335328703	0
10	314	1	30	1151335383984	1
10	206	5	15	1151335478109	0
10	609	3	20	1151335609515	0
10	325	5	15	1151335664015	1
10	109	5	10	1151335721374	0
10	109	4	10	1151335785999	0
10	124	3	30	1151335832296	1
10	314	3	30	1151335945453	1
10	116	5	20	1151335956249	1
10	506	3	25	1151336038437	1
10	505	4	25	1151336133999	0
10	420	1	30	1151336157999	1
10	617	2	10	1151336230406	1
10	124	4	30	1151336247171	1
10	512	4	15	1151336261218	0
10	400	5	25	1151336295578	1

ID	TR	TECH	DIFF	TIME	RESP
10	505	5	25	1151336321640	1
10	122	4	15	1151336351749	1
10	604	2	20	1151336378031	0
10	510	1	25	1151336420718	1
10	510	5	25	1151336450624	1
10	102	4	15	1151336523421	0
10	510	4	25	1151336562999	1
10	122	1	15	1151336583218	0
10	113	4	10	1151336610421	1
10	400	2	25	1151336625031	0
10	304	3	20	1151336665843	0
10	102	1	15	1151336676062	1
10	503	5	25	1151336729015	1
10	225	1	30	1151336743406	0
10	503	3	25	1151336751062	1
10	225	4	30	1151336775343	1
10	604	3	20	1151336830812	0
10	124	1	30	1151336844578	1
10	325	4	15	1151336878062	1
10	210	2	10	1151336890796	0
10	512	1	15	1151336907343	0
10	325	1	15	1151336923843	1
10	210	4	10	1151336956265	1
10	123	2	20	1151336989874	0
10	506	4	25	1151337008031	0
10	225	3	30	1151337047953	1
10	510	3	25	1151337070562	1
10	116	3	20	1151337113812	1
10	225	2	30	1151337124734	0
10	503	1	25	1151337150390	1
10	505	1	25	1151337177140	0
10	206	1	15	1151337216046	1
10	619	1	30	1151337262218	0
10	609	5	20	1151337279046	0
10	109	3	10	1151337300921	1
10	400	4	25	1151337314203	1
10	506	1	25	1151337320765	1
10	409	4	10	1151337333249	0
10	304	2	20	1151337346203	1
10	314	2	30	1151337357343	1
10	619	5	30	1151337402671	1
10	122	5	15	1151337427468	1
10	617	5	10	1151337446437	1
10	604	4	20	1151337461343	0
10	116	2	20	1151337474171	1
10	503	2	25	1151337482968	1
10	619	2	30	1151337489156	0
10	409	5	10	1151337503828	0
10	206	2	15	1151337527999	0
10	109	1	10	1151337550312	0
10	102	2	15	1151337568359	1
10	617	3	10	1151337637515	1
10	113	3	10	1151337664203	1
10	617	4	10	1151337698843	1
10	609	1	20	1151337720671	0
10	102	3	15	1151337732765	0
10	506	2	25	1151337745843	1
10	123	1	20	1151337787640	0
10	619	4	30	1151337799343	0
10	210	5	10	1151337821874	1
10	116	1	20	1151337827734	1
10	123	4	20	1151337849656	1
10	210	3	10	1151337861765	0
10	409	3	10	1151337885624	0
10	123	3	20	1151337903390	1
10	420	4	30	1151337914359	0
10	304	5	20	1151337965703	1
10	124	2	30	1151337988781	1
10	400	3	25	1151338004109	1
10	122	3	15	1151338012249	1
10	210	1	10	1151338027749	1
10	604	5	20	1151338044828	0
10	102	5	15	1151338065749	1
10	225	5	30	1151338089906	1
10	206	4	15	1151338109499	0
10	325	3	15	1151338135718	1
10	505	2	25	1151338144359	1

ID	TR	TECH	DIFF	TIME	RESP
10	512	5	15	1151338164046	1
10	113	1	10	1151338188140	1
10	505	3	25	1151338217937	1
10	206	3	15	1151338227124	0
10	609	4	20	1151338238078	0
10	512	3	15	1151338278078	0
10	116	4	20	1151338308359	1
10	420	5	30	1151338325734	1
10	304	4	20	1151338341671	0
10	617	1	10	1151338348593	1
10	400	1	25	1151338354531	0
10	113	2	10	1151338367984	1
10	314	4	30	1151338380843	1
10	113	5	10	1151338416328	1
10	506	5	25	1151338427406	1
10	512	2	15	1151338458499	0
10	314	5	30	1151338472531	1
10	604	1	20	1151338487421	1
10	109	2	10	1151338497312	0
10	304	1	20	1151338512609	1
10	619	3	30	1151338522499	1
10	420	3	30	1151338559562	1
10	503	4	25	1151338569765	1
10	123	5	20	1151338591968	1
10	510	2	25	1151338596796	1
10	420	2	30	1151338643156	1
10	409	2	10	1151338647906	0
10	122	2	15	1151338654843	1
10	325	2	15	1151338663187	1
10	409	1	10	1151338676359	1
10	124	5	30	1151338690921	1
11	123	3	20	1151343275238	0
11	503	1	25	1151343291253	0
11	304	2	20	1151343304785	1
11	604	4	20	1151343325503	0
11	210	4	10	1151343336613	1
11	510	5	25	1151343362222	1
11	124	5	30	1151343369988	1
11	113	2	10	1151343382175	1
11	102	5	15	1151343398832	1
11	225	3	30	1151343407457	1
11	510	1	25	1151343420738	0
11	116	5	20	1151343433285	1
11	123	4	20	1151343445972	0
11	124	1	30	1151343451050	1
11	116	4	20	1151343461582	1
11	210	2	10	1151343471910	1
11	420	5	30	1151343492285	0
11	210	3	10	1151343501691	0
11	122	3	15	1151343517394	1
11	113	1	10	1151343526207	1
11	206	2	15	1151343550222	1
11	123	5	20	1151343572097	1
11	304	4	20	1151343585207	0
11	113	4	10	1151343593066	1
11	506	5	25	1151343603722	0
11	109	5	10	1151343615550	1
11	109	4	10	1151343635253	1
11	619	1	30	1151343642519	0
11	609	5	20	1151343699738	0
11	512	5	15	1151343707972	1
11	113	5	10	1151343716941	1
11	400	3	25	1151343723957	1
11	325	3	15	1151343743316	0
11	409	1	10	1151343769503	0
11	510	4	25	1151343779816	1
11	314	2	30	1151343792644	0
11	122	5	15	1151343798644	1
11	617	3	10	1151343804738	1
11	210	5	10	1151343835144	0
11	619	4	30	1151343844332	0
11	400	4	25	1151343848800	1
11	225	2	30	1151343857628	1
11	102	1	15	1151343868800	1
11	512	2	15	1151343875972	1
11	420	3	30	1151343884425	1
11	617	1	10	1151343890785	1

ID	TR	TECH	DIFF	TIME	RESP
11	206	1	15	1151343899050	1
11	617	4	10	1151343911160	1
11	123	2	20	1151343922253	1
11	109	1	10	1151343928722	1
11	325	1	15	1151343940378	1
11	113	3	10	1151343947628	1
11	109	3	10	1151343954050	1
11	512	3	15	1151343971363	1
11	304	3	20	1151343983378	0
11	225	1	30	1151343989941	0
11	420	4	30	1151344003925	1
11	109	2	10	1151344010175	1
11	609	2	20	1151344026394	1
11	609	3	20	1151344032675	1
11	512	1	15	1151344045191	1
11	409	5	10	1151344062160	0
11	609	1	20	1151344074816	1
11	604	3	20	1151344084035	1
11	506	4	25	1151344097722	1
11	314	4	30	1151344136816	1
11	314	1	30	1151344144269	0
11	409	4	10	1151344162097	1
11	122	4	15	1151344172082	1
11	420	1	30	1151344176613	1
11	116	2	20	1151344187441	0
11	124	4	30	1151344195566	1
11	206	4	15	1151344208847	1
11	206	3	15	1151344219488	1
11	604	2	20	1151344225269	1
11	400	5	25	1151344231847	1
11	124	2	30	1151344241175	1
11	210	1	10	1151344255035	0
11	505	2	25	1151344266722	1
11	102	3	15	1151344287910	0
11	314	5	30	1151344299566	1
11	409	2	10	1151344320628	1
11	503	4	25	1151344327378	1
11	506	1	25	1151344332425	1
11	619	3	30	1151344345300	1
11	123	1	20	1151344356832	0
11	122	1	15	1151344365394	1
11	325	2	15	1151344377722	0
11	503	3	25	1151344384332	1
11	505	1	25	1151344400347	0
11	617	2	10	1151344405628	1
11	206	5	15	1151344414394	1
11	304	1	20	1151344420066	1
11	225	4	30	1151344430628	1
11	506	3	25	1151344438191	1
11	619	2	30	1151344450488	1
11	510	3	25	1151344457785	1
11	503	2	25	1151344472675	0
11	124	3	30	1151344484410	1
11	604	5	20	1151344520003	1
11	505	3	25	1151344538363	1
11	505	5	25	1151344550332	1
11	102	2	15	1151344560988	1
11	400	1	25	1151344567019	0
11	420	2	30	1151344576019	1
11	304	5	20	1151344588722	1
11	325	4	15	1151344606332	1
11	400	2	25	1151344612738	1
11	314	3	30	1151344642832	1
11	617	5	10	1151344650300	1
11	225	5	30	1151344661972	1
11	619	5	30	1151344671613	1
11	409	3	10	1151344701816	0
11	116	3	20	1151344710582	1
11	325	5	15	1151344715785	1
11	116	1	20	1151344719691	1
11	604	1	20	1151344726191	0
11	505	4	25	1151344732003	1
11	122	2	15	1151344740816	1
11	102	4	15	1151344747535	0
11	609	4	20	1151344756378	0
11	510	2	25	1151344771050	1
11	512	4	15	1151344786566	1

ID	TR	TECH	DIFF	TIME	RESP
11	506	2	25	1151344795394	0
11	503	5	25	1151344808847	1
14	210	2	10	1151351339050	1
14	225	3	30	1151351404097	1
14	116	1	20	1151351504941	1
14	510	3	25	1151351549410	0
14	409	5	10	1151351670472	1
14	510	5	25	1151351725566	1
14	619	4	30	1151351777894	1
14	604	2	20	1151351836144	1
14	109	1	10	1151351877800	1
14	617	3	10	1151351953769	1
14	609	4	20	1151352035753	0
14	506	2	25	1151352046941	1
14	619	5	30	1151352074519	1
14	102	4	15	1151352205753	0
14	619	1	30	1151352212128	1
14	325	2	15	1151352250457	1
14	604	4	20	1151352286800	1
14	206	2	15	1151352296691	0
14	206	3	15	1151352312535	0
14	604	5	20	1151352335300	1
14	512	4	15	1151352349441	0
14	123	3	20	1151352375753	1
14	122	5	15	1151352388253	0
14	325	1	15	1151352418441	0
14	109	4	10	1151352430253	1
14	505	2	25	1151352439316	0
14	617	5	10	1151352451503	1
14	124	2	30	1151352464644	1
14	325	5	15	1151352477410	1
14	210	5	10	1151352488832	1
14	619	3	30	1151352522175	1
14	116	5	20	1151352552566	1
14	506	1	25	1151352585910	0
14	512	1	15	1151352592066	1
14	225	1	30	1151352614972	0
14	512	2	15	1151352627941	1
14	420	1	30	1151352637363	0
14	400	1	25	1151352658800	0
14	505	3	25	1151352673457	0
14	113	2	10	1151352688707	0
14	604	1	20	1151352721582	1
14	113	5	10	1151352737175	0
14	304	4	20	1151352748910	1
14	505	5	25	1151352767582	0
14	123	1	20	1151352789347	0
14	400	5	25	1151352810566	1
14	206	1	15	1151352839628	0
14	409	4	10	1151352862347	0
14	304	3	20	1151352890332	0
14	116	3	20	1151352903253	0
14	420	3	30	1151352913847	0
14	314	4	30	1151352931644	1
14	420	2	30	1151352963644	0
14	503	3	25	1151353035144	0
14	314	3	30	1151353053785	1
14	617	1	10	1151353073785	0
14	304	1	20	1151353098238	0
14	113	3	10	1151353127816	1
14	109	3	10	1151353137613	1
14	609	2	20	1151353166378	1
14	314	1	30	1151353195644	1
14	510	4	25	1151353218050	1
14	420	5	30	1151353238675	0
14	102	3	15	1151353244050	0
14	604	3	20	1151353254582	1
14	124	4	30	1151353265910	1
14	102	2	15	1151353288566	1
14	510	2	25	1151353306269	1
14	409	3	10	1151353313457	1
14	206	4	15	1151353338269	1
14	124	5	30	1151353364144	1
14	505	4	25	1151353380113	1
14	510	1	25	1151353402675	0
14	116	4	20	1151353432457	1
14	512	3	15	1151353473175	1

ID	TR	TECH	DIFF	TIME	RESP
14	400	4	25	1151353498878	0
14	609	1	20	1151353517207	1
14	102	5	15	1151353542878	0
14	512	5	15	1151353572972	0
14	124	3	30	1151353592378	1
14	122	3	15	1151353614050	1
14	609	5	20	1151353638847	1
14	304	2	20	1151353650628	1
14	503	2	25	1151353707175	0
14	304	5	20	1151353762066	0
14	123	5	20	1151353807285	1
14	122	4	15	1151353823207	0
14	109	5	10	1151353966738	1
14	617	4	10	1151353978910	1
14	206	5	15	1151354006316	0
14	124	1	30	1151354011175	0
14	225	2	30	1151354028207	0
14	325	3	15	1151354051519	0
14	503	5	25	1151354070613	1
14	400	2	25	1151354081847	0
14	225	4	30	1151354086472	1
14	505	1	25	1151354095160	1
14	122	2	15	1151354105832	0
14	506	4	25	1151354136378	1
14	225	5	30	1151354154207	1
14	506	5	25	1151354170441	0
14	123	4	20	1151354189675	1
14	420	4	30	1151354201316	1
14	503	1	25	1151354212128	1
14	210	3	10	1151354234488	1
14	210	4	10	1151354250347	1
14	102	1	15	1151354260019	0
14	506	3	25	1151354287660	1
14	619	2	30	1151354302550	0
14	314	5	30	1151354318503	0
14	609	3	20	1151354337113	0
14	123	2	20	1151354350222	0
14	314	2	30	1151354360566	0
14	210	1	10	1151354395128	0
14	116	2	20	1151354405332	1
14	400	3	25	1151354417675	1
14	122	1	15	1151354461519	1
14	113	1	10	1151354467660	1
14	503	4	25	1151354486019	1
14	617	2	10	1151354494160	1
14	325	4	15	1151354510378	0
14	409	1	10	1151354527582	0
14	113	4	10	1151354552707	0
14	109	2	10	1151354562175	0
14	409	2	10	1151354591285	1
16	409	4	10	1151358939628	0
16	409	3	10	1151358963128	0
16	124	3	30	1151358968144	1
16	503	3	25	1151358975644	1
16	206	4	15	1151358984753	1
16	619	5	30	1151358994082	1
16	123	4	20	1151359006457	0
16	409	2	10	1151359012988	0
16	409	5	10	1151359024035	0
16	122	2	15	1151359030253	1
16	206	2	15	1151359038082	0
16	304	5	20	1151359048894	0
16	225	3	30	1151359057441	1
16	116	5	20	1151359063988	1
16	113	1	10	1151359071597	1
16	113	4	10	1151359076753	1
16	314	2	30	1151359086082	1
16	617	2	10	1151359100128	1
16	609	1	20	1151359105519	1
16	210	2	10	1151359114253	1
16	420	1	30	1151359120082	0
16	102	3	15	1151359127660	1
16	102	4	15	1151359173144	0
16	109	3	10	1151359182222	1
16	609	3	20	1151359197035	0
16	505	2	25	1151359201519	1
16	400	5	25	1151359210394	1

ID	TR	TECH	DIFF	TIME	RESP
16	304	3	20	1151359218503	0
16	510	2	25	1151359228128	0
16	225	1	30	1151359234441	0
16	124	4	30	1151359240910	0
16	503	5	25	1151359249300	1
16	512	4	15	1151359257472	1
16	109	4	10	1151359268003	0
16	314	1	30	1151359278363	1
16	314	5	30	1151359287316	1
16	400	2	25	1151359291847	0
16	123	1	20	1151359299019	1
16	619	2	30	1151359307660	1
16	102	5	15	1151359321613	1
16	505	3	25	1151359340316	1
16	325	2	15	1151359349847	1
16	609	5	20	1151359387503	1
16	506	2	25	1151359393285	0
16	109	1	10	1151359399410	1
16	124	2	30	1151359409097	0
16	109	5	10	1151359430785	1
16	304	4	20	1151359455160	1
16	619	4	30	1151359462628	1
16	314	4	30	1151359475910	1
16	225	5	30	1151359484738	1
16	123	2	20	1151359489441	1
16	510	5	25	1151359501613	1
16	512	3	15	1151359514394	1
16	325	4	15	1151359521847	1
16	506	4	25	1151359534316	0
16	400	1	25	1151359540503	1
16	116	1	20	1151359549972	1
16	304	2	20	1151359555035	0
16	122	4	15	1151359560675	1
16	109	2	10	1151359573300	1
16	409	1	10	1151359580222	0
16	400	3	25	1151359586769	1
16	505	1	25	1151359595019	0
16	619	1	30	1151359609769	0
16	210	4	10	1151359622222	0
16	604	5	20	1151359634316	1
16	506	1	25	1151359642566	1
16	102	1	15	1151359646785	1
16	420	2	30	1151359653988	0
16	304	1	20	1151359662113	1
16	116	3	20	1151359669925	1
16	512	5	15	1151359677535	1
16	225	4	30	1151359684222	1
16	510	4	25	1151359692097	0
16	617	1	10	1151359697128	1
16	113	3	10	1151359701894	1
16	609	2	20	1151359706410	1
16	122	5	15	1151359713019	1
16	617	4	10	1151359720628	1
16	113	5	10	1151359728816	1
16	210	3	10	1151359733222	0
16	512	1	15	1151359738519	1
16	506	3	25	1151359746425	0
16	510	3	25	1151359944769	1
16	325	5	15	1151359951160	1
16	619	3	30	1151359958644	1
16	325	3	15	1151359965675	1
16	124	5	30	1151359987050	1
16	325	1	15	1151359992394	1
16	506	5	25	1151359999644	0
16	420	4	30	1151360014972	0
16	604	1	20	1151360019347	1
16	210	5	10	1151360025285	1
16	420	5	30	1151360031753	1
16	124	1	30	1151360036332	1
16	503	2	25	1151360042222	0
16	314	3	30	1151360049863	1
16	505	5	25	1151360057300	1
16	116	4	20	1151360070800	0
16	116	2	20	1151360083769	1
16	420	3	30	1151360099347	1
16	503	4	25	1151360109613	1
16	617	3	10	1151360114988	1

ID	TR	TECH	DIFF	TIME	RESP
16	617	5	10	1151360123457	1
16	503	1	25	1151360127738	1
16	210	1	10	1151360131394	0
16	225	2	30	1151360141738	1
16	505	4	25	1151360153425	0
16	206	3	15	1151360163285	0
16	123	5	20	1151360171394	1
16	400	4	25	1151360177316	1
16	206	5	15	1151360184957	0
16	604	4	20	1151360191441	1
16	206	1	15	1151360198019	1
16	122	3	15	1151360209097	1
16	512	2	15	1151360213175	1
16	510	1	25	1151360219628	1
16	113	2	10	1151360225832	1
16	604	2	20	1151360230175	1
16	604	3	20	1151360243472	1
16	609	4	20	1151360252347	1
16	102	2	15	1151360262691	1
16	123	3	20	1151360270128	0
16	122	1	15	1151360275238	0
21	102	5	15	1151420918259	1
21	122	3	15	1151420923962	1
21	409	5	10	1151420936712	1
21	619	4	30	1151420948962	1
21	505	3	25	1151420961462	1
21	420	1	30	1151420970025	0
21	617	1	10	1151420986994	1
21	314	3	30	1151421005822	1
21	506	5	25	1151421026087	1
21	409	4	10	1151421032869	1
21	400	5	25	1151421042306	1
21	206	2	15	1151421071697	1
21	113	1	10	1151421120916	1
21	116	1	20	1151421145103	0
21	314	4	30	1151421179431	0
21	512	3	15	1151421192072	1
21	505	1	25	1151421204541	1
21	510	2	25	1151421225947	1
21	124	4	30	1151421237541	0
21	210	4	10	1151421248806	1
21	325	5	15	1151421273322	1
21	409	1	10	1151421316744	0
21	609	5	20	1151421331931	0
21	124	1	30	1151421374462	0
21	206	1	15	1151421403978	0
21	102	2	15	1151421433259	1
21	512	4	15	1151421456291	0
21	116	5	20	1151421485837	0
21	512	5	15	1151421496587	1
21	109	4	10	1151421505384	0
21	210	3	10	1151421528181	1
21	109	3	10	1151421538416	1
21	122	5	15	1151421555994	1
21	506	1	25	1151421583462	0
21	225	1	30	1151421595619	1
21	122	2	15	1151421611572	1
21	506	4	25	1151421634322	0
21	123	5	20	1151421668634	0
21	304	4	20	1151421683697	1
21	123	3	20	1151421725853	1
21	113	4	10	1151421753697	1
21	113	2	10	1151421785541	1
21	124	3	30	1151421822837	1
21	210	1	10	1151421844275	0
21	510	4	25	1151421858603	1
21	604	2	20	1151421873744	1
21	609	3	20	1151421887869	1
21	503	1	25	1151421895556	1
21	116	2	20	1151421916853	0
21	617	3	10	1151421931150	1
21	503	4	25	1151421941462	1
21	109	1	10	1151421946822	1
21	619	3	30	1151421961166	1
21	210	2	10	1151421990650	0
21	510	5	25	1151422010681	1
21	400	4	25	1151422017478	1

ID	TR	TECH	DIFF	TIME	RESP
21	314	1	30	1151422036150	1
21	116	4	20	1151422073275	1
21	304	1	20	1151422087947	0
21	409	3	10	1151422107619	1
21	304	2	20	1151422136353	0
21	409	2	10	1151422171556	0
21	609	4	20	1151422205900	1
21	225	3	30	1151422219306	1
21	109	2	10	1151422238525	0
21	420	5	30	1151422264462	1
21	109	5	10	1151422277416	1
21	325	1	15	1151422291291	1
21	604	1	20	1151422302525	1
21	314	2	30	1151422313619	1
21	102	1	15	1151422323775	0
21	510	3	25	1151422363369	1
21	617	5	10	1151422374978	1
21	304	5	20	1151422401212	1
21	503	2	25	1151422430759	0
21	206	4	15	1151422471494	1
21	123	4	20	1151422488306	1
21	225	5	30	1151422522384	1
21	102	3	15	1151422534212	0
21	617	2	10	1151422578916	1
21	420	3	30	1151422601931	1
21	503	3	25	1151422615869	1
21	619	1	30	1151422667228	0
21	225	2	30	1151422681853	1
21	304	3	20	1151422694759	0
21	400	2	25	1151422709228	1
21	325	3	15	1151422728447	0
21	325	4	15	1151422748853	0
21	314	5	30	1151422762650	1
21	113	5	10	1151422780228	1
21	123	1	20	1151422800947	0
21	122	4	15	1151422827181	1
21	400	1	25	1151422837478	1
21	124	2	30	1151422892369	1
21	420	2	30	1151422905869	1
21	604	4	20	1151422934759	1
21	619	5	30	1151422947916	1
21	619	2	30	1151422965009	1
21	206	3	15	1151422999197	1
21	420	4	30	1151423007837	1
21	510	1	25	1151423020869	1
21	604	3	20	1151423029603	1
21	102	4	15	1151423045556	0
21	113	3	10	1151423063587	1
21	505	5	25	1151423078634	1
21	512	1	15	1151423084619	1
21	206	5	15	1151423111728	1
21	604	5	20	1151423123119	1
21	325	2	15	1151423151775	0
21	123	2	20	1151423160166	1
21	512	2	15	1151423171806	1
21	116	3	20	1151423219431	0
21	506	2	25	1151423236634	0
21	506	3	25	1151423265212	1
21	225	4	30	1151423287494	1
21	210	5	10	1151423301447	1
21	124	5	30	1151423328462	1
21	400	3	25	1151423340275	1
21	609	1	20	1151423345947	1
21	505	4	25	1151423360978	1
21	503	5	25	1151423385900	1
21	617	4	10	1151423391447	1
21	505	2	25	1151423405712	1
21	122	1	15	1151423417275	1
21	609	2	20	1151423432572	1

Table A.6: Participant responses from User Study 3.3

ID	TR	TECH	TIME	RESP
90	24	4	1151284164958	1
90	45	3	1151284169630	1
90	40	3	1151284191489	1
90	45	5	1151284195802	1
90	35	2	1151284200567	1
90	24	5	1151284224474	1
90	24	2	1151284236864	1
90	24	1	1151284250317	0
90	42	5	1151284254552	1
90	40	5	1151284262770	1
90	34	3	1151284267161	1
90	32	1	1151284282833	1
90	52	3	1151284286989	1
90	52	2	1151284296849	1
90	52	1	1151284308817	0
90	32	3	1151284315474	1
90	42	4	1151284321255	1
90	32	2	1151284326270	1
90	03	5	1151284330989	1
90	40	5	1151284335864	1
90	24	4	1151284355208	1
90	03	4	1151284368020	1
90	24	3	1151284375614	1
90	34	1	1151284388661	0
90	50	3	1151284395817	1
90	32	4	1151284401442	1
90	35	3	1151284405239	1
90	03	1	1151284422520	1
90	52	2	1151284426130	1
90	32	4	1151284430208	0
90	50	4	1151284439333	1
90	40	4	1151284445067	1
90	40	3	1151284448927	1
90	32	3	1151284452692	1
90	50	2	1151284455911	1
90	32	2	1151284458880	1
90	50	1	1151284463333	0
90	45	2	1151284466395	1
90	14	2	1151284469427	1
90	52	3	1151284474020	1
90	05	5	1151284476974	1
90	50	4	1151284480349	1
90	24	2	1151284490880	1
90	14	4	1151284494177	1
90	14	1	1151284499458	1
90	50	2	1151284504474	1
90	31	1	1151284507442	1
90	42	2	1151284511208	1
90	03	2	1151284514583	1
90	53	3	1151284518442	1
90	45	4	1151284521442	1
90	40	1	1151284528645	1
90	42	3	1151284531724	1
90	05	4	1151284534489	1
90	14	5	1151284538020	1
90	32	1	1151284543833	1
90	50	5	1151284549067	1
90	52	5	1151284552427	1
90	24	5	1151284557130	1
90	53	2	1151284560395	1
90	52	1	1151284565739	1
90	31	5	1151284568536	1
90	32	5	1151284574505	1
90	52	4	1151284580442	1
90	32	5	1151284582849	1
90	03	2	1151284586817	1
90	50	5	1151284590958	1
90	45	1	1151284593708	1
90	32	1	1151284601145	0
90	50	3	1151284603864	1
90	50	3	1151284606630	1
90	14	3	1151284608755	1
90	35	5	1151284611599	1
90	05	1	1151284613958	1
90	03	3	1151284617474	1
90	14	4	1151284620270	1
90	52	4	1151284623724	1
90	52	4	1151284626567	1
90	34	5	1151284629520	1
90	32	2	1151284635427	1
90	24	4	1151284645864	1
90	50	1	1151284656224	1
90	24	3	1151284662630	1
90	03	1	1151284664864	1
90	40	2	1151284670052	1
90	05	3	1151284672583	1
90	52	5	1151284674286	1
90	32	4	1151284679474	1
90	24	2	1151284683364	1
90	40	1	1151284690083	1
90	35	1	1151284693974	1
90	31	4	1151284696442	1
90	14	2	1151284699489	1
90	53	1	1151284710083	1
90	03	3	1151284713114	1
90	52	3	1151284715880	1
90	40	4	1151284734083	1
90	14	1	1151284737817	1
90	32	3	1151284740724	1
90	03	5	1151284743724	1
90	50	2	1151284746099	1
90	52	2	1151284749208	1
90	14	3	1151284751927	1
90	35	4	1151284754442	1
90	32	5	1151284760067	1
90	34	2	1151284764552	1
90	52	1	1151284773145	1
90	05	2	1151284775724	1
90	40	2	1151284779427	1
90	24	1	1151284786724	1
90	03	4	1151284790505	1
90	34	4	1151284795739	1
90	53	4	1151284799708	1
90	42	1	1151284803286	1
90	31	3	1151284805614	1
90	24	1	1151284813614	1
90	14	5	1151284815864	1
90	50	5	1151284818474	1
90	52	5	1151284823536	1
90	50	1	1151284825770	1
90	31	2	1151284827770	1
90	50	4	1151284832942	1
90	24	5	1151284837255	1
90	53	5	1151284839974	1
90	24	3	1151284842958	1
0	03	2	1150922415758	1
0	45	4	1150922417898	1
0	42	5	1150922420133	1
0	45	1	1150922422101	1
0	52	4	1150922423914	1
0	03	1	1150922428226	1
0	45	2	1150922430117	1
0	34	4	1150922432836	1
0	24	4	1150922439117	1
0	05	4	1150922441430	1
0	50	1	1150922447945	1
0	40	2	1150922450711	1
0	50	3	1150922456008	1
0	24	3	1150922459164	1
0	32	2	1150922461492	1
0	42	2	1150922464180	1
0	24	4	1150922467289	1
0	03	5	1150922470211	1
0	52	3	1150922472476	1
0	52	3	1150922474711	1
0	50	1	1150922481101	1
0	14	1	1150922484305	0
0	52	5	1150922487492	1
0	32	4	1150922490476	1
0	40	3	1150922493398	1
0	40	4	1150922498914	1

ID	TR	TECH	TIME	RESP
0	52	4	1150922501445	1
0	35	2	1150922503430	1
0	52	1	1150922506789	1
0	50	5	1150922510445	1
0	52	2	1150922512305	1
0	14	3	1150922514414	1
0	32	4	1150922516758	1
0	50	2	1150922519133	1
0	34	5	1150922522101	1
0	24	1	1150922528336	0
0	14	5	1150922534508	1
0	42	1	1150922537633	1
0	35	1	1150922541242	1
0	32	2	1150922547180	0
0	31	1	1150922549945	1
0	35	4	1150922553039	1
0	34	2	1150922556539	1
0	32	1	1150922558898	0
0	14	3	1150922560883	1
0	53	4	1150922562570	1
0	24	2	1150922564461	1
0	03	4	1150922566398	1
0	32	3	1150922568758	1
0	05	2	1150922570633	1
0	32	1	1150922572648	1
0	24	5	1150922575008	1
0	14	5	1150922581180	1
0	35	3	1150922583492	1
0	40	3	1150922586336	1
0	52	1	1150922588570	0
0	34	1	1150922597430	1
0	52	2	1150922600383	1
0	52	3	1150922602336	1
0	52	5	1150922604461	1
0	24	1	1150922607289	0
0	50	1	1150922610930	1
0	14	4	1150922613039	1
0	53	3	1150922615289	1
0	50	2	1150922624226	1
0	40	1	1150922626726	1
0	24	1	1150922629851	0
0	34	3	1150922632023	1
0	32	4	1150922634226	1
0	03	3	1150922636086	1
0	52	4	1150922638351	1
0	14	2	1150922640570	1
0	05	3	1150922642992	1
0	32	2	1150922645414	1
0	53	1	1150922647867	1
0	24	5	1150922674195	1
0	03	3	1150922676508	1
0	50	4	1150922679055	1
0	32	1	1150922681320	1
0	50	4	1150922684539	1
0	50	5	1150922688008	1
0	53	5	1150922689976	1
0	50	4	1150922692789	1
0	32	3	1150922695851	1
0	42	3	1150922699726	1
0	31	2	1150922701851	1
0	03	2	1150922704133	1
0	32	5	1150922706445	0
0	50	5	1150922709055	1
0	40	1	1150922711242	1
0	50	2	1150922713305	1
0	14	2	1150922715289	1
0	40	5	1150922716914	1
0	52	2	1150922719023	1
0	52	5	1150922721336	1
0	32	5	1150922723336	1
0	50	3	1150922725961	1
0	40	4	1150922728523	1
0	45	3	1150922730523	0
0	32	3	1150922732898	1
0	40	2	1150922734992	1
0	03	1	1150922737383	1
0	05	1	1150922739242	1

ID	TR	TECH	TIME	RESP
0	03	4	1150922745586	1
0	40	5	1150922747867	1
0	14	4	1150922750320	1
0	31	4	1150922752320	1
0	05	5	1150922754601	1
0	24	4	1150922762305	1
0	24	3	1150922764930	1
0	24	5	1150922768055	1
0	42	4	1150922770101	1
0	03	5	1150922774055	1
0	31	3	1150922776180	1
0	53	2	1150922778383	1
0	14	1	1150922781726	1
0	24	3	1150922785351	1
0	50	3	1150922788367	1
0	31	5	1150922790711	1
0	32	5	1150922801570	1
0	52	1	1150922803898	1
0	24	2	1150922806836	1
0	35	5	1150922809320	1
0	24	2	1150922812039	1
0	45	5	1150922814992	1
2	52	4	1151074793969	1
2	24	1	1151074800359	1
2	05	1	1151074804500	1
2	53	3	1151074809328	1
2	05	5	1151074816250	1
2	03	5	1151074825578	1
2	35	5	1151074829640	1
2	53	4	1151074834047	1
2	50	5	1151074839546	1
2	40	2	1151074846265	1
2	03	4	1151074863702	1
2	40	5	1151074869405	1
2	24	2	1151074880374	1
2	50	1	1151074884546	1
2	31	3	1151074888218	1
2	32	3	1151074891827	1
2	03	3	1151074895640	1
2	45	5	1151074899811	1
2	52	1	1151074906764	0
2	32	4	1151074912639	1
2	03	3	1151074915905	1
2	50	2	1151074920389	1
2	35	4	1151074934795	1
2	32	1	1151074941451	1
2	50	4	1151074946170	1
2	40	2	1151074957295	1
2	24	4	1151074964936	1
2	42	3	1151074968529	1
2	45	4	1151074974014	1
2	40	3	1151074979185	1
2	14	4	1151074987841	1
2	32	3	1151074991138	1
2	53	2	1151074994216	1
2	50	5	1151074996826	1
2	40	4	1151075006247	1
2	05	4	1151075009669	1
2	35	3	1151075012372	1
2	24	3	1151075026138	1
2	34	2	1151075033466	1
2	42	2	1151075036685	1
2	45	1	1151075040497	1
2	24	2	1151075046481	1
2	14	4	1151075052138	1
2	50	5	1151075056684	1
2	05	3	1151075060637	1
2	32	4	1151075064075	1
2	32	1	1151075069590	0
2	24	4	1151075076278	0
2	50	2	1151075078872	1
2	31	5	1151075081590	1
2	34	5	1151075095996	1
2	34	4	1151075102309	0
2	24	1	1151075106574	1
2	31	4	1151075110684	1
2	45	2	1151075113434	1

ID	TR	TECH	TIME	RESP
2	52	2	1151075115824	1
2	34	3	1151075119824	1
2	50	3	1151075122762	1
2	14	1	1151075126496	1
2	52	5	1151075129965	1
2	52	1	1151075134136	1
2	52	3	1151075137699	1
2	24	5	1151075143214	1
2	50	4	1151075150136	0
2	52	4	1151075153792	1
2	03	2	1151075157371	1
2	31	2	1151075159636	1
2	32	5	1151075164120	1
2	03	2	1151075166730	1
2	24	4	1151075187058	0
2	32	1	1151075190667	0
2	24	5	1151075195245	1
2	50	1	1151075199183	0
2	32	2	1151075202151	1
2	35	1	1151075206386	1
2	50	2	1151075209495	1
2	52	3	1151075214260	1
2	03	1	1151075217370	1
2	03	4	1151075221135	1
2	32	5	1151075224667	1
2	50	1	1151075228354	1
2	52	5	1151075233995	1
2	24	2	1151075237307	1
2	50	3	1151075240744	1
2	42	4	1151075250010	1
2	52	2	1151075254119	1
2	34	1	1151075260838	0
2	52	5	1151075265572	1
2	50	4	1151075270150	1
2	05	2	1151075273463	1
2	52	4	1151075276541	1
2	24	3	1151075280103	1
2	14	5	1151075283947	1
2	14	2	1151075286056	1
2	03	5	1151075289369	1
2	45	3	1151075291353	1
2	24	1	1151075294666	1
2	14	2	1151075297806	1
2	40	1	1151075301369	1
2	52	1	1151075305291	1
2	32	2	1151075309462	1
2	24	3	1151075314962	1
2	42	1	1151075320556	1
2	14	5	1151075324650	1
2	32	2	1151075327165	1
2	32	3	1151075330009	1
2	31	1	1151075333056	1
2	24	5	1151075341196	1
2	53	1	1151075345259	1
2	32	5	1151075349040	1
2	50	3	1151075352243	1
2	40	4	1151075363227	1
2	03	1	1151075370196	1
2	32	4	1151075373868	1
2	42	5	1151075378149	1
2	40	1	1151075380461	1
2	14	3	1151075383071	1
2	53	5	1151075386133	1
2	40	5	1151075388852	1
2	14	1	1151075393602	0
2	35	2	1151075396477	1
2	40	3	1151075399196	1
2	14	3	1151075402039	1
2	52	3	1151075405321	1
2	52	2	1151075408320	1
22	03	1	1151424020759	1
22	34	2	1151424031728	0
22	05	5	1151424042666	1
22	52	3	1151424052056	1
22	14	5	1151424056541	1
22	42	2	1151424072416	1
22	03	1	1151424083900	0

ID	TR	TECH	TIME	RESP
22	53	2	1151424098884	1
22	14	3	1151424101603	1
22	52	5	1151424104806	1
22	45	4	1151424120337	0
22	32	2	1151424127306	1
22	40	3	1151424131900	1
22	24	2	1151424138900	1
22	50	5	1151424144197	1
22	40	1	1151424158869	1
22	03	2	1151424164275	1
22	24	1	1151424171994	1
22	32	4	1151424178134	1
22	24	3	1151424189056	0
22	35	2	1151424197181	1
22	50	1	1151424213697	1
22	50	5	1151424217275	1
22	40	5	1151424221525	1
22	14	1	1151424325275	0
22	53	3	1151424332556	1
22	50	1	1151424345587	1
22	31	3	1151424349884	1
22	52	4	1151424370212	1
22	32	3	1151424375541	1
22	24	4	1151424384931	1
22	32	4	1151424391650	1
22	34	4	1151424406306	0
22	32	1	1151424425337	1
22	24	3	1151424432509	1
22	31	1	1151424439166	1
22	03	3	1151424446900	1
22	32	5	1151424450869	1
22	52	1	1151424458869	1
22	50	3	1151424467353	1
22	03	4	1151424478822	1
22	31	4	1151424482603	1
22	42	1	1151424491119	1
22	24	4	1151424508978	1
22	50	2	1151424513462	1
22	53	1	1151424526900	1
22	35	3	1151424535306	1
22	45	5	1151424539134	1
22	52	1	1151424543416	1
22	52	3	1151424549259	1
22	50	3	1151424552353	1
22	40	4	1151424586384	1
22	24	5	1151424596259	1
22	52	2	1151424598681	1
22	52	5	1151424600978	1
22	52	1	1151424615150	0
22	14	1	1151424632759	1
22	05	4	1151424637166	1
22	31	5	1151424640056	1
22	50	4	1151424643556	1
22	31	2	1151424646134	1
22	14	2	1151424648322	1
22	45	3	1151424651603	1
22	03	2	1151424655791	1
22	52	2	1151424659525	1
22	14	2	1151424662119	1
22	34	3	1151424687462	1
22	32	3	1151424691400	1
22	35	1	1151424696119	1
22	34	5	1151424708384	1
22	45	2	1151424715087	1
22	52	5	1151424718853	1
22	32	5	1151424722587	1
22	24	2	1151424725712	1
22	14	5	1151424728056	1
22	32	4	1151424730728	1
22	32	1	1151424751072	1
22	53	5	1151424756119	1
22	50	1	1151424761447	1
22	42	4	1151424766384	1
22	52	4	1151424771400	1
22	03	5	1151424773791	1
22	24	5	1151424778634	1
22	05	1	1151424783962	1

ID	TR	TECH	TIME	RESP
22	14	4	1151424789181	1
22	14	3	1151424793400	1
22	24	3	1151424799056	1
22	24	2	1151424803166	1
22	40	4	1151424806587	0
22	03	4	1151424811119	1
22	40	2	1151424818369	1
22	42	3	1151424820291	1
22	50	4	1151424822197	1
22	32	3	1151424825478	1
22	32	2	1151424831962	1
22	50	2	1151424835306	1
22	40	3	1151424838509	1
22	05	2	1151424841369	1
22	24	4	1151424863619	0
22	32	5	1151424871447	1
22	40	2	1151424873494	1
22	24	5	1151424875697	1
22	32	1	1151424879306	1
22	50	5	1151424882197	1
22	40	5	1151424885931	1
22	42	5	1151424888791	1
22	24	1	1151424895869	1
22	52	3	1151424899478	1
22	50	4	1151424906884	1
22	50	2	1151424915462	1
22	53	4	1151424935150	1
22	32	2	1151424938400	1
22	24	1	1151424946525	1
22	50	3	1151424951009	1
22	34	1	1151424977337	0
22	05	3	1151424982603	1
22	45	1	1151424985056	1
22	40	1	1151424986869	1
22	14	4	1151424988994	1
22	03	3	1151424991587	1
22	52	2	1151424995181	1
22	35	5	1151425000212	1
22	52	4	1151425006431	1
22	03	5	1151425009978	1
22	35	4	1151425013291	0
95	31	3	1151369860176	1
95	31	1	1151369863035	1
95	32	2	1151369868801	1
95	24	4	1151369887707	1
95	40	2	1151369893817	1
95	14	2	1151369897082	1
95	32	3	1151369901395	1
95	34	3	1151369907192	1
95	14	1	1151369915676	1
95	45	2	1151369919129	1
95	24	2	1151369924348	1
95	34	5	1151369928660	1
95	05	2	1151369932379	1
95	24	2	1151369941176	1
95	45	5	1151369945254	1
95	40	5	1151369956035	1
95	32	1	1151369964113	0
95	50	4	1151369970707	1
95	03	5	1151369974301	1
95	52	3	1151369977895	1
95	34	2	1151369982910	1
95	42	2	1151369985817	1
95	14	3	1151369990770	1
95	14	3	1151369993988	1
95	31	2	1151369997754	1
95	24	4	1151370032129	1
95	50	1	1151370036410	1
95	40	1	1151370042926	1
95	24	1	1151370050629	1
95	52	2	1151370053817	1
95	50	2	1151370057613	1
95	52	4	1151370063973	1
95	42	1	1151370069488	1
95	34	4	1151370075879	0
95	50	3	1151370081770	1
95	50	5	1151370085567	1

ID	TR	TECH	TIME	RESP
95	50	5	1151370088848	1
95	53	5	1151370094817	1
95	32	1	1151370099598	1
95	40	1	1151370108832	1
95	24	5	1151370114270	1
95	32	2	1151370118410	1
95	31	5	1151370124410	1
95	03	1	1151370134442	1
95	45	3	1151370138317	1
95	03	3	1151370141442	1
95	14	1	1151370145176	1
95	52	2	1151370149067	1
95	42	4	1151370155895	1
95	35	4	1151370158988	1
95	40	5	1151370162910	1
95	42	3	1151370166426	1
95	52	1	1151370170488	1
95	45	4	1151370174535	1
95	40	4	1151370181317	1
95	35	1	1151370185348	1
95	03	3	1151370189301	1
95	24	1	1151370196098	1
95	32	5	1151370200942	1
95	24	5	1151370205801	1
95	32	4	1151370209301	1
95	35	2	1151370212317	1
95	35	5	1151370215848	1
95	53	1	1151370236488	1
95	03	2	1151370240395	1
95	50	3	1151370245238	1
95	52	5	1151370247942	1
95	50	5	1151370250910	1
95	50	2	1151370254379	1
95	35	3	1151370257051	1
95	14	4	1151370260317	1
95	52	4	1151370265067	1
95	32	4	1151370269676	1
95	32	1	1151370285535	1
95	32	5	1151370290160	1
95	24	2	1151370296723	1
95	32	3	1151370301582	1
95	14	5	1151370303910	1
95	03	4	1151370308910	1
95	32	3	1151370313567	1
95	50	4	1151370318723	1
95	14	2	1151370323270	1
95	24	1	1151370329629	1
95	52	4	1151370334504	1
95	24	3	1151370340113	1
95	14	5	1151370343113	1
95	52	5	1151370346957	1
95	03	1	1151370349629	1
95	50	4	1151370353285	1
95	05	5	1151370357317	1
95	24	3	1151370362582	1
95	42	5	1151370365676	1
95	52	1	1151370374848	0
95	50	2	1151370379692	1
95	32	4	1151370385676	1
95	40	3	1151370388629	1
95	50	1	1151370394223	1
95	05	3	1151370397832	1
95	24	5	1151370402395	1
95	45	1	1151370405801	1
95	52	3	1151370411910	1
95	50	1	1151370414832	1
95	32	5	1151370417660	1
95	05	1	1151370419926	1
95	52	1	1151370424473	0
95	53	2	1151370429363	1
95	34	1	1151370437160	0
95	52	2	1151370444879	1
95	05	4	1151370449129	1
95	31	4	1151370452457	0
95	32	2	1151370457270	1
95	50	3	1151370459723	1
95	03	2	1151370463301	1

ID	TR	TECH	TIME	RESP
95	03	4	1151370466051	1
95	53	4	1151370469660	1
95	24	4	1151370473270	1
95	24	3	1151370477582	1
95	52	3	1151370480520	1
95	03	5	1151370483238	1
95	14	4	1151370485051	1
95	53	3	1151370488692	1
95	40	2	1151370492801	1
95	40	4	1151370499192	0
95	40	3	1151370501660	1
95	52	5	1151370504504	1

BIBLIOGRAPHY

[ACKT96] T. Asano, D. Z. Chen, N. Katoh, and T. Tokuyama. Polynomial-time solutions to image segmentation. In *Proceedings of the 7th Annual SIAM-ACM Conference on Discrete Algorithms*, pages 104–113, 1996.

[AE98] Ulrike Axen and Herbert Edelsbrunner. Auditory morse analysis of triangulated manifolds. In Hans-Christian Hege and Konrad Polthier, editors, *Mathematical Visualization*, pages 223–236. Springer-Verlag, Heidelberg, 1998.

[Axe99] Ulrike Axen. Computing morse functions on triangulated manifolds. In *Symposium on Discrete Algorithms*, pages 850–851, 1999.

[BA05] J. Andreas Baerentzen and Member-Henrik Aanaes. Signed distance computation using the angle weighted pseudonormal. *IEEE Transactions on Visualization and Computer Graphics*, 11(3):243–253, 2005.

[BB90] A. Blake and H. Bülthoff. Does the brain know the physics of specular reflection? *Nature*, 343:165–168, 1990.

[Ben75] Jon Louis Bentley. Multidimensional binary search trees used for associative searching. *Commun. ACM*, 18(9):509–517, 1975.

[BHW05] Alethea Bair, Donald House, and Colin Ware. Perceptually optimizing textures for layered surfaces. In *APGV '05: Proceedings of the 2nd symposium on Applied perception in graphics and visualization*, pages 67–74, New York, NY, USA, 2005. ACM Press.

[BKSBL87] B. Bauer-Kirpes, W. Schlegel, R. Boesecke, and W. J. Lorenz. Display of organs and isodoses as shaded 3-d objects for 3-d therapy planning. *Int'l J. Radiation Oncology, Biology, Physics*, 13:135–140, 1987.

[Bli77] James F. Blinn. Models of light reflection for computer synthesized pictures. In *SIGGRAPH Conference Proceedings*, pages 192–198, New York, NY, USA, 1977. ACM Press.

[BQG86] G. K. Binning, C. Quate, and C. Gerber. Atomic force microscope. *Physics Review Letters*, 56:930, 1986.

[BS97] T. Barth and J. Sethian. Numerical schemes for the Hamilton-Jacobi and level set equations on triangulated domains. *J. Comp. Phys.*, 145(1), 1997.

[BVI91] Chakib Bennis, Jean-Marc Vézien, and Gérard Iglésias. Piecewise surface flattening for non-distorted texture mapping. In *SIGGRAPH Conference Procedings*, pages 237–246, New York, NY, USA, 1991. ACM Press.

[BW01] David E. Breen and Ross T. Whitaker. A level-set approach for the metamorphosis of solid models. *IEEE Transactions on Visualization and Computer Graphics*, 7(2):173–192, 2001.

[Cas01] U. Castiello. Implicit processing of shadows. *Vision Research*, 41:2305–2309, 2001.

[CJ96] William Curran and Alan Johnston. The effect of illuminant position on perceived curvature. *Vision research*, 36(10):1399–1410, 1996.

[CJP93] B. Cumming, E. Johnston, and A. Parker. Effects of different texture cues on curved surfaces viewed stereoscopically. *Vision Research*, 33(5/6):827–838, 1993.

[CK97] Chris G. Christou and Jan J. Koenderink. Light source dependence in shape from shading. *Vision research*, 37(11):1441–1449, 1997.

[CL89] P. Cavanagh and Y. Leclerc. Shape from shadows. *Journal of Experimental Psychology: Human Perception and Performance*, 15(1):3–27, 1989.

[Con83] M.L. Connolly. Solvent-accessible surfaces of proteins and nucleic acids. *Science*, 221:709–713, 1983.

[COSL98] Daniel Cohen-Or, Amira Solomovic, and David Levin. Three-dimensional distance field metamorphosis. *ACM Trans. Graph.*, 17(2):116–141, 1998.

[Des04] Mathieu Desbrun. Applied geometry: discrete differential calculus for graphics. *Comput. Graph. Forum*, 23(3), 2004.

[DHEN95] Erik De Haan, Roderik G. F. Erens, and André J. Noest. Shape from shaded random surfaces. *Vision research*, 35(21):2985–3001, 1995.

[DM06] Tony DeRose and Mark Meyer. Harmonic coordinates. In *SIGGRAPH Conference Proceedings*. ACM, 2006.

[DMA02] M. Desbrun, M. Meyer, and P. Alliez. Intrinsic parameterizations of surface meshes. In *Eurographics Conference Proceedings*, 2002.

[DPRL04a] J. Dongarra, Roldan Pozo, Karin Remington, and Andrew Lumsdaine. IML++: iterative methods library, March 2004.

[DPRL04b] J. Dongarra, Roldan Pozo, Karin Remington, and Andrew Lumsdaine. SparseLib++, March 2004.

[DRG00] M. D'Zmura, O. Rinner, and K. R. Gegenfurtner. The colors seen behind transparent filters. *Perception*, 29(8), 2000.

[DWE02] J. Diepstraten, D. Weiskopf, and T. Ertl. Transparency in interactive technical illustration. *Computer Graphics Forum*, 21(3), 2002.

[DWE03] J. Diepstraten, D. Weiskopf, and T. Ertl. Interactive cutaway illustrations. *Computer Graphics Forum*, 22(3):523–532, 2003.

[DYT05] Huong Quynh Dinh, Anthony J. Yezzi, and Greg Turk. Texture transfer during shape transformation. *ACM Trans. Graph.*, 24(2):289–310, 2005.

[EDT+95] M. Eck, T. DeRose, T.Duchamp, H. Hoppes, M. Lounsbery, and W. Stuetzle. Multiresolution analysis of arbitrary meshes. In *SIGGRAPH Conference Proceedings*, pages 173–182. ACM, 1995.

[EHP02] Jeff Erickson and Sariel Har-Peled. Optimally cutting a surface into a disk. In *Proceedings of the 18th annual Symposium on Computational Geometry*, pages 244–253, New York, NY, USA, 2002. ACM Press.

[EKK93] R. Erens, A. Kappers, and J. Koenderink. Perception of local shape from shading. *Perception and Psychphysics*, 54:145–147, 1993.

[ERC02] C. Everitt, A. Rege, and C. Cebenoyan. Hardware shadow mapping. In *SIGGRAPH Conference Proceedings*. ACM Press, 2002.

[Eve01] C. Everitt. Interactive order-independant transparency. Technical report, Nvidia, 2001.

[FJ89] P. J. Flynn and A. K. Jain. On reliable curvature estimation. In *Proceedings of the International Conference on Computer Vision and Pattern Recognition*, pages 110–116, 1989.

[FKR05] Michael S. Floater, Géza Kós, and Martin Reimers. Mean value coordinates in 3d. *Computer Aided Geometric Design*, 22(7):623–631, 2005.

[Flo97] M. Floater. Parametrization and smooth approximation of surface triangulations. *Computer Aided Geometric Design*, 14(3):231–250, 1997.

[Flo03] Michael S. Floater. Mean value coordinates. *Computer Aided Geometric Design*, 20(1):19–27, 2003.

[GD03] Philippe Guigue and Olivier Devillers. Fast and robust triangle-triangle overlap test using orientation predicates. *Journal of Graphics Tools*, 8(1):25–42, 2003.

[Ger92] Nahum D. Gershon. Visualization of fuzzy data using generalized animation. In *IEEE Visualization*, pages 268–273, 1992.

[GI04] Jack Goldfeather and Victoria Interrante. A novel cubic-order algorithm for approximating principal direction vectors. *ACM Trans. Graph.*, 23(1):45–63, 2004.

[Gib50] J. J. Gibson. *The perception of the visual world*. Houghton Mifflin, Boston, 1950.

[Gib98] Sarah F. Frisken Gibson. Using distance maps for accurate surface representation in sampled volumes. In *IEEE Symposium on Volume Visualization*, pages 23–30, 1998.

[GLM96] S. Gottschalk, M. C. Lin, and D. Manocha. Obbtree: A hierarchical structure for rapid interference detection. *Computer Graphics*, 30(Annual Conference Series):171–180, 1996.

[GMTF89] J. Goldfeather, S. Molnar, G. Turk, and H. Fuchs. Near real-time CSG rendering using tree normalization and geometric pruning. *IEEE Computer Graphics and Applications*, 9(3):20–28, 1989.

[GPRJ00] Sarah F. Frisken Gibson, Ronald N. Perry, Alyn P. Rockwood, and Thouis R. Jones. Adaptively sampled distance fields: a general representation of shape for computer graphics. In *SIGGRAPH Conference Proceedings*, pages 249–254. ACM, 2000.

[GR02] Gevorg Grigoryan and Penny Rheingans. Probabilistic surfaces: Point based primitives to show surface uncertainty. In *IEEE Visualization*, 2002.

[GR04] Gevorg Grigoryan and Penny Rheingans. Point-based probabilistic surfaces to show surface uncertainty. *IEEE Trans. Vis. Comput. Graph.*, 10(5):564–573, 2004.

[GSL+98] A. Gregory, A. State, M. Lin, D. Manocha, and M. Livingston. Feature-based surface decomposition for correspondence and morphing between polyhedra. In *Proceedings of the Computer Animation*, page 64, Washington, DC, USA, 1998. IEEE Computer Society.

[GY03] Xianfeng Gu and Shing-Tung Yau. Global conformal surface parameterization. In *Proceedings of the 2003 Eurographics/ACM SIGGRAPH Symposium on Geometry Processing*, pages 127–137, Aire-la-Ville, Switzerland, 2003. Eurographics Association.

[Hea96] Chistopher Healey. Choosing effective colours for data visualization. In *Proceedings of Visualization '96*, pages 263–270. IEEE Computer Society, 1996.

[HW02] D. House and C. Ware. A method for the perceptual optimization of complex visualizations. In *Advanced Visual Interface*, pages 148–155, 2002.

[IFP96] Victoria Interrante, Henry Fuchs, and Steven Pizer. Illustrating transparent surfaces with curvature-directed strokes. In *Proceedings of Visualization '96*, pages 211–218. IEEE Computer Society, 1996.

[IFP97] Victoria Interrante, Henry Fuchs, and Steven Pizer. Conveying the 3d shape of smoothly curving transparent surfaces via texture. *IEEE Transactions on Visualization and Computer Graphics*, 3(2):98–117, 1997.

[Int97] Victoria Interrante. Illustrating surface shape in volume data via principal direction-driven 3d line integral convolution. In *SIGGRAPH Conference Proceedings*, pages 109–116, New York, NY, USA, 1997. ACM Press/Addison-Wesley Publishing Co.

[Ish94] Shinobu Ishihara. *Ishihara tests for colour-blindness*. Kanehara Shuppan, Ltd., 1994.

[JC96] Alan Johnston and William Curran. Investigating shape-from-shading illusions using solid objects. *Vision research*, 36(18):2827–2835, 1996.

[KHSI03] Sunghee Kim, Haleh Hagh-Shenas, and Victoria Interrante. Showing shape with texture: two directions seem better than one. In *Human Vision and Electronic Imaging VIII*, pages 332–339. SPIE, 2003.

[KHSI04] S. Kim, H. Hagh-Shenas, and V. Interrante. Conveying shape with texture: experimental investigations of texture's effects on shape categorization judgments. *IEEE Transactions on Visualization and Computer Graphics*, 10(4):471–483, 2004.

[KMC97] N. G. Kanwisher, J. McDermott, and M. M. Chun. The fusiform face area: a module in human extrastriate cortex specialized for face perception. *Journal of Neuroscience*, 17(11):4302–4311, 1997.

[KMK97] D. Knill, P. Mamassian, and D. Kersten. Geometry of shadows. *Journal of the Optical Society of Ameriaca*, 14(12):3216–3232, 1997.

[Koe84] J. J. Koenderink. What does the occluding contour tell us about solid shape? *Perception*, 13:321–330, 1984.

[Koe90] J. J. Koenderink. *Solid Shape*. MIT Press, Cambridge, Massachusetts, 1990.

[KS98a] R. Kimmel and J. Sethian. Computing geodesic paths on manifolds. In *National Academy of Sciences*, volume 95, pages 8431–8435, 1998.

[KS98b] R. Kimmel and J.A. Sethian. Fast marching methods on triangulated domains. In *Proc. Nat. Acad. Sci.*, volume 95, pages 8341–8435, 1998.

[KSK00] Takashi Kanai, Hiromasa Suzuki, and Fumihiko Kimura. Metamorphosis of arbitrary triangular meshes. *IEEE Comput. Graph. Appl.*, 20(2):62–75, 2000.

[KVD95] J. J. Koenderink and A. Van Doorn. Relief: pictoral and otherwise. *Image and Vision Computing*, 13(5):321–334, 1995.

[LB00] M. S. Langer and H. H. Bülthoff. Measuring visual shape using computer graphics psychophysics. In *Proceedings of Eurographics Workshop on Rendering Techniques*, pages 1–9. Springer, 2000.

[Lev01] B. Levy. Constrained texture mapping for polygonal meshes. In *SIGGRAPH Conference Proceedings*, pages 417–424. ACM, 2001.

[LFP+90] Mark Levoy, Henry Fuchs, Stephen M. Pizer, Julian Rosenman, Edward L. Chaney, George W. Sherouse, Victoria Interrante, and Jeffrey Kiel. Volume rendering in radiation treatment planning. In *First Conference on Visualization in Biomedical Computing*. IEEE, 1990.

[LGLM00] Eric Larsen, Stefan Gottschalk, Ming C. Lin, and Dinesh Manocha. Fast distance queries with rectangular swept sphere volumes. In *ICRA*, pages 3719–3726, 2000.

[LHV04] Chang Ha Lee, Xuejun Hao, and Amitabh Varshney. Light collages: lighting design for effective visualization. In *Proceedings of the Conference on Visualization '04*, pages 281–288, Washington, DC, USA, 2004. IEEE Computer Society.

[LHV05] C. H. Lee, X. Hao, and A. Varshney. Geometry-dependent lighting. *IEEE Transactions on Visualization and Computer Graphics*, 2005.

[LPRM02] B. Levy, S. Petitjean, N. Ray, and J. Maillot. Least squares conformal maps for automatic texture atlas generation. In *SIGGRAPH Conference Proceedings*. ACM, 2002.

[LR71] B. Lee and F.M. Richards. The interpretation of protein structures: estimation of static accessibility. *Journal of Molecular Biology*, 55:379–400, 1971.

[LSPW96] Suresh K. Lodha, Bob Sheehan, Alex T. Pang, and Craig M. Wittenbrink. Visualizing geometric uncertainty of surface interpolants. In *Proceedings of Graphics Interface*, pages 238–245, 1996.

[LSS+98] Aaron W. F. Lee, Wim Sweldens, Peter Schröder, Lawrence Cowsar, and David Dobkin. MAPS: Multiresolution adaptive parameterization of surfaces. *Computer Graphics*, 32(Annual Conference Series):95–104, 1998.

[LZ00] A. Li and Q. Zaidi. Perception of three-dimensional shape from texture is based on patterns of oriented energy. *Vision Research*, 40:217–242, 2000.

[MÖ97] Tomas Möller. A fast triangle-triangle intersection test. *Journal of Graphics Tools*, 2(2):25–30, 1997.

[MDSB02] M. Meyer, M. Desbrun, P. Schroder, and A. Barr. Discrete differential geometry operators for triangulated 2-manifolds. In *VisMath*, 2002.

[Mea82] Donald Meagher. Geometric modeling using octree encoding. *Journal of Computer Graphics and Image Processing*, 19(2):129–147, 1982.

[Met74] F. Metelli. Achromatic color conditions in the perception of transparency. *Perception*, pages 95–116, 1974.

[Mil94] Gavin S. P. Miller. Efficient algorithms for local and global accessibility shading. In *SIGGRAPH Conference Proceedings*, pages 319–326. ACM Press, 1994.

[MK96] Pascal Mamassian and Daniel Kersten. Illumination, shading and the perception of local orientation. *Vision research*, 36(15):2351–2367, 1996.

[MKK98] P. Mamassian, D. Knill, and D. Kersten. The perception of cast shadows. *Trends in Cognitive Science*, 2(8):288–295, 1998.

[MLBD02] M. Meyer, H. Lee, A. Barr, and M. Desbrun. Generalized barycentric coordinates for irregular polygons. *Journal of Graphics Tools*, 7(1):13–22, 2002.

[NM00] J. D. Northrup and Lee Markosian. Artistic silhouettes: a hybrid approach. In *Proceedings of the 1st International Symposium on Non-Photorealistic Animation and Rendering*, pages 31–37, New York, NY, USA, 2000. ACM Press.

[NT00] F. Nooruddin and G. Turk. Interior/exterior classification of polygonal models. In *Proceedings of IEEE Visualization '00*, pages 415–422, 2000.

[Ola05] Marc Olano. Modified noise for evaluation on graphics hardware. In *Proceedings of the ACM SIGGRAPH/EUROGRAPHICS Conference on Graphics Hardware*, pages 105–110, New York, NY, USA, 2005. ACM Press.

[PC05] Gabriel Peyré and Laurent Cohen. Geodesic computations for fast and accurate surface remeshing and parameterization. *Progress in Nonlinear Differential Equations and Their Applications*, 63:157–171, 2005.

[PFH00] Emil Praun, Adam Finkelstein, and Hugues Hoppe. Lapped textures. In *SIGGRAPH Conference Proceedings*, pages 465–470, 2000.

[Pho75] B. T. Phong. Illumination for computer generated pictures. *Communications of the ACM*, 18:311–317, 1975.

[PHWF01] Emil Praun, Hugues Hoppe, Matthew Webb, and Adam Finkelstein. Real-time hatching. In *SIGGRAPH Conference Proceedings*, page 581, New York, NY, USA, 2001. ACM Press.

[PR03] A. Plaza and M. Rivara. Mesh refinement based on the 8-tetrahedra longest-edge partition. In *12th International Meshing Roundtable*, pages 67–78, 2003.

[PWL96] Alex T. Pang, Craig M. Wittenbrink, and K. Lodha, Suresh. Approaches to uncertainty visualization. Paper, Computer Science Department, University of California, Santa Cruz, CA 95064, USA, 1996.

[Ram88] V. Ramachandran. Perceiving shape from shading. *Scientific American*, 259:58–65, 1988.

[RC99] Ramesh Raskar and Michael Cohen. Image precision silhouette edges. In *Proceedings of the 1999 Symposium on Interactive 3D Graphics*, pages 135–140, New York, NY, USA, 1999. ACM Press.

[Rhe96] Penny Rheingans. Opacity-modulating triangular textures for irregular surfaces. In *Proceedings of Visualization '96*, pages 219–225. IEEE Computer Society, 1996.

[RR05] M. Robinson and K. Robbins. Towards perceptual enhancement of multiple intersecting surfaces. In *Visualization and Data Analysis*, pages 339–349, 2005.

[RS00] Sam Roweis and Lawrence Saul. Nonlinear dimensionality reduction by locally linear embedding. *Science*, 290(5500):2323–2326, 2000.

[RSC87] W. T. Reeves, D. H. Salesin, and P L. Cook. Rendering antialiased shadows with depth maps. In *SIGGRAPH Conference Proceedings*, volume 21, pages 283–291. ACM Press, 1987.

[SAPH04] John Schreiner, Arul Asirvatham, Emil Praun, and Hugues Hoppe. Inter-surface mapping. *ACM Trans. Graph.*, 23(3):870–877, 2004.

[Set96] J. Sethian. A fast marching level set method for monotonically advancing fronts. In *Proc. Nat. Acad. Sci.*, volume 93, pages 1591–1595, 1996.

[Si06] Hang Si. TegGen: a quality tetrahedral mesh generator and three-dimensional delaunay triangulator, July 2006.

[Sin00] P. Sinha. Perceiving illumination inconsistencies. *Investigative Ophthalmology and Visual Science*, 41(4):1192, 2000.

[Sin04] M. Singh. Lightness constancy through transparency: Internal consistency in layered surface representations. *Vision Research*, 44:1827–1842, 2004.

[SKvW+92] Mark Segal, Carl Korobkin, Rolf van Widenfelt, Jim Foran, and Paul Haeberli. Fast shadows and lighting effects using texture mapping. In *SIGGRAPH Conference Proceedings*, pages 249–252. ACM Press, 1992.

[SM97] P. Samson and J.-L. Mallet. Curvature analysis of triangulated surfaces in structural geology. *Math. Geol.*, 29(3):391–412, 1997.

[SML98] W. Schroeder, K. Martin, and W. Lorensen. *The Visualization ToolKit: An object-oriented approach to 3D graphics*. Prentice-Hall, 2nd edition, 1998.

[SSK+05] Vitaly Surazhsky, Tatiana Surazhsky, Danil Kirsanov, Steven J. Gortler, and Hugues Hoppe. Fast exact and approximate geodesics on meshes. *ACM Trans. Graph.*, 24(3):553–560, 2005.

[SW04] G. Sweet and C. Ware. View direction, surface orientation and texture orientation for perception of surface shape. In *Proceedings of Graphics Interface 2004*, 2004.

[SWG+03] Pedro V. Sander, Zoë J. Wood, Steven J. Gortler, John Snyder, and Hugues Hoppe. Multi-chart geometry images. In *Symposium on Geometry Processing*, pages 146–155, 2003.

[Tau95] Gabriel Taubin. Estimating the tensor of curvature of a surface from a polyhedral approximation. In *ICCV*, pages 902–907, 1995.

[TO02a] J. T. Todd and A. H. Oomes. Generic and non-generic conditions for the perception of surface shape from texture. *Vision Research*, 42(7):837–850, 2002.

[TO02b] Greg Turk and James F. O'Brien. Modelling with implicit surfaces that interpolate. *ACM Trans. Graph.*, 21(4):855–873, 2002.

[TSS+98] William Thompson, Peter Shirley, Brian Smits, Daniel Kersten, and Cindee Madison. Visual glue. Technical Report UUCS-98-007, University of Utah, Department of Computer Science, 12 1998.

[Tur91] Greg Turk. Generating textures on arbitrary surfaces using reaction-diffusion. In *SIGGRAPH Conference Proceedings*, pages 289–298, 1991.

[vdB97] Gino van den Bergen. Efficient collision detection of complex deformable models using AABB trees. *Journal of Graphics Tools*, 2(4):1–13, 1997.

[War88] C. Ware. Color sequences for univariate maps: Theory, experiments and principles. *IEEE Computer Graphics and Applications*, pages 41–49, September 1988.

[War04] C. Ware. *Information visualization: Perception for design, 2nd Edition*. Morgan Kaufmann, San Francisco, CA, USA, 2004.

[WE02] Daniel Weiskopf and Thomas Ertl. Real-time depth-cueing beyond fogging. *J. Graph. Tools*, 7(4):83–90, 2002.

[Wil78] L. Williams. Casting curved shadows on curved surfaces. In *SIGGRAPH Conference Proceedings*, pages 270–274. ACM Press, 1978.

[WPL95] Craig Wittenbrink, Alex Pang, and Suresh Lodha. Verity visualization: Visual mappings. Technical Report UCSC-CRL-95-48, University of California, Santa Cruz, 1995.

[WTI05] Chris Weigle and Russell M. Taylor II. Visualizing intersecting surfaces with nested-surface techniqes. In *Proceedings of IEEE Visualization 2005*, pages 503–510, Minneapolis, Minnesota, 2005. IEEE Computer Society.

[Yat06] Liron Yatziv. A fast O(N) implementation of the fast marching algorithm. *Journal of Computational Physics*, 212:393–399, 2006.

[ZMT05] Eugene Zhang, Konstantin Mischaikow, and Greg Turk. Feature-based surface parameterization and texture mapping. *ACM Trans. Graph.*, 24(1):1–27, 2005.